REPUBLIC OF CAMEROON
PEACE-WORK-FATHERLAND
****
THE UNIVERSITY OF YAOUNDE I
****
FACULTY OF SCIENCE
****
POSTGRADUATE SCHOOL OF SCIENCE TECHNOLOGY AND GEOSCIENCES
****
RESEARCH AND POSTGRADUATE TRAINING UNIT FOR CHEMISTRY AND APPLICATIONS

REPUBLIQUE DU CAMEROUN
PAIX-TRAVAIL-PATRIE
****
UNIVERSITE DE YAOUNDE I
****
FACULTE DES SCIENCES
****
CENTRE DE RECHERCHE ET DE FORMATION DOCTORALE EN SCIENCES, TECHNOLOGIES ET GEOSCIENCES
****
UNITE DE RECHERCHE ET DE FORMATION DOCTORALE CHIMIE ET APPLICATIONS

DEPARTMENT OF ORGANIC CHEMISTRY
DEPARTEMENT DE CHIMIE ORGANIQUE

Speciality : Natural Products
****
Spécialité : Substances Naturelles
****

Chemical and Antiplasmodial activity of three Cameroonian medicinal plants: *Sida rhombifolia* Linné C., *Sida acuta* Burm F. (Malvaceae) and *Garcinia ovalifolia* Oliv. (Clusiaceae).

Thesis

Presented and defended publicly for the fulfilment of the award of the degree of Doctorat/PhD.

By

KAMDOUM Blaise Cédric

Ph.D. student, Organic chemistry

Registration number: 05U221

Under the Co-direction of

SIMO KONGA Ingrid
Associate Professor
University of Dschang

NGAMENI Bathelemy
Professor
University of Yaoundé 1

Year 2022/2023

REPUBLIQUE DU CAMEROUN
Paix-Travail-Patrie
.....
UNIVERSITE DE YAOUNDE I
.....
FACULTE DES SCIENCES
.....
CENTRE DE RECHERCHE ET DE FORMATION DOCTORALE EN SCIENCES, TECHNOLOGIES ET GEOSCIENCES
.....
UNITE DE RECHERCHE ET DE FORMATION DOCTORALE CHIMIE ET APPLICATIONS
.....

REPUBLIC OF CAMEROON
Peace-Work-Fatherland
.....
UNIVERSITY OF YAOUNDE I
.....
FACULTY OF SCIENCE
.....
POSTGRADUATE SCHOOL OF SCIENCE, TECHNOLOGY AND GEOSCIENCES
.....
RESEARCH AND POSTGRADUATE TRAINING UNIT FOR CHEMISTRY AND APPLICATIONS
.....

DEPARTEMENT DE CHIMIE ORGNIQUE

DEPARTMENT OF ORGANIC CHIMISTRY

ATTESTATION DE CORRECTION DE MEMOIRE DE THÈSE DE DOCTORAT/PhD DE MONSIEUR KAMDOUM BLAISE CEDRIC

Titre de la thèse: **Chemical and Antiplasmodial activity of three Cameroonian medicinal plants: *Sida rhombifolia* Linné C., *Sida acuta* Burm F. (Malvaceae) and *Garcinia ovalifolia* Oliv. (Clusiaceae).**

Nous soussignés, enseignant ci-dessous nommés membre du jury de soutenance de thèse de Doctorat /PhD de Monsieur **KAMDOUM BLAISE CEDRIC**, Matricule **05U221**, attestons que ce candidat a bel et bien pris en compte dans la mouture finale de sa thèse, toutes corrections et recommandations qui lui ont été faites au cours de sa soutenance en date du 27 Avril 2023.

En foi de quoi, la présente attestation de correction lui est délivrée pour servir et valoir ce que de droit.

Fait à Yaoundé, le .....

Président du jury

MBAZE MEVA'A Luc Léonard

Professeur

Rapporteurs

NGAMENI Bathélémy

Professeur

SIMO KONGA Ingrid

Maître de Conférences

Membres

MBAZOUA DJAMA Céline

Professeur

FEKAM BOYOM Fabrice

Professeur

KAMDEM WAFO Alain

Professeur

ZONDEGOUMBA Ernestine

Maître de Conférences

‘ »UNIVERSITÉ DE YAOUNDÉ I **Faculté des Sciences** Division de la Programmation et du Suivi des Activités Académiques		THE UNIVERSITY OF YAOUNDE I **Faculty of Science** Division of Programming and Follow-up of Academic Affaires
LISTE DES ENSEIGNANTS PERMANENTS		**LIST OF PERMANENT TEACHING STAFF**

OFFICIAL LIST OF LECTURERS OF THE FACULTY OF SCIENCE

ACADEMIC YEAR 2021/2022

(*By Department and by Grade*)

LAST UPDATED: Jun 22, 2022

ADMINISTRATION

Dean: TCHOUANKEU Jean- Claude, Associate Professor
Vice Dean in Charge of Academic Affairs: ATCHADE Alex de Théodore, Professor
Vice Dean in Charge of Student Affairs: AJEAGAH Gideon AGHAINDUM, Professor
Vice Dean in Charge of Research and Cooperation: ABOSSOLO Monique, Associate Professor
Head of Administrative and Financial Division: NDOYE FOE Marie C. F., Associate Professor
Head of Academic Affairs Division, Keeping of Terms and Research: MBAZE MEVA’A Luc Léonard, Professor

1- DEPARTMENT OF BIOCHIMISTRY (BCH) (39)			
N°	**NAME AND SURNAME**	**GRADE**	**OBSERVATIONS**
1	BIGOGA DIAGA Jude	Professor	In service
2	FEKAM BOYOM Fabrice	Professor	In service
3	FOKOU Elie	Professor	In service
4	KANSCI Germain	Professor	In service
5	MBACHAM FON Wilfried	Professor	In service
6	MOUNDIPA FEWOU Paul	Professor	**Head of Department**
7	NINTCHOM PENLAP V. épse BENG	Professor	In service
8	OBEN Julius ENYONG	Professor	In service
9	ACHU Merci BIH	Associate Professor	In service
10	ATOGHO Barbara Mma	Associate Professor	In service
11	AZANTSA KINGUE GABIN BORIS	Associate Professor	In service
12	BELINGA née NDOYE FOE M. C. F.	Associate Professor	**Chief DAF / FS**
13	BOUDJEKO Thaddée	Associate Professor	In service

14	DJUIDJE NGOUNOUE Marcelline	Associate Professor	In service
15	EFFA NNOMO Pierre	Associate Professor	In service
16	NANA Louise épouse WAKAM	Associate Professor	In service
17	NGONDI Judith Laure	Associate Professor	In service
18	NGUEFACK Julienne	Associate Professor	In service
19	NJAYOU Frédéric Nico	Associate Professor	In service
20	MOFOR née TEUGWA Clotilde	Associate Professor	**Insp. Serv. MINESUP**
21	TCHANA KOUATCHOUA Angèle	Associate Professor	In service
22	AKINDEH MBUH NJI	Senior Lecturer	In service
23	BEBOY EDZENGUELE Sara N.	Senior Lecturer	In service
24	DAKOLE DABOY Charles	Senior Lecturer	In service
25	DJUIKWO NKONGA Ruth Viviane	Senior Lecturer	In service
26	DONGMO LEKAGNE Joseph Blaise	Senior Lecturer	In service
27	FONKOUA Martin	Senior Lecturer	In service
28	BEBEE Fadimatou	Senior Lecturer	In service
29	KOTUE KAPTUE Charles	Senior Lecturer	In service
30	LUNGA Paul KEILAH	Senior Lecturer	In service
31	MANANGA Marlyse Joséphine	Senior Lecturer	In service
32	MBONG ANGIE M. Mary Anne	Senior Lecturer	In service
33	PECHANGOU NSANGOU Sylvain	Senior Lecturer	In service
34	Palmer MASUMBE NETONGO	Senior Lecturer	In service
35	MBOUCHE FANMOE Marceline J.	Assist. Lecturer	In service
36	OWONA AYISSI Vincent Brice	Assist. Lecturer	In service
37	WILFRIED ANGIE Abia	Assist. Lecturer	In service
38	FOUPOUAPOUOGNIGNI Yacouba	Assist. Lecturer	In service
39	MBOUCHE FANMOE Marceline Joëlle	Assist. Lecturer	In service
2- DEPARTMENT OF ANIMAL BIOLOGY AND PHYSIOLOGY (A. B. P.) (52)			
1	AJEAGAH Gideon AGHAINDUM	Professor	**Vice Dean/DSSE**
2	BILONG BILONG Charles-Félix	Professor	**Head of Department**
3	DIMO Théophile	Professor	In service
4	DJIETO LORDON Champlain	Professor	In service
5	ESSOMBA née NTSAMA MBALA	Professor	**Vice dean/FMSB/UYI**

6	FOMENA Abraham	Professor	In service
7	KAMTCHOUING Pierre	Professor	In service
8	NJAMEN Dieudonné	Professor	In service
9	NJIOKOU Flobert	Professor	In service
10	NOLA Moïse	Professor	In service
11	TAN Paul VERNYUY	Professor	In service
12	TCHUEM TCHUENTE Louis Albert	Professor	**Insp. Serv. Coord. Progr. in HEALTH**
13	ZEBAZE TOGOUET Serge Hubert	Professor	In service
14	BILANDA Danielle Claude	Associate Professor	In service
15	DJIOGUE Séfirin	Associate Professor	In service
16	DZEUFIET DJOMENI Paul Désiré	Associate Professor	In service
17	JATSA BOUKENG Hermine épse M.	Associate Professor	In service
18	KEKEUNOU Sévilor	Associate Professor	In service
19	MEGNEKOU Rosette	Associate Professor	In service
20	MONY Ruth épse NTONE	Associate Professor	In service
21	NGUEGUIM TSOFACK Florence	Associate Professor	In service
22	TOMBI Jeannette	Associate Professor	In service
23	ALENE Désirée Chantal	Senior Lecturer	In service
26	ATSAMO Albert Donatien	Senior Lecturer	In service
27	BELLET EDIMO Oscar Roger	Senior Lecturer	In service
28	DONFACK Mireille	Senior Lecturer	In service
29	ETEME ENAMA Serge	Senior Lecturer	In service
30	GOUNOUE KAMKUMO Raceline	Senior Lecturer	In service
31	KANDEDA KAVAYE Antoine	Senior Lecturer	In service
32	LEKEUFACK FOLEFACK Guy B.	Senior Lecturer	In service
33	MAHOB Raymond Joseph	Senior Lecturer	In service
34	MBENOUN MASSE Paul Serge	Senior Lecturer	In service
35	MOUNGANG LucianeMarlyse	Senior Lecturer	In service
36	MVEYO NDANKEU Yves Patrick	Senior Lecturer	In service
37	NGOUATEU KENFACK Omer Bébé	Senior Lecturer	In service
38	NGUEMBOK	Senior Lecturer	In service
39	NJUA Clarisse Yafi	Senior Lecturer	**Chief of Division/UBA**

40	NOAH EWOTI Olive Vivien	Senior Lecturer	In service
41	TADU Zephyrin	Senior Lecturer	In service
42	TAMSA ARFAO Antoine	Senior Lecturer	In service
43	YEDE	Senior Lecturer	In service
44	BASSOCK BAYIHA Etienne Didier	Assist. Lecturer	In service
45	ESSAMA MBIDA Désirée Sandrine	Assist. Lecturer	In service
46	KOGA MANG DOBARA	Assist. Lecturer	In service
47	LEME BANOCK Lucie	Assist. Lecturer	In service
48	YOUNOUSSA LAME	Assist. Lecturer	In service
49	AMBADA NDZENGUE GEORGIA ELNA	Assist. Lecturer	In service
50	FOKAM Alvine Christelle Epse KEGNE	Assist. Lecturer	In service
51	MAPON NSANGOU Indou	Assist. Lecturer	In service
52	NWANE Philippe Bienvenu	Assist. Lecturer	In service
3- DEPARTMENT OF PLANT BIOLOGY AND PHYSIOLOGY (P. B. P.) (33)			
1	AMBANG Zachée	Professor	**Chief of Division/UYII**
2	BELL Joseph Martin	Professor	In service
3	DJOCGOUE Pierre François	Professor	In service
4	MOSSEBO Dominique Claude	Professor	In service
5	YOUMBI Emmanuel	Professor	**Head of Department**
6	ZAPFACK Louis	Professor	In service
7	ANGONI Hyacinthe	Associate Professor	In service
8	BIYE Elvire Hortense	Associate Professor	In service
9	KENGNE NOUMSI Ives Magloire	Associate Professor	In service
10	MALA Armand William	Associate Professor	In service
11	MBARGA BINDZI Marie Alain	Associate Professor	**CT/ MINESUP**
12	MBOLO Marie	Associate Professor	In service
13	NDONGO BEKOLO	Associate Professor	**CE/MINRESI**
14	NGODO MELINGUI Jean Baptiste	Associate Professor	In service
15	NGONKEU MAGAPTCHE Eddy L.	Associate Professor	In service
16	TSOATA Esaïe	Associate Professor	In service
17	TONFACK Libert Brice	Associate Professor	In service

18	DJEUANI Astride Carole	Senior Lecturer	In service
19	GOMANDJE Christelle	Senior Lecturer	In service
20	MAFFO MAFFO Nicole Liliane	Senior Lecturer	In service
21	MAHBOU SOMO TOUKAM G.	Senior Lecturer	In service
22	NGALLE Hermine BILLE	Senior Lecturer	In service
23	NGOUO Lucas Vincent	Senior Lecturer	In service
24	NNANGA MEBENGA Ruth Laure	Senior Lecturer	In service
25	NOUKEU KOUAKAM Armelle	Senior Lecturer	In service
26	ONANA JEAN MICHEL	Senior Lecturer	In service
27	GODSWILL NTSOMBAH N.	Assist. Lecturer	In service
28	KABELONG BANAHO Louis-P.-R.	Assist. Lecturer	In service
29	KONO Léon Dieudonné	Assist. Lecturer	In service
30	LIBALAH Moses BAKONCK	Assist. Lecturer	In service
31	LIKENG-LI-NGUE Benoit C	Assist. Lecturer	In service
32	TAEDOUNG Evariste Hermann	Assist. Lecturer	In service
33	TEMEGNE NONO Carine	Assist. Lecturer	In service
4- DEPARTMENT OF INORGANIC CHEMISTRY (I. C.) (35)			
1	AGWARA ONDOH Moïse	Professor	**Head of Department**
2	ELIMBI Antoine	Professor	In service
3	Florence UFI CHINJE épouse MELO	Professor	**Rector Univ. Ngaoundere**
4	GHOGOMU Paul MINGO	Professor	**Minister in Charge of Mission. P.R.**
5	NANSEU Njiki Charles Péguy	Professor	In service
6	NDIFON Peter TEKE	Professor	**C.T. MINRESI**
7	NGOMO Horace MANGA	Professor	**Vice Chancellor/U.B**.
8	NDIKONTAR Maurice KOR	Professor	**Vice-Dean Un. Bamenda**
9	NENWA Justin	Professor	In service
10	NGAMENI Emmanuel	Professor	**Dean F.S. U.Ds**
11	BABALE née DJAM DOUDOU	Associate Professor	**Charge of Mission P.R.**
12	DJOUFAC WOUMFO Emmanuel	Associate Professor	In service
13	KAMGANG YOUBI Georges	Associate Professor	In service
14	KEMMEGNE MBOUGUEM Jean C.	Associate Professor	In service
15	KONG SAKEO	Associate Professor	In service

16	NDI NSAMI Julius	Associate Professor	In service
17	NJIOMOU C. épse DJANGANG	Associate Professor	In service
18	NJOYA Dayirou	Associate Professor	In service
19	YOUNANG Elie	Associate Professor	In service
20	ACAYANKA Elie	Senior Lecturer	In service
21	BELIBI BELIBI Placide Désiré	Senior Lecturer	**CS/ ENS Bertoua**
22	CHEUMANI YONA Arnaud M.	Senior Lecturer	In service
23	EMADACK Alphonse	Senior Lecturer	In service
24	KENNE DEDZO GUSTAVE	Senior Lecturer	In service
25	KOUOTOU DAOUDA	Senior Lecturer	In service
26	MAKON Thomas Beauregard	Senior Lecturer	In service
27	MBEY Jean Aime	Senior Lecturer	In service
28	NCHIMI NONO KATIA	Senior Lecturer	In service
29	NEBA nee NDOSIRI Bridget N.	Senior Lecturer	**CT/ MINFEM**
30	NYAMEN Linda Dyorisse	Senior Lecturer	In service
31	PABOUDAM GBAMBIE A.	Senior Lecturer	In service
32	TCHAKOUTE KOUAMO Hervé	Senior Lecturer	In service
33	NJANKWA NJABONG N. Eric	Assist. Lecturer	In service
34	PATOUOSSA ISSOFA	Assist. Lecturer	In service
35	SIEWE Jean Mermoz	Assist. Lecturer	In service
5- DEPARTMENT OF ORGANIC CHIMISTRY (O. C.) (40)			
1	DONGO Etienne	Professor	**Vice Dean/CSA/ *F. SED***
2	GHOGOMU TIH Robert Ralph	Professor	**Director B. A. I Foumban**
3	NGOUELA Silvère Augustin	Professor	**Head of Department UDs**
4	NKENGFACK Augustin Ephrem	Professor	Retired
5	NYASSE Barthélemy	Professor	In service
6	PEGNYEMB Dieudonné Emmanuel	Professor	**Head of Department Director/MINESUP/**
7	WANDJI Jean	Professor	In service
8	Alex de Théodore ATCHADE	Professor	**Vice-Dean/CAA**
9	EYONG Kenneth OBEN	Associate Professor	In service
10	FOLEFOC Gabriel NGOSONG	Associate Professor	In service

11	FOTSO WABO Ghislain	Associate Professor	In service
12	KEUMEDJIO Félix	Associate Professor	In service
13	KEUMOGNE Marguerite	Associate Professor	In service
14	KOUAM Jacques	Associate Professor	In service
15	MBAZOA née DJAMA Céline	Professor	In service
16	MKOUNGA Pierre	Associate Professor	In service
17	NOTE LOUGBOT Olivier Placide	Associate Professor	**Chief Service/MINESUP**
18	NGO MBING Joséphine	Associate Professor	**Sous/Direct. MINERESI**
19	NGONO BIKOBO Dominique Serge	Associate Professor	**Chargé d'Études Ass. n°3/MINESUP**
20	NOUNGOUE TCHAMO Diderot	Associate Professor	In service
21	TABOPDA KUATE Turibio	Associate Professor	In service
22	TCHOUANKEU Jean-Claude	Associate Professor	**Dean/FS/ UY1**
23	TIH née NGO BILONG E. Anastasie	Associate Professor	In service
24	YANKEP Emmanuel	Associate Professor	In service
25	MVOT AKAK Carine	Associate Professor	In service
26	AMBASSA Pantaléon	Associate Professor	In service
27	TAGATSING FOTSING Maurice	Associate Professor	In service
28	ZONDENDEGOUMBA Ernestine	Associate Professor	In service
29	KAMTO Eutrophe Le Doux	Associate Professor	In service
30	NGNINTEDO Dominique	Senior Lecturer	In service
31	NGOMO Orléans	Senior Lecturer	In service
32	OUAHOUO WACHE Blandine M.	Senior Lecturer	In service
33	SIELINOU TEDJON Valérie	Senior Lecturer	In service
34	MESSI Angélique Nicolas	Senior. Lecturer	In service
35	TSEMEUGNE Joseph	Senior. Lecturer	In service
36	TCHAMGOUE Joseph	Senior Lecturer	In service
37	TSAFACK Maurice	Senior Lecturer	In service
38	TSAMO Armelle	Senior. Lecturer	In service
39	NONO Eric Carly	Senior Lecturer	In service
40	OUETE NANTCHOUANG Judith Laure	Senior Lecturer	In service
6- DEPARTMENT OF COMPUTER SCIENCE (C. S.) (25)			

1	ATSA ETOUNDI Roger	Professor	**Chief Div.MINESUP**
2	FOUDA NDJODO Marcel Laurent	Professor	**Head of Dpt HTTC/Chief IGA. MINESUP**
3	NDOUNDAM Réné	Associate Professor	In service
4	AMINOU Halidou	Senior Lecturer	**Head of Department**
5	DJAM Xaviera YOUH - KIMBI	Senior Lecturer	In service
6	EBELE Serge Alain	Senior Lecturer	In service
7	KOUOKAM KOUOKAM E. A.	Senior Lecturer	In service
8	MELATAGIA YONTA Paulin	Senior Lecturer	In service
9	MOTO MPONG Serge Alain	Senior Lecturer	In service
10	TAPAMO Hyppolite	Senior Lecturer	In service
11	ABESSOLO ALO'O Gislain	Senior Lecturer	In service
12	MONTHE DJIADEU Valery M.	Senior Lecturer	In service
13	OLLE OLLE Daniel Claude Delort	Senior Lecturer	**C/D Enset. Ebolowa**
14	TINDO Gilbert	Senior Lecturer	In service
15	TSOPZE Norbert	Senior Lecturer	In service
16	WAKU KOUAMOU Jules	Senior Lecturer	In service
17	BAYEM Jacques Narcisse	Assist. Lecturer	In service
18	DOMGA KOMGUEM Rodrigue	Assist. Lecturer	In service
19	EKODECK Stéphane Gaël Raymond	Assist. Lecturer	In service
20	HAMZA Adamou	Assist. Lecturer	In service
21	JIOMEKONG AZANZI Fidel	Assist. Lecturer	In service
22	MAKEMBE. S. Oswald	Assist. Lecturer	In service
23	MESSI NGUELE Thomas	Assist. Lecturer	In service
24	MEYEMDOU Nadège Sylvianne	Assist. Lecturer	In service
25	NKONDOCK. MI. BAHANACK.N.	Assist. Lecturer	In service
7- DEPARTMENT OF MATHEMATICS (MAT) (31)			
1	EMVUDU WONO Yves S.	Professor	**CD Info/Inspecteur MINESUP**
2	AYISSI Raoult Domingo	Associate Professor	**Head of Department**
3	NKUIMI JUGNIA Célestin	Associate Professor	In service
4	NOUNDJEU Pierre	Associate Professor	**Chief serv. certif. prog.**
5	MBEHOU Mohamed	Associate Professor	In service

6	TCHAPNDA NJABO Sophonie B.	Associate Professor	**Director/AIMS Rwanda**
7	AGHOUKENG JIOFACK Jean G.	Senior Lecturer	**Chief Cell MINPLAMAT**
8	CHENDJOU Gilbert	Senior Lecturer	In service
9	DJIADEU NGAHA Michel	Senior Lecturer	In service
10	DOUANLA YONTA Herman	Senior Lecturer	In service
11	FOMEKONG Christophe	Senior Lecturer	In service
12	KIANPI Maurice	Senior Lecturer	In service
13	KIKI Maxime Armand	Senior Lecturer	In service
14	MBAKOP Guy Merlin	Senior Lecturer	In service
15	MBANG Joseph	Senior Lecturer	In service
16	MBELE BIDIMA Martin Ledoux	Senior Lecturer	In service
17	MENGUE MENGUE David Joe	Senior Lecturer	In service
18	NGUEFACK Bernard	Senior Lecturer	In service
19	NIMPA PEFOUNKEU Romain	Senior Lecturer	In service
20	POLA DOUNDOU Emmanuel	Senior Lecturer	In service
21	TAKAM SOH Patrice	Senior Lecturer	In service
22	TCHANGANG Roger Duclos	Senior Lecturer	In service
23	TCHOUNDJA Edgar Landry	Senior Lecturer	In service
24	TETSADJIO TCHILEPECK M. E.	Senior Lecturer	In service
25	TIAYA TSAGUE N. Anne-Marie	Senior Lecturer	In service
26	MBIAKOP Hilaire George	Assist. Lecturer	In service
27	BITYE MVONDO Esther Claudine	Assist. Lecturer	In service
28	MBATAKOU Salomon Joseph	Assist. Lecturer	In service
29	MEFENZA NOUNTU Thiery	Assist. Lecturer	In service
30	TCHEUTIA Daniel Duviol	Assist. Lecturer	In service
31	TENKEU JEUFACK Yannick Léa	Assist. Lecturer	In service
8- DEPARTMENT OF MICROBIOLOGY (MIB) (21)			
1	ESSIA NGANG Jean Justin	Professor	**Head of Department**
2	BOYOMO ONANA	Associate Professor	In service
3	NWAGA Dieudonné M.	Associate Professor	In service
4	NYEGUE Maximilienne Ascension	Associate Professor	In service
5	RIWOM Sara Honorine	Associate Professor	In service

6	SADO KAMDEM Sylvain Leroy	Associate Professor	In service
7	ASSAM ASSAM Jean Paul	Senior Lecturer	In service
8	BODA Maurice	Senior Lecturer	In service
9	BOUGNOM Blaise Pascal	Senior Lecturer	In service
10	ESSONO OBOUGOU Germain G.	Senior Lecturer	In service
11	NJIKI BIKOÏ Jacky	Senior Lecturer	In service
12	TCHIKOUA Roger	Senior Lecturer	In service
13	ESSONO Damien Marie	Assist. Lecturer	In service
14	LAMYE Glory MOH	Assist. Lecturer	In service
15	MEYIN A EBONG Solange	Assist. Lecturer	In service
16	NKOUDOU ZE Nardis	Assist. Lecturer	In service
17	SAKE NGANE Carole Stéphanie	Assist. Lecturer	In service
18	TOBOLBAÏ Richard	Assist. Lecturer	In service
19	MONI NDEDI Esther Del Florence	Assist. Lecturer	In service
20	NKOUE TONG ABRAHAM	Assist. Lecturer	In service
21	SAKE NGANE Carole Stéphanie	Assist. Lecturer	In service

9- DEPARTMENT OF PHYSICS (PHY) (46)			
1	BEN-BOLIE Germain Hubert	Professor	In service
2	ESSIMBI ZOBO Bernard	Professor	In service
3	EKOBENA FOUDA Henri Paul	Associate Professor	**Chief of Division. UN**
4	KOFANE Timoléon Crépin	Professor	Retired
5	NANA ENGO Serge Guy	Professor	In service
6	NDJAKA Jean Marie Bienvenu	Professor	**Head of Department**
7	NOUAYOU Robert	Professor	In service
8	NJANDJOCK NOUCK Philippe	Professor	**Under Director/ MINRESI**
9	PEMHA Elkana	Professor	In service
10	TABOD Charles TABOD	Professor	**Dean Univ. Bda**
11	TCHAWOUA Clément	Professor	In service
12	WOAFO Paul	Professor	In service
13	BIYA MOTTO Frédéric	Associate Professor	**G. D./HYDRO Mekin**
14	BODO Bertrand	Associate Professor	In service
15	DJUIDJE KENMOE épouse A.	Associate Professor	In service

16	EYEBE FOUDA Jean sire	Associate Professor	In service
17	FEWO Serge Ibraïd	Associate Professor	In service
18	HONA Jacques	Associate Professor	In service
19	MBANE BIOUELE César	Associate Professor	In service
20	NANA NBENDJO Blaise	Associate Professor	In service
21	NDOP Joseph	Associate Professor	In service
22	SAIDOU	Associate Professor	**MINRESI**
23	SIEWE SIEWE Martin	Associate Professor	In service
24	SIMO Elie	Associate Professor	In service
25	VONDOU Derbetini Appolinaire	Associate Professor	In service
26	WAKATA née BEYA Annie	Associate Professor	**Under Dir./ MINESUP**
27	ZEKENG Serge Sylvain	Associate Professor	In service
28	ABDOURAHIMI	Senior Lecturer	In service
29	EDONGUE HERVAIS	Senior Lecturer	In service
30	ENYEGUE A NYAM épse BELINGA	Senior Lecturer	In service
31	FOUEDJIO David	Senior Lecturer	**Chief of Cell MINADER**
32	MBINACK Clément	Senior Lecturer	In service
33	MBONO SAMBA Yves Christian U.	Senior Lecturer	In service
34	MELI'I Joelle Larissa	Senior Lecturer	In service
35	MVOGO ALAIN	Senior Lecturer	In service
38	OBOUNOU Marcel	Senior Lecturer	**DA/U. Int. Etat/Sangma.**
39	WOULACHE Rosalie Laure	Senior Lecturer	In service
40	AYISSI EYEBE Guy François V.	Assist. Lecturer	In service
41	CHAMANI Roméo	Assist. Lecturer	In service
42	TEYOU NGOUPOU Ariel	Assist. Lecturer	In service
43	KAMENI NEMATCHOUA Modeste	Assist. Lecturer	In service
44	LAMARA Maurice	Assist. Lecturer	In service
45	NGA ONGODO Dieudonné	Assist. Lecturer	In service
46	WANDJI NYAMSI William	Assist. Lecturer	In service
10- DEPARTMENT OF EARTH SCIENCES (E. S.) (43)			
1	BITOM Dieudonné	Professor	**Dean/FASA/UDs**
2	FOUATEU Rose épse YONGUE	Professor	In service
3	KAMGANG Pierre	Professor	In service

4	NDJIGUI Paul Désiré	Professor	**Head of Department**
5	NDAM NGOUPAYOU Jules-Remy	Professor	In service
6	NGOS III Simon	Professor	**DAAC/Uma**
7	NKOUMBOU Charles	Professor	In service
8	NZENTI Jean-Paul	Professor	In service
9	ABOSSOLO née ANGUE Monique	Associate Professor	**Vice-Dean/DRC**
10	GHOGOMU Richard TANWI	Associate Professor	**CD/Uma**
11	MOUNDI Amidou	Associate Professor	**CT/ MINIMDT**
12	NGUEUTCHOUA Gabriel	Associate Professor	**CEA/MINRESI**
13	NJILAH Isaac KONFOR	Associate Professor	In service
14	ONANA Vincent Laurent	Associate Professor	**Chief serv. Mater. Maint**.
15	BISSO Dieudonné	Associate Professor	**Director/Project Barrage Memve'ele**
16	EKOMANE Emile	Associate Professor	In service
17	GANNO Sylvestre	Associate Professor	In service
18	NYECK Bruno	Associate Professor	In service
19	TCHOUANKOUE Jean-Pierre	Associate Professor	In service
20	TEMDJIM Robert	Associate Professor	In service
21	YENE ATANGANA Joseph Q.	Associate Professor	**Chief Div. /MINTP**
22	ZO'O ZAME Philémon	Associate Professor	**G. D./ART**
23	ANABA ONANA Achille Basile	Senior Lecturer	In service
24	BEKOA Etienne	Senior Lecturer	In service
25	ELISE SABABA	Senior Lecturer	In service
26	ESSONO Jean	Senior Lecturer	In service
27	EYONG JOHN TAKEM	Senior Lecturer	In service
28	FUH Calistus Gentry	Senior Lecturer	**Sec. D'Etat/MINMIDT**
29	LAMILEN BILLA Daniel	Senior Lecturer	In service
30	MBESSE CECILE OLIVE	Senior Lecturer	In service
31	MBIDA YEM	Senior Lecturer	In service
32	METANG Victor	Senior Lecturer	In service
33	MINYEM Dieudonné-Lucien	Senior Lecturer	**CD/Uma**
34	NGO BELNOUN Rose Noël	Senior Lecturer	In service
35	NGO BIDJECK Louise Marie	Senior Lecturer	In service

36	NOMO NEGUE Emmanuel	Senior Lecturer	In service
37	NTSAMA ATANGANA Jacqueline	Senior Lecturer	In service
38	TCHAKOUNTE J. épse NOUMBEM	Senior Lecturer	**Chief of cell/MINRESI**
39	TCHAPTCHET TCHATO De P.	Senior Lecturer	In service
40	TEHNA Nathanaël	Senior Lecturer	In service
41	TEMGA Jean Pierre	Senior Lecturer	In service
42	FEUMBA Roger	Assist. Lecturer	In service
43	MBANGA NYOBE Jules	Assist. Lecturer	In service

Classification of teaching staff at the faculty of Science of the University of Yaoundé 1

NUMBER OF LECTURERS					
Department	**Professor**	**Associate Professor**	**Senior Lecturer**	**Assist. Lecturer**	**Total**
BCH	9 (1)	13 (09)	14 (06)	3 (2)	**39 (18)**
A. B. P.	13 (1)	09 (06)	19 (05)	05 (2)	**46 (14)**
P. B. P.	06 (0)	11 (02)	9 (06)	07 (01)	**33 (9)**
I. C.	10 (1)	09 (02)	12 (02)	03 (0)	**34 (5)**
O. C.	7 (0)	19 (06)	09 (03)	05 (01)	**40 (10)**
C. S.	2 (0)	1 (0)	13 (01)	09 (01)	**25 (2)**
MAT	1 (0)	5 (0)	19 (01)	05 (02)	**30 (3)**
MIB	1 (0)	5 (02)	06 (01)	06 (02)	**18 (5)**
PHY	12 (0)	15 (02)	10 (03)	03 (0)	**40 (5)**
E. S.	8 (1)	14 (01)	19 (05)	02 (0)	**43 (7)**
Total	**69 (4)**	**99 (28)**	**130 (33)**	**45 (10)**	**348 (78)**

A total of: **348 (78)** including:

Professors **69 (4)**

Associate Professors **101 (30)**

Senior Lecturers **130 (33)**

Assist. Lecturers **48 (11)**

( ) = Number of women **75**

The Dean of the Faculty of Science

Prof. TCHOUANKEU Jean-Claude

DEDICATION

To

My Parents

KAMDOUM DANIEL

And

BODIE SIMONE

ACKNOWLEDGEMENTS

I would like to express my gratitude to:

- The German Academic Exchange Service (DAAD), for having fully funded this work through the YaBiNaPA (Yaounde-Bielefeld Bilateral Graduate School Natural Products with antiparasitic and antimicrobial) project;
- Open Lab Africa of university of East Anglia for analysis of hemisynthetic products
- Laboratory of phytobiochemistry and medicinal plants studies for the antiplasmadial test
- My supervisor Professor NGAMENI B., your orientations were very beneficial to me for the realisation of this work. Your scientific rigor and your way of working have allowed me to be more attentive and critical towards my work;
- Professor SIMO I., director of this work, for completely investing her time energy and knowledge to train me in this field of Natural Product Chemistry/Pharmacognosy and through whose guidance, motivation and connections enabled the realisation of this work in due time;
- Emeritous Professor NGADJUI B.T., for your constant support, he is like a father to me;
- Professor PEGNYEMB D.E, Head of the Department of Organic Chemistry for their countless advices and the immense knowledge imparted on me;
- All the lecturers of the Department Organic Chemistry of the University of Yaounde 1 for their selfless advices and most specifically:
- Professor NKENGFACK E., whose precious guidance, assistance, , and encouragement contributed to the completion of this research work;
- Professor KEUMEDJIO F., for kind behavior during the course of my studies;
- Professor FOTSO W. G**.,** for every valuable guidance offered, not excluding the priceless advice, patience throughout the course of this study;
- Professor AMBASSA P**.**, for guidance and all the meaningful criticisms he made in order to give the required standard to this work;
- Professors LENTA N. B. and SEWALD N., Coordinators of the YaBiNaPA graduate school, Yaounde and Bielefeld respectively for the opportunies they offered me to carry out this work in well-equipped laboratories and with other research facilities;

- Professor TABOPDA T., for encouragement.
- Professor FEKAM B., for carring out the biological activity tests reported in this work;
- My seniors in the laboratory, Doctors KAMGA J., KENGAP R., SIMO CC, NGNINTEDO D, ACHE R, CHI G, OUETE J, GUEDEM A, TCHAMGOUE J., for the availability in guiding this work;
- My laboratory mates, most especially NOULALA C, NGANGOUE M., and KAMSU.V. MOUAFO T., for their support and collaboration without which this work would not have been completed;
- Drs TEKAPI W., TABEKOUENG B., for mentoring me throughout this work;
- All the members of Laboratory 278 of the University of Yaounde 1 for collaboration during bench work;
- All the students of the YaBiNaPA graduate school and some students of the University of Yaounde 1 especially MBOCK A., FEUMOE U., WAMBA S., TCHATAT B., for their immense support and collaboration;
- My elder brother, KAMDOUM E., for financial support throughout my studies;
- Those whose names have not been mentioned here your varied contributions and support remain boldly and colourfully engraved in my heart.

TABLE OF CONTENTS

LIST OF ABBREVIATIONS AND CHEMICAL SYMBOLS

APCI: Atmospheric Pressure Chemical Ionisation

CC: Column Chromatography

CI : Chemical Ionisation

CoA : Coenzyme A

COSY : COrrelation SpectroscopY

d: doublet

DAAD: *Deutscher Akademischer Austausch Dienst*

dd: doublet of doublet

ddd: doublet of doublet of doublet

DEPT: Distortionless Enhancement by Polarization Transfer

DI: Desorption Ionisation

dt: doublet of triplet

EA: Ethylacetate

ESI-MS: Electro Spray Ionization Mass Spectrometry

FPP: Farnesyl diPhosPhate

FAB: Fast Atom Bombardment

Go: *Garcinia ovalifolia*

GPP: Geranyl diPhosPhate

GGPP: Geranyl Geranyl diPhosPhate

Hex: Hexene

HMBC: Heteronuclear Multiple Bond Correlation

HMQC: Heteronuclear Multiple Quantum Coherence

HPLC: High Performance Liquid Chromatography

HR-ESIMS: High Resolution ElectroSpray Ionization Mass Spectrometry

HSQC: Heteronuclear Single Quanctum Coherence

IPP: Isopentenyl diphosphate

IR: Infra Red

IC_{50}: Concentration causing 50% inhibition

J (Hz): Coupling constant (NMR) in Hertz

m: multiplet

m.p: melting point

NOESY: Nuclear Overhauser Enhanced SpectroscopY

ppm: Part per million

q : quadruplet

RDA : Retro Diels-Alder

ROESY: Rotating frame Overhausser enhancement spectroscopy

^{13}C NMR: Carbon-13 Nuclear Magnetic Resonance

^{1}H NMR: Proton Nuclear Magnetic Resonance

Rf: Retention factor

s: singlet

Sr: *Sida rhombifolia*

Sa : *Sida acuta*

SI : Selectivity Index

t : triplet

TLC: Thin Layer Chromatography

UV : Ultra Violet

VLC : Vacuum Liquid Chromatograpghy

WHO: World Health Organization

δ (ppm) : Chemical shift in part per million

LIST OF TABLES

LIST OF FIGURES

LIST OF SCHEMES

ABSTRACT

This work consists of the chemical investigation of three medicinal plants: *Sida rhombifolia* Linné.C, *Sida acuta* Burm. F. (Malvaceae) and *Garcinia ovalifolia* Oliv. (Clusiaceae) and their antiplasmodial activity against 3D7 and Dd2 strains. The studies led to the isolation and characterization of twenty-four (24) compounds by means of chromatographic and spectroscopic techniques (IR, UV, Mass, 1D and 2D NMR) and by comparison with literature data. Among these, twelve were obtained from *Sida rhombifolia,* seven from *Sida acuta* and five from *Garcinia ovalifolia* stem bark, grouped as follows: Two alkaloids: 4-methoxy-1-methylquinolin-2(1H)-one and cryptolepine**;** One ceramide: rhombifoliamide**;** Eleven phenolic compounds: kaempferol-3-*O*-*D*-glucopyranoside, kaempferol-3-*O*-*β*-*D*-(6-*E*-*P*-coumaroyl)**,** 1,6-dihydroxy-xanthone**,** xanthyletin**,** isogarcinol, taxifolin 6-*C*-glucoside, 7-epiisogarcinol, rheediaxanthone, suberenol, thamnosmonin, 2,6-dimethoxy-p-benzoquinone; Three steroids: 3-*O*-*β*-*D*-glucopyranosyl-*β*-sitosterol, mixure of *β*-sitosterol and stigmasterol, 20-hydroxyecdysone and seven triterpenes: lupeol, oleanolic acid, taraxeryl acetate, leontosise A**,** taraxerol, ursolic acid, betulinic acid.

Hemi-synthesis on isogarcinol led to five derivatives: 13,14-dioxaethylisogarcinol**,** 13,14-di-*O*-(4-bromobenzyl)isogarcinol**,** 13,14-di-*O*-benzylisogarcignol**,** 13,14-di-*O*-propargylisogarcinol and 13,14-di-*O*-(2-bromobenzyl)isogarcinol.

The crude extracts, some fractions and twenty (20) compounds were evaluated for their antiplasmodial activity against chloroquine-sensitive (3D7) and chloroquine-resistant (Dd2) of *Plasmodium falciparum* strains. The results showed that, extracts and fractions exhibited moderate to strong antiplasmodial activities against 3D7 (IC_{50} values: 0.18-20.11 µg/mL) and Dd2 (IC_{50} values: 0.74-63.09 µg/mL) of *P. falciparum* strains. In addition, cryptolepine from *Sida acuta* and oleanolic acid from *Sida rhombifolia* displayed promising antiplasmodial activities with $IC_{50} < 3.0$ µg/mL. The semisynthetic products 13, 14-dioxaethylisogarcinol and 13,14-di-*O*-benzyliso-garcignol exhibited promising antiplasmodial activities with $IC_{50} < 3.0$ µg/mL.

Cryptolepine and oleanolic acid are potential antimalarials and can be explored in the design of drugs against *Plasmodium falciparum* that justifying the traditional use of *Sida rhombifolia* and *Sida acuta* as antimalarial agents.

Keywords: *Garcinia ovalifolia, Sida rhombifolia, Sida acuta,* Antiplasmodial activity, Rhombifoliamide, Oleanolic acid, Cryptolepine, Hemi-synthesis.

RESUME

Le présent travail porte sur l'étude chimique de trois plantes médicinales camerounaise : *Sida rhombifolia* Linné. C, *Sida acuta* Burm. F. (Malvaceae) et *Garcinia ovalifolia* Oliv. (Clusiaceae) et leur activité antiplasmodiale sur les souches 3D7 et Dd2. Au moyen des techniques chromatographiques et spectroscopiques usuelles (IR, UV, MS, RMN-1D et 2D) et par comparaison avec les données de la littérature, cette étude a conduit à l'isolement et la caractérisation de vingt-quatre composés dont douze de *Sida rhombifolia*, sept de *Sida acuta* et cinq de l'écorce de la tige de *Garcinia ovalifolia* regroupés comme suit : Deux alcaloides: 4-méthoxy-1-méthylquinolin-2(1H)-one, cryptolépine; Un céramide: rhombifoliamide; Onze composés dérivés phénoliques: kaempférol-3-*O*-D-glucopyranoside**,** kaempférol-3-*O*-*β*-D-(6-*E*-*P*-coumaroyl) **,** 1,6- dihydroxy-xanthone, subérénol, isogarcinol**,** taxifoline 6-*C*-glucoside**,** 7-épiisogarcinol, rheediaxanthone, thamnosmonine, xanthylétine, 2,6-diméthoxy-*p*-benzoquinone; Trois stéroïdes: 3-*O*-*β*-D-glucopyranosyl-*β*-sitostérol, le mélange *β*-sitostérol et stigmastérol, 20-hydroxyecdysone; Sept tri terpènes: lupéol, acide oléanolique, acétate de taraxéryle, léontosise A, taraxérol, acide ursolique, acide bétulinique;

L'hémisynthèse sur l'isogarcinol a conduit à cinq dérivés: 13,14-dioxaéthylisogarcinol**,** 13,14-di-*O*-(4-bromobenzyl)isogarcinol**,** 13,14-di-*O*-benzylisogarcinol, 13,14-di-*O*-propargyliso-garcinol; 13,14-di-*O*-(2-bromobenzyl)isogarcinol et 13,14-di-*O*-propargylisogarcinol.

Les extraits bruts, fractions et 20 composés ont été évalués pour leur activité antiplasmodiale contre deux souches de *Plasmodium falciparum*: sensible à la chloroquine (3D7) et résistante à la chloroquine (Dd2). Les résultats ont révélés que les extraits et les fractions présentent une activité antiplasmodiale modérée contre les deux souches testées, 3D7 (valeurs CI_{50} : 0,18-20,11 µg/mL) et Dd2 (valeurs CI_{50} : 0,74-63,09 µg/mL). La cryptolepine obtenue de *Sida acuta* et l'acide oléanolique de *Sida rhombifolia* ont montré une activité antiplasmodiale significative avec une CI_{50} < 3,0 µg/mL. De même, deux des composés hémisynthétiques 13,14-dioxaéthylisogarcinol et 13,14-di-*O*-benzylisogarcinol présentent également une activité significative avec une CI_{50} < 3,0 µg/mL.

La cryptolepine et l'acide oléanolique sont de potentiels antimalariques et peuvent être explorés dans la conception des médicaments contre le *Plasmodium falciparum* justifiant ainsi l'usage traditionnel de *Sida rhombifolia* et *Sida acuta* comme des agents antimalariques.

Mots clés : *Garcinia ovalifolia, Sida rhombifolia, Sida acuta,* activité antiplasmodiale, Rhombifoliamide, Acide oléanolique, Cryptolépine, Hémisynthèses.

GENERAL INTRODUCTION

Introduction

Malaria is a human life-threatening disease caused by several species of the protozoan parasite *Plasmodium* transmitted through female anopheles mosquitoes. According to the recently published world malaria report, malaria remains an important parasitic disease affecting about 229 million patients globally (**WHO, 2020**). Reported malaria-associated deaths are evaluated to 409,000 people globally, with children under the age of five years being the most affected. Almost all cases are reported from low- and middle-income countries (LMICs) of the subtropical regions, and Africa accounts for about 94% of the total burden, with around 215 million cases and 384,000 malaria-associated deaths (**WHO, 2020**). In light of these statistics, the high mortality rates of malaria and its associated economic burden are of great concern. The increased incidence of drug-resistant parasites is a global concern for prophylaxis and treatment, as it leads to an increase in deaths [**Yu-Qing et *al.*, 2020**]. Moreover, reported toxicities and side effects caused by conventional antimalarial agents limit their effectiveness in malaria therapy. Among the first-line treatment strategies, artemisinin-based combination therapies (ACTs) are recommended for complicated cases of malaria, while artesunate monotherapy is directed to complicate and severe cases of malaria. Though these treatments have widely contributed to the decrease of malaria-associated deaths, increasing evidence suggest that their efficacy is declining due to the increase of resistant strains (**Yu-Qing et *al.*, 2020**). Therefore, there is a need to identify new antimalarial drugs. A reliable therapeutic source which remains explored in the traditional pharmacopeia. Plants of the genus *Sida* (Malvaceae) and *Garcinia* are widely used by indigenous communities for the treatment of malaria (**Gupta et *al.*, 2009; Hemshekhar et *al.*, 2011**).

The widespread uses of the aforementioned for the treatment of several ailments, including malaria justifies our choice. Thus, the aim of this work was to search for new, safe and efficient antiplasmodial therapetic agents, from the species *Sida acuta, Sida rhombifolia and Garcinia ovalifolia.*

More specifically:

- Extract and isolate the secondary metabolites from the fractions obtained;
- Characterise the secondary metabolites obtained;
- Carry out hemi-synthesis on promising compounds;
- Evaluate the antiplasmodial activities of extracts, fractions and compounds derivatives obtained;

This thesis, which summarizes the essential of our work, has three main parts: the first covers the bibliographic study with a brief overview on malarial and a brief botanical description as well as the previous chemical and biological works on the studied plants: the second gives the results and discussions, and third part gives the various experimental procedures used and applied following by the bibliography.

CHAPTER I

LITERATURE REVIEW

I-1-Malaria

Malaria is a parasitic disease caused by a protozoan of the genus *Plasmodium*. Nowadays, despite the significant progress in the area of drug research, malaria is one of the major causes of death and the most dangerous parasitic infection in Africa. As a result of this, the search for new antimalarial drugs is imperative and probably one of the greatest public health challenges facing humanity (**Gontijo et *al*., 2019**).

I-1-1-Epidemiology

Despite several attempts to reduce the spread of this desease, many people around the world keep dying. It is reported that in 2018, 228 million people were infected among which 213 million in Africa (93%) leading to approximately 405,000 deaths (**WHO, 2019**). Five species of the single-celled protozoan parasite *Plasmodium* can cause malaria in humans: *P. falciparum*, *P. vivax*, *P. ovale*, *P. knowlesi* and *P. malaria*. Of these, *P. falciparum* with Chroquine-resistant (Dd2) and Chloroquine sensitive (3D7) strains are dominant in Africa. It is the deadliest and is responsible for approximately 90% of malaria deaths cases per year. However, it has been estimated that many people worldwide live at risk from *P. vivax* than *P. falciparum* and as a result suffer increased morbidity from *P. vivax*.

- **The *Plasmodium* parasite life cycle**

The *Plasmodium* parasite has a complex life cycle characterized by alternating extracellular and intracellular forms, involving sexual reproduction in the mosquito and asexual reproduction in the liver cells and RBCs of humans (see Scheme1) **(Minodier et *al*., 2011)**. The parasite enters the human body when an infected mosquito takes a blood meal. Sporozoites from the mosquito's salivary glands are injected into the host's bloodstream. Within 30 minutes, the sporozoites enter the host's liver cells. The sporozoites feed on the cell contents, grow and change to form schizonts. Over the next 5–8 days, they divide rapidly, forming thousands of merozoites. The liver cells balloon and burst, releasing merozoites into the bloodstream where they invade the RBCs. While the parasite is within the liver, the person does not feel sick and shows no signs or symptoms of the disease. *P. vivax* and *P. ovale* can have a dormant stage in the liver called hypnozoites. These can remain in the liver for several years, causing relapses in later life. While in the liver and the RBCs, the parasite is protected from the host's antibodies. Inside the RBCs the individual merozoites develop into trophozoites and finally into schizonts which contain up to 32 distinct merozoites, depending upon the species of Plasmodium. After 2–3 days, the RBCs rupture, releasing the merozoites

back into the bloodstream. These merozoites go on to invade uninfected RBCs and the cycle continues. As the RBC ruptures toxins are released from the merozoites **(Minodier et *al*., 2011)**.

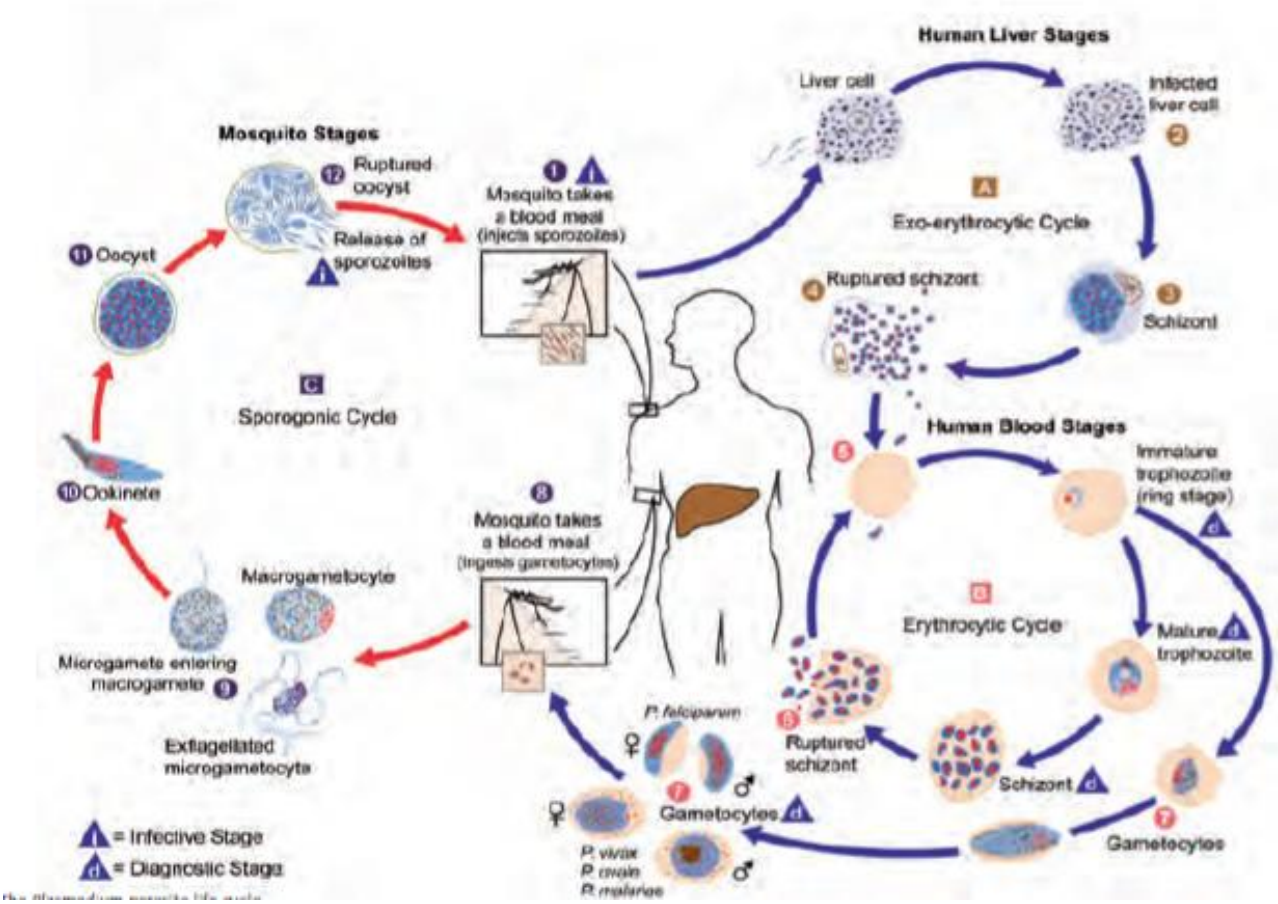

Scheme 1 : The *Plasmodium* parasite life cycle

- **Symptom and diagnosis of Malaria**

Malaria is diagnosed by clinical symptoms, microscopic examination of the blood or rapid diagnostic tests (RDTs). RDTs use blood from a pinprick to identify infection based on the presence of antigens. Fever, headache, chills and vomiting the classic flu-like symptoms of malaria appear around 9–14 days after the initial mosquito bite. The time differs according to the species of *Plasmodium*. WHO currently recommends that all cases of suspected malaria should be confirmed before starting treatment. Currently, approximately 35% of cases in Africa are confirmed using a RDT. Malaria may lead to anemia and jaundice because RBCs are destroyed faster than they can be replaced; severe anemia is the leading cause of death in children with malaria. Blood transfusions can be used to treat anemia, but in areas where AIDS is endemic, this exposes the patient to the risk of infection with HIV. Cerebral malaria

may arise after infection with *P. falciparum*. It is characterized by coma and convulsions, and often results in death. 10–20% of children with cerebral malaria die and around 7% of those that survive are left permanently brain damaged **(Casalino, 2004).**

I-1-2- Malaria treatment

Malaria can normally be treated with antimalarial drugs. The type of drugs and duration of treatment depend on the type of malaria diagnosed, place of infection, age of the patient and severity of disease. Travelers visiting endemic areas can take antimalarial drugs to prevent infection. Depending on the type of drug prescribed, it can be taken even up to 2 weeks before travelling. Artemisinin-based combination therapies (ACTs) are now the standard treatment for malaria. These therapies combine artemisinin or one of its derivatives with another antimalarial drug **(WHO, 2017).** Current recommended drugs are:

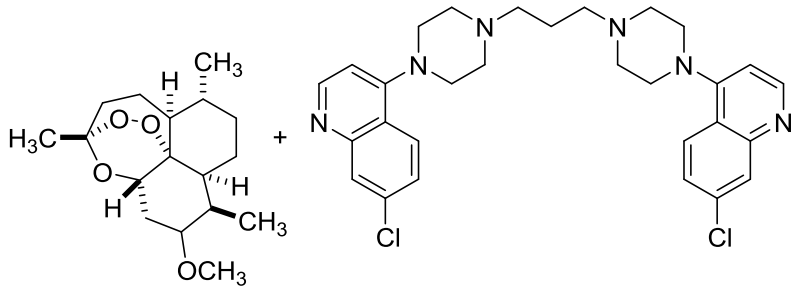

1

Artemether and Piperaquin

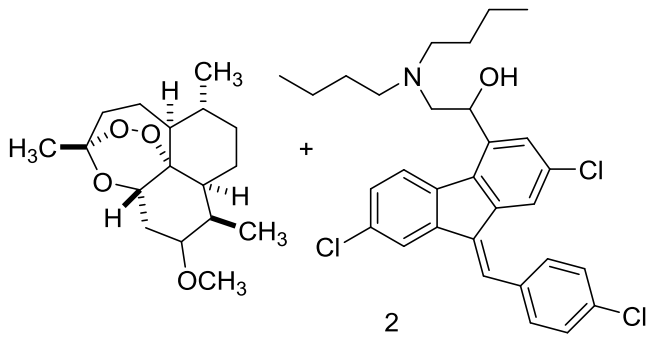

2

Artemether and Lumefantrine

The continuous spread of *Plasmodium falciparum* resistance to antimalarial drugs poses a serious threat to malaria. The ever increasing number of differents mechanism of resistance, urges the development of novel antimalarial agents. The high cost of malaria treatment has compelled low income individuals to rely on traditional practitioners and medicinal plants for treatment **(WHO, 2017).**

I.1.2.1 Resistance

It is the ability of a parasite strain to survive and/or multiply despite the administration and absorption of a drug in doses equal to or higher than those usually recommended but within the limits of tolerance of the subject.

- **Resistance of antimalarial drugs**

a) Chloroquine

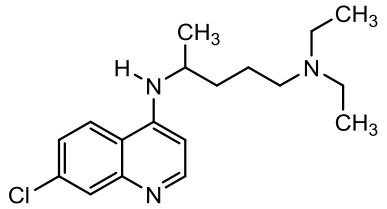

Since its development in the 1940s, the high efficacy, good tolerance, chemical stability, low cost , ease of chemical stability and ease of production have contributed to making chloroquine (CQ) the most widely used antimalarial drug in the world. However, resistance to CQ in *P. falciparum* was first detected in 1957 on the Cambodia-Thailand and Colombia-Venezuela borders (**Payne, 1987**). Genetic analyses later demonstrated the existence of at least 4 different outbreaks of chloroquine resistance emergence: one in Asia that then spread to Africa, one in Papua New Guinea, and two in South America (**Wootton et *al*., 2002**); Chloroquine resistance then spread to other countries in Asia and, over the next 30 years, to Africa (1st documented case in the East in 1977 (**Fogh et *al*., 1979**) with catastrophic consequences. By 1989, chloroquine resistance had spread throughout sub-Saharan Africa (**Payne, 1987**). Today, *P. falciparum* resistance to CQ is present in all malaria-endemic countries except for a few countries in Central America and the Caribbean (**WHO, 2014**). Although the emergence of *P. falciparum* resistance to CQ has forced malaria-endemic countries to abandon this molecule, CQ is still recommended for malaria caused by non-*falciparum Plasmodium* species. However, the emergence of *P. vivax* resistance to CQ in Papua New Guinea and later in South America; also limits its use, ACT being recommended in these countries (**Rieckmann et *al*., 1989**).

b) Artemisinin

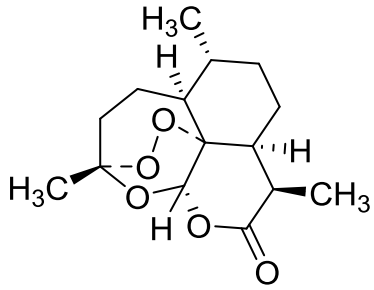

The discovery of artemisinin by Professor Youyou Tu's team in the 1970s is one of the greatest advances in medicine of the 20th century that was awarded the Nobel Prize in Medicine in 2015. The chemical structure of artemisinin was obtained in 1976 (**Zhang, 2005**), which allows the development of semi-synthetic derivatives (artemether, artesunate (AS) in 1987, dihydroartemisinin (DHA) in 1992). Outside of China, these compounds remained unknown for a long time. However, faced with the spread of resistance to all available antimalarial drugs in South-East Asia, these molecules have been the subject of clinical studies demonstrating their very good efficacy and tolerability.

Since the early 1980s, the effect of artemisinin-based monotherapy combined with a partner molecule has been studied in order to reduce treatment time and costs, but also partner molecule was studied in order to reduce treatment time and costs, but also to limit the risk to limit the risk of resistance development. Artemisinin allows to strongly reduce the parasite load in the first 3 days of treatment while the partner molecule eliminates the remaining parasites. The WHO has recommended the use of ACTs (Artemisinin-based Combination Therapies) in the treatment of uncomplicated malaria in 2001. In the following years, the majority of endemic countries have adopted ACTs, with the number of ACT treatments delivered increasing from 11 million in 2005 to over 300 million in 2015 (**WHO, 2017**).

Unfortunately, the first cases of resistance were reported in 2008 (**Noedl et *al*., 2008**). *P. falciparum* resistance to artemisinin is currently detected in five countries in the of the Greater Mekong Subregion: Cambodia, Myanmar, Lao PDR, Thailand and People's Democratic Republic of Laos, Thailand and Vietnam (**Amaratunga et *al*., 2012)**.

Resistance to ART is characterized by a higher treatment failure rate and slowed parasite clearance (**Ashley et *al*., 2014**) with no change in susceptibility to DHA as assessed by standard growth inhibition methods (**Amaratunga et *al*., 2012**). In the majority of cases, patients respond well to treatment with an effective partner molecule. However, at the Cambodia-Thailand border, parasites have become resistant to almost all available antimalarial drugs

Containing resistance to ARTs and preventing its spread to other countries, particularly in Africa where parasite endemicity is highest, is a major public health priority today, as no other antimalarial drug of the same efficacy and tolerance is currently available. Recommendations have been published in this sense in 2011 (GPARC: Global Action Plan for Artemisinin Resistance Containment). Regular monitoring of the status of resistance in malaria-endemic countries is an essential prerequisite for developing strategies to better prevent its spread.

I.1.2.2. Mechanism of resistance

Numerous mechanisms of resistance to antimalarial drugs coexist within the different organelles of the parasite (**Blasco** et ***al.*, 2017**). In general, three types of mechanisms are involved in resistance:

The biological target of the antimalarial drug may be altered. Certain mutations in key players of the parasite key players in parasite metabolism can confer resistance to one or more antimalarial drugs. This is the case, for example, for resistance to SP (Sulfadoxine-pyriméthamine), acquired by point mutations in the genes coding for the DHFR (Dihydrofolate Reductase Inhibitors) and DHPS (Dihydropteroate Synthase Inhibitors Enzymes). The acquisition of resistance by modification of the target generally occurs rapidly (**Sibley et *al.*, 2001**)

Resistance can also be acquired by limiting the concentration of antimalarial drugs in the parasite. This mechanism is mainly generated by the modification of transporters allowing the entry or exit of antimalarial molecules into or out of the digestive vacuole of the parasite. For example, mutations in the Pfcrt gene, coding for the PfCRT (Choroquine resistance transporter) transporter, allow inhibit the accumulation of 4-aminoquinolines such as CQ and PPQ (Pipéraquine) in the digestive vacuole. Polymorphisms in the Mdr1 (Multi-drug resistance) gene, which codes for the PGH1 (P-glycoprotein homolog 1) glycoprotein, also affect CQ and AQ (Amodiaquine), concentrations, and concentrations of CQ and AQ, MQ (Méfloquine) and LM (Luméfantrine) of the parasite in the digestive vacuole (**Sibley et *al.*, 2001**). Finally, resistance can be conferred to the parasite via a mechanism of detoxification or repair. The modification of parasite proteins involved in the management of oxidative stress, or in DNA repair and malformed proteins is notably involved in ART resistance (**Sibley et *al.*, 2001**).

I.I.3 Fight against malaria

Malaria has been recognized as a priority public health problem since the mid 19th century. In 2018, $2.7 billion was invested in the fight against malaria (**W H O, 2019**). In response, many global control strategies have been put in place. The latest was developed in 2015 and covers the period 2016-2030 (**W H O, 2015**) It involves various partners such as: governments of endemic countries, research institutes, health research institutes, health professionals, and funders such as the Global Fund. To reduce the number of malaria cases and deaths by 90% by 2030, eliminate malaria 2030, to eliminate malaria in at least 35 countries and to prevent the re-emergence of the disease in countries where it has been eliminated. Its strategy is essentially based on the fight against anopheles, and patient

management combining reliable diagnosis followed by effective drug treatments to fight the parasites.

- **Vector control**

Vector control consists to fight vector to limit human/vector contact. The main methods used are: the use of long-lasting insecticide-impregnated nets (LLINs) and indoor residual spraying (IRS) of mosquitoes with insecticidal insecticide (LLINs) and indoor residual spraying (IRS) of mosquitoes with insecticidal and/or insecticide. Other control methods can be used in addition, such as elimination of breeding sites or personal protection against mosquito bites. During the 20th century, the insecticide Dichloro-diphenyl-trichloroethane (DDT), belonging to the organochlorine class, has been used for a long time in IRS. This product was originally intended for agricultural against crop pests (**Roberts et *al.*, 2013**).

The discovery of its action against mosquitoes led to its massive use and gave hope for the eradication of malaria in the 1950s (**Nájera et *al.*, 2011**). DDT has shown good efficacy and has saved nearly a billion lives (**Roberts et *al.*, 2013**). However, its widespread use has selected resistant vectors. Since then, pyrethroids, organophosphates carbamates, or organochlorines have been used. Vector control has made it possible to reduce the number of cases of malaria, but resistance to insecticides regularly threatens the progress made. Resistance is generally hereditary which results in an increase over generations of the resistant vector population (National Vector Expertise Center 2014). It is measured at the phenotypic level using standardized procedures that involve exposing mosquitoes to standard doses of insecticides and then assess their mortality. WHO defines insecticide resistance as the ability of mosquitoes to survive a standard dose due to physiological or behavioral adaptation (**W H O, 2018**).

To survive, they develop different mechanisms (**W H O, 2018**):

- Metabolic resistance, which corresponds to enzymatic actions that allow to break down or block the insecticide,
- Resistance by modification of the target which corresponds to genetic mutations initially present in the population that lead to changes in the receptors. Insecticides are not responsible for the appearance of these mutations (absence of mutagenic effect) but only for the selection of individuals that carry them (National Vector Expertise Center 2014).
- Cuticular resistance, which reduces the absorption of the molecule at the cuticle level,
- Behavioral resistance, which limits mosquito/treated surface contact.

Resistance (mortality <90% with standard tests) is now confirmed in all major malaria vector species and for the four classes of insecticides available, pyrethroids, organophosphates,

carbamates, and organochlorines (**WH O, 2018**). Despite this, IRS and LLINs are still widely deployed and sometimes show their effectiveness.

In order to limit the appearance of resistance to insecticides but also the impact on the environment, it is essential to have an adapted and reasoned use of these molecules. From new insecticides such as neonicotinoids and pyrroles are being developed (**W H O, 2018**).

- **Vaccines**

The development of a vaccine is essential in the fight against a disease. In many cases, it makes it possible to make significant progress in terms of mortality, or even to eradicate it. In the case of malaria, this development is long and delicate due to the important diversity and plasticity of the targeted parasite. Several vaccines acting on different parasitic stages (hepatic, erythrocytic, asexual, or sexual) are currently in clinical trials to control *P. falciparum* and *P. vivax* (**Draper et *al*. 2018**). After more than 30 years of research, the RTS, S vaccine is the most promising. It targets *P. falciparum* sporozoites and is the only vaccine to have shown effective protection in children under the age of five. It has been validated by the WHO and is being tested since April, May, and September 2019 in Malawi, Ghana, and Kenya, respectively (**W H O, 2019**). Another very promising vaccine, PfSPZ, which can provide effective protection against the disease will be tested in people aged 2 to 50 years soon on the island of Bioko in Africa (Butler 2019). If validated, these vaccines could save tens of thousands of lives.

- **Antimalarial drugs**

In the absence of an effective vaccine against malaria, antimalarial drugs, along with insecticides remain an essential component in the fight against the disease in humans. Antimalarials have been used for centuries and have consistently reduced the mortality and transmission of malaria worldwide. The first ones to exist and those currently most recommended are of natural origin, initially used in traditional medicine to treat cases of fever (**Meshnick and Dobson 2001**).

These natural molecules were then joined by synthetic chemical compounds. The antimalarial drugs currently in use fall into therapeutic classes (**Mishra et *al.*, 2017**): derivatives of quinolines (e.g.quinine, chloroquine), antifolates (e.g.proguanil, sulfadoxine), and naphthoquinones (e.g.naphthoquinones (e.g.atovaquone), artemisinin derivatives (e.g. artesunate, artemether) and antibiotics (e.g. tetracycline, doxycycline).

- **Quinoline derivatives**

The first compound to be used in this class of antimalarials was quinine. This molecule of natural origin was isolated in 1820 by two French chemists, Pierre Pelletier and Joseph Caventou (**Meshnick and Dobson, 2001**). It was extracted from the bark of trees native to the Andes, the Cinchona such as *Cinchona pubescens* (red cinchona) and *Cinchona calisaya* (yellow cinchona). This bark was used by the indigenous people of South America to treat fever. It was introduced in Europe at the beginning of the 17th century where it was called "Jesuit powder." During the 19th century, quinine was the standard treatment for malarial fevers. Because of its delicacy of use and the side effects it causes, quinine is now recommended as a second-line treatment for severe cases (World Health treatment for severe cases (**W H O, 2015**) It is usually used in combination with a tetracycline (most often doxycyline). It is also one of the treatments for uncomplicated *P. falciparum* infections in pregnant women during the first six months of pregnancy, along with atovaquone/proguanil. Despite its ancestral use, the first resistance appeared in the early 20th century in Brazil (**Da Silva and Benchimol 2014**).To date, it is the least widespread resistance on the surface of the globe (**Okombo et *al.*, 2011**).

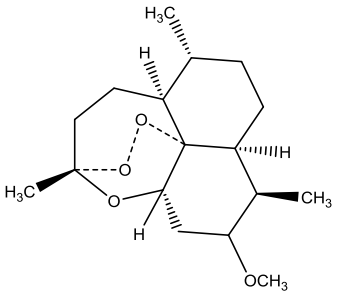

Arthemether

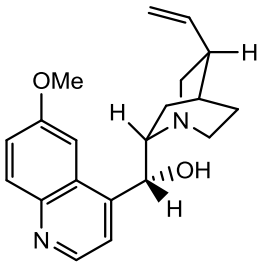

Quinin

- **Antifolates**

The first antifolates were also developed during the Second World War. To this class belong, proguanil, pyrimethamine, and sulfadoxine (**Mishra et *al.*, 2017**). The proguanil is used in combination with atovaquone belonging to the class of naphthoquinones. Sulfadoxine is used in combination with pyrimethamine. The loss of chloroquine's effectiveness led to the use of sulfadoxine/pyrimethamine as an alternative in the 1970s (**Meshnick and Dobson, 2001**). However, resistance to this combination therapy was very quickly selected. It first appeared in South-East Asia and Cambodia-Thailand border and then in South America, resistance then spread to Africa spread to Africa following the same path as chloroquine resistance a few years earlier (**Achan et *al.*, 2018**).

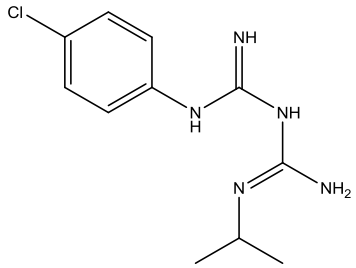

Proguanil

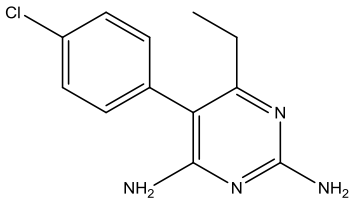

Pyrimethamine

- **Naphthoquinones**

Atovaquone is used in dual therapy with proguanil. This combination therapy (Malarone TM) is currently used for prophylaxis or to treat uncomplicated *P. falciparum* in travelers returning from endemic (**W H O, 2015**). It is not recommended in endemic areas because the selection of atovaquone-resistant parasites is very rapid (**Cottrell et *al.*, 2014**).

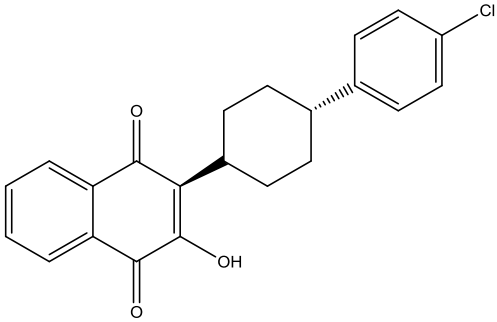

Atovaquone

- **Antibiotics**

Some antibiotics such as doxycycline, tetracycline, clindamycin or azithromycin also have antimalarial activities (**Mishra et *al.*, 2017**). They can be used as prophylaxis or curative treatment as monotherapy or dual therapy (**W H O, 2015**). In addition to tetracyclines and macrolides, new families of antibiotics are being identified (e.g., tigecyclines, thiopeptides) and are in clinical development (**Gaillard et *al.*, 2016**). Antibiotics have different modes of action than the antimalarial drugs mentioned above. They have the advantage of not having cross-resistance, which makes them good partners for the development of new therapeutic combinations.

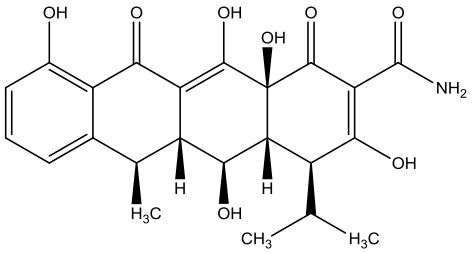

Doxycycline

- **Plants in the fight against malaria**

Medicinal plants are valuable sources of bioactive secondary metabolites for innovation on malaria chemotherapy (**Gupta et *al*., 2009**).With respect to this, plants of genus *Sida* (Malvaceae) have been widely used by indigenous communities as a food and for the treatment of gonorrhoea, piles, rheumatism, gastrointestinal infections, varicella, variola, and malaria (**Gupta et *al*., 2009**).The predominant plant species used in traditional medicine for the treatment of malaria infections as reported by **Bandeira et *al*., 2001** are *Acacia karroo Hayne*, Acacia *nilotica, Senna abbreviata, Adansonia digitata, Alepidea amatymbica, Bridelia cathartica, Crossopteryx febrifuga, Euclea natalensis, Lippia javanica, Momordica balsamina, Rauwolfia caffra, Salacia kraussii, Senna occidentalis, Spirostachys africana, Tabenaemontana ele-gans, Trichilia emetic* and *Zanthoxylum capense***.**

Results presented by Ramalhete and collaborators in 2008, on plant material collected in Mozambique, showed significant antiplasmodial activity. The ethyl acetate extract from aerial parts of *M. balsamina* has an activity value of (1.0 µg/mL) and 19.3 µg/mL for the hexane extract from leaves of *S. occidentalis*. The ethanol extracts of the leaves of *S. occidentalis* showed high *in vitro* antimalarial activity against a *P. falciparum* CQ-sensitive strain (< 3 µg/mL) (**Tona et *al*., 2004**). Interesting *in vitro* antimalarial activity was also revealed by Jurg *et al*. 1991 from the ethanol and aqueous root and stem bark extract of *B. cathartica* at a concentration of 0.05 µg/mL. Moreover, the *in vitro* antimalarial activity of methanol and alkaloid-rich extracts of *C. febrifuga* showed that this plant could be a promising source of malaria treatment (**Sanon et *al*., 2003**). This was confirmed in subsequent *in vivo* assays. The ethanol stem bark extract of *C. febrifuga* was investigated against malaria infections *in vivo* and the eradication of parasitaemia at the highest dose (400 mg/kg) was similar to CQ at 5 mg/kg and pyrimethamine at 1.2 mg/kg (**Elufioye and Agbedahunsi 2004**).

Some plants have shown *in vitro* antiplasmodial activities with possibilities of establishing new antimalarial drugs. For example work on antimalarial plants from Burkina Faso by Sanon and collaborators in 2003, showed good antiplasmodial activity of alkaloids isolated from *Pavetta crassipes* and *Achanthospermum hispidum*. Similarly, extracts of *Nauclea latifolia* and *Gadenia sokotensis* have been very active against *Plasmodium* strains (**Banzouzi et *al*., 2004**).

Natural products come with a great variety of chemical structures and some have been screened for antiplasmodial activity as potential sources of new antimalarial drugs examples of which are:

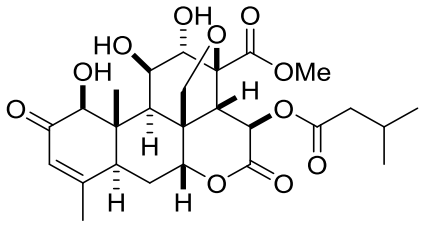

3

Isobrucein A (IC_{50} = 0.05 µM, 3D7)

3D7 sensitive strains

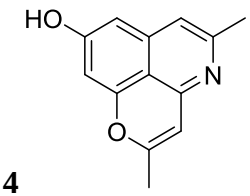

4

Cassiarin A (IC_{50} = 0.02 µM, K1)

K1 Resistanse strains

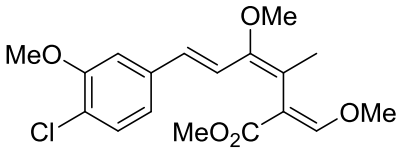

5

Strobilurins (IC_{50} 0.06 µM, K1)

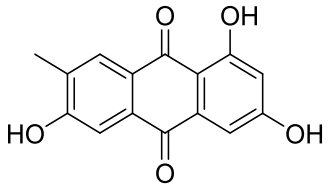

6

Methylmacrosporine (IC_{50} = 0.3 µM, K1)

I-2-Botanical aspect of Malvaceae and Clusiacaea famillies

I-2-1- Botanical aspect of Malvaceae

Malvaceae is a family of flowering plants estimated to contain 243 genera with more than 4225 species including *Abutilon*, *Urena*, *Pavonia*, *Kydia*, *Decaschistia*, *Hibiscus*, *Bombax*, *Eriodendron*, *Thespesia*, *Cullenia*are and *Sida* **(Vadivel, 2016)**. The phytoconstituents present in the plant extracts (*Abutilum indicum*, *Hibiscus sabdariffa*, *Sida acuta*, and *Sida rhombifolia*) belong to categories such as flavonoids, phenolics, acids, and polysaccharides. Phytoconstituents are naturally occurring chemical compounds, responsible for the color, odor, and therapeutic potential of plants (**De Lima et *al*., 2021**). These therapeutic properties include anticancer agents, antioxidant, antifungic, anticonvulsant, antiseptic, aphrodisiac, astringent, cholagogue, demulcent, digestive, purgative, resolvent, anthelmintic, and antiulcerogenic activities (**De Lima et *al*., 2021**).

I-2-2 Botanical aspect of Genus *Sida*

Plants of the genus *Sida* are annual or perennial herbs. They are shrubs of 0.5–2.0 m high. The leaves of the plants are simple, narrowly ovate and the flowers are solitary or paired. Fruits have 5-carpels with slender mericarps and relatively large calyces that enclose

and conceal the fruits (**Dinda et *al.*, 2015**). The table1 below shows different species of the genus *Sida* identified in Africa.

Table 1. **Some species of the genus *Sida* identified in Africa**

Species	**Countries**	**References**
S. acuta	Burundi, DR Congo Congo, Egypt, Gabon, Ghana, Kenya Cameroon,	(**Forno et *al.*, 1992**)
S. cordifolia	Angola, Benin, Botswana, Burkina, Faso, Burundi, Cameroon	(**Dinda et *al.*, 2015**)
S. rhombifolia	Angola, Botswana, Cameroon,	(**Dinda et *al.*, 2015**)

Our research work was focused on *Sida acuta* and *Sida rhombifolia*.

I-2-3 Botanical aspect of *Sida rombifolia* and *Sida acuta*

Sida rhombifolia. Linné. C *is* a small erect woody, and perennial shrub of about 1.5 m high with rough branches and stellate hairs. Leaves vary in shape up to 5 mm by 18 mm, short petioled, rhomboid-lanceolate (**Kumar et *al.*, 2011**). Flowers are yellow or white, axillary, solitary or in pairs. The fruits are depressed enclosed within the calyx, separating into one-seeded unit. The seeds are black and smooth **(Kumar et *al.*, 2011).**

Sida acuta Burm.f is a small perennial herb which is erected, branched or shrub of about 1.5 m in height **(Sreedevi et *al.*, 2009)**. The bark is smooth and greenish. The root is thin, long, cylindrical and very rough. The leaves are lanceolate. The flowers are yellow, solitary or in pairs. Seeds are smooth and black. It grows abundantly on cultivated fields, waste areas and roadsides in Cameroon and is called "sengh". Its common name is sida. The plant can be propagated both by seed and stem cuttings (**Sreedevi et *al.*, 2009**).

(a) Whole plant of *Sida rhombifolia* -collected in February 2017 at Bangangte by Mr. KAMDOUM

(b) Whole plant of *Sida acuta* collected in September 2017 at Ebolowa by Mr. KAMDOUM

I-2-4 Ethnobotanical use of the genus *Sida*

This section presents the ethnobotanical description of the family Malvaceae. It encompasses folk medicine use of *Sida rhombifolia*, *Sida acuta* and some plants of the genus *Sida*.

Table 2: Ethnobotanical use of *Sida*

Species	Plant part used	Ethnomedicinal Use	Country	Mode of preparation	References
S.acuta	Leaf	Wound	Nigeria	Decoction of leaves	**(Adetutu et *al.*, 2011)**
	Leaf	Dandruff	India	Leaf juice is mixed with coconut oil and applied on head	**(Silja et *al.*, 2008)**
	Root	Rheumatism, breathing problems	India	Decoction of freshroots	
	Root	Dysentery	Papua New Guinea	Fresh root is chewed	**(Holdsworth and Lacanienta 1981)**
	Root	Nervous disorders	India	N/S	**(Reddy et *al.*, 2017)**
S. veronicifolia (= *S. cordata*)	Whole plant	Pregnancy and childbirth complaints to shorten and reduce the labour pain	Cameroon, Ghana	Maceration orally for 6 months	(**Yemele et *al.*, 2015**)
	Leaf	Diarrhea	India	Juice	(**Asif et *al.*, 2019**)
	Leaf	Cuts and bruises	India	Poultice	
	Root bark	Leucorrhea and Genito urinary-treck infections	India	N/S	
S. cordata	Leaf	Boils	India	Paste of leaves is topically	(**Adhikari et *al.*, 2010a**)

				applied	
	Root	Boils or abscesses	India	Root paste is topically applied on boils	
		Severe fever, liver disease and body pain	Thailand	Decoction orally	(**Abat et *al.*, 2017**)
S. alnifolia	Root	Abortion	India	N/S	(**Dinda, et *al.*, 2015**)
S. glutinosa (= *S. mysorensis*)	Whole plant	Tuberculosis and rheumatism	India	N/S	
	Whole plant	Asthma and other chest ailments	India	N/S	(**Sobreira, 2019**)
S. rhombifolia	Root	Antivenom	India	N/S	(**Dinda, et *al.*, 2015**)
	Root	Boils or abscesses	India	Root paste is applied on boils	(**Adhikari et *al.*, 2010**)
	Root	Tuberculosis and malaria	India	Decoction	(**Girach et *al.* 1994**)
	Root	Dysentery, diarrhoea and indigestion	Australia, Cameroon, Papua New Guinea	Root infusion orally	(**Noumi and Yomi 2001**)

N/S : not stated

I-2-4-1 Botanical aspect of Clusiaceae

Also known by the name Guttiferae, the Clusiaceae constitute a family of about 1340 species divided into 47 genera, mostly in tropical regions and temperate regions; it is one of the most important families of Spermaphytes (**Aubreville, 1959**). The Trees, shrubs, grasses and rarely lianas are generally hairless, sometimes unduly stellate hairs and are easily recognized due to the yellow or orange resinous latex which drains, often slowly from the wound of bark, flowers, fruits, more difficult for twigs and leaves (**Bamps, 1970**). The wood is hard, shaped with medium-sized pores whose rays are clearly visible (**Busson, 1965**).

From the point of view of the general classification of Guttiferaceae, it seems that the genera represented in Cameroon can be grouped together in natural divisions (**Hutchinson, 1972**). Among the most widespread genera in Cameroon, we can cite among others: *Allanblackia, Mammea, Vismia, Calophyllum, Hypericum, Pentadesma, Bonnetia, Kielmyera, Garcinia, Platonia Rheedia, Symphonia* and *Pentadesma*.

Clusiaceae are easily distinguished by the yellow resinous latex that drains from the gash in bark, twigs or petioles. Some species are rather rare and grow outside the forest, especially in the savannah or often at the edge of rivers (**Guedje et *al.*, 2000**).

I-2-4-2 Botanical aspect of *Garcinia genus*

Plants of this genus are often refered as the monkey fruit. The trees are ever green and the shrubs dioecious (**Wong, 2008**).

They have an edible fruit, and some are used for food supply source depending on the location. This is the case of *G.mangostana*, which is now cultivated throughout South of Asia and other tropical countries and *G.forbesii* with its small round red fruits with an acid taste and tender flesh. *Garcinia* are also known for their resin in the form of yellow-brownish gum (**Wong, 2008**).

Table 3 : Geographical distribution of some species of the genus *Garcinia* in Cameroon

N°	Species	Aspect	Geographical distribution
1	*G. smeatmannii*	Tree	Nkambé, Bafoussam, Bamenda, Eseka, Foumban
2	*G.punctata*	Small tree	Banyo, Foumban, Yaoundé, Kribi, Bafia, Ebolowa, Sangmélima
3	*G. polyantha*	Shrub	Nkambé, Kumba, AbongMbang, Yaoundé
4	*G. lucida*	Tree	Manfé, Akonolinga, Mfou, Yaoundé, Kribi, Ebolowa
5	*G. ovalifolia*	Shrub	Guider, Tibati, Kribi, Bertoua, Nanga-Eboko
6	*G. barteri*	Shrub	Ngaoundéré, Tcholiré
7	*G. epunctata*	Small tree	Banyo, Foumban, Kribi, akwaya
9	*G.kola*	Big tree	Manfé, Mfou, Batouri, Yaoundé
10	*G. manii*	Small tree	Tignère, Kribi, Matom, Mfou, Douala
11	*G. conrauna*	Small tree	Manfé, Bafang, Eseka

Among these species we focused on *Garcinia Ovalifolia*

I-2-4-3 Garcinia ovalifolia

G. ovalifolia whose height ranges between 10– 19 m has a yellow sticky latex and generally is distributed in 20 fringing forests and riverbanks in West and central Africa (**Pieme et *al.*, 2015**).

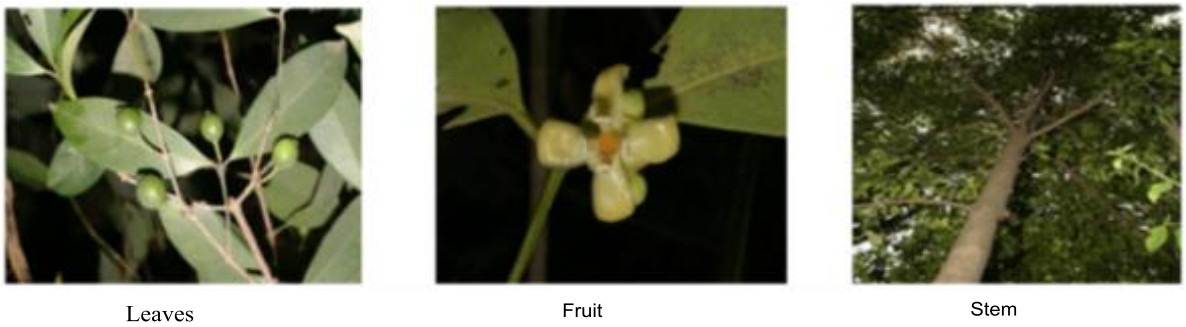

Figure 1: Different parts of *Garcinia ovalifolia* (Photo Kamdoum, May 2018 at Mont-Kala, Centre region of Cameroon).

Garcinia are an important source of secondary metabolites. In the traditional pharmacopoeia and the Cameroonian diet, *G. kola, G. lucida and G. manii* are the most widely used species.

I-2-4-4 Uses of *Garcinia* genus.

- **Therapeutic use**

The genus *Garcinia* is made up of a group of medicinal plants with potential therapeutic agents. The different parts like the fruit, rind, flower, leaves, bark and stem have been globally used in the folk medicine to treat several disorders such as inflammation, oxidative stress, microbial infection, cancer, and obesity (**Padye et *al.*, 2009**).

In Cameroon, the seeds of *G. kola, G. polyantha* are used as an antidote to poison or venom. They are used for drugs production and these drugs can treat multiple gastrointestinal infections (**G. *lucida, G. kola***) and pulmonary ailments. They are also astringents *(G. kola*). Their pulp is consumed for the supply of minerals, vitamins and amino acids contained in these fruits, making them complementary supplementary foods, sometimes essential, during the lean season for local forest populations (**Guedje et *al.*, 2000**).

Polyantha's trunk sores exude a thick, sticky chrome yellow resin; this resin is used in Senegal by the populations for dressing of wounds. (**Bouquet, 1969**). *Garcinia punctata* Oliv is used in the Boko region (Congo Brazzaville) to treat rib pain and coughs; the juice of the barks or their aqueous decoction is taken as a drink, while the preparation of the juice of the leaves with the addition of hunting powder and charcoal of *Schwenkia americana* and *Dichrostachys glomerata* is applied for after epidermal scarification. The bark powder is used to treat snake bites (**Bouquet, 1969**).

The oral aqueous decoction bark of the trunk of *G. kola*, is used for the treatment of high blood pressure. Likewise, the leaves are generally used for the treatment of gastrointestinal and lungs infections. The seeds consumed with palm wine would cleanse the stomach and above all would be aphrodisiac (**Bouquet, 1969**).

Epunctata Stapf is used in Congo (Brazzaville) for the treatment of stomach pain (**Bouquet, 1969**).

- **Other uses of *Garcinia* genus**

The economic benefit of *Garcinia* wood is very low, because inspite of their hardness, these woods are quite alterable; on the other hand, they are resistant to termites. They are not

only used by the populations in the construction of canoes and bridges but also in the making of works of art and decoration (**Normand, 1955**).

In Cameroon, the seeds of *G. kola, G. lucida, G. Polyantha* are used as an additive in kola nut. The stem bark of *G. kola, G. lucida, G.mannii, G. klaineana* is commonly used for the fermentation of palm and / or raffia wine and for the distillation of these wines in traditional drinks (**Guedje et *al*., 2000**).

In South of Asia, *mangostana*, mango's tree, is an important source of food (**Burkill et *al*., 1966**).

I-3-Pharmacological overview of *Sida* and *Garcinia* genus

In view of their numerous uses in traditional medicine, several biological assay have been done to confirm the ethnopharmacological claim, as listed in the table below.

I-3-1- Pharmacological overview of *Sida genus*

Table 4 : Phamarcological uses of *Sida*

Species	Extract/Part	Biological Effects	References
S. acuta	Aqueous extract leaves	Laxative activity in Loperamide-Induced Constipated Rats	(**Chukwuemeka et *al.*, 2019**)
		Antibacterial activity against *Escherichia coli*	(**Senthilkumar et *al.*, 2019**)
	methanol extracts Whole plant	Prominent anti-bacterial activity against *Staphylococcous aureus*	(**Asha et *al.*, 2018**)
	Leaf Extract	Good antibacterial activity on *Pseudomonas aeruginosa* and *Candida albicans*	(**Nisha et *al.*, 2017**)
	Methanolic extract aerial part	. Good antibacterial activity.	(**Mathew et *al.*, 2017**)
	fungal endophytes stem	Significant antibacterial potential against *Staphylococcus aureus* and *Escherichia coli*. MIC in the range of 15.6-62.5 µg/mL	(**Murali et *al.*, 2017**)
	Chloroform extract whole plant	Significant cytotoxic effet against A-431 cell lines (human epidermoid carcinoma) with an inhibit cell growth by 50% (IC_{50}) of 375±0.00	(**Kanthal et *al.*, 2017**)
S. acuta	Ethanolic whole plant extracts	Significant results against *Trypanossoma cruzi* with an IC_{50} of 341.3 and 227 µg/mL	(**Thondawada et *al.*, 2016**)
	hexane and ethyl acetate Leaf	Good Hepatoprotective activity	(**Mgbemena et *al.*, 2015**)
	Leaves and aqueous extracts	Good antimicrobial activity on *Staphylococcus aureus, Escherichia coli* and *Candida albican*	(**Johnson et *al.*, 2014**)
S. rhombifolia	Ethanolic extract Aerial parts	Good acute toxicity in rats	(**Ramalho et *al.*, 2019**)
	Ethanolic leaf	Good acute toxicity in rats	(**Ukpanukpong et *al.*, 2019**)
	Ethanolic extract aerial parts	Significant Hepatoprotective activity	(**Gurjar and Pal 2021**)
	Ethanol extract leaves	Strong anti-diabetic properties.	(**Bati et *al.*, 2018**)
	Aqueous-ethanolic extracts leaves	Antibacterial activities against *Escherichia coli, Salmonella typhi* and *Staphylococcus aureus*	(**Debalke et *al.* 2018**)
	Ethanol extract root	Significant anti-inflammatory activity.	(**Tanumihardja et *al.*, 2016**)
	Aqueous Leaf	Synergistic Antibacterial Effect	

	Extracts	against *S. Pneumoniae and E. coli*	**(Desalegn and Andualem, 2014**)
S. rhombifolia	Ethyl acetate extract of Leaves and Roots	Good antitubercular activity against the Standard strain of *M.tuberculosis* H37RV and clinical isolate of *M.tuberculosis* resistant to S, H, R and E	(**Papitha et *al.*, 2013**)
	Ethanol leaves extract	Anti-Inflammatory activity	(**Martins et *al.*, 2017**)

Garcinia species are reported to have a range of biological activities including cytotoxicity antimicrobial, antifungal, antioxidant, antimalarial and HIV-1 protease inhibitory activity (**Anyango et *al.*, 2019**).

I-3-2- Pharmacological overview of *Garcinia* genus

Table 5 : Phamarcological uses of Garcinia

Species	Extract	Biological assay	References
G. brasiliensis	Ethanolic extract	Anti-inflammatory activity	(**Arwa et *al.*, 2015**)
G. brasiliensis	Hexane extract	Leishmania activity on extracellular (promastigote) and intracellular (amastigote)	(**Gontijo et *al.*, 2012**)
	Hydroalcoholic extract	Significant antiproliferative activities in breast neoplastic lines in animals	(**Subeki et *al.*, 2004**)
G. gardneriana	Hexane and chloroform extracts	Antioxidant activity	(**Jayaprakasha et *al.*, 2003**)
G. cambogia	Ethanolic extract	Significant hepatoprotective, cardioprotective, and hypoglycemic activities in the treatment of Long Evans rats with a daily dose of 1000 mg/kg for 21 days	(**Hung et *al.*, 2015**)
	methanolic extract	Antioxidant activity	(**Sarma et *al.*, 2016**)
	ethanolic extract	Antiobesity activities	(**Chen et *al.*, 1996**)

Previous phytochemical investigations on some species of the genus *Sida* led to the isolation of alkaloids, flavonoids, terpenoids, steroids, saponins, fatty acids and ceramides.

I-4-Previous chemical studies of *Sida* and *Garcinia* genus

I-4-1 Previous chemical studies of Genus *Sida*

I-4-1-1 Alkaloids

These are natural nitrogen containing organic compounds, more or less basic and endowed with distinct pharmacological properties at low doses. Most alkaloids are bio-genetically derived from C_4 (ornithrine) and C_5 (lysine) amino acids (**Bruneton, 1993**).

Examples of some alkaloids isolated from the genus *Sida*

Table 6 : Alkaloids isolated from the genus *Sida*

Structures and names	Plants	Activity	References
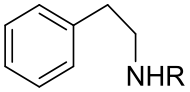 β -Phenethylamine **(7)** (**R=H**) *N*-Methyl-b-phenethylamine **(8)** (**R=Me**)	*S. acuta*		(**Jain et *al.*, 2011**).
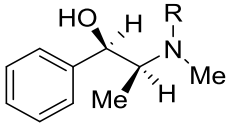 Ephedrine **(9)** (**R=H**) *N*-Methyl ephedrine **(10)** (**R=Me**)		Antidiabetic	
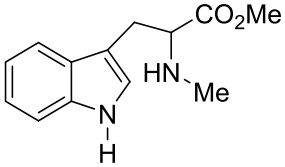 *S*-(+)-*Nb*-Methyltryptophan methyl ester **(11)**		Anti-inflammatory	**(Tanumihadja et *al.*, 2019)** (**Prakash et *al.*, 1981**)
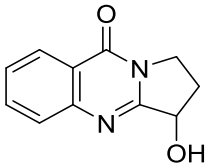 Vasicinone (**12**)		Antiproliferative	**(Dey et *al.*, 2018)**
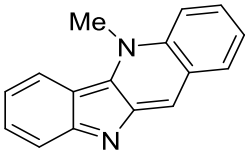 Cryptolepine (**13**)	*S. acuta*	Antibacterial	(**Banzouzi et *al.*, 2004**) (**Osafo et *al.*, 2017**)
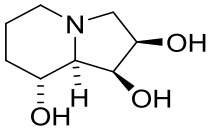 Swainsonine (**14**)	*S. carpinifolia*	Antidiabetic	(**Dorling et *al.*, 1983**) (**Colodel et *al.*, 2002**)

I-4-1-2 Flavonoids

Flavonoids are a group of natural products that play an important role in the growth, development and defense of the plant against the harmful effects of microorganisms (**Gonzalez and Rosazza 2004**). These compounds are responsible for the colouring of flowers, fruits and sometimes leaves (**Bruneton, 1993**). They are also important components in the human diet where they act as important antioxidants through free radicals scavenging of peroxides (**Gonzalez and Rosazza, 2004**). The basic skeleton has fifteen carbon atoms. They have a common biosynthetic origin and therefore have the same basic structural element, namely the C6-C3-C6 chain corresponding to diphenylpropane (**Bruneton, 1993**).

The table below shows some Flavonoids isolated from the genus *Sida*

Table 7 : Flavonoids isolated from the genus *Sida*

Structures and names	Plants	activity	References
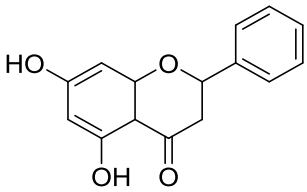 Chrysin(**15**)	*S. glutinosa*	Anticancer	(**Marques et *al.*, 2012**) **(Talebi et *al.*, 2021)**
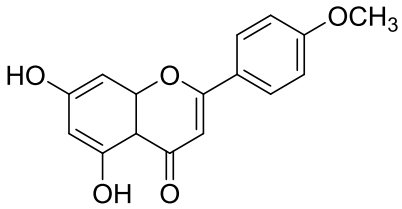 5,7-Dihydroxy-4'-methoxy flavone (**16**)	*S. rhombifolia*	Anticancer	**(Kim et *al.*, 2014)** (**Chaves et *al.*, 2020**)
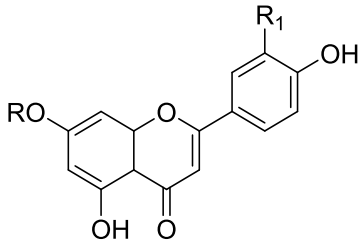 Apigenin R=H R1=H (**17**) Luteolin R=H R1=OH (**18**)	*S.galheirens*	Anticancer	**(KIM et *al.*, 2020)** (**Silva et *al.*, 2016**)

I-4-1-3 Steroids

Steroids are a group of lipids mostly derived from squalene. They are characterised by a partially or fully hydrophobic cyclopentanophenanthrenic ring. Plants produces many of them with a great structural diversity, including ecdysteroids and stigmastanes.

- On table 8 , Some Steroids are isolated from the genus Sida

Table 8 : Steroids isolated from the genus *Sida*

Structures and names	Plants	Activity	References
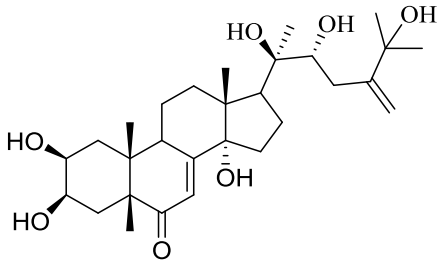 24-Dehydromakisterone A (**19**)	*S. glutinosa*	Antidiabetic	**(Lafont et *al*., 2003)** (**Das et *al*., 2014**)
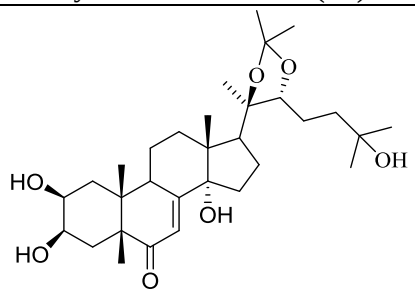 20-Hydroxyecdysone-20,22-(**20**) monoacetonide	*S. spinosa*	Anticancer	(**Darwish and Reinecke, 2003**) (**Das et *al*., 2021**)
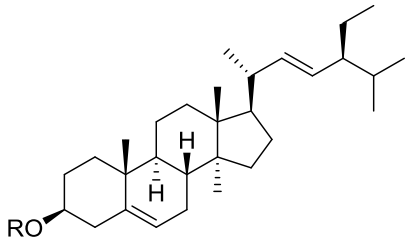 Stigmasterol (**21**) **R=H** Stigmasterol-3-*O*-*β*–D glucopyranoside (**22**) **R**=Glc	*S. rhombifolia*	Antidiabetic	**(Zeb et *al*., 2017)** **(Chaves et *al*., 2013**)

I-4-1-4 Terpenes

Terpenes are compounds made up of isoprene units 5- carbon atom units, often called, put together in a regular pattern, usually head-to-tail. They are a great importance for the cosmetic and good industries diverse and pharmaceutical and chemical industries.

Terpenoids have been quoted as the most diverse group of plants known compounds (**Goodwin and Mercer, 1983**).

- Some Terpenoids isolated from the genus *Sida* are listed on the table below

Table 9 : Terpenoids isolated from the genus *Sida*

Structures and names	Plants	Activity	References
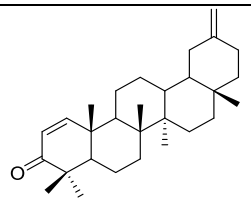 Taraxast-1,20(30)-dien-3-one (**23**)	*S. acuta*	Antioxydant	**(Aminah et *al*., 2021)**
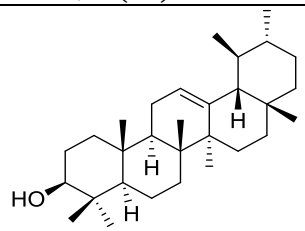 *α*-Amyrin (**24**)		Citotoxic	**(Neto et *al*., 2021)** (**Chen et *al*., 2007**)
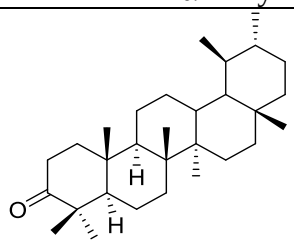 Taraxasterone (**25**)		Antioxydant	**(Aminah et *al*., 2021)**

I-4-1-5 α-tocopheroids

These are compounds related to tocopherols. Tocopherols are prenylated derivatives of benzodihydropyran. They are natural anti-oxidants that resist the oxidation of fatty acids.

Table 10 : Tocopheroids isolated from the genus *Sida*

Structures and names	Plants	Activity	References
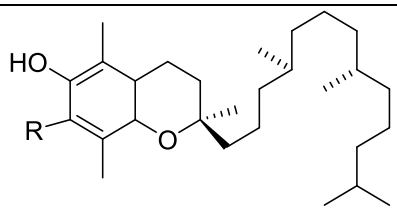 **α** -Tocopherol (**26**) R=Me 7-Methylmethoxy-a -tocopherol (**27**) R= CH_2OMe *β*-Tocopherol (**28**) R=H	*S. acuta*	Antioxydant	(**Chen et *al*., 2007**)
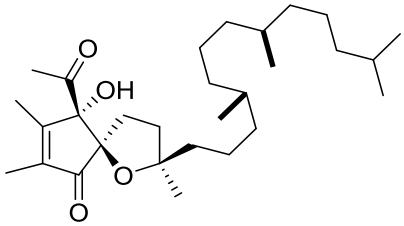 **α** -Tocospiro B (**29**)		Antioxydant	

I-4-1-6 Lignans

Lignans and neolignans are dimers of phenylpropane, and conventionally classified into three classes: lignans, neolignans, and oxyneolignans, based on the character of the C–C bond and Oxygen Bridge joining the two typical phenyl propane units that make up their general structures (**Teponno et *al.*, 2016**) as shown in the table 11.

Table 11 : Lignans isolated from the genus *Sida*

Structures and names	Plants	Activity	References
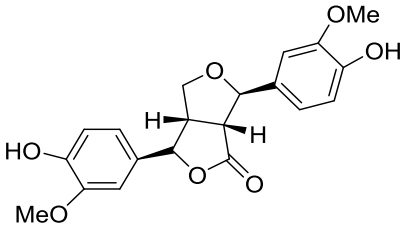 4-Ketopinoresinol (**30**)	*S. acuta*	Anticancer	**(Chen et *al.*, 2012)**
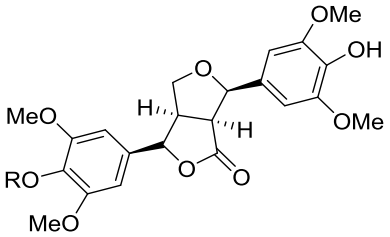 (±) Syringaresinol (**31) R=H** Acanthoside B (**32) R=Glc)**		Antioxydant	(**Chen et *al.*, 2007**) **(Karthivashan et *al.*, 2019)**

I-4-1-7- Coumarins

The word coumarin is derived from "coumarou", a South American vernacular name taken from *Dypteryx odorata*, also called tonga bean, from which the first coumarin was isolated in 1820. Coumarins are 2H-1-benzopyran-2-one which are lactones of *O*-hydroxy-2-cinnamic acids (**Bruneton, 1993**).

Table 12 : Coumarins isolated from the genus *Sida*

Structures and names	Plants	Activity	References
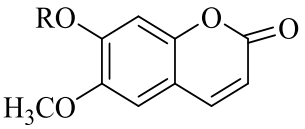 Scopoletin (**33**) **R=H** Scopoletin 7-*O*- -D-glucoside (**34**) **R**=Glc 6,7-Dimethoxy coumarin (**35**) **R**= Me	*S. acuta*	Anti-inflammatory	(**Yao et *al.*, 2012**) (**Jang et *al.*, 2003**)
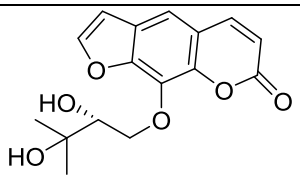 Heraclenol (**36**)		Anti-inflammatory	**(Benkiki et *al.*, 2002)**

I-4-1-8- Phenolic

Table 13 : Phenolic isolated from the genus *Sida*

Structures and names	Plants	Activity	References
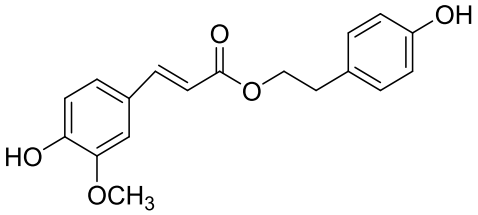 *β*-Hydroxyphenethyl*trans*-ferulate (**37**)	*S. spinosa*	Phytotoxic	**(Sbai et *al.*, 2017)** (**Darwish and Reinecke, 2003**)
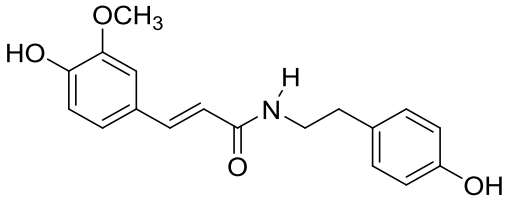 *N-trans*-feruloyltyramine (**38**)		Antioxydant	**(Park et *al.*, 2011)**
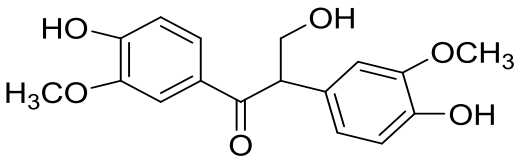 Evofolin-B (**39**)	*S. acuta*	Anticancer	(**Jang et *al.*, 2003**)
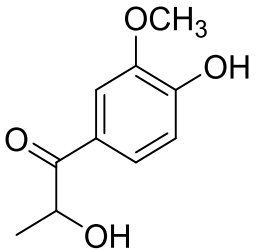 Evofolin-A (**40**)		Anticancer	

I-4-2- Previous chemical studies of Genus *Garcinia*

I-4-2-1 Xanthones

Xanthones are a class of yellowish oxygenated heterocycles based on dibenzo-γ-pyrone and are structurally related to the chromone (benzo-γ-pyrone) from which they are derived (**Meli, 2004**). Table 14 represents some examples.

Table 14 : Xanthones isolated from the genus *Garcinia*

Structures and names	Activity	Plants	References
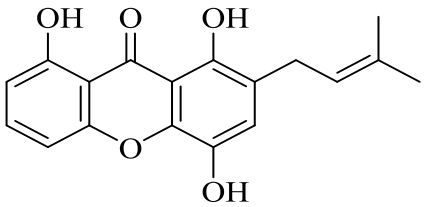 Bangangxanthone B (**41**)	Antioxydant	Bark of *G. polyantha*	(**Meli et *al*., 2005**)
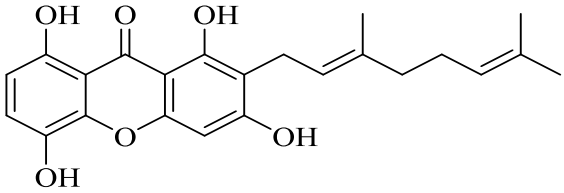 Smeathxanthone A (**42**)	Antimicrobial	Bark of *G. smeathmannii*	(**Komguem et *al*., 2005**) (**Chin et *al*., 2008**)
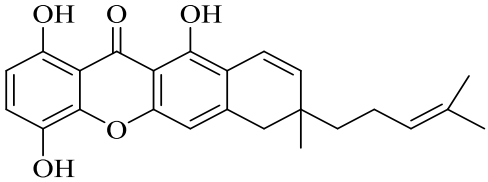 Smeathxanthone B (**43**)	Antioxydant		
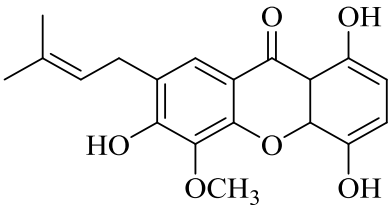 1,4,6-trihydroxy-5-methoxy-7-(3-methylbut-2-enyl)xanthone (**44**)	Antioxydant	Bark of *G. multiflora*	(**Lin et *al*., 1997**) (**Chin et *al*., 2008**)
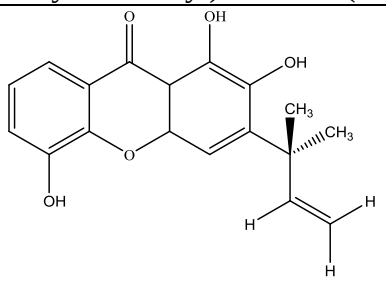 Banfoxanthone (**45**)		Bark of *G. ovalifolia*	(**Noudou et *al*., 2015**)

I-4-2-2 Benzophenones

Benzophenones are symmetrical ketones with a C6-C1-C6 in their backbone and are known to be biogenic precursors of xanthones. Biogenitically, they are derived either from the metabolism of phenylalanine (β-phenyl-α-aminopropionic acid) by a mixed pathway or from the polyacetate metabolism of acetic acid. Table 15 shows some examples of benzophenones.

Table 15 : Benzophenones isolated from the genus Garcinia

Structures and names	Plants	Activity	References
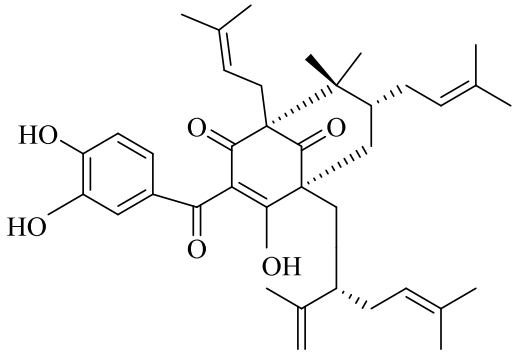 Garcinol (**46**)	*G.epunctata*	Anticancer	(**Biloa et *al*., 2014**) (**Schobert et *al*., 2019**)
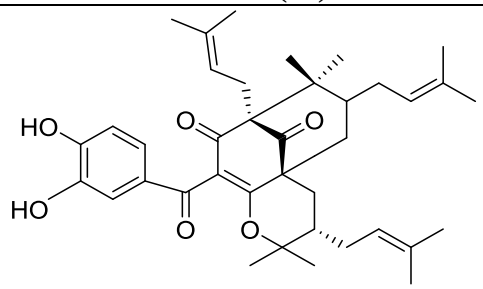 Isogarcinol (**47**)	*G. ovalifolia*	Anticancer	(**Pieme et *al*., 2015**)
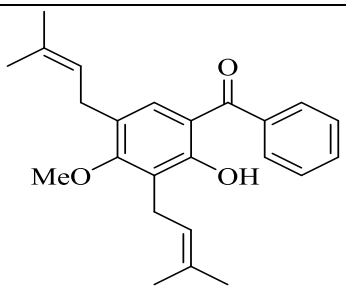 Vismiapherone-C (**48**)	*G. Pseudoguttifera*		(**Ali et *al*., 2000**)
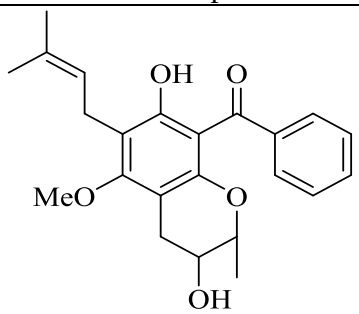 Pseudoguttiapherone-A (**49**)			
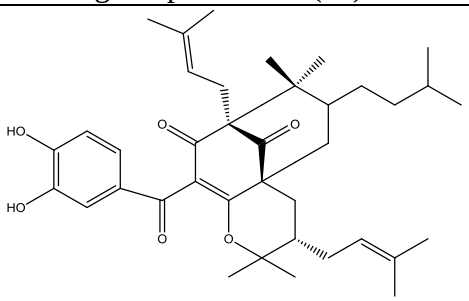 Epunctanone (**49**)	*G. epunctata*		**(Fotso et *al*., 2014)**

I-4-2-3 Triterpenes

Terpenes are compounds made up of isoprene units, coupled in a regular pattern, usually head-to-tail. They hold potential interest practical application especially in the food and cosmetic industries, as well as in the pharmaceutical and chemical industries. Terpenoids have been cited as the most diverse group of plants products known (**Goodwin and Mercer, 1983**)

- Table 16 shows some triterpenes isolated from the genus *Garcinia*

Table 16 : Triterpenes isolated from the genus *Garcinia*

Structures and names	Plants	Activity	References
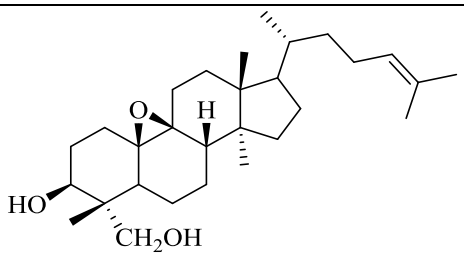 30-hydroxycycloarténol(**50**)	*G.lucida*		(**Nyemba et *al*., 1990**)
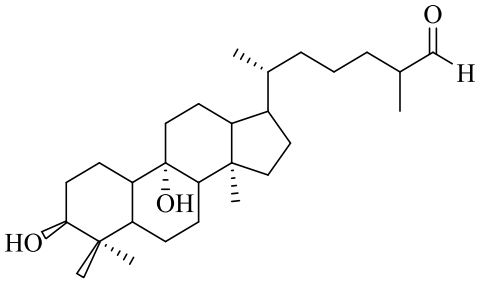 3β, 9 α -dihydroxylanost-24-èn-26-ol (**51**)	*G. speciosa*	cytotoxic	(**Shao et *al*., 2005**) (**Viera et *al*., 2004**)
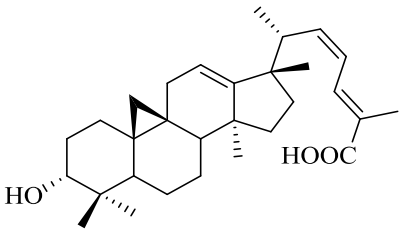 (22*Z*,24*E*)-3α-hydroxy-17,13-friedocycloarta-12,22,24-trien-26-oïc acid (**52**)	*G. benthami*	Antimicrobial	**(Giang et *al*.,2018)** (**Nguyen et *al*., 2012**)
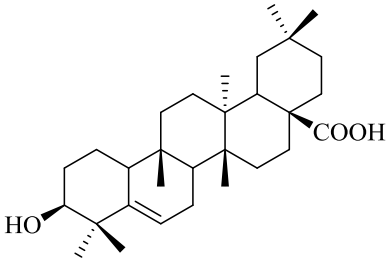 **3β**-Hydroxy-5-glutinen-28-oic acid (**53**)	*Garcinia spp*	Cytotoxic	**(Zakaria et *al*., 2018)**

Structures and names	Plants	Activity	References
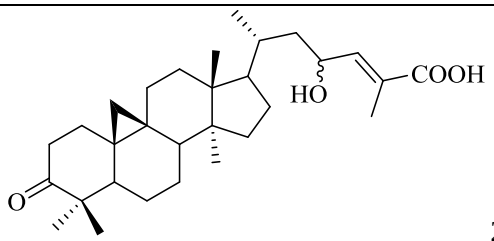 23-Hydroxy-3-oxocycloart-24-en-26-oic acid (**54**)	*Garcinia* spp	Cytotoxic	**(Li et *al.*, 2009)**
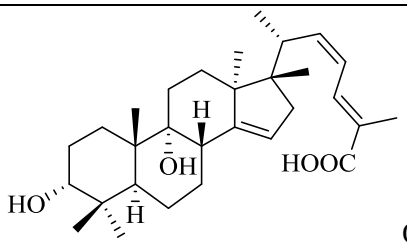 Garcihombronane G (**55**)	*G. hombroniana*	Anticancer	**(Rosli et *al.*, 2020)** **(Vatcharin et *al.*, 2005)**

I-5-Overview of Ceramides

Ceramides consist of a long-chain or sphingoid base linked to a fatty acid via an amide bond (**55**) (**William, 2014**). The core of sphingolipids is the long-chain amino alcohol, sphingosine (**56**). The sphingolipids include the sphingomyelins (sulfatides, globosides and gangliosides). Sphingolipids are components of all membranes but are particularly abundant in the myelin sheath of animals (**Michael, 2013**). Besides animals, ceramides are found in herbs, leguiminous plant and other higher plant species.

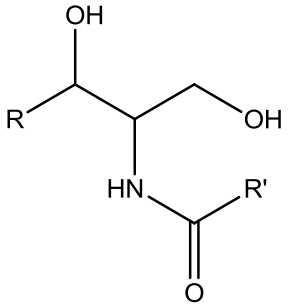

55 R, R′ = Long saturated or unsaturated aliphatic chain

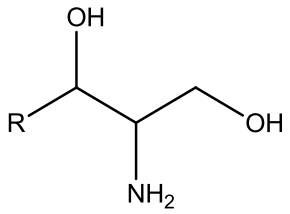

56 **R** = Long saturated or unsaturated aliphatic chain

About 50 % of the mammalian myelin sheath is made up of ceramides and more than 200 structurally distinct molecular species of ceramides have been characterised from the mammalian cells. The N-acyl group of the fatty acid could be hydroxylated (**57**) or non-

hydroxylated (**58**). The animal and plant composition differs in the basic skeleton due to the presence of hydroxyl group at position-4 (**60**) (**William, 2014**).

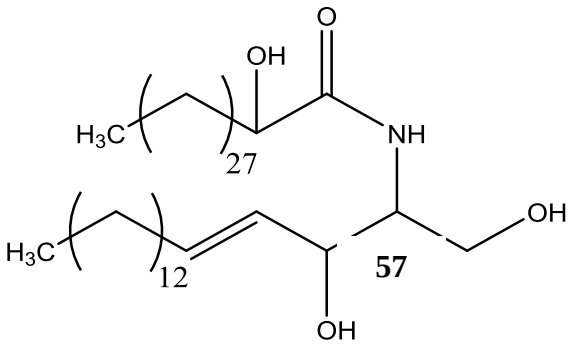

57

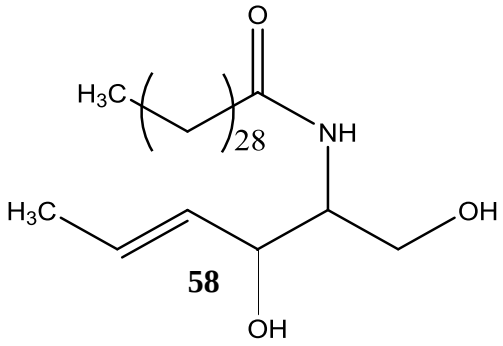

58

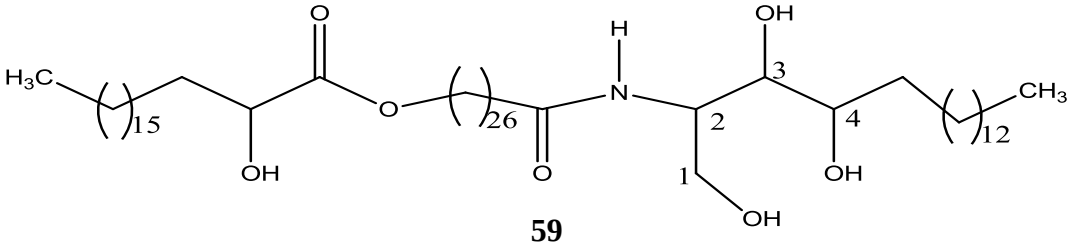

59

I-5-1- Nomenclature of ceramides

There is a systematic nomenclature that permits the naming of ceramides which is based on the nature of the skeleton and the length of the long chain base as seen in the case of Trolliamide also called 2-hydroxy-tetracosanoic acid (2,3-dihydroxy-1-hydroxymethyl-heptadec-7-enyl)-amide (**60**), isolated from *Trollius chinensis* (**Wang et *al.*, 2010**).

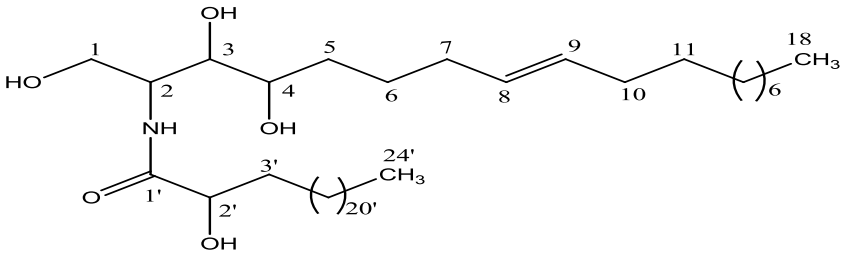

60

I-5-2- Biosynthesis of ceramides

Ceramide biosynthesis begins with the condensation of palmitoyl coenzyme A and serine to give 3-ketodihydrosphingosine. This reaction is catalysed by serine palmitoyltransferase. Subsequently, 3-ketodihydrosphingosine is reduced to dihydrosphingosine. Dihydrosphingosine or sphingonine undergoes acetylation reaction

catalysed by dihydroceramide synthase to give dihydroceramide. The final reaction is catalysed by dihydroceramide desaturase to give ceramide (**Li Guan et *al*., 2006).**

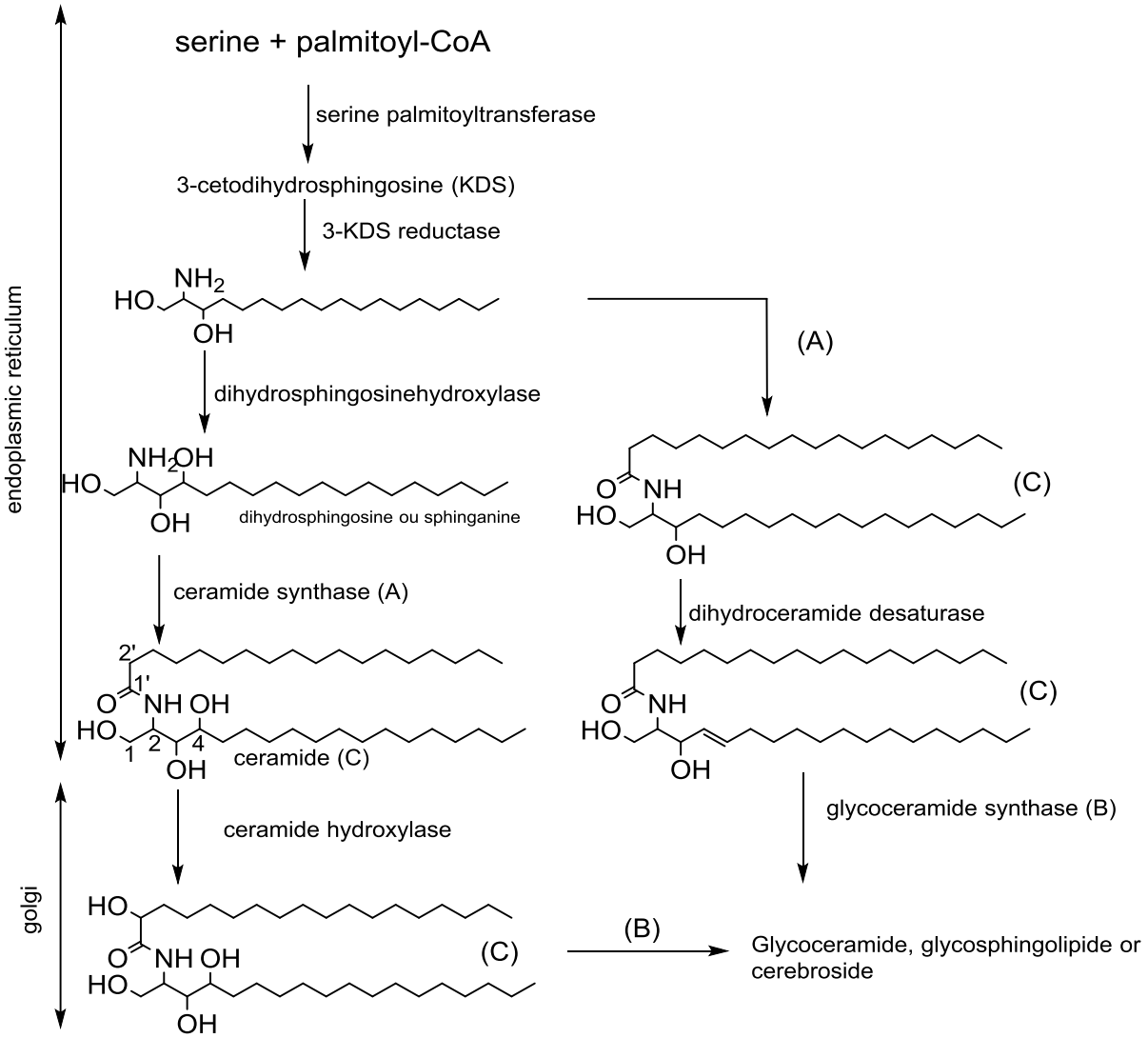

Scheme 2 : Overview of the biosynthetic pathway of ceramides

I-5-3- Identification of ceramides

Thin-layer chromatography is a popular and convenient technique for separation and identification of ceramide monohexoside (CMH), and is the first step in analysis of glycosphingolipids, requiring only small amounts (3–4 nM) of material (**Scandroglio et *al.*, 2009**). This technique does not allow determination of chemical structures, but can give preliminary information on their structures based on chromatographic mobility, in comparison with standards and the reaction with specific staining reagents (**Scandroglio et *al.*, 2009**). Mass spectrometry (MS) is a powerful tool for the analysis of lipids. However, in the early days of its development, the intact lipids could not be directly analysed by MS, since the available ionisation sources produced ions by accelerating electrons electron ionisation (EI),

which should provide the molecules in a gaseous phase, to transfer their energy on ionisation. This was the limiting factor for its application, since the molecules must have a sufficient vapor pressure to enter into the gaseous phase of the mass spectrometer's ion source. Briefly, MS with EI was coupled to gas chromatography (GC–MS) and lipids could be analysed. However, in order to become analysable, CMHs should be converted to their constituent moieties (sugar, fatty acids, LCB), submitted to appropriate chemical derivatization and then identified by GC–MS.

To overcome the requirements for volatilisation, the glycosphingolipids were methanolyzed and their components analysed as fatty acid methyl esters (FAMEs) (**Duarte et *al.*, 1998**). The monosaccharide components of glycosphingolipids were analysed by GC–MS, by conversion to alditol acetate derivatives after being liberated by acid hydrolysis (**Sawardeker et *al.*, 1965**). Long-chain bases were released (LCB or sphingoid base) from CMH by methanolysis and analysed by GC–MS as the TMS derivatives after treatment with bis-(trimethylsilyl) -trifluoroacetamide/pyridine (**Zanetta et *al.*, 1999**). A simple derivatization method established by **Sassaki et *al.*,** (**2008**) can also be employed for, GC–MS identification of monosaccharides and LCB, present in glycosphingolipids.

The highly energetic electrons (70 eV) in EI produce radical ions, but a secondary effect associated with EI is an intense production of fragment-ions, due to the extensive covalent-linkage breakdown promoted by the absorbed energy by the molecules.

In order to overcome the tendency of fragmentation during the ionisation process, other ion sources have been developed, called soft ionisation methods. The soft ionisation technologies allow ionisation and transferring non-volatile and thermolabile molecules to the gaseous phase without extensive production of fragments, impossible with EI. This type of source became available from 1980s with the introduction of fast atom bombardment-mass spectrometry (FAB-MS), followed by electrospray ionisation mass spectrometry (ESI-MS), and matrix-assisted laser desorption ionisation (MALDI). Another important characteristic is that these techniques allow changing the ion polarity, since it is possible to produce ions via cation or anion interactions, such as protonation, sodiation, lithiation or deprotonation, chlorination, and so on. Nowadays, variations of these techniques are also found, such as nano-ESI-MS, photospray ionisation, as well as those called ambient MS, which include direct analysis in real time-mass spectrometry (DART-MS) and desorption electrospray (DESI), (**Barreto-Bergter et *al.*, 2004**). Fungal cerebrosides suitable for analysis of analytes deposited on a surface, such as with HPTLC. The ions obtained from intact molecules provide information on their molecular weight, as well as fragmentation being an important tool for

structural analysis. The MS instrumentation allow separation of a specific ion and subjecting it to a fragmentation process, as occurring in collision-induced dissociation (CID) or collision-activated dissociation (CAD). This type of analysis is usually referred to as tandem-MS and the spectrometers operating in tandem mode consist of conjugated analyzers, such as triple quadrupole (TQ or QQQ), quadrupole-time of flight (Q-TOF) or the ion trap, and Fourier-transform ion cyclotron resonance (FTICR) analysers, which allow the re-fragmentation of product ions (fragment-ions from MS/MS) usually referred to as MSn. Fast atom bombardment was first introduced by (**Morris et *al.*, 1981**). The sample is dissolved in a nonvolatile liquid matrix (e.g., glycerol, thioglycerol,t riethanolamine), and the mixture is bombarded by a beam of accelerated atoms (typically argon or xenon). Non-volatile, polar, and thermolabile molecules, such as lipids, could be ionised directly analysed (**Murphy et *al.*, 1982**). FAB-MS is considered to be a relatively soft ionisation technique, since it produces primary the molecular ion (quasi- or pseudo-molecular ions), although numerous fragments ions are typically generated. Since FAB-MS allowed the analysis of a broad range of intact molecules, it rapidly became one of the most commonly used techniques for structural characterisation of lipids, including a wide variety of fungal cerebrosides, using native and peracetylated samples (reviewed by **Levery, 2005**).

I-5-4-Biological potential of ceramides

The wide occurence in nature and structural diversity of ceramide have attracted attention on their biological potential. Ceramide have been implicated in many fundamental cellular processes including growth, differentiation, and morphogenesis. Ceramide may also modulate cell signaling by controlling the assembly and specific activities of plasma membrane proteins (**Kasahara and Sanai 2000**). Soya- ceramide from soybeans was reported to exhibit moderate tyrosinase inhibitory activity, and applied for making skin-care cosmetics for removal of (black) freckles (**Michio, 2011**). Ceramide from edible Chinese mushroom were shown to induce neuronal differentiation in rat PC12 cells (**Qi et *al.*, 2000**). Some ceramide have been noted to exhibit a potent and selective antifungal, antimicrobial, antitumor, antiviral, cytotoxic, and immunomodulatory activities **(Shi-Yie et *al.*, 2012**).

I-6-Overview of pentacyclic terpenes

Terpenes are compounds made up of 5- carbon units, often called isoprene units, put together in a regular pattern, usually head-to-tail. They hold potential interest, practical application especially in the fragrance and flavor industries, as well as in the pharmaceutical and chemical industries. Terpenoids have been cited as the most diverse group of plants

products known (**Goodwin and Mercer, 1983**). Many of these products have functions known to be essential to plant life (e.g. carotenoids, chlorophyll side-chain and some hormones). The volatile monoterpernoids are the major components of essential oils and often function as floral odour glands (**Goodwin and Mercer, 1983**). However, diterpenoids, triterpenoids, and sersterterpenoids are also known and have been found to be of great biological significance. The classification of terpenoids is based on the number of isopreneoid units they contain; for example monoterpenes (C10), sesquiterpenes (C15), diterpenes (C20), sesterterpenes (C25), triterpenes (C30) and tetraterpenes (C_{40}) respectively (**Muffler et *al.*, 2011**). The immediate biological precursor of the diverse polycyclic terpenoid is squalene (**62**) produced through the head-to-tail condensation of two C_{15} units of farnesyl diphosphate (FPP) (**Muffler et *al.*, 2011**). Cyclization of squalene via intermediate squalene-2,3-epoxide followed by a series of concerted Wagner Meerwein migration of methyl and hydrides occurring in the presence of specific enzymes, so-called cylases, leads to the formation of the various units. The resulting products are dependent on the folding of squalene unit (**62**), prior to the process of cylisation

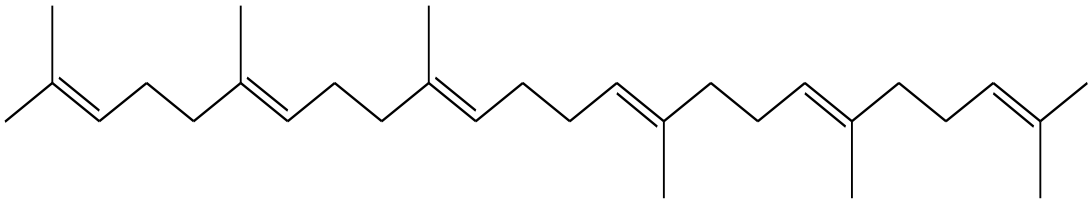

62

Pentacyclic triterpenoids have been identified as predominant constituents in this study. The wide investigation based on literature sources, permits their classification into 12 structural groups (**Mahato et *al.*, 1994**) as presented in the figure 2 below.

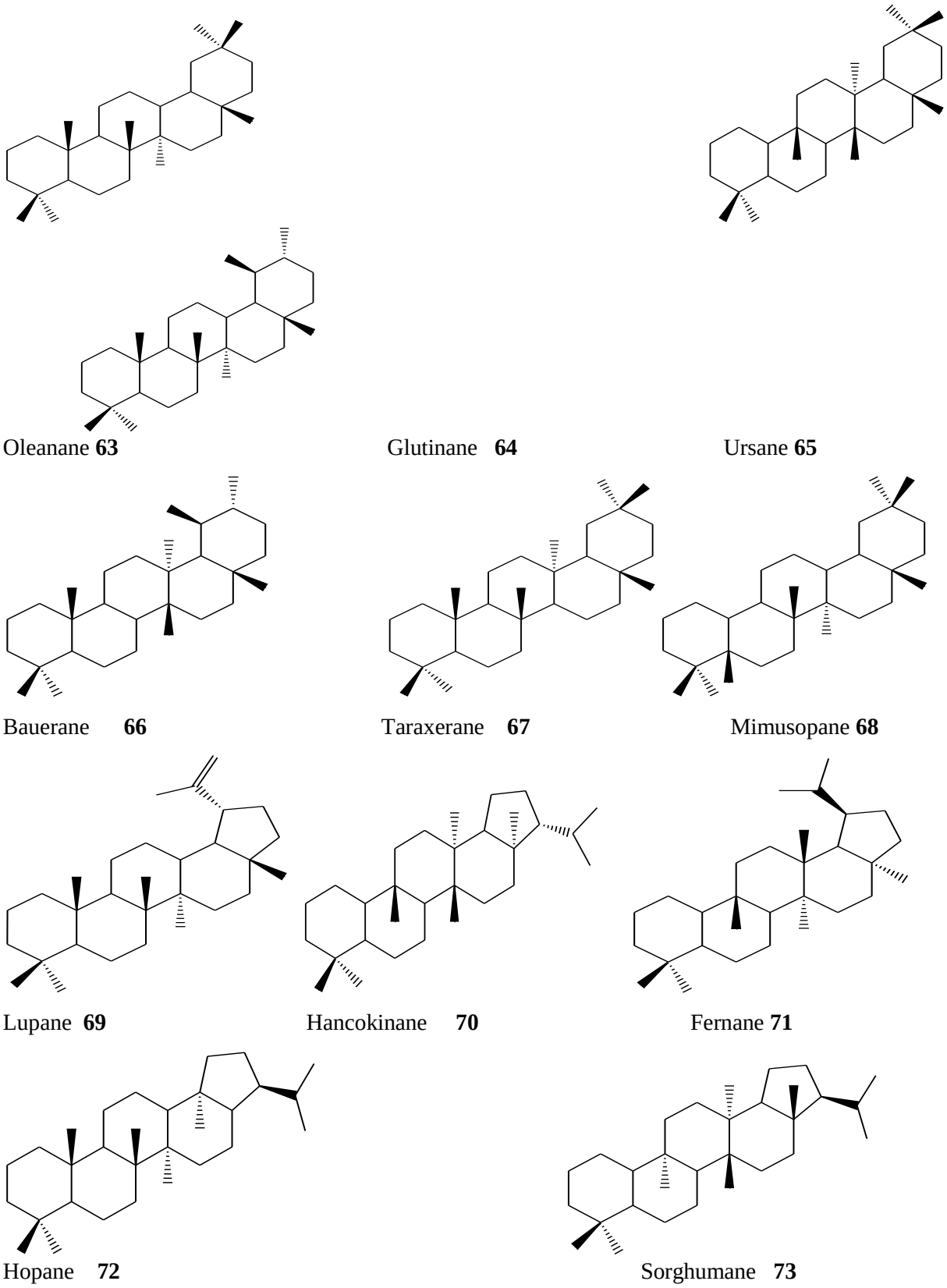

Figure 2 : Different structural groups of pentacyclic triterpenoids

I-6-1 Nomenclature and Stereochemistry of triterpenoids

Just like any other family of secondary metabolites, there is a systematic approach in naming triterpenoids. Pentacyclic triterpenoids are made up of cycles labelled A, B, C, D and E. The concept of triterpenoid nomenclature was introduced by Allard and Ourisson in 1957). The nomenclature of triterpenoids is based on about seven rules. The first rule is to determine its name according to its skeleton. Thus, the main name comes from the class of compounds. The number of the carbons in the backbone forms the second rule. These numberings are used to define the position of substituents or functionalities, which are added as prefixes or suffixes to the main name. Their stereochemistry inside the core is highlighted by employing Greek letters α and β or whether it is trans (E) or Cis (Z), R or S as illustrated by the examples below (**Allard and Ourisson 1957**) **.**

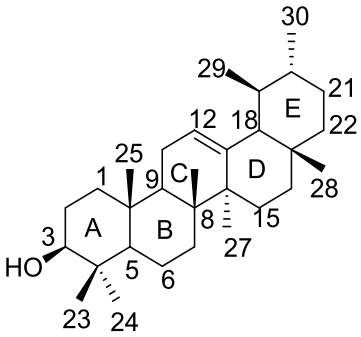

Urs-12-en-3- β-ol (**74**)

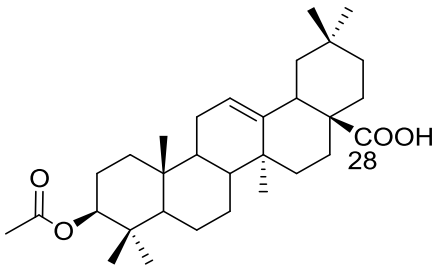

3- β-acetoxy-olean-12-en-28-oic acid (**75a**)

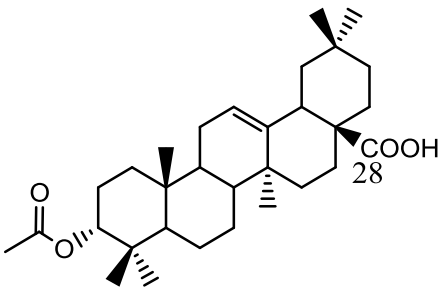

3- α-acetoxy-olean-12-en-28-oic acid (**75b**)

I-6-2 Elucidation of structures of triterpenoids

The task of treating a crude extract right up to the point of obtaining a pure compound is not an easy one. Even when the pure compounds are obtained, the next herculean assignment is that of identification and determination of their structures. Thanks to several 1D (^{1}H, ^{13}C, DEPT) and 2D (COSY, NOESY, HSQC, HMBC, TOCSY) NMR experiments in

association with IR, UV, mass spectrometry and even X-ray crystallography in some cases characterisation of the various classes of secondary metabolites has been made possible.

Infra-red (IR) spectroscopy gives information on the presence of functional groups such as carbonyls, alcohols, amines as well as for gem dimethyls double bonds functionalities and others.

Triterpenoids are easily identified on the ^{1}H NMR by the appearance of signals between four and eight very intense peaks in the δ_H 0.50 to 2.00 region, each integrating for three protons (Ageta et Arai, 1983). These readily discernable peaks are the angular methyls on the triterpenoid structure. Protons attached to unsaturated carbons appear further downfield after δ_H 5.00. Most triterpenoids are hydroxylated at position 3 of the triterpenoids structure, hence the oxymethine proton appears between δ_H 3.00 and 4.00. But if the proton attached to the oxygen is substituted by an ester or ether bond, then the oxymethine proton will appear further downfield after δ_H 4.00 due to the deshielding of its environment. Protons attached to any other oxygenated carbon appear downfield after δ_H 3.00. In lup-(20) (29)-enes characteristic exocyclic olefenic protons appear between δ_H 4.30 and 4.80. In the ^{1}H NMR spectrum of ursane-type triterpenoids, H-18 appears as a doublet around δ_H 2.55 while in oleanane series, it appears around δ_H 2.20 as a doublet of doublet. When the methyl on C-17 or C-28 is oxidized to carboxylic acid, the proton H-18 undergoes an attractor effect of the acid which then moves it downfield to about δ_H 2.84 for oleanane-type molecules and around δ_H 2.40 for ursane-type **(Furuya et *al*., 1987)** In friedelane triterpenes, there is absence of the double bond and consequently the vinylic proton signal after δ_H 5.00. The proton NMR spectrum in most cases is not sufficient even for known compounds to be identified and must be associated to other NMR and spectroscopic techniques.

The ^{13}C NMR experiment is very important for structure elucidation. It is different even for very similar compounds and so is very diagnostic for a particular compound. Triterpenoids show 30 signals on their broad band decoupled ^{13}C NMR spectrum, except in cases where more than one carbon atoms possess the same magnetic environment and hence the same chemical shift value, reducing the number of signals or when other molecules like sugar moieties, esters, phenyl groups etc, add up to the triterpenoids, increasing the number of signals. The different classes of pentacyclic triterpenes are easily distinguished on their ^{13}C NMR spectrum by the appearance of some diagnostic signals pertaining to the olefinic carbons at C-12 and C-13: Olean-12-enes have signals approximately at δ_C 122.0 and 145.0 respectively Urs-12-enes have signals at δ_C 124.0 and 139.0 and lup-(20)(29)-enes have

signals at δ_C 109.0 and 150.0 for C-20 and C-29) respectively. For friedelanes, C-23 appears around δ_C 11.0 when C-3 is hydroxylated and around δ_C 7.0 when C-3 is completely oxidised to a keto function However, these resonances are affected by the introduction of substituents (**Mahato and Kundu, 1994**).

The ^{13}C DEPT experiments, especially DEPT 135 helps in classifying the carbons as primary (CH_3), secondary (CH_2), tertiary (CH) or quartenary (C). 2D NMR experiments (COSY, NOESY, HSQC, HMBC, and TOCSY) are very necessary for the unequivocal establishment of the structures of molecules. The HMQC or HSQC experiment permits attribution of protons to particular carbon atoms.The HMBC spectrum allows us to establish links between protons and the carbon atoms adjacent to the one bearing the proton usually up to 2, 3 and in rare cases 4 bonds. The HMBC experiment is very important in locating the positions of substituent groups in a molecule. COSY on its part useful in locating adjacent protons through bonds while NOESY helps in the attribution of the relative stereochemistry around stereogenic centres and locating protons that have spatial proximities. Finally, HOHAHA or TOCSY is very useful in the elucidation of the structure of saponins because it helps in dividing the proton signals into groups or coupling networks.

Mass spectroscopy is used to establish the molecular weight of the compound under analysis. Apart from soft ionisation techniques such as ESI, FAB, DI, MALDI, and CI are commonly used to establish the mass of steroids, triterpenoids and their saponins from pseudomolecular ion peaks on the spectrum (**Li et *al.*, 2006**).The most prominent fragmentation pattern shown by pentacyclic triterpenoids is that due to a RDA reaction common in tritepenoids with a double bond. This usually leads to a base peak at m/z 218 and a prominent peak at m/z 203 on simple unsubstituted triterpenoids like α and β-amyrin. It is thus possible to get more information about the structure of a substituted triterpenoid by making deductions from the distinctive peaks. Oleanolic and ursolic acid show base peak at m/z 203 and other prominent peaks at m/z 203 + COOH and 218 + COOH (**Thanakijcharoenpath and Theanphong 2007**).

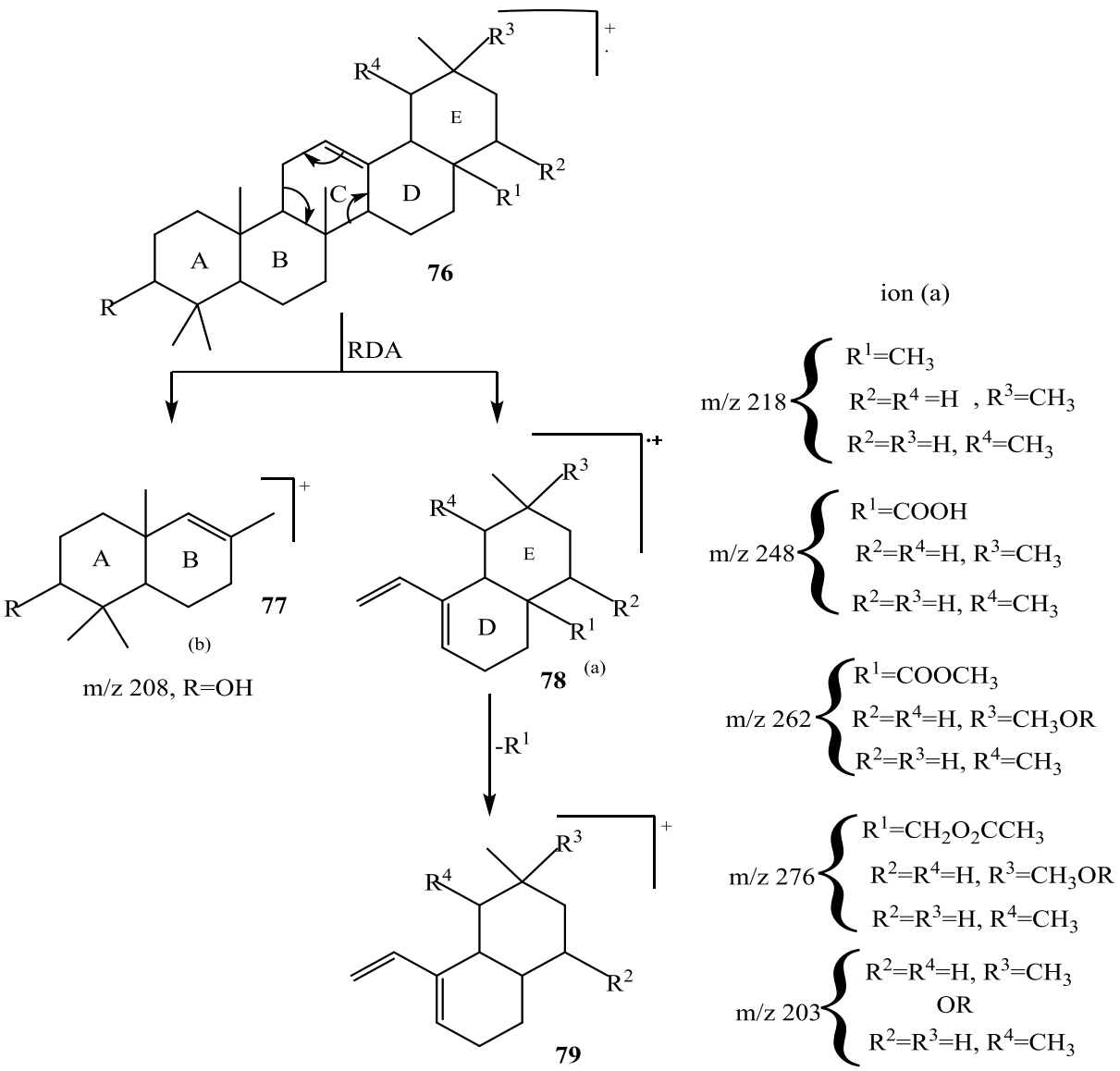

Scheme 3 : Retro-Diels-Alder fragmentation pattern for Oleanane and Ursane type triterpenoids (Ogunkoya, 1981).

I-6-3-Biosynthesis

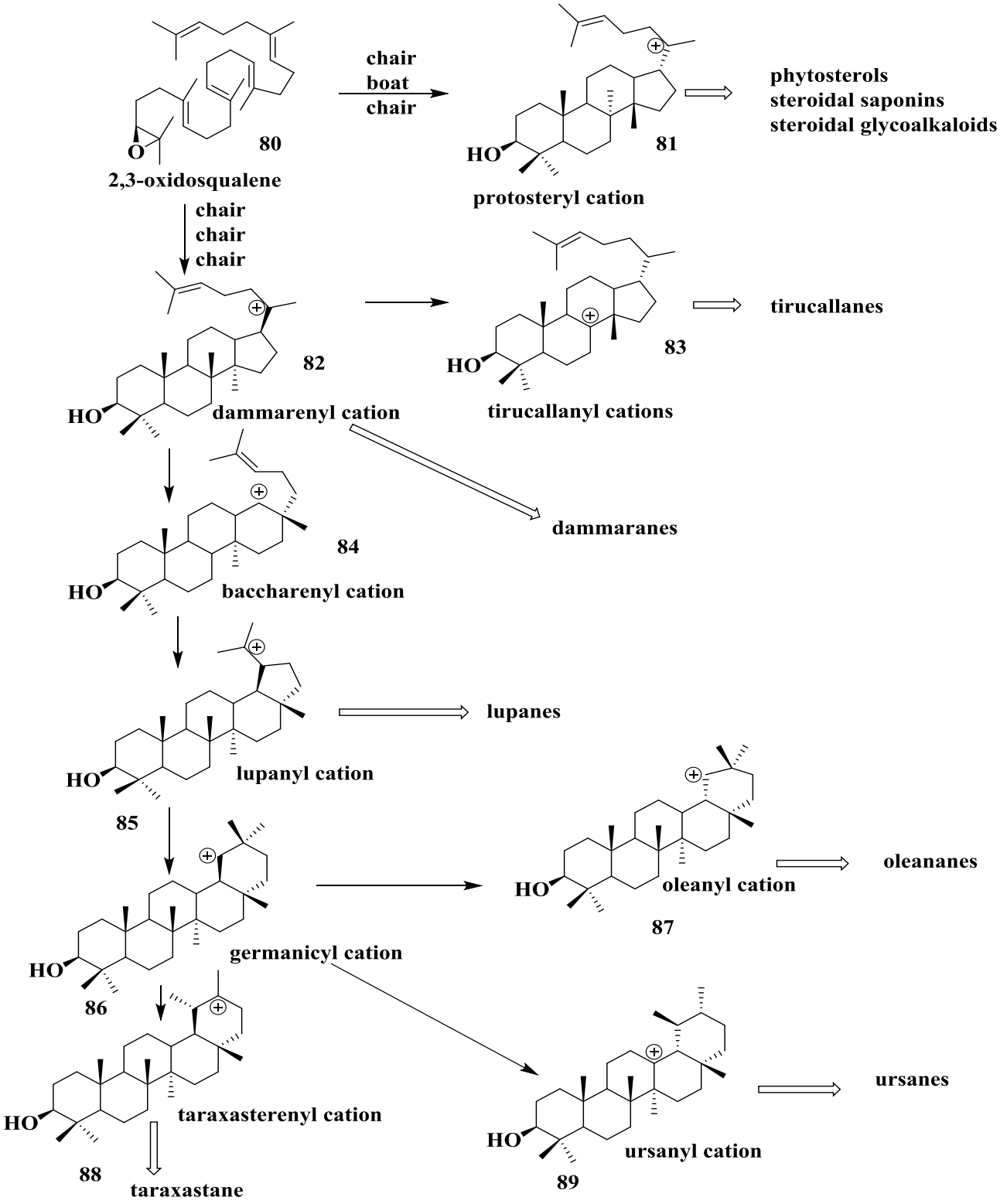

Scheme 4 : Biosynthesis of triterpenoids (Augustin et *al*., 2011)

CHAPTER II

RESULT AND DISCUSSION

II.1 COLLECTION, EXTRACTION AND ISOLATION OF COMPOUNDS

II.1.1 Collection of plant materials

The whole plant *Sida rhombifolia* L.was collected in February 2017 at Bagangté in the Western region of Cameroon. This plant was identified by Mr. Nana Victor, botanist at the National Herbarium in Yaounde, where a voucher specimens was conserved under the specimen N^{o}: 20113/HNC.

The whole plant *Sida acuta* Burm. F.was collected in September 2017 at Ebolowa in the South region of Cameroon. This plant was identified by Mr. Nana Victor, botanist at the National Herbarium in Yaounde, where voucher specimens was conserved under the specimen N^{o}: 46188/HNC.

The Stem bark of *Garcinia ovalifolia* Oliv. was collected in October 2018 at Mont Kala. This plant was identified by Mr. *Nana Victor*, botanist at the National Herbarium, Yaoundé, Cameroon, where a voucher specimen N° 55523/HNC was deposited.

II.1.2 Extraction of different powders

II.1.2.1 Extraction of whole plant of *Sida rhombifolia* L

The whole plant *Sida rhombifolia* L, was air dried and ground to give 2.5 kg of powder. This powder was extracted by maceration at room temperature with EtOH/H_2O (7:3) (3×10 L) for 72 hours. After evaporation of the solvent (40°C) under reduced pressure, we obtained 105.3 g of crude extract. This extract, was poured into distilled water and extracted successively with by *n*-hexane, EtOAc and *n*-butanol fraction.

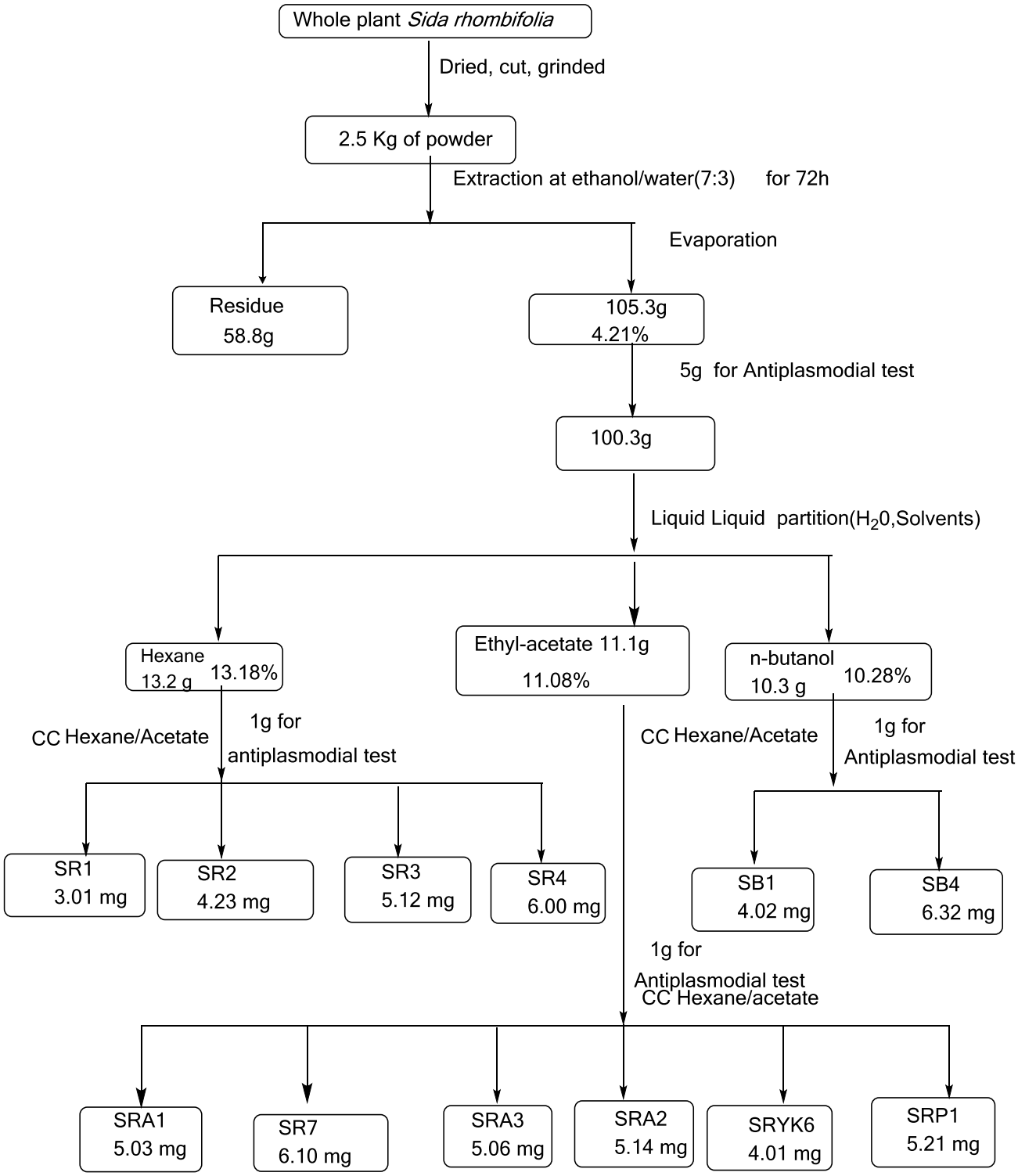

Scheme 5: Extraction and isolation of compounds from *Sida rhombifolia*

II.1.2.2 Extraction of whole plant of *Sida acuta*

The whole plant of *Sida acuta* Burm was air dried and ground to give 3 kg of powder. This powder was extracted by maceration at room temperature with EtOH/H_2O (7:3) (3×10 L)

for 72 hours. After evaporation of the solvent under reduced pressure 40 °C, we obtained 130.3 g of crude extract. This extract, was poured into distilled water and extracted progressively with *n*-hexane, EtOAc and *n*-butanol fraction.

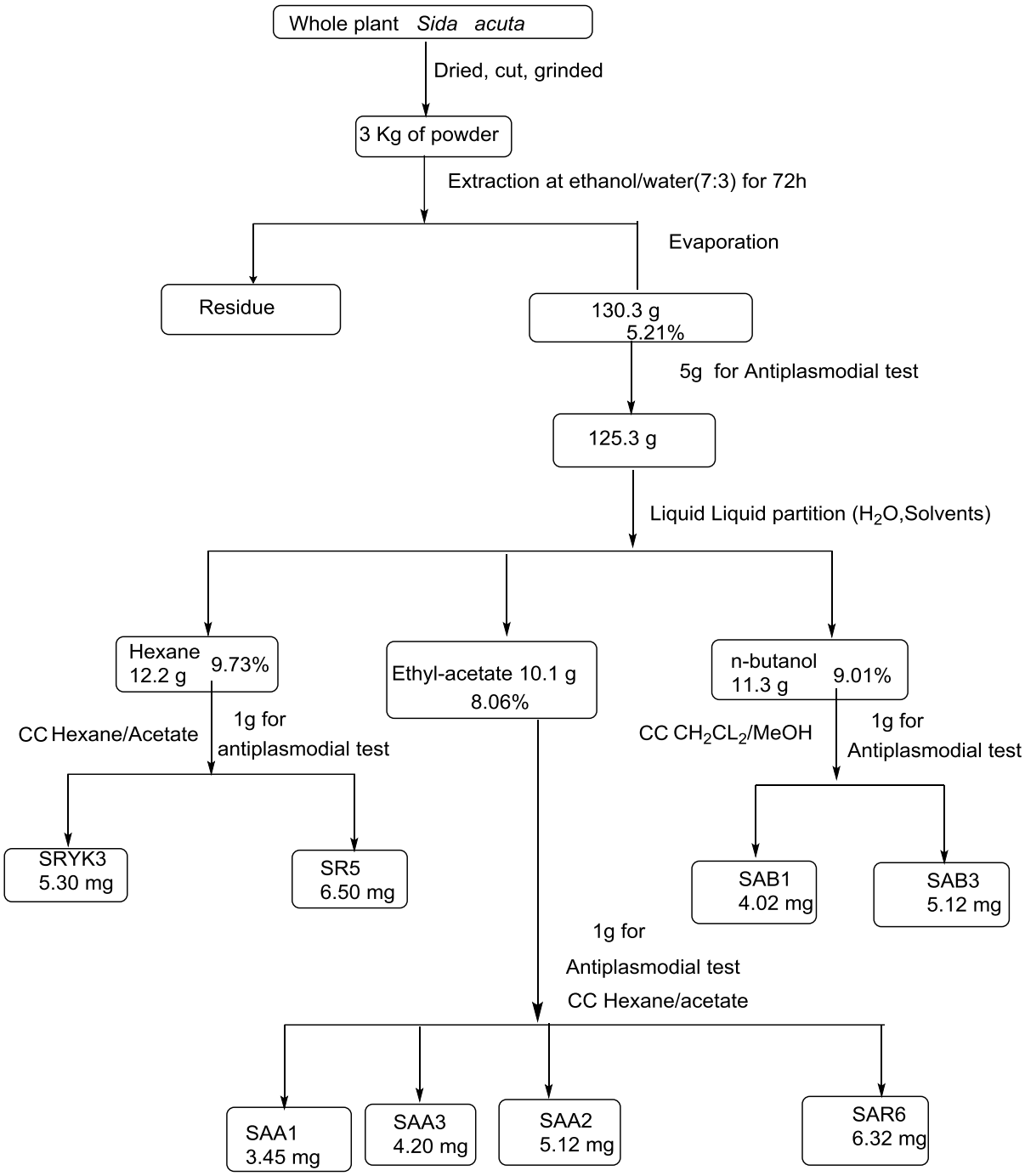

Scheme 6: Extraction and isolation of compounds from *Sida acuta*

II.1.2.3 Extraction of stem bark of *Garcinia ovalifolia*

The air-dried and powdered stem bark of *G. ovalifolia* (1 kg) was macerated at room temperature in a mixture of CH_2Cl_2/MeOH (1:1) for 48h and MeOH for 24h, respectively. The removal of solvent under reduced pressure yielded 45 g of brown extract. A mass of 40 g of this organic extract was submitted to flash liquid chromatography on silica gel 60 (220 g) and eluted with a mixture hexane- ethyl acetate (1:1) and (1:3), and finally with pure EtOAc to give 40 fractions of 250 ml each. A total of 5 compounds were isolated from the fraction hexane- ethyl acetate (1:1) of *G. ovalifolia*.

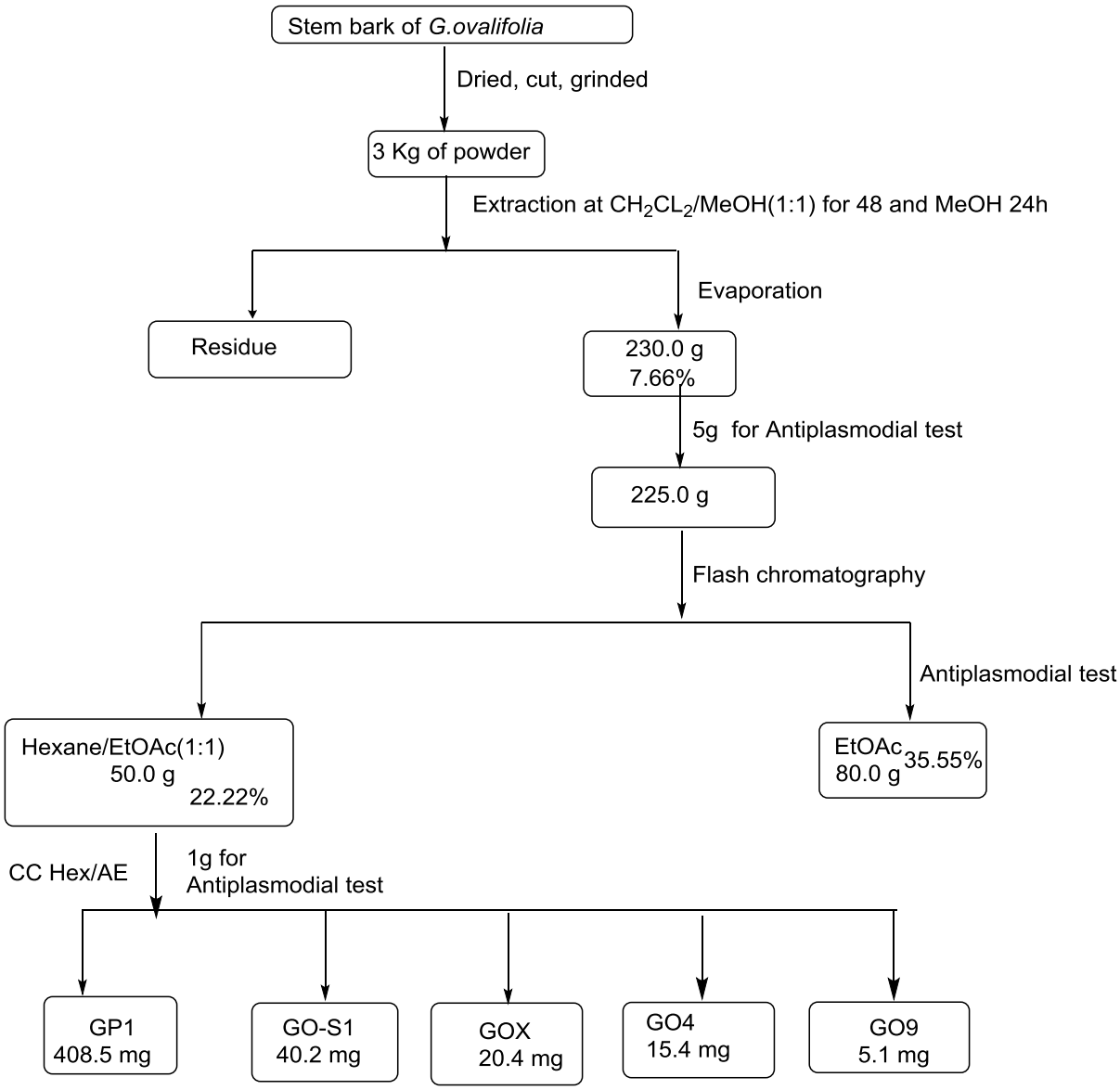

Scheme 7: Extraction and isolation of compounds from the stem bark of *G. ovalifolia*

II.2 CHARACTERISATION OF COMPOUNDS ISOLATED FROM THE THREE SPECIES

II.2.1 Ceramide

II.2.1.1 Characterization of SRP1

SRP1 was obtained as a white powder. Its molecular formula $C_{43}H_{85}NO_5$ was established from its HRESI-MS spectrum (Figure 3), showing the pseudo-molecular ion peak $[M+H]^+$ at *m/z* 696.6506 ($C_{43}H_{86}NO_5^+$; calcd. 696.6501), indicating two degrees of unsaturation.

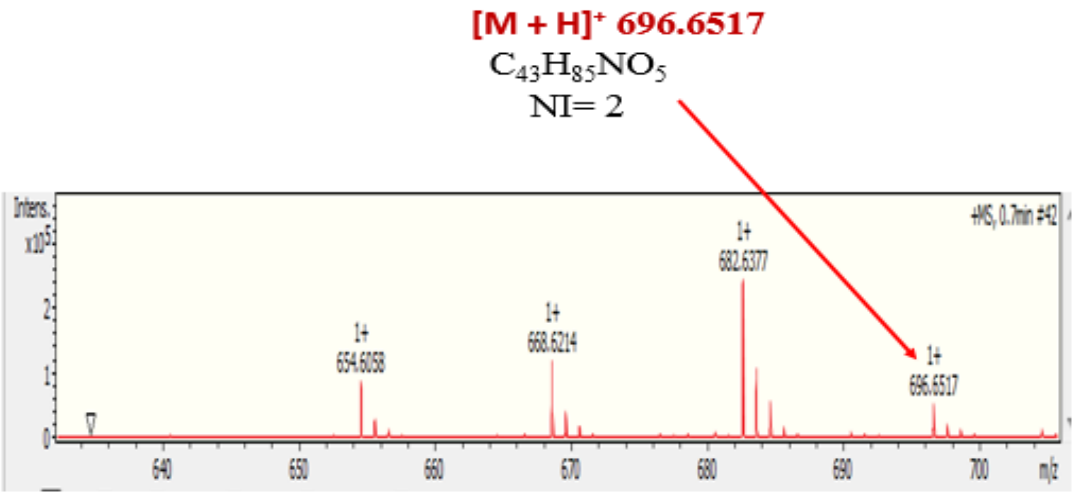

Figure 3: HR-ESI-MS spectrum of SRP1

Its IR spectrum (Figure 4) showed characteristic absorption bands for free OH groups (3329-3215 cm^{-1}) and an amide group (1620 cm^{-1}) (**Yue et *al*., 2001**).

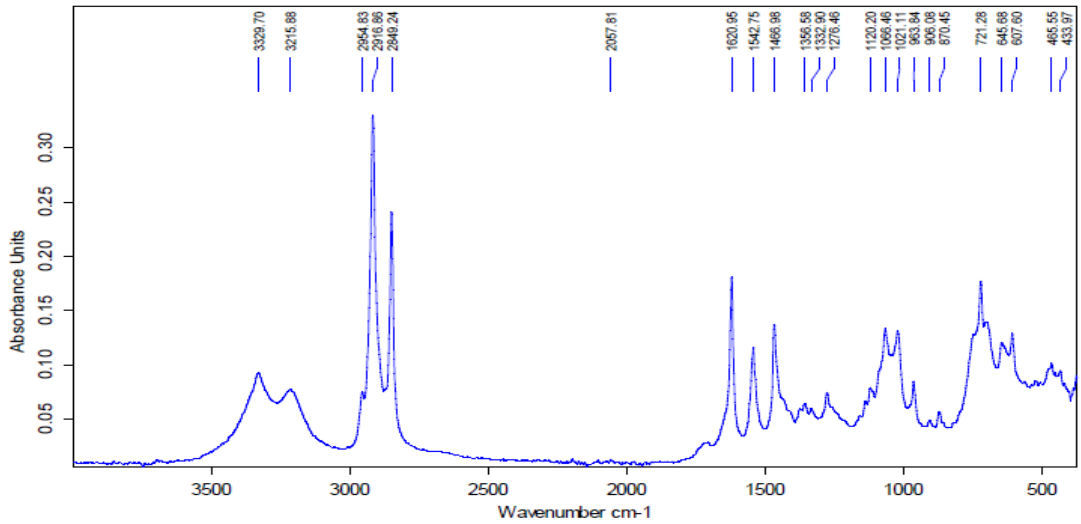

Figure 4: FT-IR spectrum of SRP1

The ^{1}H NMR spectrum of SRP1 (Figure 5) in conjunction with ^{13}C-NMR, DEPT 135 and HSQC (Figure 5–8) displayed a set of signals characteristic of a ceramide as described by Simo et al. 2008. This was confirmed by the signals of the carbonyl of an amide at δ_C 175.4 and the signal of a nitrogen- attached Sp_3 carbon at δ_C 51.5. The amino methine NC-H proton appeared at δ_H/δ_C 4.03 (1H, m)/51.5 while the broad signal centered at δ_H 1.18 was attributed to the methylene protons of the aliphatic long chain, and a distorted triplet at δ_H 0.79 (6H, t, 6.9) indicated the presence of two terminal methyl groups. In addition, the spectrum displayed two diastereotopic protons of an oxymethylene at δ_H/δ_C 3.72 (1H, dd, 4.6, 11.5, H-1a) / 60.9 and 3.66 (1H, dd, 4.6, 11.4, H-1b) / 60.9 as well as three oxymethine protons at δ_H/δ_C 3.46/75.3 (C-3), 3.45/72.1 (C-4) and 3.95 / 71.8 (C-2') respectively.

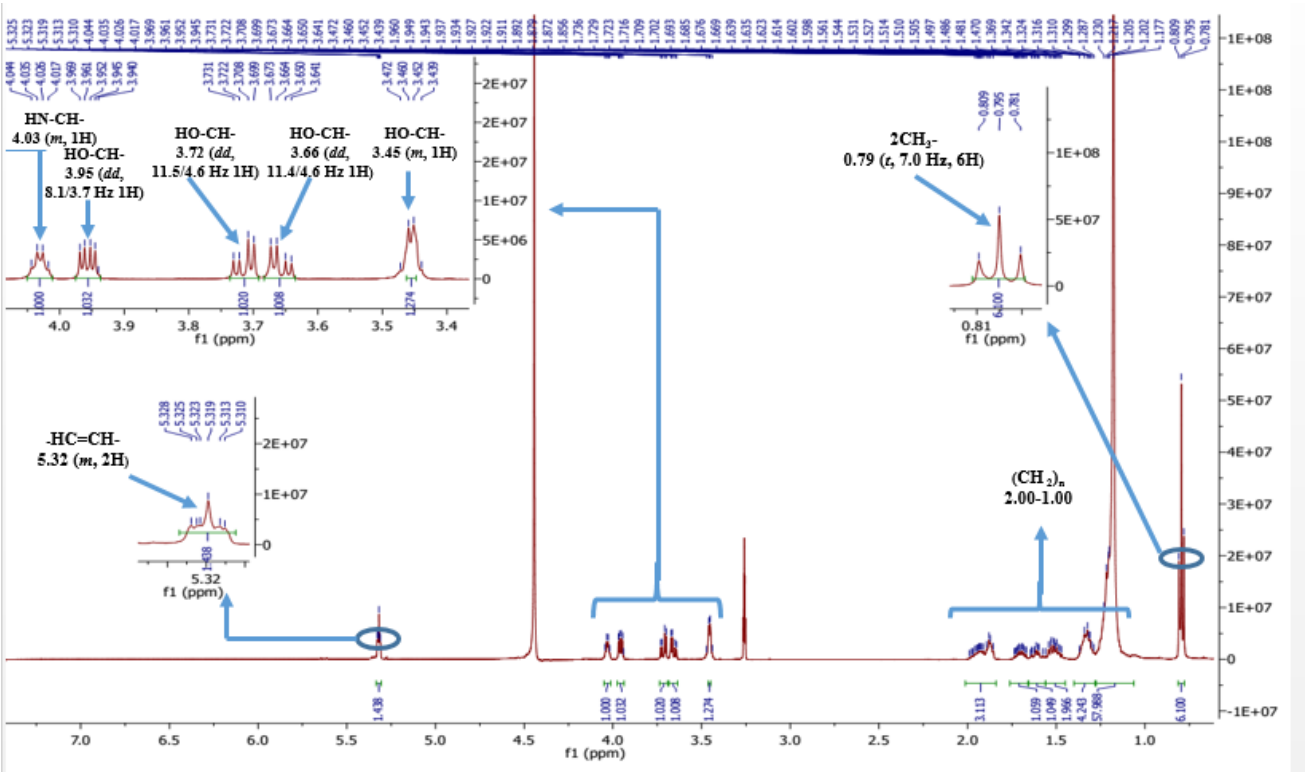

Figure 5: ^{1}H-NMR spectrum (600 MHz, $CDCl_3$ /CD_3OD) of SRP1

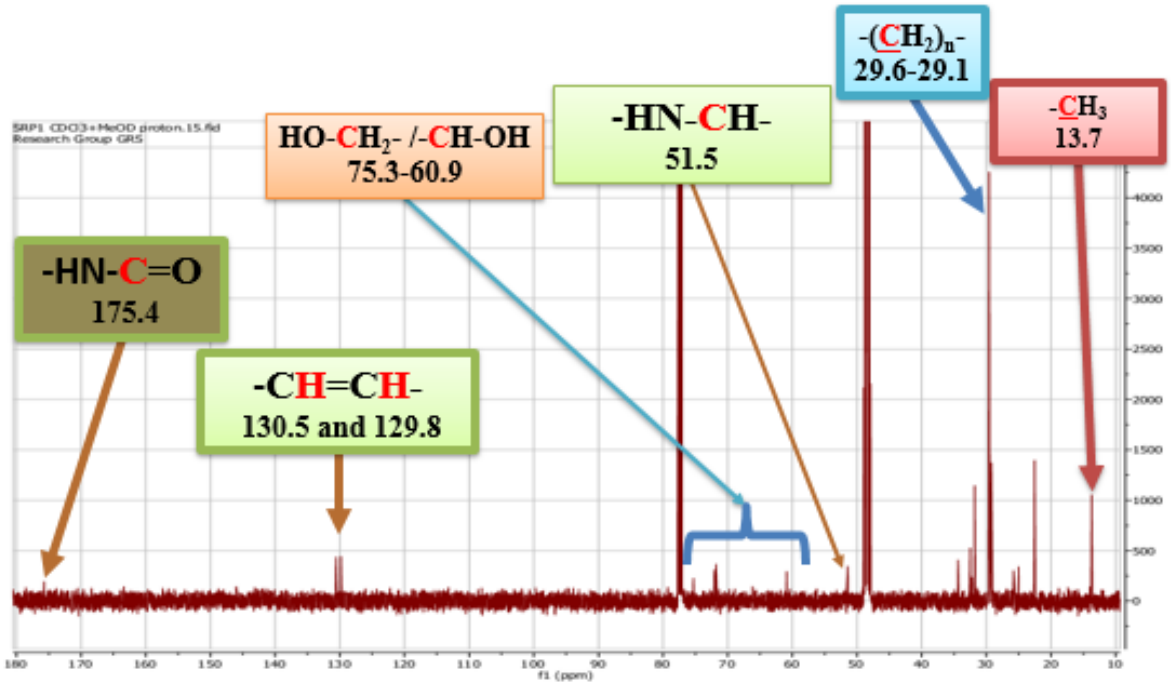

Figure 6: ^{13}C-NMR broadband decoupled spectrum (150 MHz, $CDCl_3/CD_3OD$) of SRP1

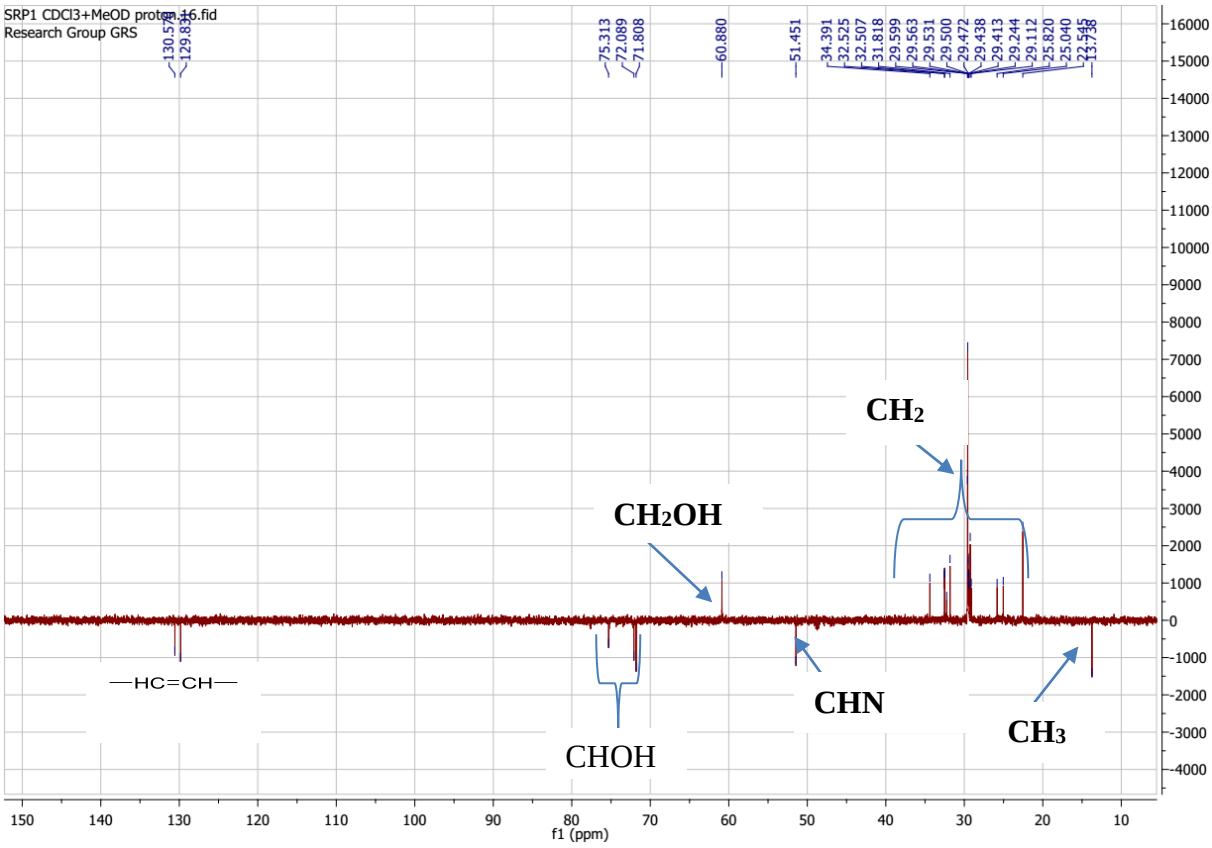

Figure 7: DEPT 135 spectrum of SRP1

The Correlations between these protons were observed on the $^{1}H–^{1}H$ COSY spectrum . In addition, the presence of a signal at δ_H 5.32(2H, m) showing cross peaks on the HSQC with two olefinic carbons at 129.8 and 130.5 ppm suggested the presence of a double bond in the structure of SRP1 (**Wouamba et *al*., 2020**).

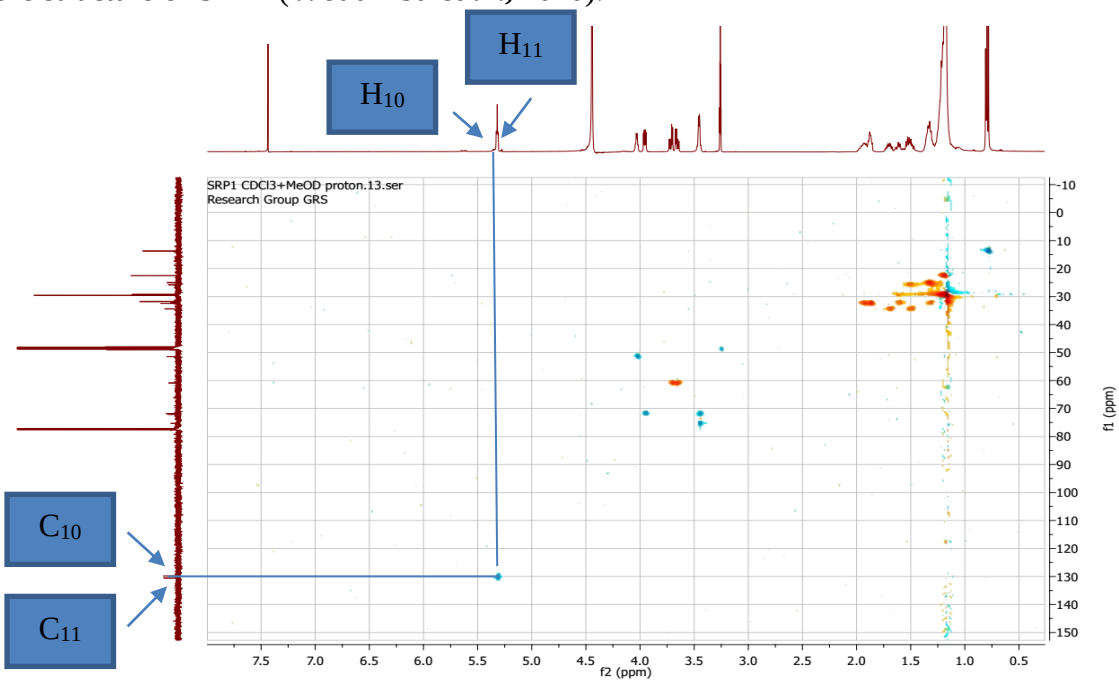

Figure 8: HSQC spectrum of SRP1

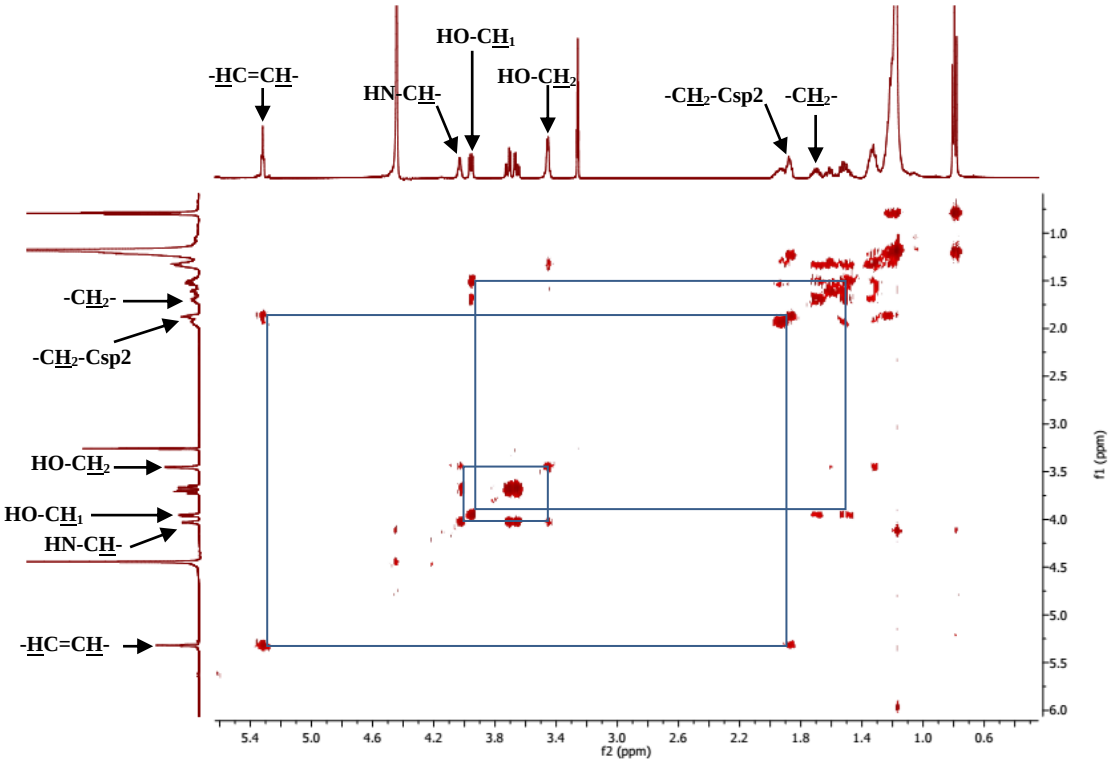

Figure 9: $^{1}H—^{1}H$COSY spectrum of SRP1

The length of this fatty acid moiety was deduced by the analysis of the ESI-MS/MS spectra of SRP1 (Figure 10) showing the fragment ion peak $[(CH_3(CH_2)_{22}CH(OH)CO -H_2O + 2H]^+$ at m/z 363.5 and further confirmed by the methanolysis using 0.9 N, HCl/MeOH, at 70 ◦C for 20h to yield the fatty acid methyl ester (1a) and the sphingosine (1b) (**Simo et *al*., 2008**).

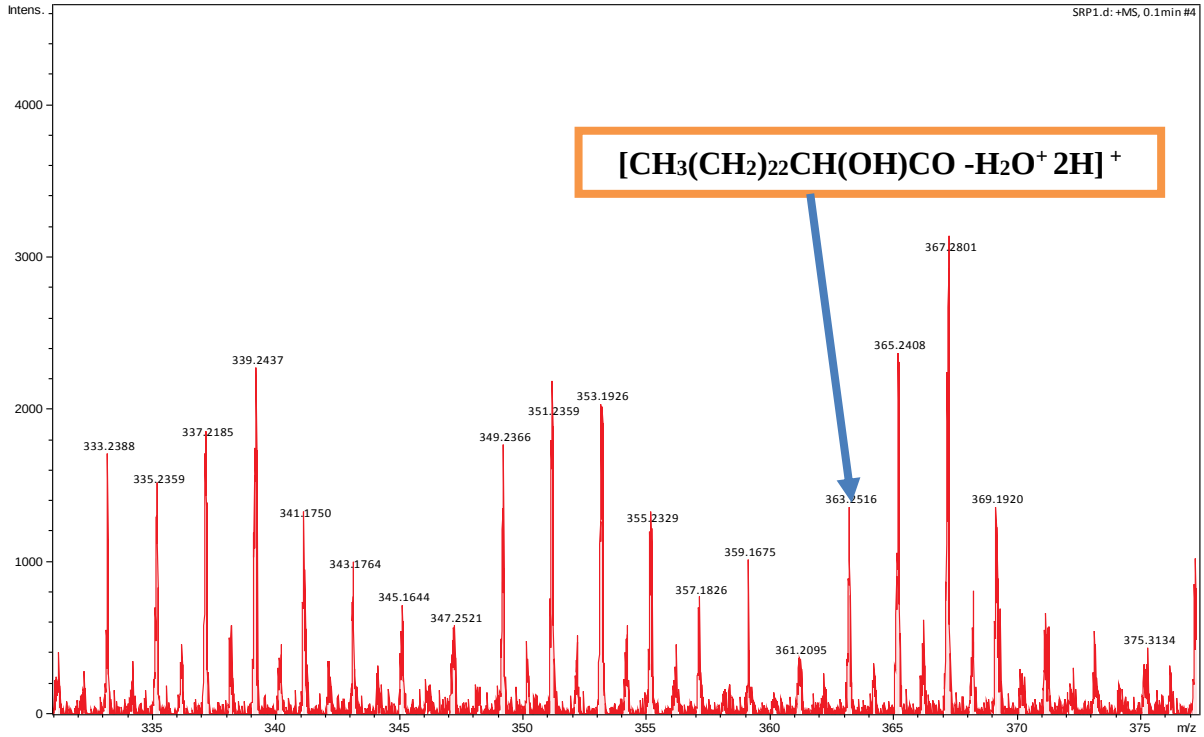

Figure 10: ESI-MS/MS spectrum of methanolysis of SRP1

In fact, the peak at m/z 316.19 $[M+H]^+$ corresponding to molecular formula $C_{18}H_{37}NO_3^+$ was attributable to the long chain base (1b) and implying one degree of unsaturation. Furthermore, this molecular formula of sphingosine suggested that the olefinic moiety is located in the long chain base (LCB).

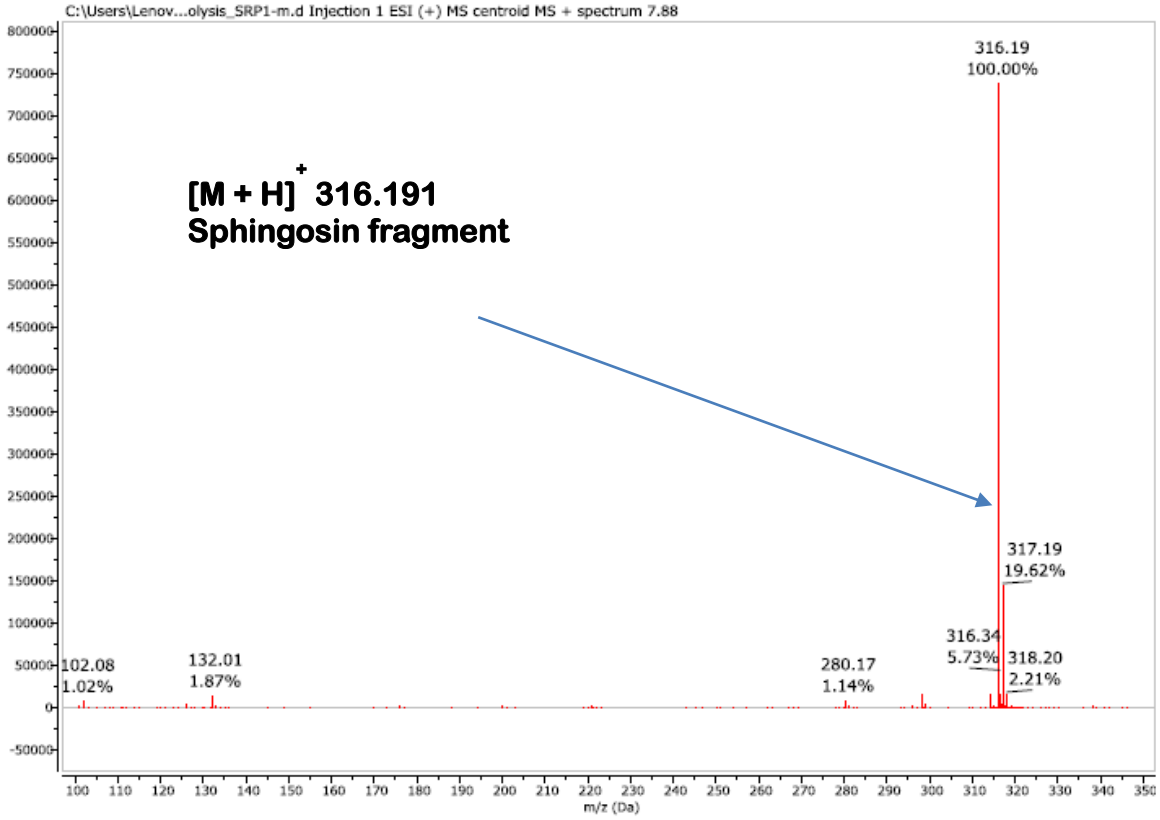

Figure 11: ESI-MS spectrum of methanolysis of SRP1

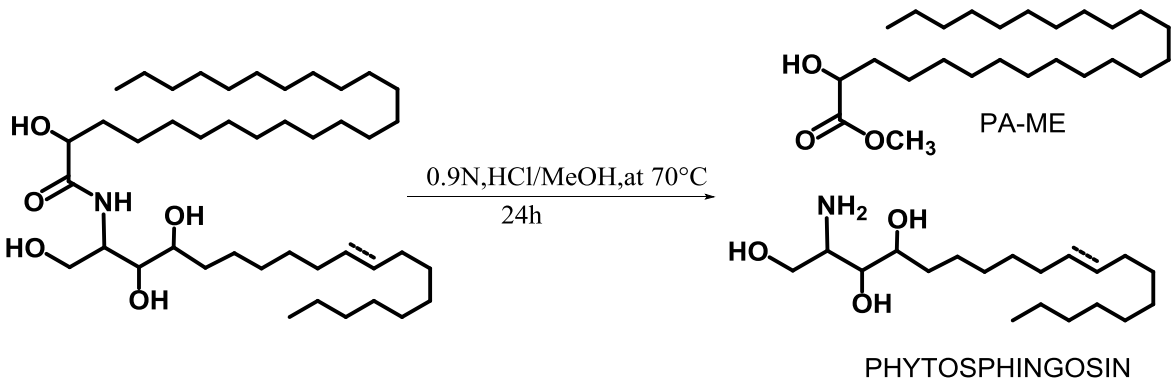

In the HMBC spectrum of SRP1 (Figure 13), ^{2}J correlations were observed between the olefinic proton at δ_H 5.32 and carbon C-12 (δ_C 32.5); H-15 at δ_H 1.21 with C-16 carbon (δ_C 31.8). Finally, H-17 at δ_H 1.20 showed a ^{3}J correlation with C-18 of the terminal methyl. All of these correlations (Figure 12) made it possible to locate the double bond at Δ^{10} on the long basic chain.

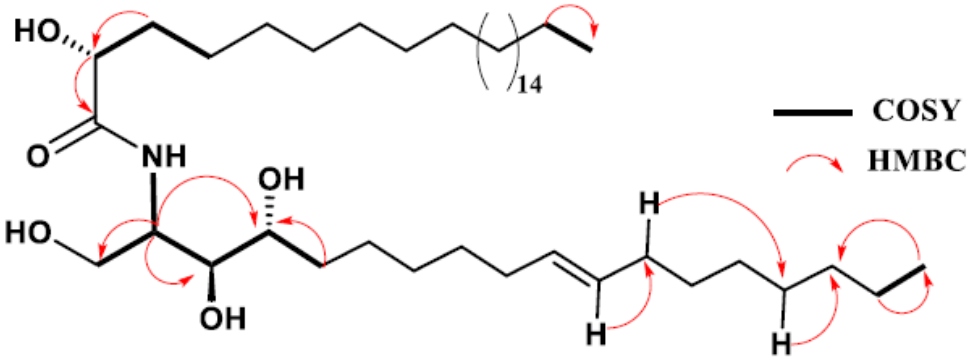

Figure 12: Important HMBC and COSY correlations of SRP1

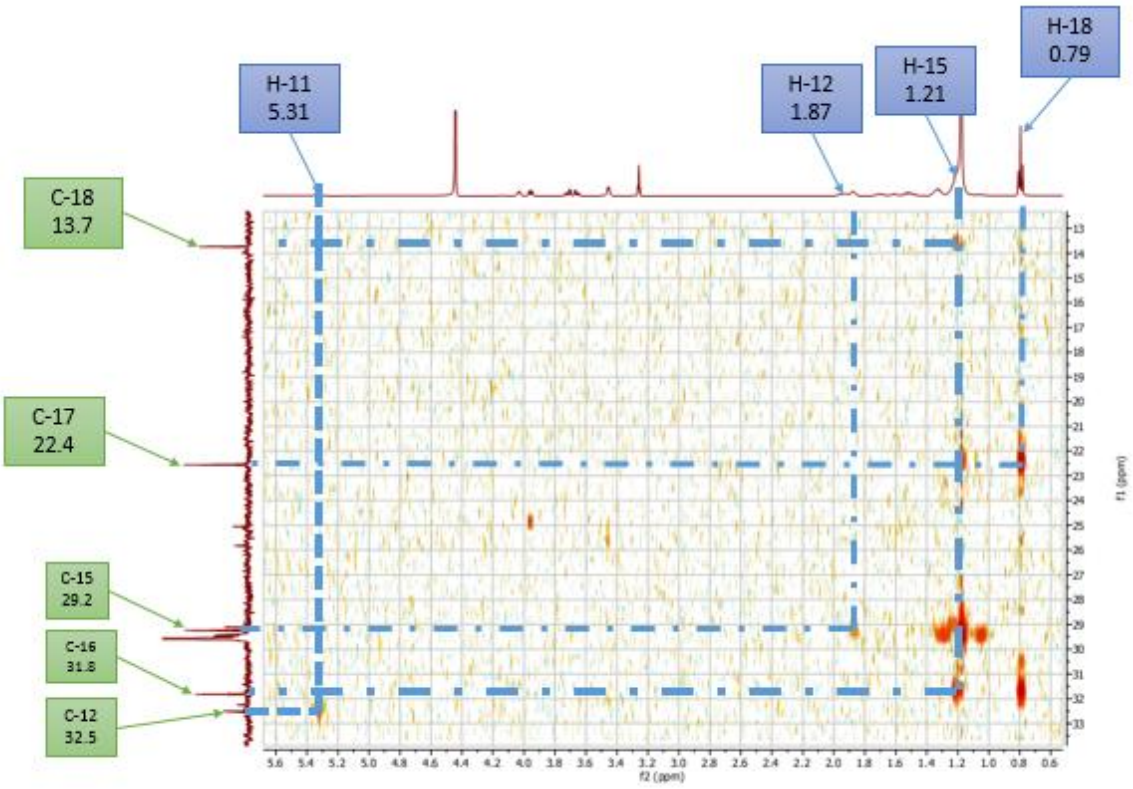

Figure 13 : HMBC spectrum of SRP1

This information was confirmed by the ESI-MS/MS spectrum (Figure 15) on which the ions peaks $[M+H-C_9H_{17}]^+$ at *m/z* 571.5 and $[M+H-C_7H_{15}]^+$ at *m/z* 619.5 corresponding to the allylic cleavages of the double bond, respectively for C9-C10 and C11-C12 were observed (Figure 14).

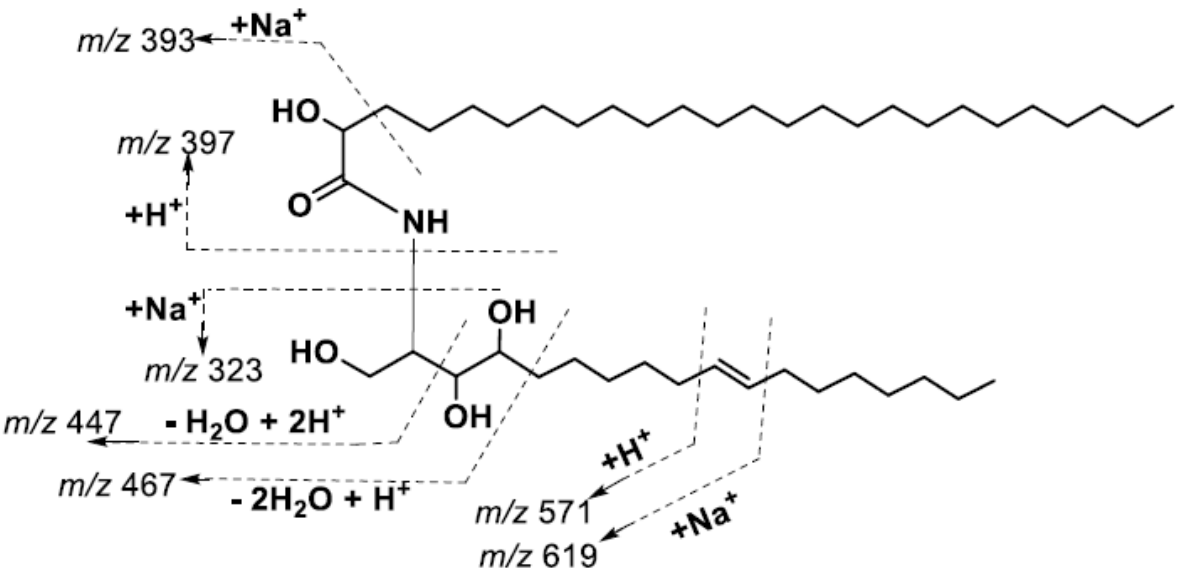

Figure 14: Mass fragmentation pattern of SRP1

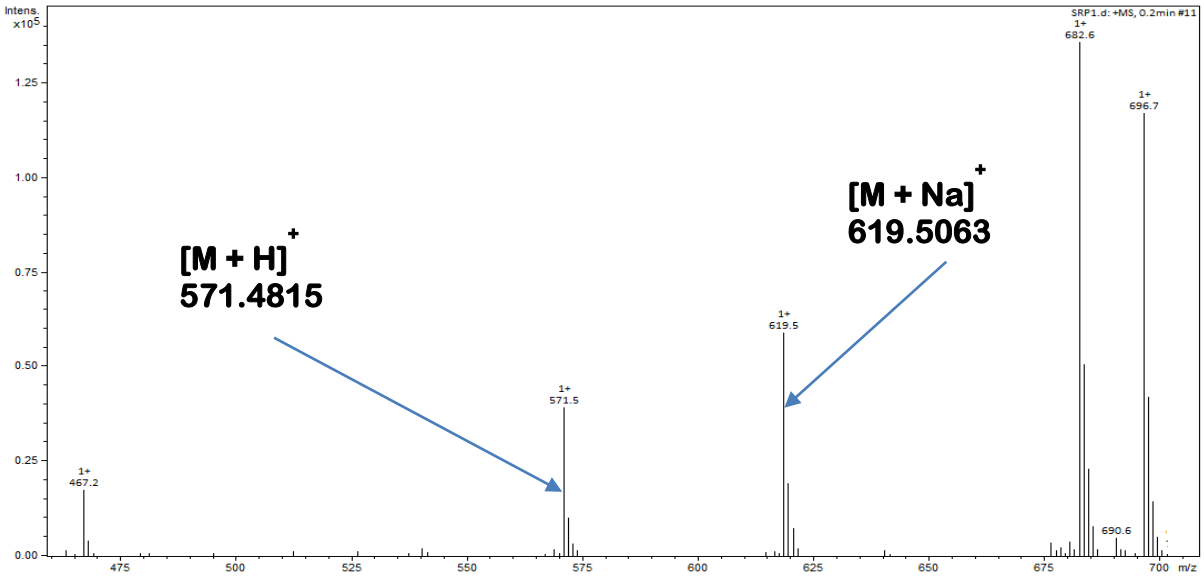

Figure 15: ESI-MS/MS spectrum of SRP1

The trans configuration of the C=C bond was evident from the chemical shifts of the allylic C-atoms at δ_C 32.5 and 32.0, which should have been less than 29.0 ppm if the configuration was cis (Simo et al. 2008, Wouamba et al. 2020). In addition, the absolute configurations at C(2), C(3), C(4), and C(2') were determined as (S), (S), (R), and (R) according to biogenetic consideration and previously reported data (**Ishii *et al.*, 2006**). Therefore, the structure of **90** was unambiguously determined as (2S,2'R,3S,4R,10E)-N-[2'hydroxypentacosanoyl]-2-amino-octadec-10-ene-1,3,4-triol, to which the trivial name rhombifoliamide was given and described here for the first time.

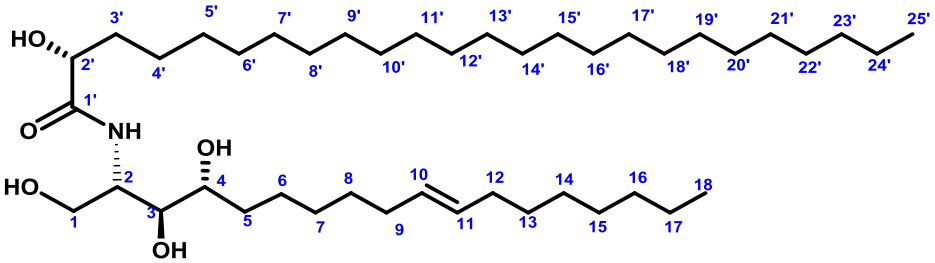

90

(2S,2'R,3S,4R,10E)-N-[2'hydroxypentacosanoyl]-2-amino-octadec-10-ene-1,3,4-triol

Table 17: ^{1}H (600 MHz) and ^{13}C (150 MHz) NMR data of SRP1 in $CDCl_3$

Position	*δH*	*δC*	DEPT
Long chaine base			
1a, 1b	3.72 (dd,*J*=4.6 ;11.5) 3.66 (dd,J=4.6 ;11.4)	60.9	CH2
2	4.3 (m)	51.5	CH
3	3.46 (m)	75.3	CH
4	3.45 (m)	72.1	CH
5a,5b	1.55 (m) 1.55 (m)	25.5	CH2
6----8, 13, 14 (CH_2 groups)	1.18 (br s)	29,1-----29.6	CH2
9	1.87 (m)	32.5	CH2
10	5.32 (m)	129.8^{β}	CH
11	5.32 (m)	130.5^{β}	CH
12	1.87 (m)	32.5	CH2
15	1.21 (m)	29.2	CH2
16	1.64 (m)	31.8	CH2
17	1.20 (m)	22.5^{γ}	CH2
18	0.69 (t, *J*=6.9)	13.7	CH3
NH	-----	------	---
N-acyl moety			
1'	-----	175.4	C
2'	3.95 (dd, *J*=3.7 ; 8.1)	71.8	CH
3'a, 3'b	1.70 (m) 1.50 (m)	34.4	CH2
4'---23'(CH_2 groups)	1.18 (br, s)	29,1-----29.6	CH2
24'	1.20 (m)	22.5^{γ}	CH2
25'	0.69 (t, *J*=6.9)	13.7	CH3

II.2.2 Phenolic compounds

II.2.2.1 Coumarines

II.2.2.1.1 Identification of SAA2

SAA2 obtained as a white powder from *Sida acuta* in a gradient elution of Hex-EA (65-35). Its ^{1}H NMR spectrum (Figure 16) displayed a typical AB system, characteristic of a coumarin lactone at δ_H 6.26 (1H, *d*, *J* = 9.5 Hz) and 7.96 (1H, *d*, *J* = 9.5 Hz) assigned to H-3 and H-4, respectively (**Steck et *al*., 1972**). In addition, two signals of aromatic protons were obtained at δ_H 7.78 (1H, *s*) and 6.97 (1H, *s*) and two more olefinic protons signal at δ_H 6.88 (1H, *d*, *J* = 16.2 Hz) and 6.47 (1H, *d*, *J* = 16.2 Hz) which confirm the (E) configuration.

The presence of the methoxyl group was evident from the sharp singlet at δ_H 3.98 (3H, *s*). Moreover, the signal at δ_H 1.34 (6H,s) was attributed to both methyl groups.

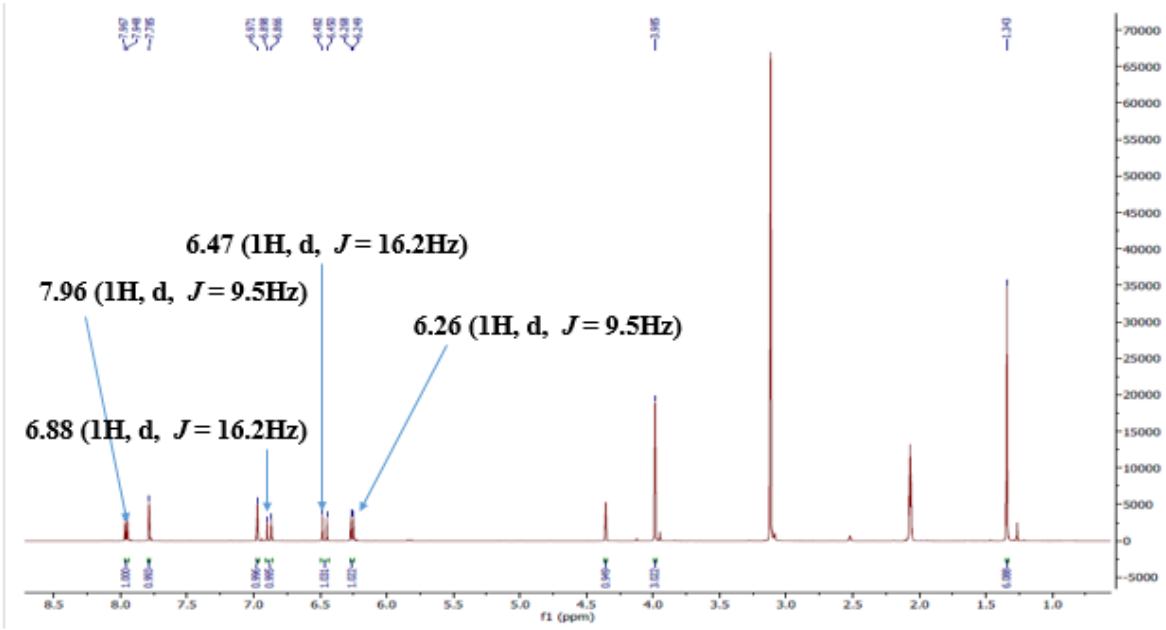

Figure 16: ^{1}H NMR (500 MHz, CD_3COCD_3) spectrum of SAA2

The ^{13}C NMR spectrum of SAA2 (Figure 17) exhibited fourteen signals, corresponding to fifteen carbon atoms which were sorted out into 6 quaternary carbons at δ_c 160.1 (C-2), 159.8 (C-7) , 155.2 (C-8a), 124.0 (C-6), 113.0 (C-4a), 69.8 (C-3') , 6 methines at δ_c 144.1 (C-4), 140.5 (C-2'), 125.4 (C-5), 118.5 (C-1'), 112.9 (C-3), 99.0 (C-9), one methoxyl at δ_c 55.9 and a methyl at δ_c 29.8.

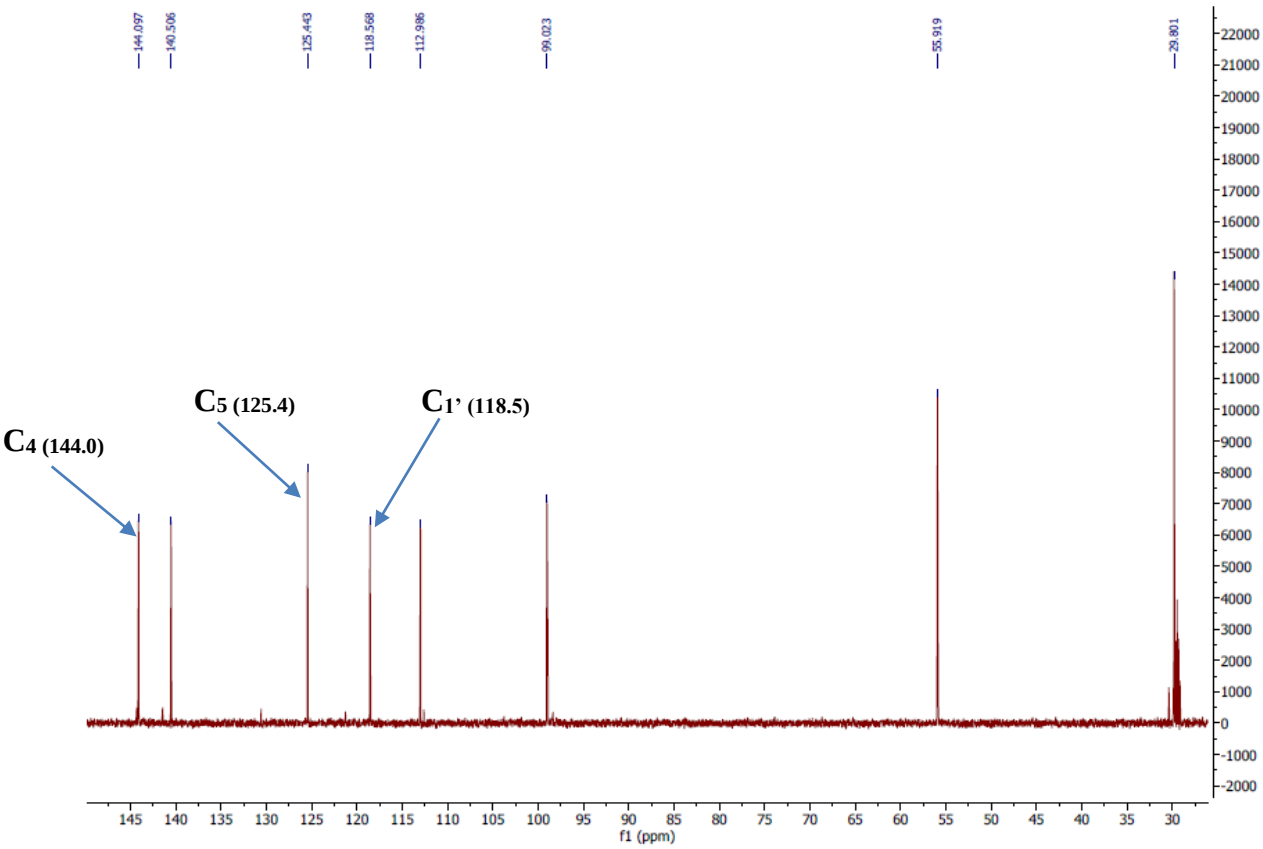

Figure 17: ^{13}C NMR broadband decoupled (125 MHz, CD_3COCD_3) spectrum of SAA2

The NMR (^{13}C: 125 MHz, CD_3COCD_3 and ^{1}H: 500 MHz, CD_3COCD_3) data of SAA2 in comparison with (E)-Suberenol of the literature are represented in the table 18 below:

Table 18: NMR (13C: 125 MHz, CD3COCD3 and 1H: 500 MHz, CD3COCD3) data of SAA2 in comparison with (E)-Suberenol of the literature (Herath et al., 2004).

	^{1}H NMR (500 MHz, CD_3COCD_3) SAA2	^{13}C NMR (125 MHz, CD_3COCD_3) SAA2	^{1}H NMR (200 MHz, $CDCl_3$) Suberenol	^{13}CNMR (50 MHz, $CDCl_3$)
2		160.1		162.3
3	6.26 (1H , d, 9.5Hz)	112.9	6.27 (1H , d, J = 9.4 Hz)	112.8
4	7.96 (1H, d, 9.5Hz)	144.1	7.75 (1H d, J = 9.4 Hz),	144.3
4a		113.2		112.3
5	7.78 (1H, s)	125.4	7.65 (1H s)	125.5
6		124.0		124.6
7		159.8		160.3
8	6.97 (1H, s)	99.0	6.81 (1H, s)	98.8
8a		155.2		155.0
1’	6.88 (1H, d, 16.2 Hz)	118.5	6.85 (1H, d ; J = 16.0 Hz)	119 .5
2’	6.47 (1H, d, 16.2 Hz)	140.7	6.38 (1H, d J = 16.0 Hz),	139.6
3’		69.8		70.6
4’ 2x CH3	1.34 (6H, s)	29.8	1.44 (6H, s)	29.1
OCH3	3.98 (3H, s)	55.9	3.96 (3H, s)	55.7

These informations compared to those obtained from the literature data (**Herath et *al*., 2004**) led to the identification of SAA2 as (E)-Suberenol **91,** known to have a potential antimicrobial effect on *S typhi* (**Nsangou et *al*., 2021**).

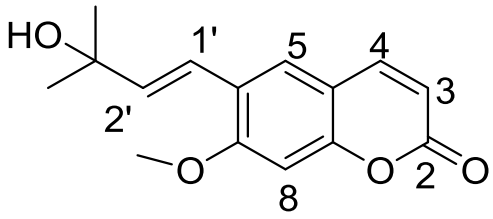

91

II.2.2.1.2 Identification of SAA1

SAA1 obtained as a white powder from *Sida acuta* in the mixure Hex-EA (90-10). Its ^{1}H NMR spectrum (Figure 18) displayed two pairs of typical AB system, at δ_H 6.19 (1H, *d*, *J* = 9.6 Hz) and 7.84 (1H, *d*, *J* = 9.5 Hz) and δ_H 6.48 (1H, *d*, *J* = 9.9 Hz) and δ_H 5.83 (1H, *d*, *J* = 9.9 Hz) belonging to proton 3,4 and 4',3' respectively . In addition, two signals of aromatic protons were obtained at δ_H 7.33 (1H, *s*) and 6.65 (1H, *s*) which were assigned to para-protons H-5 and H-8 respectively. Finally, one signal at δ_H 1.46 (6H,s) was attributed to two methyl groups.

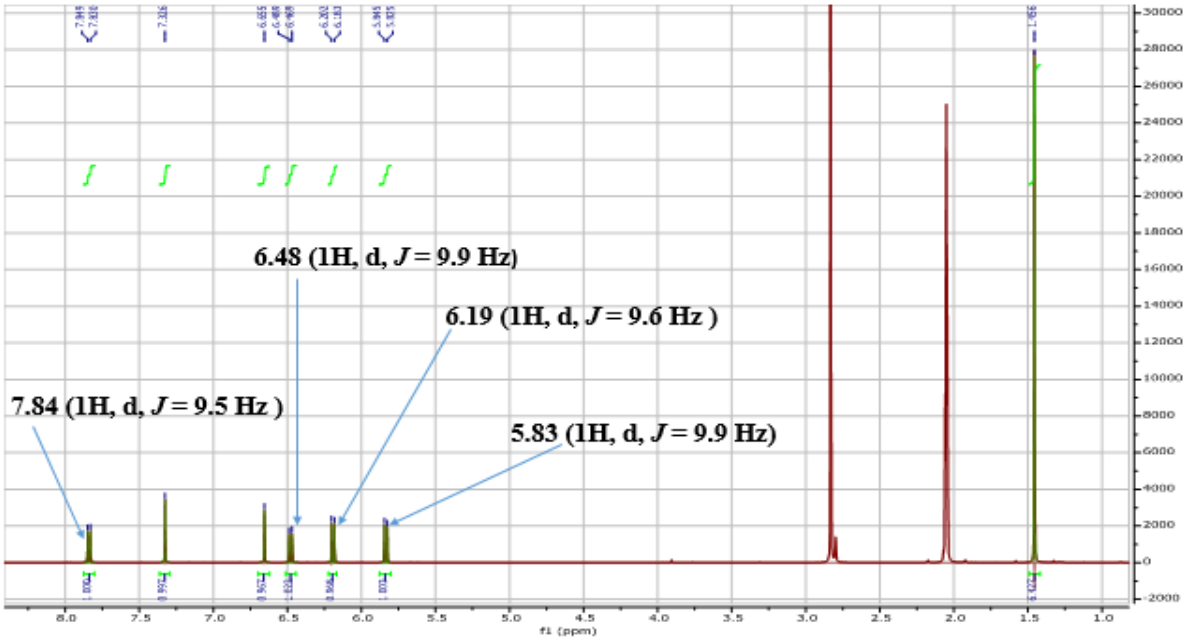

Figure 18: ^{1}H NMR (500 MHz, CD_3COCD_3) spectrum of SAA1

The ^{13}C NMR spectrum (Figure 19) of SAA1 exhibited thirteen signals, corresponding to fourteen carbon atoms determined as 6 quaternary at δ_c 159.8 (C-2), 155.5 (C-8a) , 156.6 (C-7), 118.4 (C-6), 112.8 (C-4a), 77.5 (C-2') , 6 methines at δ_c 131.1(C-3'), 120.6 (C-4') 143.5 (C-4), 125.4(C-5), 112.9(C-3), 103.5 (C-8) and a methyl at δ_c 27.5.

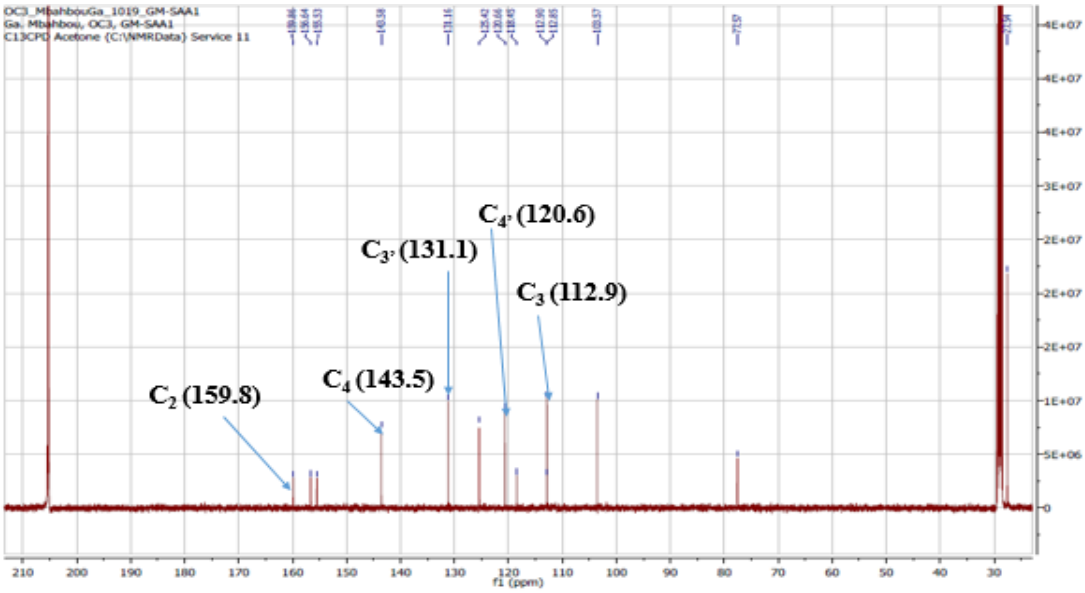

Figure 19: ^{13}C NMR broadband decoupled (125 MHz, CD_3COCD_3) spectrum of SAA1

The NMR (^{13}C: 125 MHz, CD_3COCD_3 and ^{1}H: 500 MHz, CD_3COCD_3) data of SAA1 in comparison with xanthyletin of the literature are represented in the table 19 below.

Table 19: NMR (^{13}C: 125 MHz, CD_3COCD_3 and ^{1}H: 500 MHz, CD_3COCD_3) data of SAA1 in comparison with xanthyletin of the literature (Tian-Shung *et al*., 1983).

	^{1}H NMR (500 MHz, CD_3COCD_3) SAA1	^{13}C NMR (125 MHz, CD_3COCD_3) SAA1	^{1}H NMR (300 MHz, $CDCl_3$) xanthyletin	^{13}C NMR (75 MHz, $CDCl_3$)
1				
2		159.8		161.1
3	6.19 (1H, d, *J* = 9.6 Hz,),	112.9	6.17 (1H, d, *J* = 9.6 Hz)	112.9
4	7.84 (1H, d, *J* = 9.5 Hz)	143.5	7.54 (1H, d, *J* = 9.6 Hz)	143.4
4a		112.8		112.7
5	7.33 (1H, s)	125.4	7.01 (1H, s)	124.8
6		118.4		118.5
7		156.6		156.8
8	6.65 (1H, s)	103.5	6.66 (1H ,s)	104.3
8a		155.5		155.4
2’		77.5		77.7
3’	5.83 (1H, d, *J* = 9.9 Hz)	131.1	5.65 (1H, d, *J* = 9.9 Hz)	131.2
4’	6.48 (1H, d, *J* = 9.9 Hz)	120.6	6.30 (1H, d, *J* = 9.9 Hz)	120.8
5’/6’	1.45 (6H, s)	27.5	1.43 (6H, s)	28.3

These informations compared to those obtained in the literature data (**Tian-Shung *et al.*, 1983**) led to identification of SAA1 as xanthyletin **92.** This compound is reported to have a potential antioxidant, anti-inflammatory, urease and anti-diabetic activities with IC_{50} values of 47.3 µM, 33.5 µM, 25.2 µM and 33.9 µM respectively (**Bissim *et al.*, 2020**).

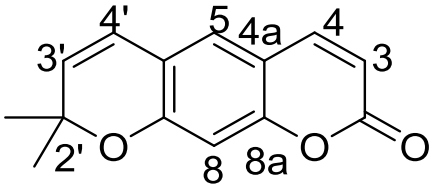

92

II.2.2.1.3 Identification of SAA3

SAA3 obtained as a white powder from *Sida acuta* in the mixure Hex-EA (60-4O). We observed here similarities with SAA2 described above but some differences can be noted.

The presence of two typical aromatic proton singlets at δ_H 6.93 (H-8) and 7.73 (H-5) in the ^{1}H NMR spectrum (Figure 20) indicated a 6, 7-disubstituted coumarin. In addition, the ^{1}H NMR spectrum showed proton signals at δ_H 4.82 (1H, d, J = 5.5 Hz, H-1'), 4.71 (1H, d, J = 5.5 Hz, H-2'), 3.93 (1H, s, H-4'), 4.83 (1H, s, H-4'), and 1.78 (3H, s, H-5') and on the other hand, the ^{13}C NMR spectrum (figure 22) showed signals at δ_C 79.3 (C-1'), 99.5 (C-2'), 145.5 (C-3'), 112.0 (C-4') and 19.4 (C-5'), indicating the existence of a 3, 4-dioxygenated-2-methyl-butylene chain.

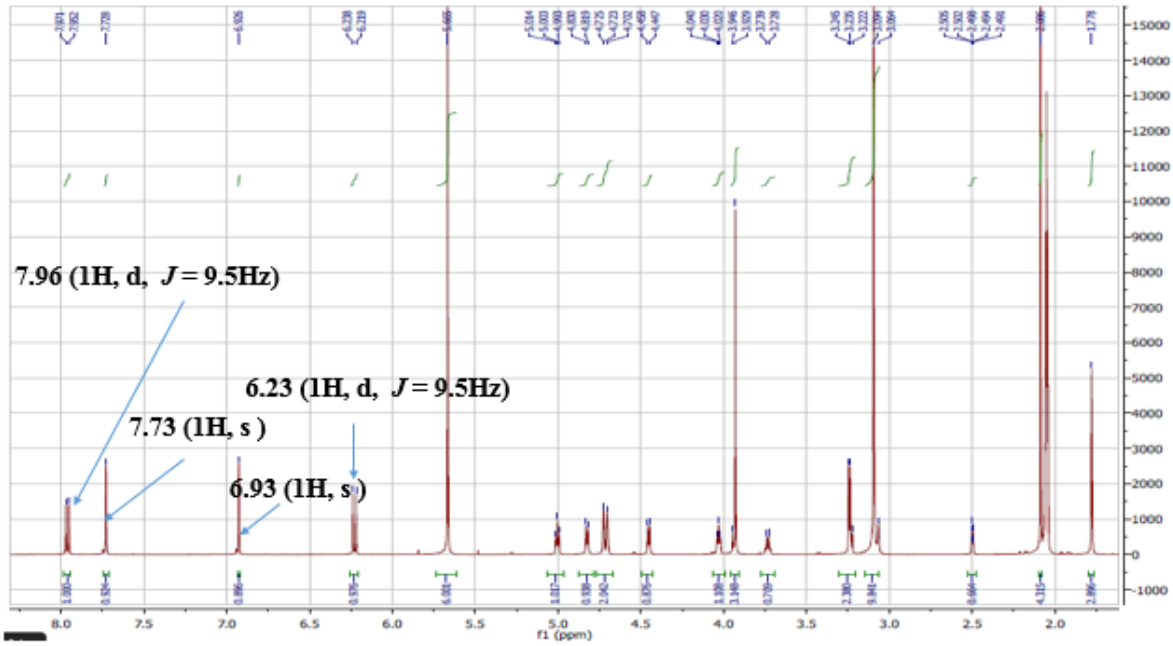

Figure 20:^{1}H NMR (500 MHz, CD_3COCD_3) spectrum of SAA3

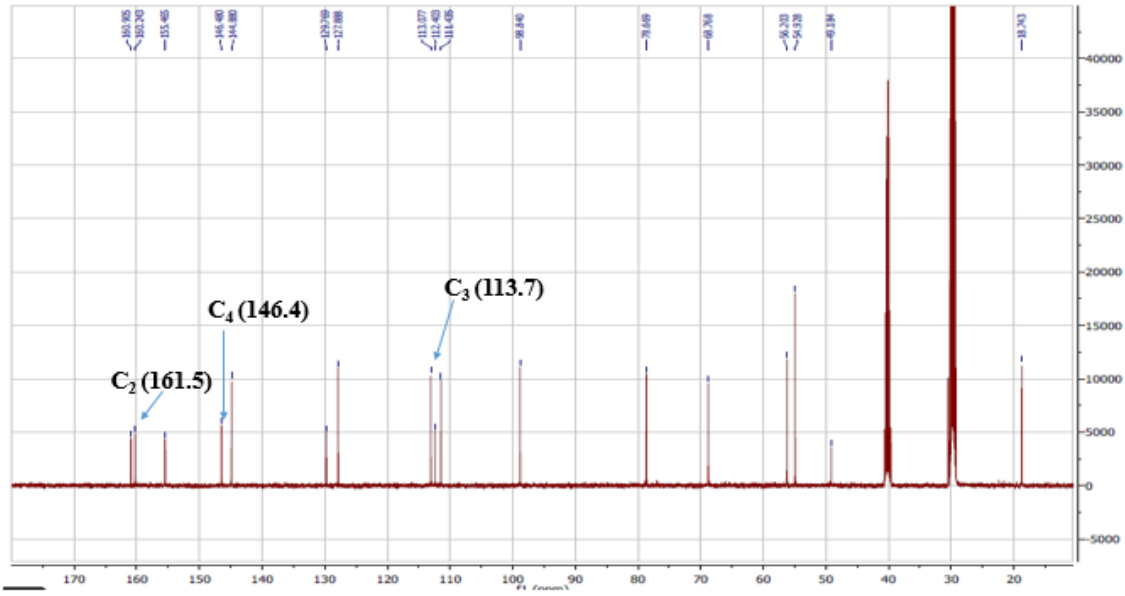

Figure 21: **^{13}C NMR broadband decoupled (125 MHz, CD_3COCD_3) spectrum of SAA3**

The NMR (^{13}C: 125 MHz, CD_3COCD_3 and ^{1}H: 500 MHz, CD_3COCD_3) data of SAA3 in comparison with thamnosmonin of the literature are represented in the table 20 below:

Table 20: NMR (^{13}C: 125 MHz, CD_3COCD_3 and ^{1}H: 500 MHz, CD_3COCD_3) data of SAA3 in comparison with thamnosmonin of the literature (Chang et *al.*, 1976).

	^{1}H NMR (500MHz, CD_3COCD_3) SAA3	^{13}C NMR (125 MHz, CD_3COCD_3) SAA3	^{1}H NMR (250 MHz, DMSO) Thamnosmonin.	^{13}C NMR (62.5 MHz, DMSO)
2		161.5		160.4
3	7.96 (1H , d, J = 9.5 Hz)	113.7	6.26 (1H, d, J = 9.4 Hz)	113.2
4	6.23 (1H,d, J = 9.5 Hz)	147.1	7.60 (1H, d, J = 9.4 Hz)	144.3
4a		113.0		112.6
5	7.73 (1H, s)	128.5	7.94 (1H, s)	128.6
6		130.4		127.2
7		156.1		150.2
8	6.93 (1H, s)	99.5	6.73 (1H, s)	99.0
8a		145.5		149.9
1’	4.82 (1H, d, J = 5.5 Hz)	69.4	5.66 (1H, d, J = 4.4 Hz)	80.6
2’	4.71 (1H, d, J = 5.5 Hz)	79.3	5.36 (1H , d, J = 4.4 Hz)	80.0
3’		143.4		145.2
4’	3.93, 4.83 (, s)	112.9	4.78, 4.83 (s)	112.8
5’	1.78 (3H, s,)	19.4	2.01 (3H s)	18.5

The comparison of SAA3 with literature data (**Chang et *al*,. 1976**) led to its characterization as Thamnosmonin.

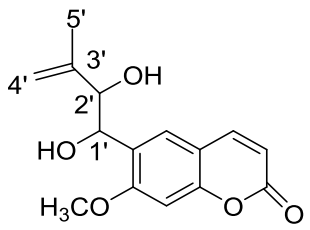

93

II.2.2.2 Xanthones

II.2.2.2.1 Identification of SRYK3

SRYK3 was obtained as a yellow powder from *Sida rhombifoila* in a mixure Hex-EA (40-6O).Its ESI-MS showed the pseudo-molecular ion peak $[M+H]^+$ at *m/z* = 229.0701 compatible with a molecular mass of 228.0423 , which in conjunction with NMR data suggested a molecular formula $C_{13}H_8O_4$ corresponding to four degree of insaturations.

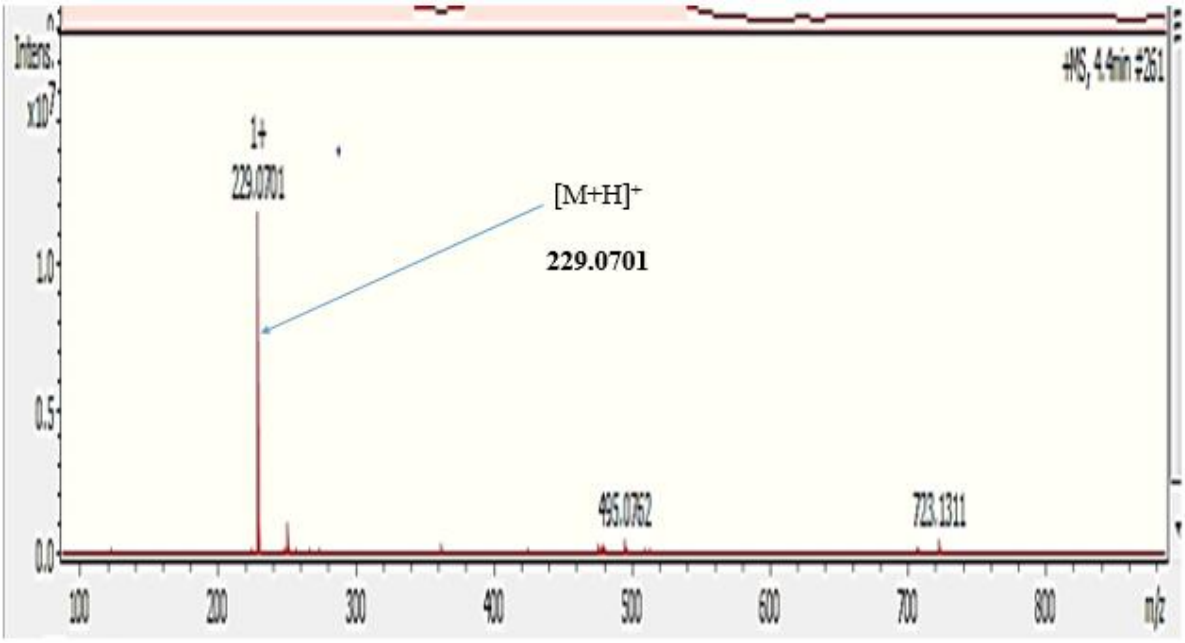

Figure 22: **ESI-MS spectrum of SRYK3**

Its ^1H NMR spectrum (Figure 23) revealed signals for an ABC spin system for a 1, 2, 3-trisubstituted benzene ring as follows:

- A triplet displayed at δ_H 7.63 (1H, t, *J* = 8.3 Hz, H_3) was shown to be mutually coupling with δ_H 6.75 (1H, dd, *J* = 8.2; 0.9 Hz, H_4), and δ_H 6.97 (1H, dd, *J* = 8.5; 0.9 Hz), all depicting the existence of an ABC spin system (Figure 23).
- Another ABX system of three protons including two doublets at δ_H 7.45 (1H ,d, *J* = 9.0 Hz, H_8) and 7.53 (1H, d, *J* = 3.0 Hz, H_5) and one doublet of doublet at δ_H 7.32 (1H, dd, *J* = 9.0; 3.0 Hz, H_7).

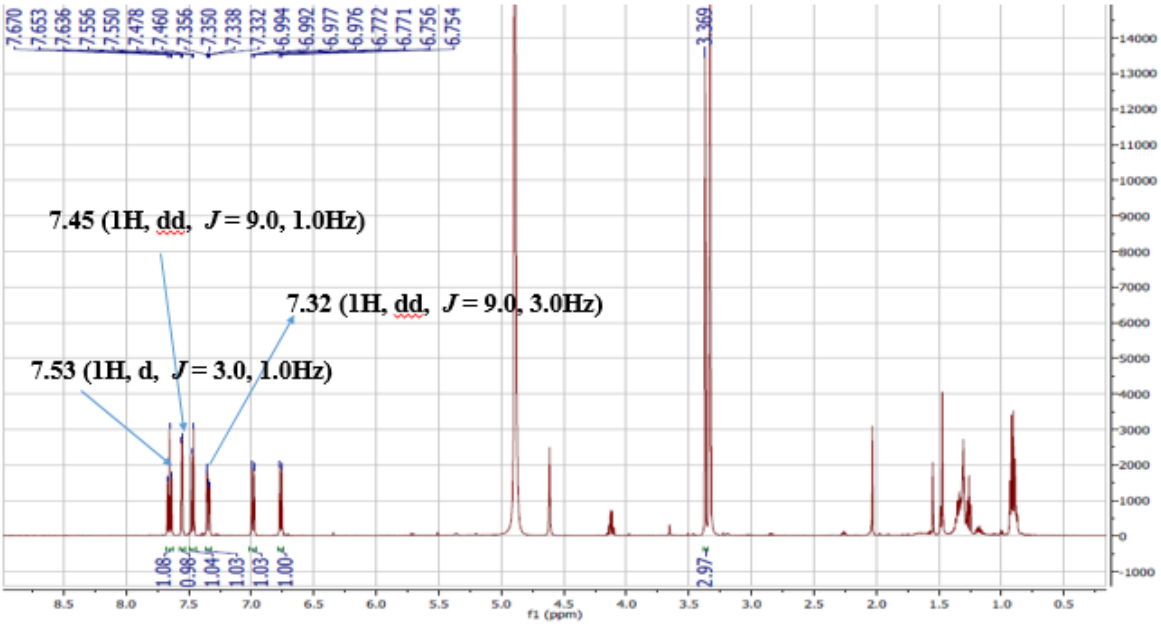

Figure 23: **^{1}H NMR (500 MHz,CD_3OD) spectrum of SRYK3**

The NMR (^{1}H: 500 MHz, CD_3OD) data of SRYK3 in comparison with 1.6-dihydroxyxanthone of the literature are represented in the table 21 below:

Table 21: NMR (^{1}H: 500 MHz, CD_3OD) data of SRYK3 in comparison with 1.6-dihydroxyxanthone of **the literature (Singh et *al.*, 1993).**

Position	^{1}HNMR (500 MHz, CD_3OD) SRYK3	^{1}HNMR (400 MHz, $CDCl_3$) 1.6-dihydroxyxanthone
2	6.97 (1H, dd, *J* = 8.5;0.9 Hz, 1H),	7.05 (1H, dd, *J* = 8.0 ; 0.8 Hz)
3	7.63 (1H, t, *J* = 8.3 Hz, 1H)	7.71 (1H, t, *J* = 8.0 Hz)
4	6.75 (1H, dd, *J* = 8.2 ; 0.9 Hz, 1H),	6.79 (1H, dd, *J* = 8.0 ; 0.8 Hz)
5	7.53 (1H, d, *J* = 3.0 Hz)	7.45 (d, *J* = 2.8 Hz)
7	7.32 (1H, dd, *J* = 9.0 ; 3.0 Hz)	7.36 (1H, dd, *J* = 8.8 ; 2.8 Hz)
8	7.45 (1H, d, *J* = 9.0 Hz, 1H),	7.55 (1H, d, *J* = 8.8 Hz)

These informations compared to 1.6-dihydroxyxanthone of the literature data led to the determination of SRYK3 as 1.6-dihydroxyxanthone **(Singh et *al.*, 1993).**

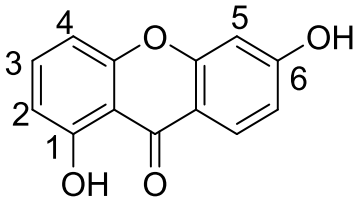

94

II.2.2.2.2 Identification of GO4

Compound GO4 was obtained from the bark of *Garcinia ovalifolia* as a yellow powder and soluble in methylene chloride. It reacts positively with ferric chloride test characteristic of phenolic compounds. The ^{1}H NMR (Figure 24) and ^{13}C NMR (Figure 25) spectra showed resonances of a chelated hydroxyl group at [δ_H 13.11 (1-OH)] and carbonyl carbon at [δ_C 183.3 (s, C-9)]. Moreover, the presence of 2 isolated penta-substituted aromatic protons at [δ_H 6.30 (1H, s, H-2); δc 99.4 (C-2)] and at [δ_H 7.52 (1H, s, H-8); δ_C 113.5 (C-8)] respectively.

We also observed a cis olefinic group at [δ_H 6.93 (1H, dd, J = 9.9Hz, H-11) and 5.65 (1H, d, J = 9.9 Hz, H-12); δ_C 127.14 (C-12) and 115.18 (C-11)]. Furthermore, another cis olefinic group was observed at [δ_H 6.49 (1H, d, J = 9.9 Hz, H-16)] and 5.78 (1H, d, J = 9.9 Hz, H-17)]; with corresponding carbons at δ_C 121.5 (d, C-16) and 131.0 (d, C-17)]. The ^{1}H NMR spectrum showed four tertiary methyls attached to the oxygenated carbon [δ_H 1.53 (6H, s, 3H-14 and H3-15), δc 79.0 (C-13) and 28.5 (C-14 and C-15); [δ_H 1.78(6H, s, H3-19 and H3-20), δc 78.2 (C-18) and 28.3 (C-19 and C-20)].

In addition, we have 9 substituted aromatic carbons at δ_C 163.1 (C-1); 160.6 (C-3); 151.6 (C-4a); 144.8 (C-10a); 132.4 (C-5); 113.5 (C-8); 117.8 (C-8a); 103.3 (C-9a) and 101.4 (C-4), five of which are oxygenated (Figure 24 and 25).

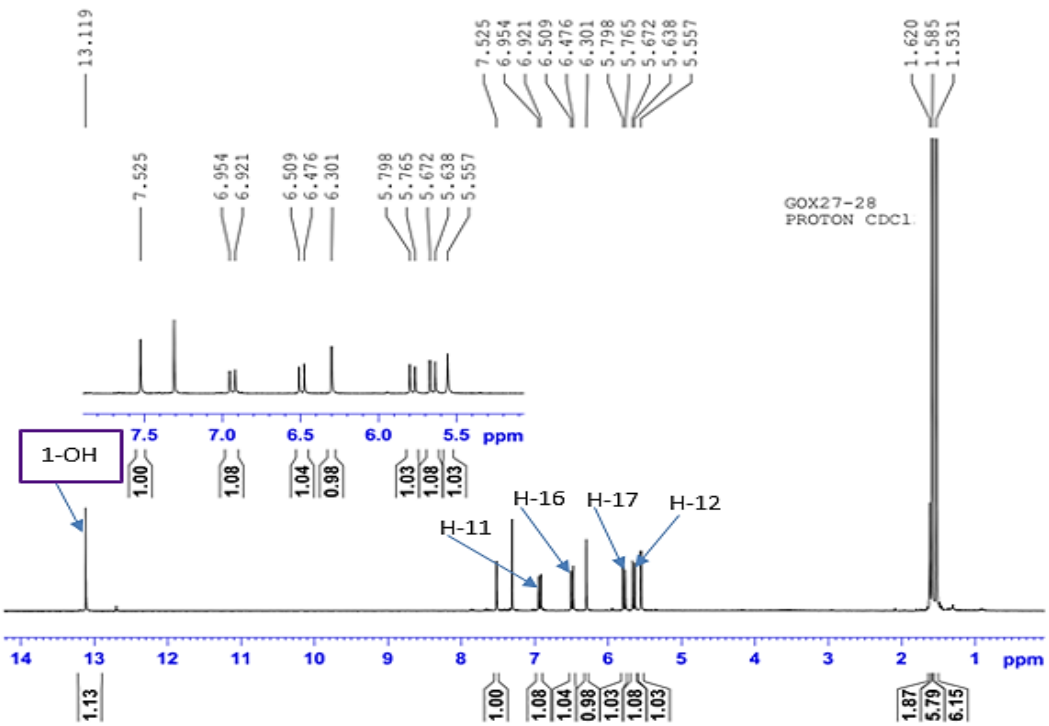

Figure 24: **^{1}H NMR spectrum of (300 MHz, $CDCl_3$) of GO4**

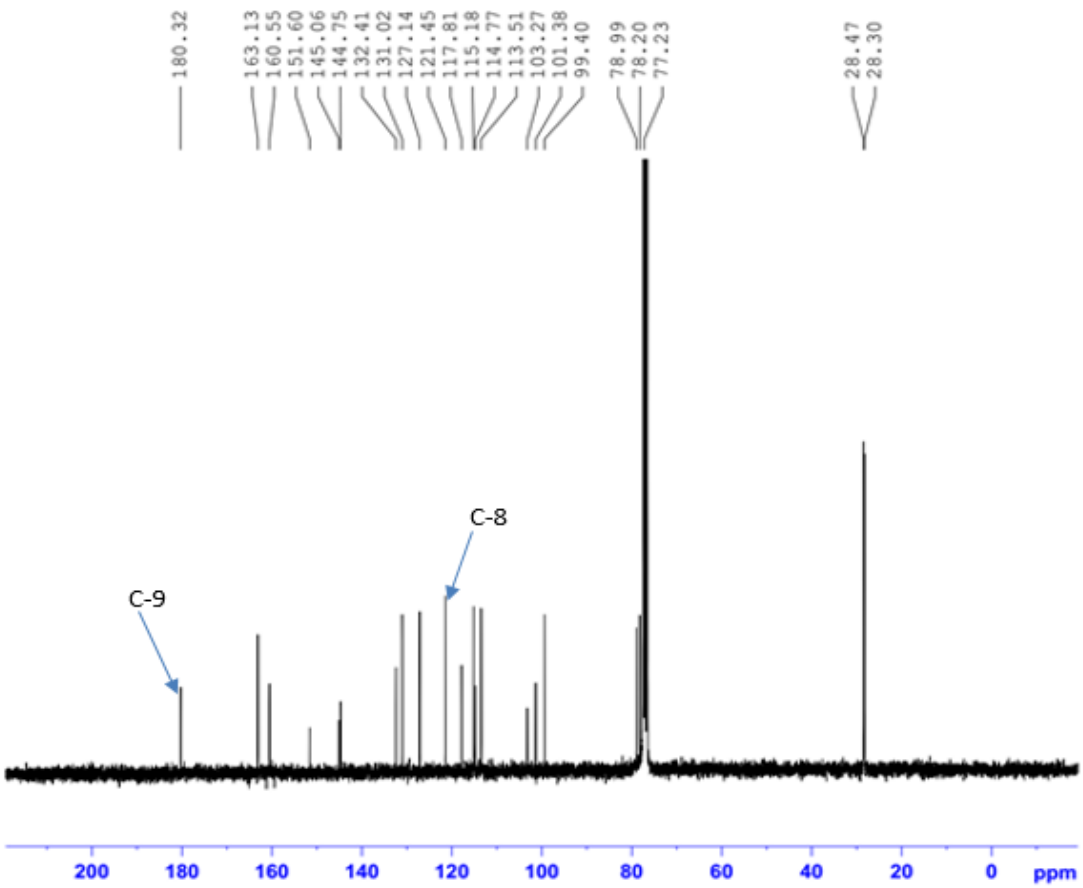

Figure 25: **^{13}C NMR broadband decoupled spectrum of (75 MHz, $CDCl_3$) of G04**

The ^{13}C NMR spectral data (75 MHz, $CDCl_3$) and ^{1}H NMR (300 MHz, $CDCl_3$) of GO4 compared rheediaxanthone A of the literature are represented in the table 22 below:

Table 22:^{13}C NMR spectral data (75 MHz, $CDCl_3$) and ^{1}H NMR (300 MHz, $CDCl_3$) of GO4 compared with rheediaxanthone A of the literature (Lien *et* al., 2003).

Position	NMR ^{13}C (75 MHz, $CDCl_3$) GO4	NMR ^{13}C (75 MHz,CD_3COCD_3) Rheediaxanthone A
1	163.1	164.5
2	99.4	99.9
3	160.6	161.6
4	101.5	102.5
4a	151.6	152.8
5	132.4	134.9
6	145.1	147.1
7	114.8	115.7
8	113.5	113.7
8a	117.8	119.9
9	180.3	181.6
9a	1033	104.1
10a	144.8	147.0

11	115.2	116.0
12	127.1	128.6
13	79.0	79.43
14	28.5	28.8
15	28.5	28.8
16	121.5	122.4
17	131.0	133.0
18	78.2	79.35
19	28.3	28.7
20	28.3	28.7

These information compared to literature data (**Lien et *al*., 2003**) led to its identification as Rheediaxanthone A. This compound is reported to have a potential antitumor-promoting activity (**Ito *et al*., 2018**).

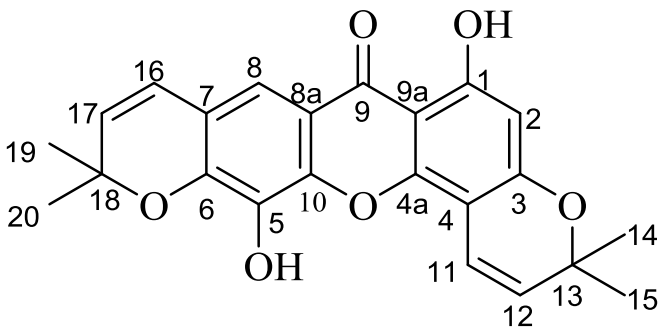

95

II.2.2.3 Flavonoids

II.2.2.3.1 Identification of SAB4

SB4 obtained as a white powder from *Sida rhombifolia* in a mixure Hex-EA (50-50), revealed in its ^{1}H NMR spectrum (Figure 26) a set of signals assignable to 7, 5, 4'-trihydroxy flavonol and a sugar unit. The kaempferol unit was confirmed by two doublets at δ_H 6.21 and δ_H 6.41 (J = 2.2 Hz) for H-6 and H-8 respectively and a pair of doublets at δ_H 8.06 and δ_H 6.90 (J = 8.8 Hz) (**Da Costa et *al*., 2007**) assignable to H-2',6' and H-3',5', respectively. These data together confirm the presence of an AA',BB' system.

On the ^{1}H NMR spectrum (Figure 26), signals at δ_H 3.40-3.87 revealed the presence of a sugar unit and also a doublet at $\delta_{H_{1''}}$ 5.26 (J = 7.3 Hz) was ascribed to the anomeric proton H-1" of glucose. The diaxial coupling (J = 7.3 Hz) between H-1" and H-2" suggested a β-configuration (**Parveen and Khan, 1987**).

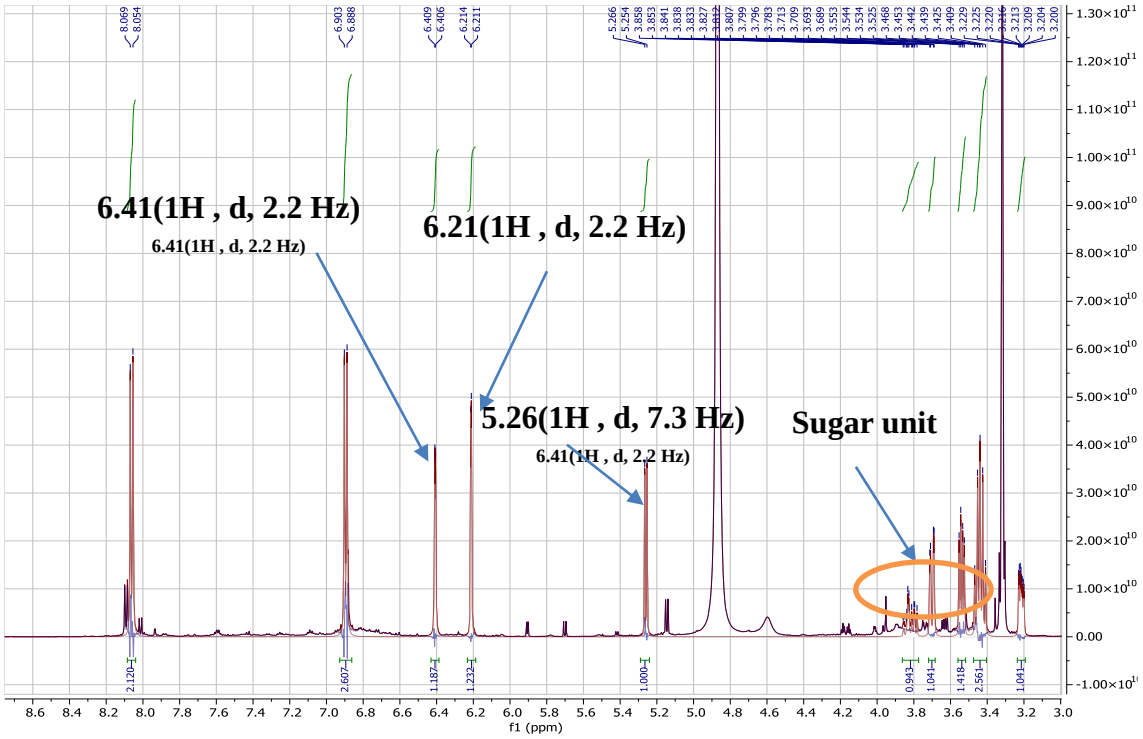

Figure 26: ^{1}H NMR (500 MHz, CD_3OD) spectrum of SAB4

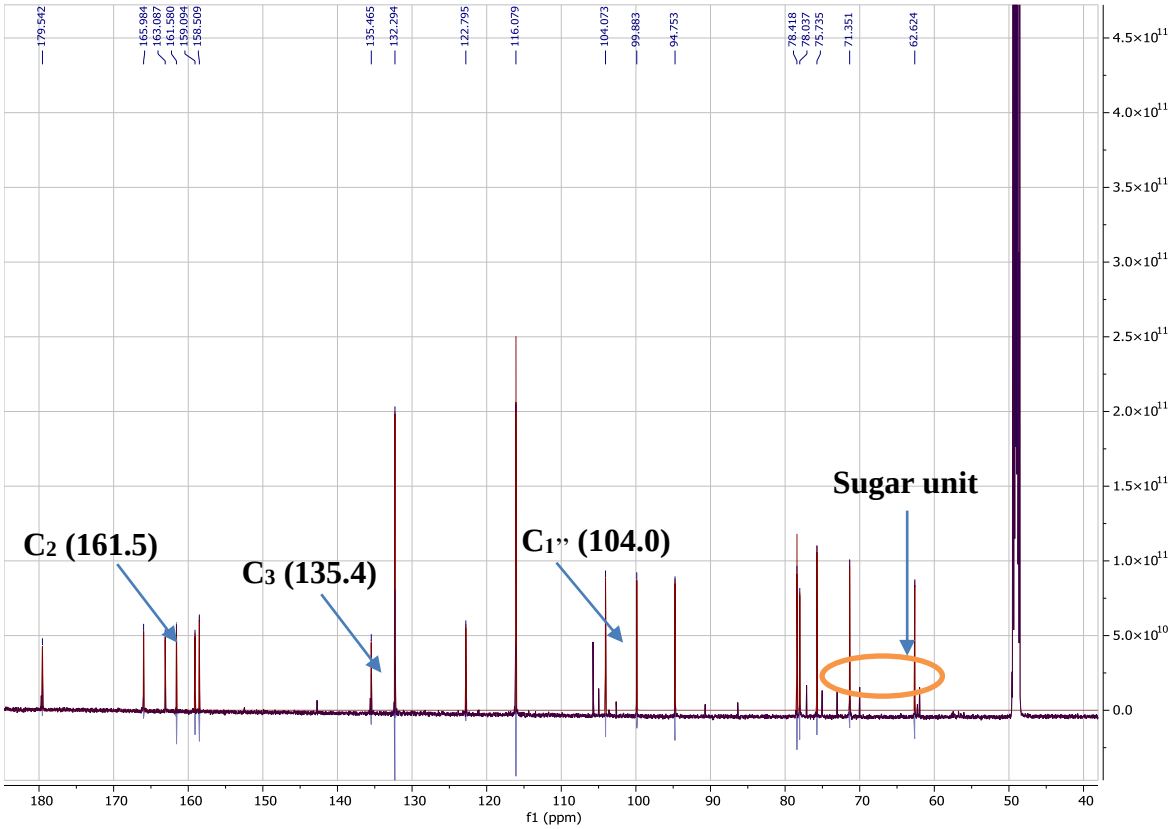

Figure 27: ^{13}C NMR broadband decoupled (125 MHz, CD_3OD) spectrum of SAB4

The NMR (^{13}C: 150 MHz, CD_3OD and ^{1}H: 600 MHz, CD_3OD) data of SAB4 in comparison with astragaline of the literature data are represented in the table 23 below:

Table 23: NMR (^{13}C: 150 MHz, CD_3OD and ^{1}H: 600 MHz, CD_3OD) data of SAB4 in comparison with astragaline of the literature (Deepralard *et al.*, 2009).

	^{1}H NMR (CD_3OD, 600 MHz):SAB4	^{13}C NMR (CD_3OD, 150 MHz): SAB4	^{1}H NMR (DMSO, 300 MHz): Astragaline	^{13}C NMR (DMSO, 75 MHz):
2		161.5		161.0
3		135.4		133.1
4		179.5		177.2
5		158.5		156.1
6	6.21 (1H, d, J = 2.2 Hz,)	99.8	6.20 (1H, d, J = 1.8 Hz)	98.7
7		163.0		164.0
8	6.41 (1H, d, J = 2.2 Hz)	94.7	6.43 (1H, d, J = 1.8 Hz)	93.6
9		157.0		156.2
10		104.0		103.9
1’		122.8		120.8
2’	8.06 (2H, d, *J* = 8.8 Hz)	132.2	8.02 (2H, d, J = 8.7 Hz)	130.7
3’	6.90 (2H, d, *J* = 8.8 Hz)	116.0	6.87 (2H, d, J = 8.7 Hz)	115.0
4’		159.0		159.8
5’		116.0		115.0
6’		132.2		130.7
1’’	5.26 (d, *J* = 7.3 Hz)	104.0	5.44 (1H, d, J = 7.2 Hz)	100.8
2’’		75.7		74.2
3’’		78.4		76.4
4’’		71.3		69.9
5’’		78.0		77.5
6’’		62.6.		60.9

This result confirmed SAB4 as astragaline (**Deepralard et *al*., 2009**).

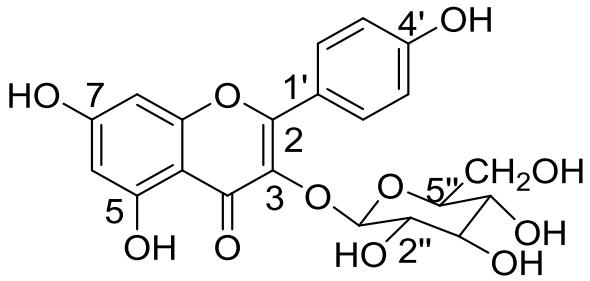

96

II.2.2.3.2 Identification of SRA3

SRA3 was obtained as a yellow powder from *Sida rhombifoila*. Its ESI-MS showed the pseudo-molecular ion peak $[M+H]^+$ at *m/z* = 595.1414, thus a molecular mass of 594.1334 in association with NMR data suggest a molecular formula $C_{30}H_{26}O_{13}$ corresponding to eighteen degree of unsaturations (Figure 28).

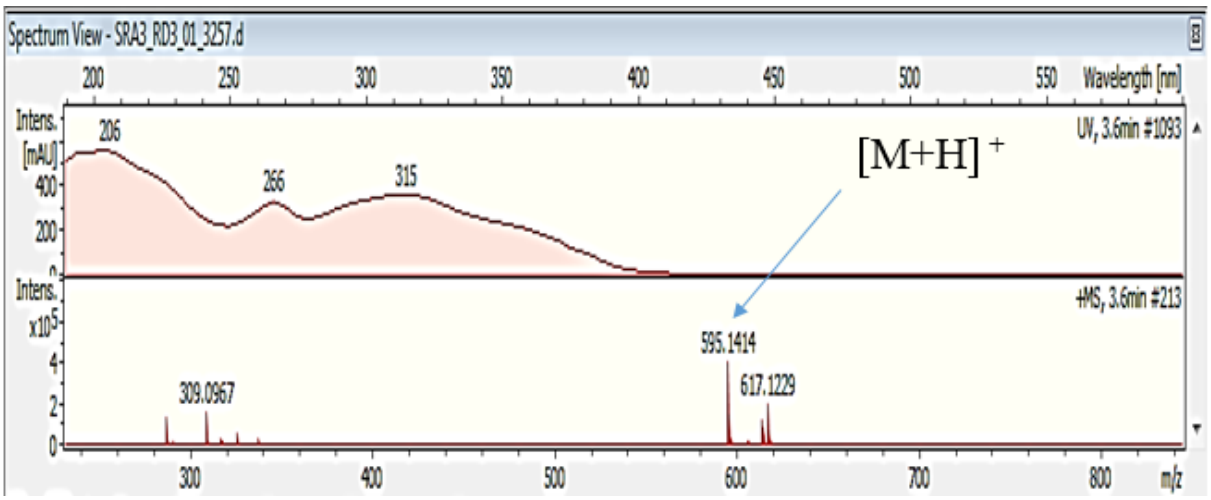

Figure 28: **ESI-MS spectrum of SRA3**

The ^{1}H NMR spectrum (Figure 29) shows similarities with SAB4 except for a set of signals characteristic of *p*-cynamoyl group. The presence of two doublets at δ_H 6.11 and δ 6.34 (*J* = 2 Hz) for H-6 and H-8 respectively and a pair of doublets at δ_H 7.95 and δ_H 7.33 (*J*= 8.9 Hz) for H-2',6' and H-3',5' respectively, indicated an AA',BB' system (**Da Costa et *al*., 2007**). Furthermore, the spectrum revealed signals between δ_H 3.33 and 4.32 suggesting the presence of a sugar unit. Also, the doublet at δ_H 5.11 (*J* = 7.3 Hz) was assignable to the anomeric proton H-1" of glucose.

The *p*-coumaroyl group was characterized by the presence of A A', B B'spin system of aromatic proton at δ 6.81 (2H, *d*, *J* = 8.5 Hz) and δ 6.74 (2H, *d*, *J* = 8.5 Hz) and two trans olefinic hydrogen signals at 6.07 (1H, *d*, *J* = 16 Hz) and 7.42 (1H, *d*, *J* = 16 Hz).

The diaxial coupling (*J* = 7.3 Hz) between H-1" and H-2" suggested a β-configuration (**Parveen and Khan, 1987**).

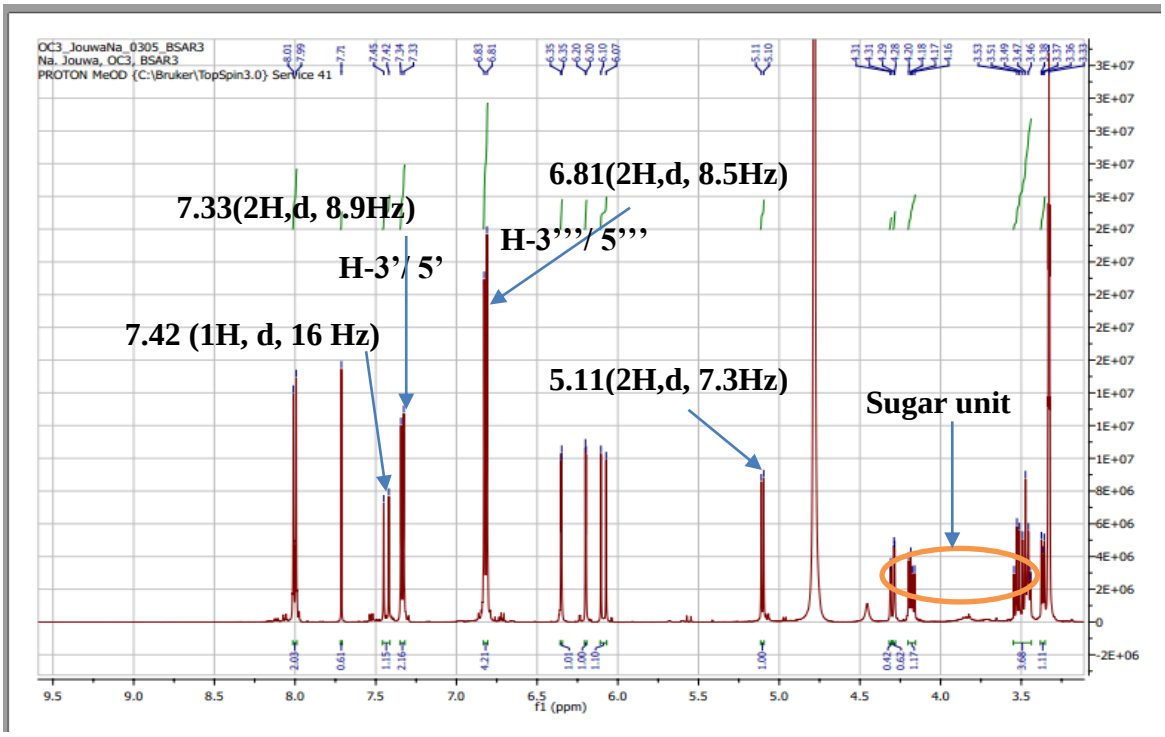

Figure 29: **^{1}H NMR (500 MHz, CD_3OD) spectrum of SAR3**

The NMR (^{1}H: 500 MHz, CD_3OD) data of SAR3 in comparison with tiliroside of the literature are represented in the table 24 below:

Table 24: NMR (^{1}H:500 MHz, CD_3OD) data of SAR3 in comparison with tiliroside of the literature (Da Costa et *al*., 2007).

Position	^{1}H NMR(500MHz, CD_3OD) SAR3	^{1}H NMR (200 MHz, CD_3 OD) Tiliroside
6	6.10 (1H , *d*, *J* = 2 Hz)	6.10 (1H , *d*, *J* = 2.2 Hz)
8	6.20 (1H, *d*, *J* = 2 Hz)	6.25 (1H, *d*, *J* = 2.2 Hz)
2'/6'	7.99 (2H , *d*, *J* = 8.9 Hz)	7.96 (2H, *d*, *J* = 8.9 Hz)
3'/5'	6.83 (2H *d*, *J* = 8.9 Hz)	6.79 (2H *d*, *J* = 8.9 Hz)
2'''/6'''	7.33 (2H *d*, *J* = 8.5 Hz)	7.26 (2H *d*, *J* = 8.5 Hz)
3'''/5'''	6.81 (2H *d*, *J* = 8.5 Hz)	6.75 (2H *d*, *J* = 8.5 Hz)
1''	5.11 (1H, *d*, *J* = 7.3 Hz)	5.24 (1H , *d*, *J* = 7.6 Hz)
2''/3''/4''/5''	3.53 (4H, *m*)	3.54 (4H, *m*)
7'''	7.42 (1H, *d*, *J* =16 Hz)	7.38 (1H, *d*, *J* =15.6 Hz)

The interpreted data of SAR3, compared to literature data led to its characterization as tiliroside. This compound is reported to have a potential relaxant activity (**Da Costa et *al*., 2007**).

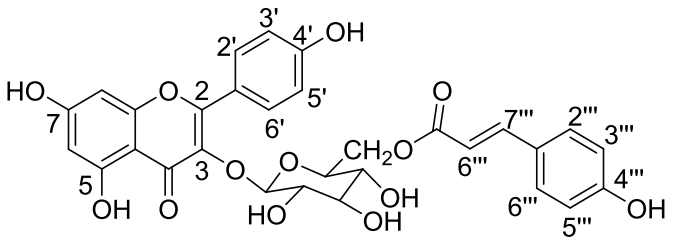

97

II.2.2.3.3 Identification of GO-S1

Compound GO-S1 was obtained from the bark of *Garcinia ovalifolia* as a white powder and is soluble in methanol. It responded positively with the ferric chloride test suggesting the existence of phenolic nature. The ^{1}H NMR spectrum (Figure 30) revealed a set of signals at δ_H 6.80 (1H, d, 8.1 Hz), δ_H 6.84 (1H, dd, 1.8;8.1 Hz) and 6,95 (1H, d,1.8 Hz), suggesting an ABX system. The singlet at δ_H 5.95 (1H, s) and signals displayed in the range of δ_H 3.38-4.79 suggested the presence of a sugar moeity. The upfield ^{1}H NMR chemical shift of H-1" in the glucose moiety δ_H (4.79) is consistent with a C-glucoside rather than an *O*-glucoside. Moreover, the upfield ^{13}C NMR chemical shift of C-6 δ_C (106.4) also indicates C substitution rather than O substitution.

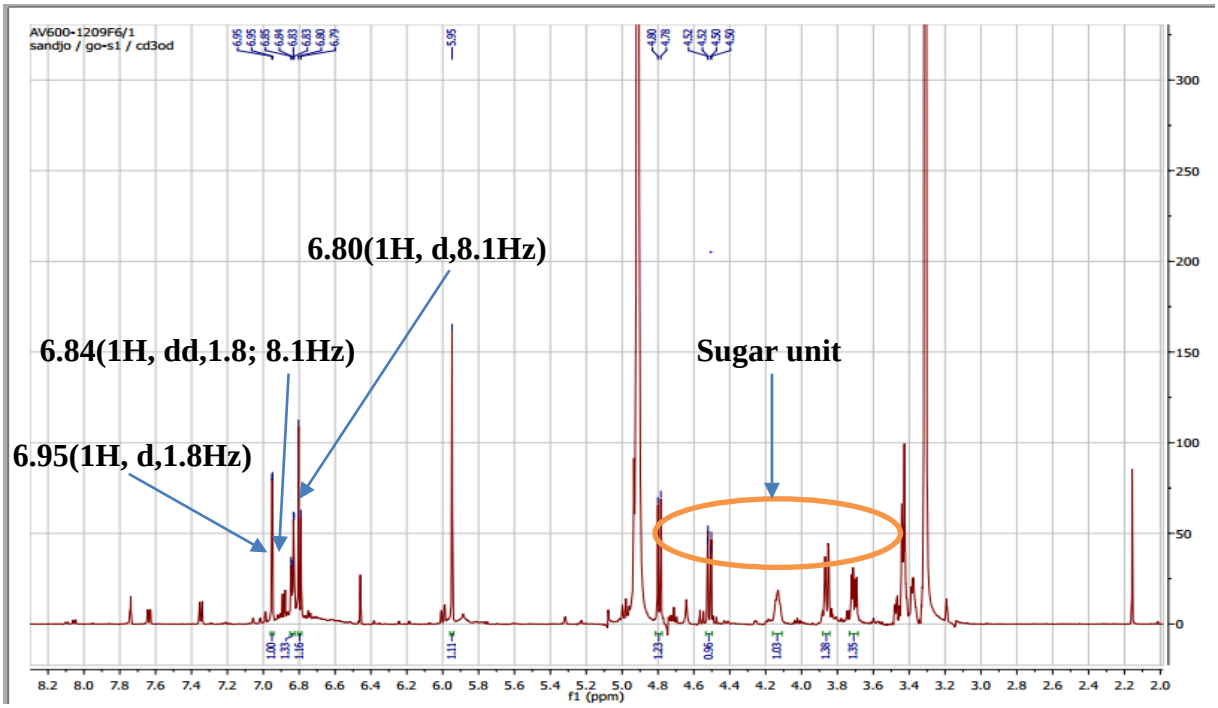

Figure 30: **^{1}H NMR (300 MHz, CD_3OD) spectrum of GO-S1**

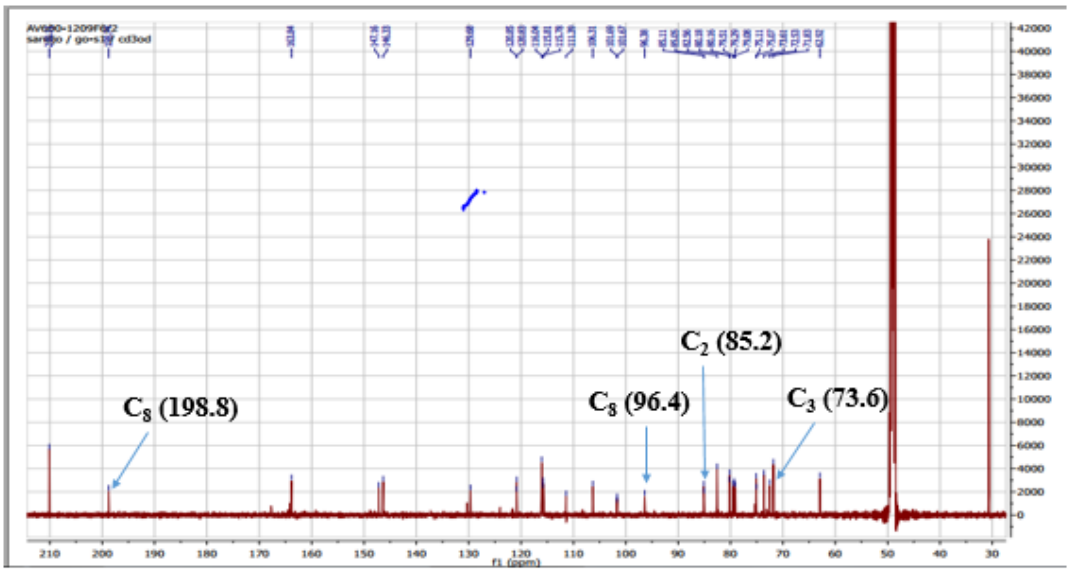

Figure 31: **^{13}C NMR broadband decoupled (75 MHz, CD_3OD) spectrum of GO-S1**

The ^{13}C NMR and ^{1}H NMR spectra data (75 MHz, CD_3OD), (300 MHz, CD_3OD) of GO-S1 compared to literature values are represented in table 25 below:

Table 25: ^{13}C NMR and ^{1}H NMR spectral data (75 MHz, CD_3OD), (300 MHz, CD_3OD) of GO-S1 compared to taxifolin 6-c-glucoside of the literature (Weihong et *al*., 2022).

Position	δ ^{1}H (300MHz, CD_3OD) **GO-S1**	δ ^{13}C (75 MHz, CD_3OD)	δ ^{1}H ((700MHz, CD_3OD) **Taxifolin 6-c-glucoside**	δ ^{13}C (175 MHz, CD_3OD)
1	-	-		
2	4.92 (1H, d, 11Hz)	85.2	4.92 (1H, d, 11.3 Hz)	85.1
3	4.51 (1H, d, 11Hz)	73.6	4.50 (1H, d, 11.3 Hz)	73.6
4	-	198.8		198.4
4a	-	101.8		101.5
5	-	164.1		164.2
6	-	106.4		106.4
7	-	167.7		168.6
8	5.95 (1H, s)	96.4	5.93 (1H, s)	96.7
8a	-	163.9		163.8
1’		129.7		129.8
2’	6,95 (1H, d, 1.8 Hz)	116.0	6.95 (1H, d, 1.9 Hz)	115.8
3’	-	147.2	-	146.3
4’	-	146.4	-	147.2
5’	6.80 (1H, d, 8.1 Hz)	115.8	6.84 (1H, d, 8.1 Hz)	116.1
6’	6.84 (1H, dd, 1.8;8.1 Hz)	120.8	6.80 (1H, dd, 1.9; 8.1 Hz)	120.4
1’’	4.79 (1H, br)	75.2	4.80 (1H, d, 9.9 Hz)	75.2
2’’	4.13 (1H, m)	72.6	4.14 (1H, t, 8.8 Hz)	72.6
3’’	3,47 (1H, m)	80.2	3.43 (1H, m)	80.2
4’’	3.47 (1H, m)	71.8	3.44 (1H, m)	71.8
5’’	3.38 (1H, m)	82.6	3.38 (1H, m)	82.5
6’’	3.88 and (1H, m)	63.0	4.48(1H, m)	62.9

The comparison of **GO-S1** with the literature source permitted its characterization as taxifolin 6-C-glucoside **(Weihong et *al*., 2022).**

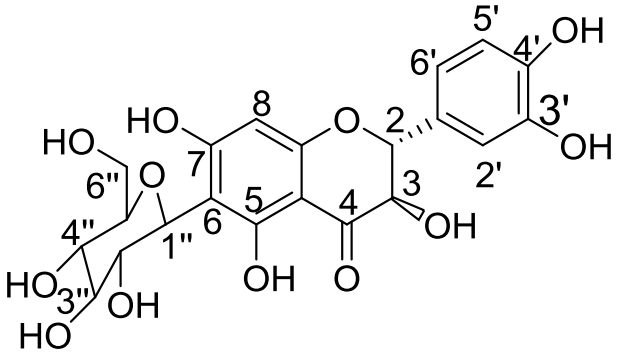

98

II.2.2.4 Benzophenone

II.2.2.4.1 Identification of GOA

GOA obtained from the bark of *Garcinia ovalifolia* as brown powder in CH_2Cl_2 / MeoH. It gave a violet coloration with $FeCl_3$ in methanol indicating the presence of phenolic group.

The ^{1}H NMR spectrum (Figure 32) of GOA showed signals at δ_H 5.87 (1H, brs), 5.56 (1H, brs), and 5.56 (1H, brs), assigned to three vinyl protons H-18, H-25, and H-35. An ABX system of three aromatic protons resonated at δ_H 8.00 (1H, brs, H-12); δ_H 7.42 (1H, d, J = 7.8 Hz, H-15) and δ_H 7.67 (1H, brd, H-16). Furthermore, ten methyl signals were observed at δ_H 2.27 (3H, s, Me-20), 2.34 (3H, s, Me-21), 1.59 (3H, s, Me-22), 1.92 (3H, s, Me-23) , 2.36 (3H, s, Me-27), 2.45 (3H, s, Me-28), 1.83 (3H, s, Me-32), 1.66 (3H, s, Me-33) and 2.25 (3H, s, Me-38) respectively.

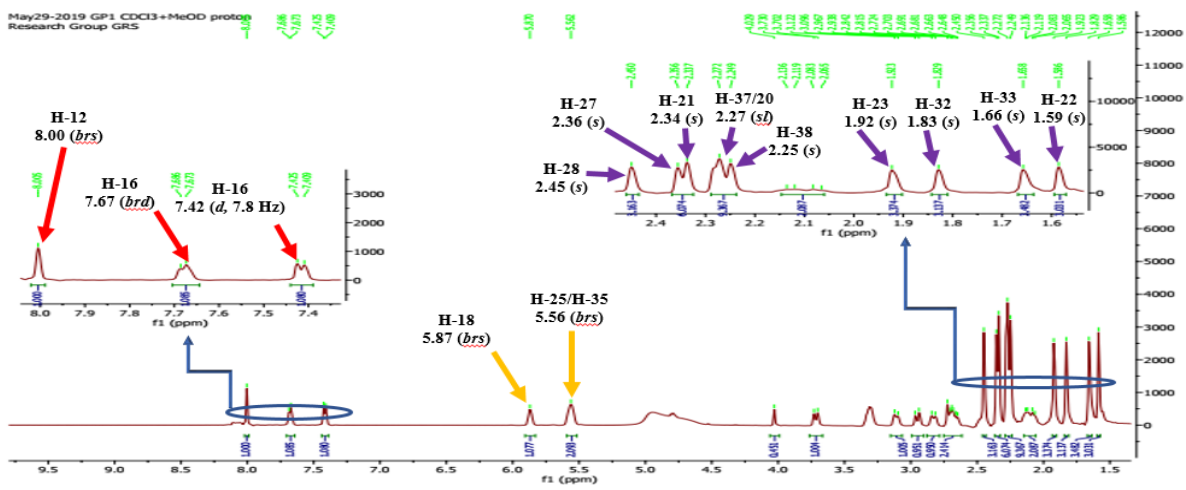

Figure 32: **^{1}H NMR spectrum ($CDCl_3/CD_3OD$, 500 MHz) of GOA**

The ^{13}C NMR spectrum (Figure 33) revealed a six-membered ring bearing a free ketone δ_C (207.2) flanked by two quaternary carbons at δ_C 51.16 (C-1) and δ_C 68.1 (C-5) respectively. The 2,4-eneolisable diketone at δ_C 171.7 (C-2), 125.1 (C-3), and 194.6 (C-4) were also observed. The appearance of a quaternary carbon at δ_C 46.0 (C-6), methine at δ_C 46.1 (C-7) and methylene at δ_C 39.2 (C-8) suggested a bicyclo [3.3.1] nonane system (**Weng *et al.*, 2004**).

According to Ciochina (2006) and Piccinelli et *al* (2005), the orientation of the substituent at C7 (axial and equatorial) can be deduced from the chemical shift of Me-22 and Me-23 in the ^{1}H and ^{13}C NMR spectra. If the C7 substituent is axial, the range would be δ_C 26-28 for Meax-22 and δ_C 22-25 for Meeq-23. In contrast, if the substituent at C7 is equatorial, the range would be δ_C 15-17 for Meax and δ_C 22-25 for Meeq.

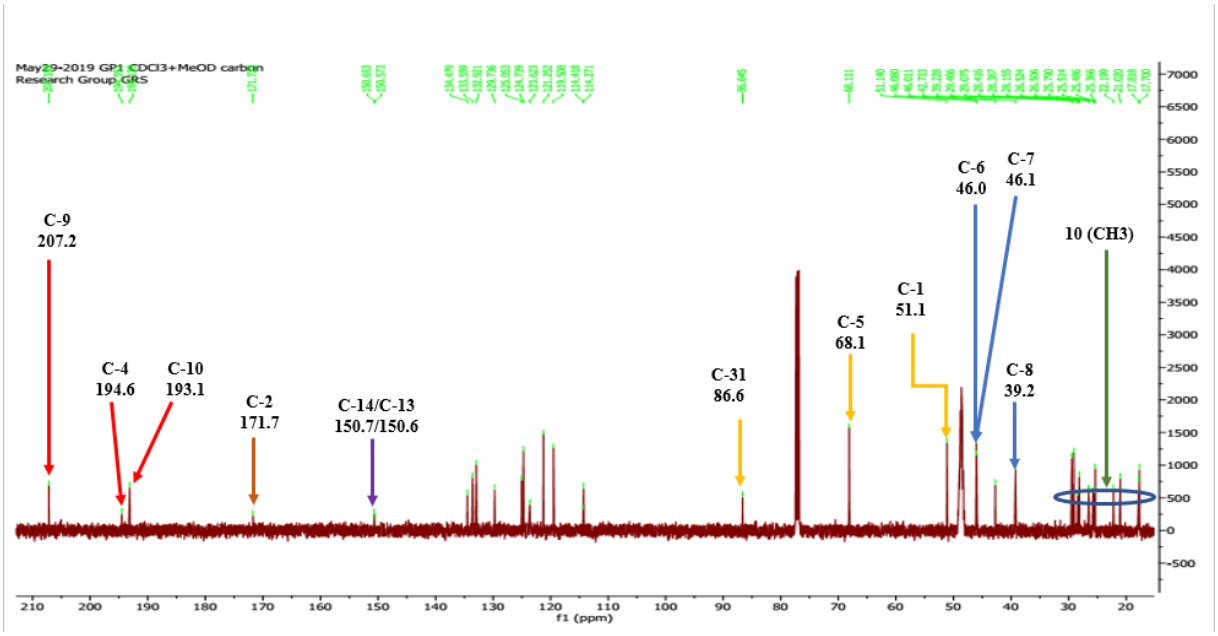

Figure 33: **^{13}C NMR broadband decoupled spectrum ($CDCl_3/CD_3OD$, 125 MHz) of GOA**

The ^{13}C NMR spectral data ($CDCl_3/CD_3OD$, 125 MHz) and ^{1}H NMR ($CDCl_3/CD_3OD$, 500MHz) of GP1 compared to isogarcinol of the literature data are represented in the table 26 below:

Table 26: 13C NMR spectral data (CDCl3/CD3OD,125 MHz) and 1H NMR (500 MHz, CDCl3/CD3OD) of GOA compared to isogarcinol of the literature (Marti et al., 2009).

Position	^{1}H (300 MHz, $CDCl_3$/ CD_3OD) GOA	δ ^{13}C (75 MHz, $CDCl_3/CD_3OD$) GOA	500 MHz ^{1}H NMR Pyridine-d_5 isogarcinol.	125MHz ^{13}C NMR
1		51.1		52.2
2		171.7		171.4
3		125.1		127.2
4		194.6		195.0
5		68.1		69.2
6		46.0		46.8
7	1.58 (1H, m)	46.1	1.59 (1H, dt, 6.2 ; 6.1 Hz)	47.0
8	2.11 (1H, dl, 14) and 2,49 (1H, m)	39.2	2.11 (1H, dd, 14.1 ;7.3 Hz) 2.43 (brd ,14.1)	39.8
9		207.2		207/9
10		193.1		193.0
11		129.7		130.9
12	8.00 (1H, brs)	114.4	8.05 (1H, d, 2 Hz)	116.6
13		150.6		147.8
14		150.7		153.7
15	7.42 (1H, d, 7.8 Hz)	114.3	7.28 (1H , d, 8.1 Hz)	116.5
16	7.67 (1H, brd)	123.6	7.68 (1H , dd, 8.1; 2 Hz)	124.3
17	2.64 (1H, dd, 8.7;13.8 Hz) and 2.44 (1H, dd, 5.4, 13.6 Hz)	25.8	2.76 (1H, dd, 13.7;5.6) 2.95 (1H, dd, 13.5; 7.6 Hz)	26.7
18	5.87 (1H, brs)	119.5	5.42(1H, brt, 6.5 Hz)	121.7
19		134.5		134.5
20	2.27 (3H, s)	26.5	1.57 s	26.6
21	2.34 (3H, s)	17.8	1.71 s	18.8
22	1.59 (3H, s)	27.4	1.05 s	27.1
23	1.92 (3H, s)	22.2	1.30 s	23.1
24	1.82 (1H, m) and 2.11 (1H, m) 3.12 (1H, dd, 14.4; 3.6 Hz)	29.5	1.82(1H, ddd, 14.2 ; 9.5 ; 9.5 Hz) 3.21 (1H, ddd, 14.4 ; 10.7 ; 9.5 Hz)	30.4
25	5.56 (1H, brd)	124.7	5.09 brt (6.5)	126.4
26		132.9		132.9
27	2.36 (3H, s)	25.5	1.74 (3H, s)	26.5
28	2.45 (3H, s)	17.8	1.91 (3H, s)	19.0
29	1.03 (1H, sl) 3.09 (1H, dd, 14 ; 2.8 Hz)	28.4	1.14 (1H, dd , 13.9; 13.7 Hz) 3.27 (1H, dd, 13.9; 3.1 Hz)	29.9

30	1.69 (m)	42.7	1.66 (dt, 9.9, 5.0)	43.8
31		87.3		87.3
32	1.83 (3H, s)	21.0	1.23 (3H, s)	21.7
33	1.66 (3H, s)	28.2	1.07 (3H, s)	29.4
34	2.06 (1H,m)	29.1	1.96 (1H, brd,14.1 Hz) 2.42 (1H, brd, 14.1 Hz)	30.4
35	5.56 (1H, brs)	121.3	5.09 (1H, brt,6.5 Hz)	122.8
36		133.6		133.7
37	2.27 (3H,s)	25.4	1.68 (3H,s)	26.2
38	2.25 (3H,s)	17.7	1.56 (3H,s)	18.3

The above data in conformity with literature source led to the characterization as isogarcinol **(Marti et *al.*, 2009).**

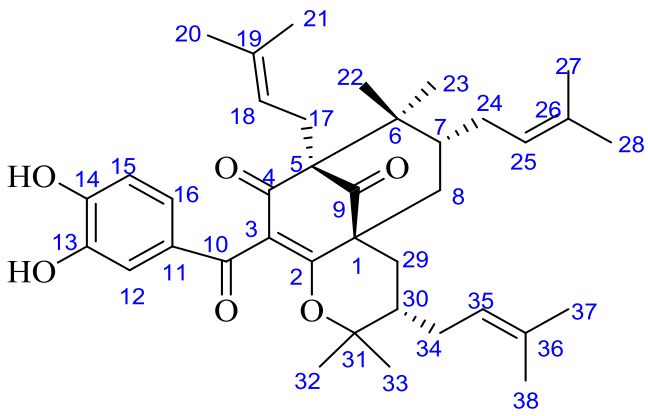

99

II.2.2.4.2 Identification of GOX

GOX was obtained as a yellow powder from the bark of *Garcinia ovalifolia* $[\alpha]_D^- = -158$ (C=1.0 ; $CHCl_3$) and gave a purple coloration with $FeCl_3$ in methanol indicating the presence of phenolic group. The ^1H NMR spectrum (Figure 34) of GOX showed signals at δ_H 4.96 (1H, t, J = 8.4HZ); 4.96 (1H, t, J = 8.4H_Z); 5.15 (1H, t, J = 6.3H_Z) assignable to the three vinyl protons H-35; H-18; H-25. Six singlets were observed integrating for three protons each at δ_H 1.29 (3H, s); 1.77 (3H, s) 1.303 (6H, s); 1.72 (3H, s); 1.31 (3H, s). Moreover, signals attributable to the six allyl protons between 1.69 and 2.70 ppm were visible.

This information confirms the presence of isopent-2-enyl groups in the structure of GOX. In addition to the vinyl methyl signals, four aliphatic methyl signals in the form of singlet are observed at δ_H 0.98 (3H, s) 1.21 (3H, s); 1.03 (3H, s); 1.08 (3H, s) assignable to protons H-20; H-21; H-32; H-33, respectively.

Furthermore, the ^{1}H NMR spectrum (Figure 34) exhibits an ABX system of three aromatic protons whose resonances are observed at δ_H 7.50 (1H, d, J = 2.1 Hz); δ_H 6.75 (1H, d, J = 8.4 Hz) and δ_H 7.11 (1H, dd, J = 2.1HZ and 8.4 Hz).

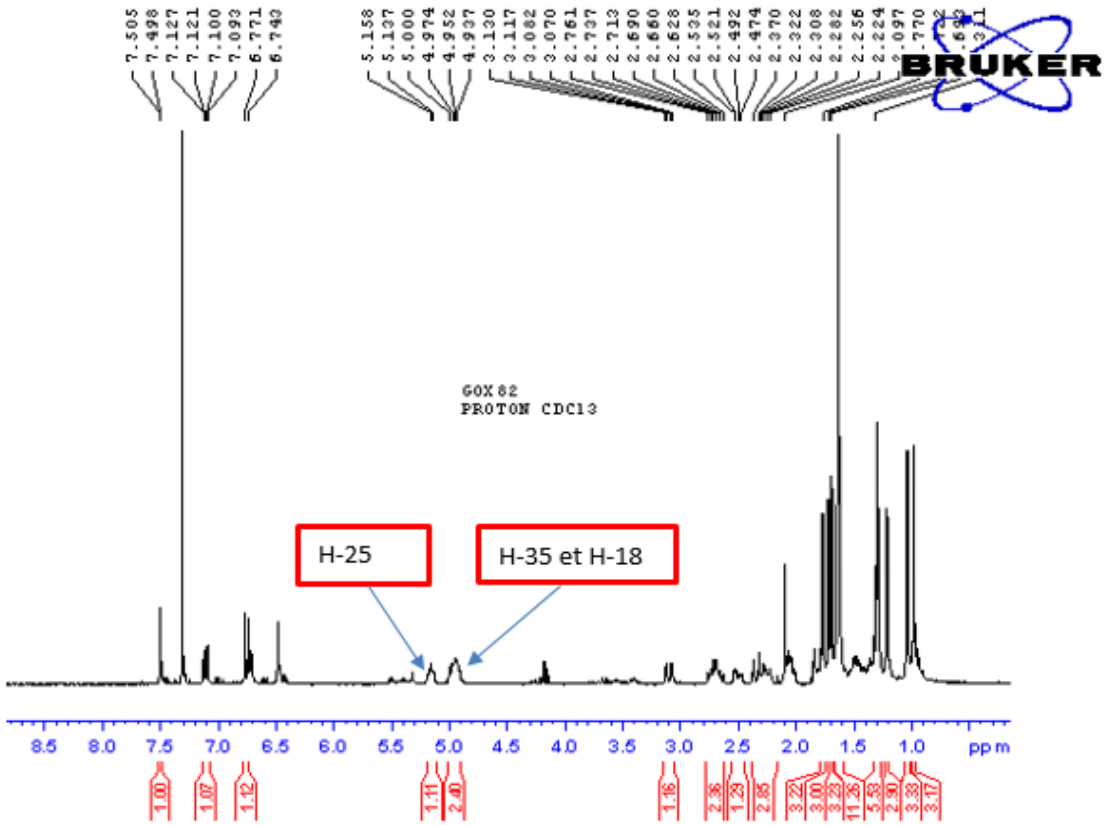

Figure 34: **^{1}H NMR spectrum of (300 MHz, $CDCl_3$) of GOX**

The ^{13}C NMR (Figure 35) data present the signals of two α,β-unsaturated carbonyl groups and a ketone group at δ_C 194.3 (C-4); 192.7 (C-10) and 207.3 (C-9) respectively. This information coupled with the signals of the two quaternary carbons at δ_C 68.4 (C-5) and 46.5 (C-6) show the structure of polycyclic polyprenylated acylphloroglucinol (PPAP) (**Marti et *al*., 2010**).

Furthermore, the ^{13}C NMR spectrum (Figure 35) shows a six-membered ring with a free ketone (δ_C 207.3) flanked by two quaternary carbons at δ_C 51.3 (C-1) and δ_C 68.4 (C-5) respectively. In addition, the 2,4-eneolisable diketone at δ_C 171.7 (C-2); 125.2 (C-3) and 194.3 (C-4) was observed in this spectrum. These data are supported by the signals of the resonance quaternary carbon at δ_C 68.4 (C-6). The methine at δ_C 39.9 (C-7) and methylene at δ_C 43.0 (C-8) were observed as part of a bicyclo [3.3.1] nonane type system (**Weng et *al*., 2004).**

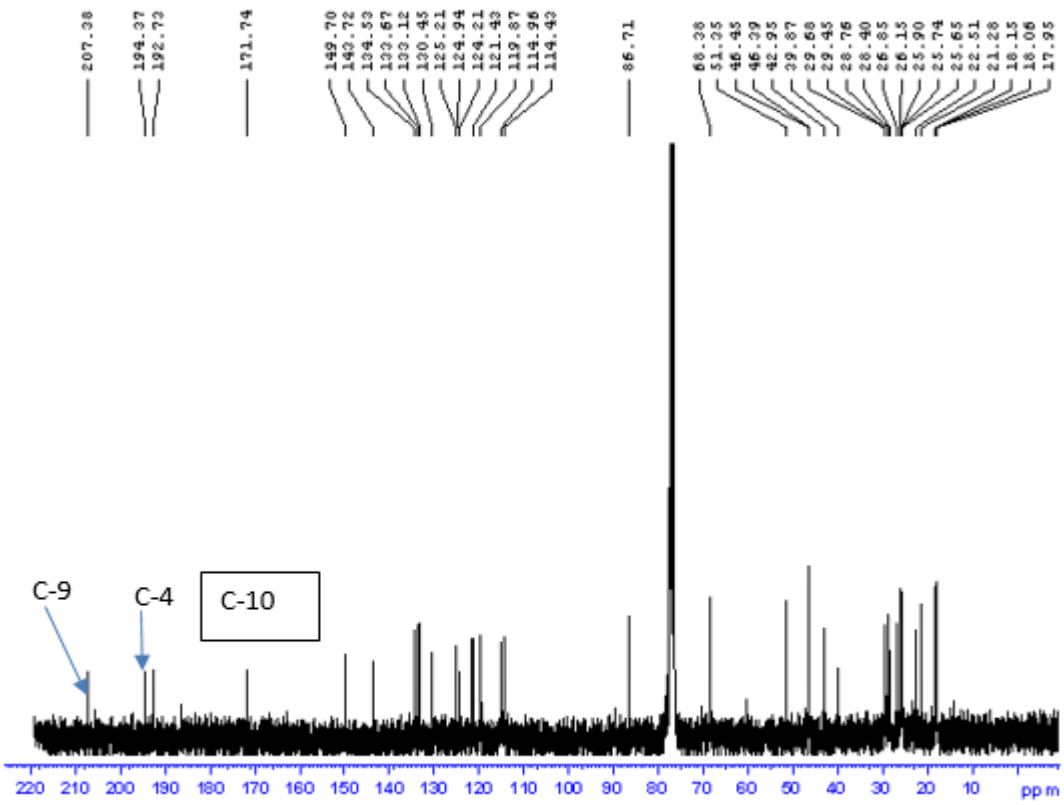

Figure 35: **^{13}C NMR broadband decoupled spectrum (75 MHz, $CDCl_3$) of GOX**

The ^{13}C NMR spectral data (75 MHz, $CDCl_3$) of GOX compared to 7-épiisogarcinol of the literature are represented in the table 27 below:

Table 27: ^{13}C NMR spectral data (75 MHz,CD_3COCD_3) of GOX compared to 7-épiisogarcinol of the literature (Marti et *al.*, 2009).

position	**^{13}C NMR (75 MHz,** $CDCl_3$**) GOX**	**^{13}C NMR** (125 MHz, pyridine-d_5) **7-épiisogarcinol**
1	51.35	52.2
2	171.7	170.8
3	125.2	129.1
4	194.3	194.9
5	63.4	71.4
6	46.4	46.8
7	39.9	42.2
8	43.0	43.1
9	207.3	207.3
10	192.7	193.3
11	130,4	131.0
12	114.4	117.1
13	143.7	147.9

14	149.7	153.7
15	114.4	116.5
16	125.0	124.4
17	25.7	25.9
18	121.4	122.1
19	134.5	134.2
20	25.9	26.2
21	21.3	18.8
22	18.0	16.6
23	25.6	22.8
24	28.4	28.5
25	124.2	123.8
26	133.1	132.9
27	26.1	26.2
28	18.1	18.8
29	28.8	28.5
30	46.4	43.8
31	86.7	87.6
32	22.5	21.7
33	29.7	29.2
34	29,4	30.4
35	119.9	122.9
36	133.6	133.7
37	26.8	26.2
38	16.6	18.3

The aforementioned led to the characterization of GOX as 7-épiisogarcinol (**Marti *et al.*, 2009)**.

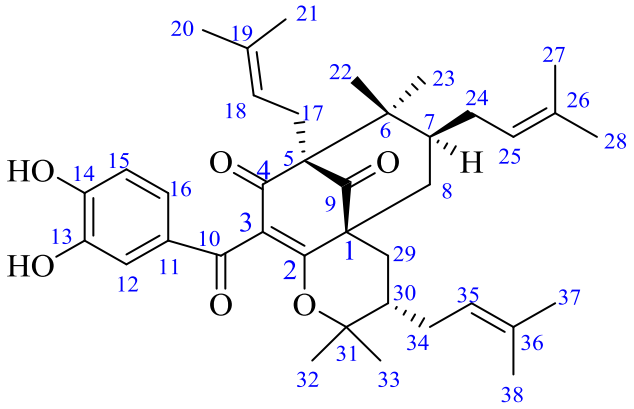

100

II.2.2.4.3 Identification of GO9

G09 was obtained from the stem bark of *Garcinia ovalifolia* as a white powder in a mixure of Hex-AE 5%.

In its ^{1}H NMR spectrum (Figure 36) was observed two groups of protons and singlet of 2 protons at δ_H 5.90 probably shielded by the presence of α-methoxyl group which were assigned to vinyl protons at positions 3 and 5. Moreover, an intense singlet at δ_H 3.87 integrated for 6 protons were assigned to the methyl protons of two methoxyl groups.

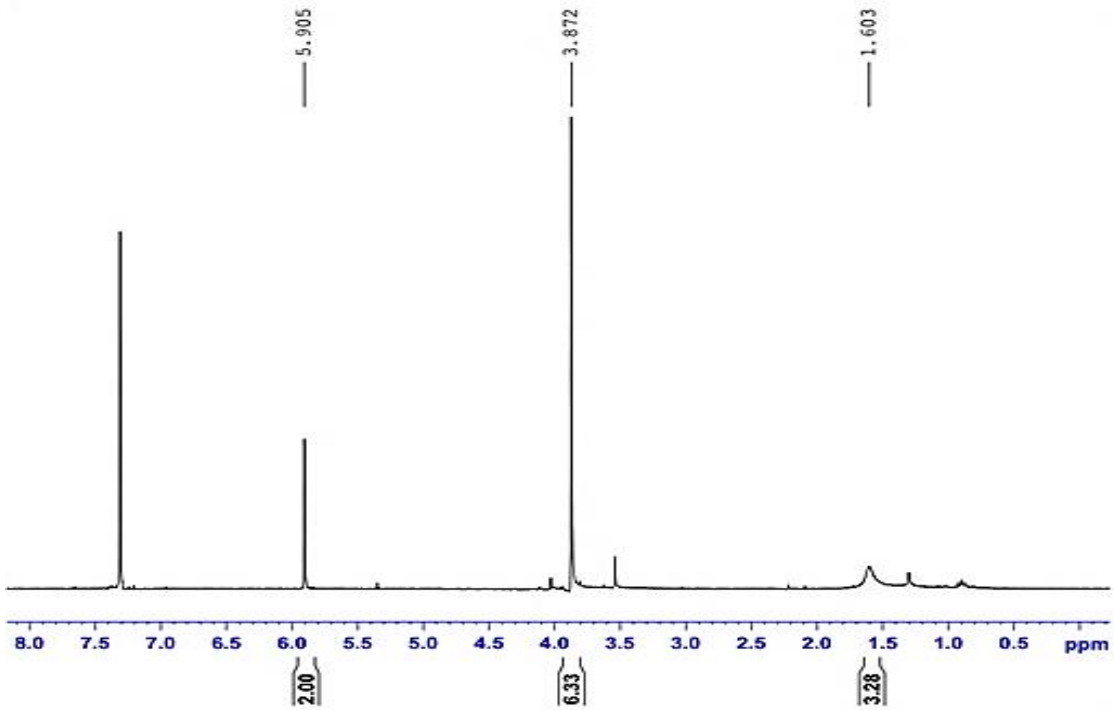

Figure 36: **^{1}H NMR spectrum (300 MHz, $CDCl_3$) of GO9**

The double integral value of these signals suggests the presence of an axis of symmetry in the molecule. In the ^{13}C NMR spectrum (Figure 37), the resonance at δ_C 186.84 were attributable to two α-β unsaturated carbonyls, while the signal at δ_C 157.38 were assigned to the two Sp^2 carbons attached to the methoxyl groups. Furthermore, the resonance at δ_C 107.45 were ascribed the two Sp^2 carbons in positions 3 and 5 and the quatriplet resonance at δ_C 56.47 assigned to two carbons of two methoxyl groups.

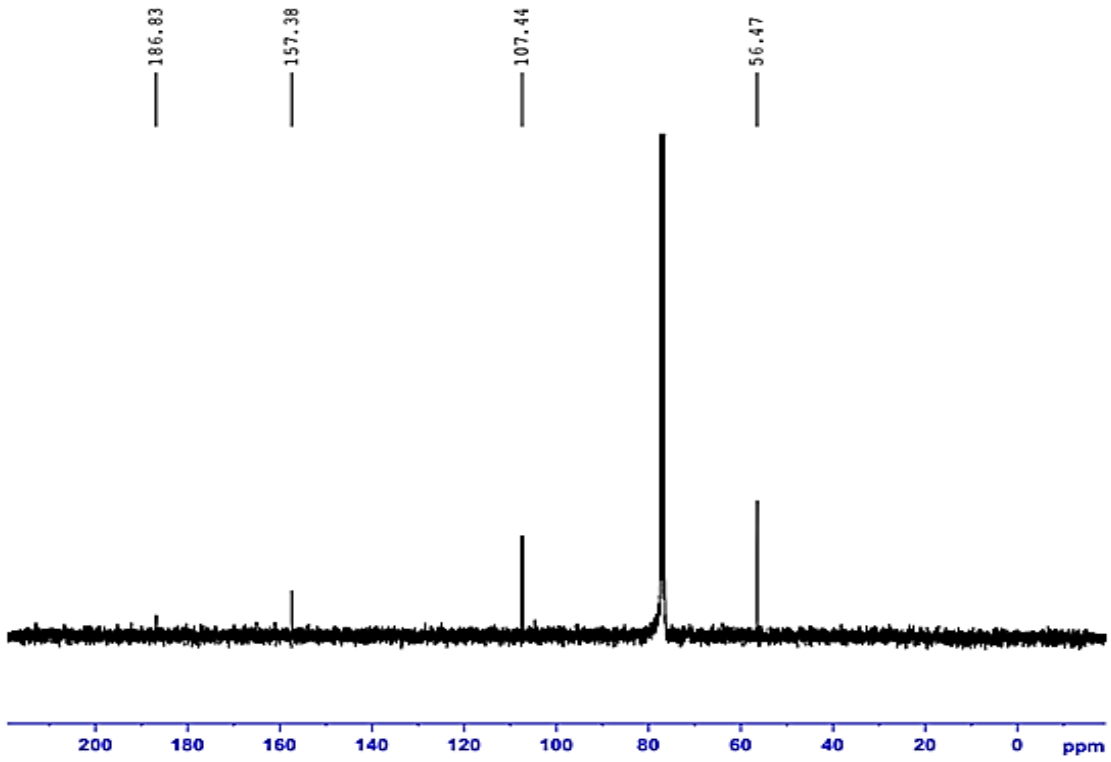

Figure 37: **^{13}C NMR broadband decoupled spectrum (75 MHz, $CDCl_3$) of GO9**

The ^{1}H NMR (300 MHz, $CDCl_3$) of GO9 compared to 2,6-dimethoxy-p-benzoquinone of the literature are represented in the table 28 below:

Table 28: ^{1}H NMR (300 MHz, $CDCl_3$) of GO9 compared to 2,6-dimethoxy-p-benzoquinone of the literature (Huang et *al*., 2019).

^{1}H NMR (300 MHz, $CDCl_3$)	^{1}H NMR (500 MHz, $CDCl_3$)
3.87 (6H, s, 2, 6-OMe)	3.82 (6H, s, 2, 6-OMe)
5.90 (2H, s, H-3, 5)	5.86 (2H, s, H-3, 5)

These informations compared to those obtained from the literature data (**Huang et *al*., 2019**) led to the identification of GO9 as 2,6-dimethoxy-p-benzoquinone.This compound have been reported to exhibit a potential antimalarial activity against *Plasmodium falciparum* (**Karaket et *al*., 2012**).

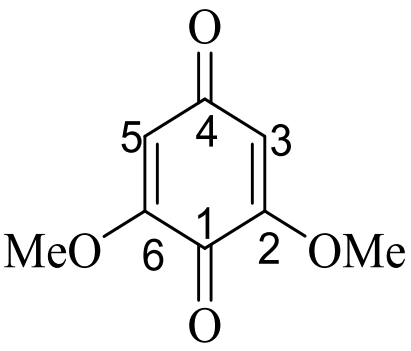

101

II.2.2.5 Alkaloids

II.2.2.5.1 Identification of SAB1

SAB1 was obtained as a crystalline solid from *Sida acuta* in the mixture Hex-EA (60-4O). In its ^{1}H NMR spectrum (Figure 38) were observed signals of four aromatic hydrogens at δ_H 7.55 (1H, ddd, J = 1.4; 7.1; 8.5 Hz), δ_H 7.94 (1H, dd, J = 1.4; 7.1 Hz), δ_H 7.33 (1H, d, J = 8.5 Hz), and δ_H 7.19-7.26 (1H, m) indicating the presence of a disubstituted aromatic ring.

The singlets at δ_H 3.66 (3H, s) and δ_H 3.93 (3H, s) were assigned to *N*-methyl and *O*-methyl groups.

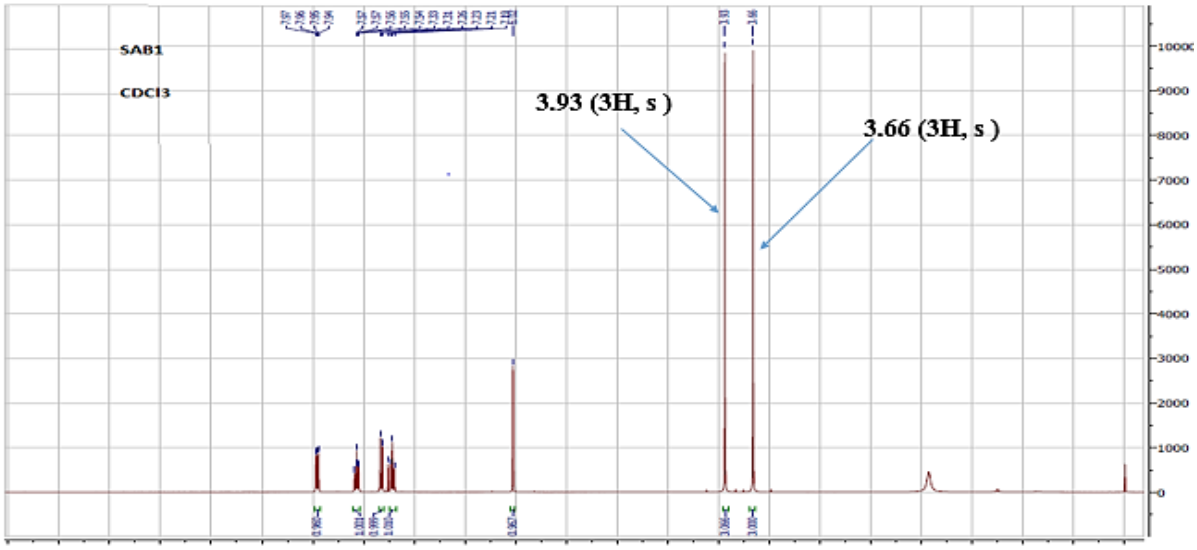

Figure 38: **^{1}H NMR (500 MHz, $CDCl_3$) spectrum of SAB1**

The ^{13}C NMR spectrum (Figure 40) showed a signal at δ_C 163.9 for a quaternary carbon, corresponding to a carbonyl group. The *N*-methyl and *O*-methyl carbon signals were observed at δ_C 29.1 and δ_C 55.9 respectively. Informations provided by the ^{1}H

and ^{13}C NMR spectra led to determination of SAB1 as quinoline alkaloid, named 4-Methoxy-1-methyl-2-quinolone (**Cuca -suarez *et al.*, 2011**).

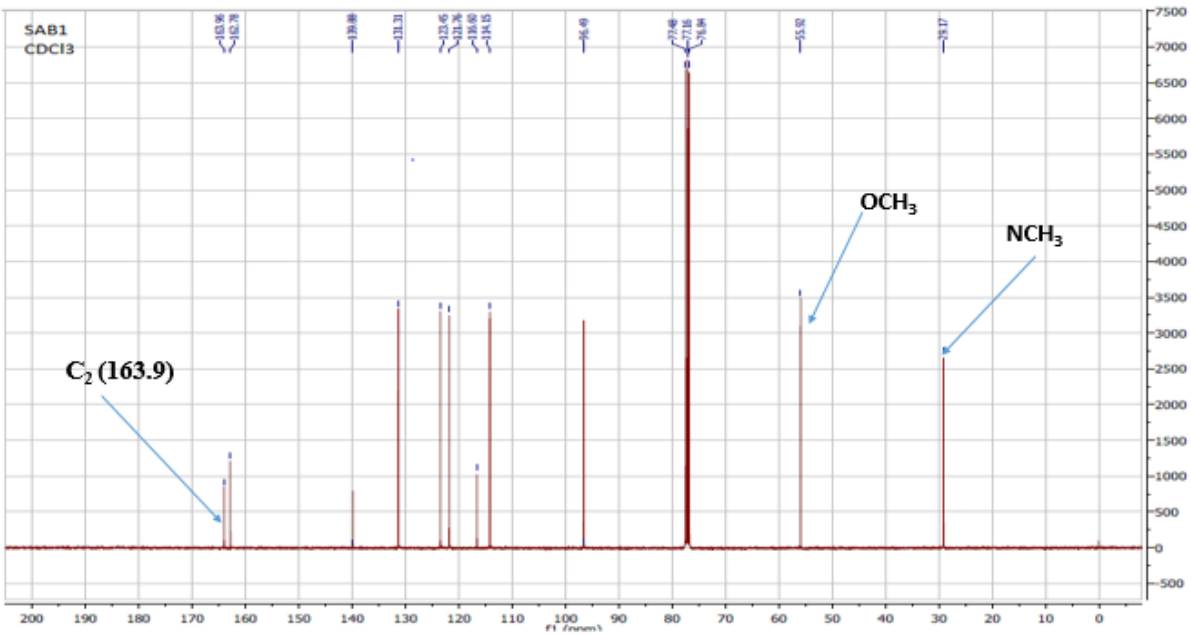

Figure 39: **^{13}C NMR broadband decoupled (125 MHz, $CDCl_3$) spectrum of SAB1**

The ^{13}C: 125 MHz, $CDCl_3$ and ^{1}H:500 MHz, $CDCl_3$) data of SAB1 in comparison with methoxy-1-methyl-2-quinolone of the literature are represented in the table 29 below:

Table 29: (^{13}C: 125 MHz, $CDCl_3$ and ^{1}H:500 MHz, $CDCl_3$) data of SAB1 in comparison with methoxy-1-methyl-2-quinolone of the literature (Cuca -suarez *et al.*, 2011).

	^{1}H NMR ($CDCl_3$, 500 MHz) SAB1	^{13}C NMR ($CDCl_3$,125 MHz) SAB1	^{1}H NMR ($CDCl_3$, 400 MHz): 4-Methoxy-1-methyl-2-quinolone	^{13}C NMR ($CDCl_3$,100 MHz)
2		163.9		163.9
3	6.03(s)	96.3	6.08 (s)	96.2
4		162.7		160.1
5	7.94 (1H ,dd, *J* =1.4; 7.1 Hz)	123.4	7.80 (1H,dd, *J* =1.5; 7.2 Hz)	123.4
6	7.19-7.26 (1H ,m)	121.7	7.22-7.28 (1H, m)	121.8
7	δ 7.55 (1H, ddd, *J* =1.4; 7.1; 8.6 Hz,)	131.3	7.50 (1H,ddd, *J* =1.5; 7.2; 8.6 Hz,)	130.0
8	7.33 (1H, d, *J* =8.5 Hz,)	114.1	7.30 (1H, d, *J* =8.6 Hz)	114.0
4a		116.6		117.8
8a		139.8		139.0
N-Me	3.66 (s)		3.70 (s)	
O-Me	3.96 (s)		3.90 (s)	

This coumpound was reported to have a potential antimalarial on *Plasmodium falciparum* strain (**Cuca -suarez *et al.* 2011**).

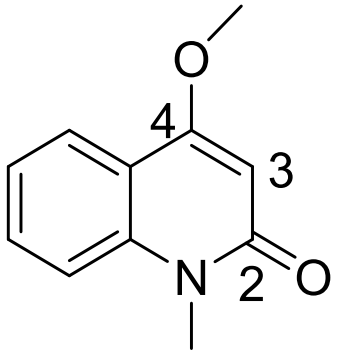

102

II.2.2.5.2. Identification of SAB3

SAB3 was obtained as a yellow powder from *Sida acuta.* Its atmospheric pressure chemical ionisation APCI showed a peak at *m/z* value of 233.27 corresponding to molecular formula $C_{16}H_{13}N_2$ with eleven degree of unsaturations.

The ^{1}H NMR spectrum (figure 41) of SAB3 showed an intense singlet signal at δ_H 4.43 which assigned to 3H of the methyl group of cryptolepine at position 5**.**

The proton NMR of cryptolepine showed signals between δ_H 6.76 and 7.92 and a singlet at δ_H 8.45 corresponding to eight aromatic protons and one aromatic hydrogen of cryptolepine respectively. The singlet at δ_H 8.46 was assignable to the hydrogen at position 11.

The multiplet revealed signals between δ_H 7.83 (d, 8.7 Hz, H-4) and 7.75 (d, 8.0 Hz, H-6) were ascribed to two hydrogens (2H) at positions 4 and 6 .

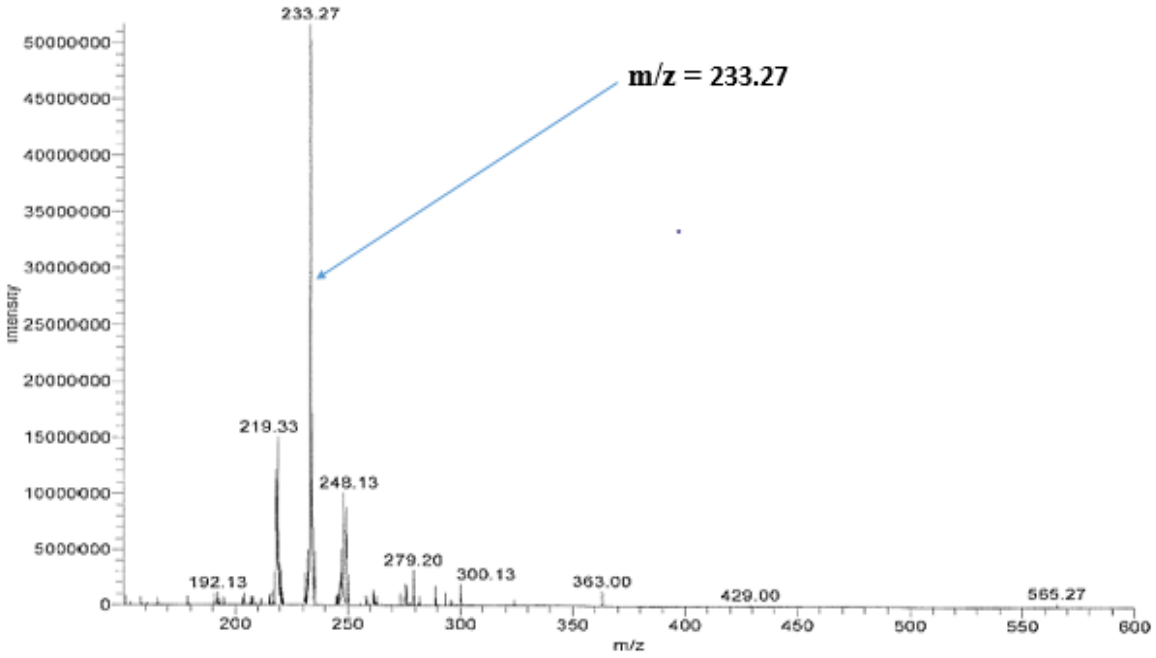

Figure 40: **ACPI spectrum of SAB3**

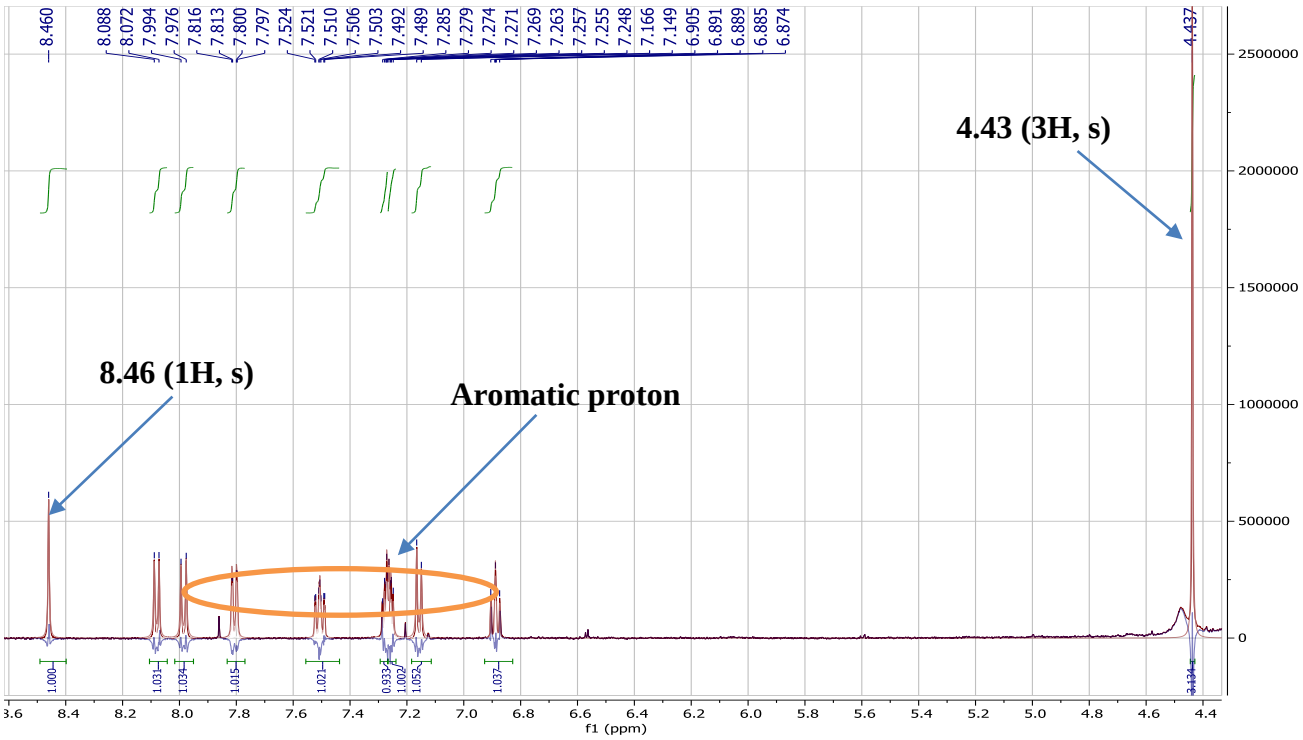

Figure 41: **^{1}H NMR (500 MHz, CD_3OD) spectrum of cryptolepine**

The NMR (^{1}H: 500 MHz, CD_3OD) data of SAB3 in comparison with cryptolepine of the literature are represented in the table below:

Table 30: NMR (^{1}H:500 MHz, CD_3OD) data of SAB3 in comparison with cryptolepine of the literature (Ablordeppey et *al*., 1990) .

Position	^{1}H ($CDCl_3$, 500Hz) SAB3	^{1}H (CD_3OD, 500Hz) Cryptolepine
1	7.92 (1H, d, *J*=8.0Hz)	8.08 (1H, d, *J*= 8.2Hz)
2	7.46 (1H, dd, *J*=8.0 ; 7.5Hz)	7.25 (1H, m)
3	7.69 (1H, dd, *J*=8.5 ; 7.5Hz)	7.51 (1H, d, *J*= 1.8Hz)
4	7.83 (1H, d, *J*= 8.7Hz)	7.99 (1H, d, *J*= 9.2Hz,)
6	7.75 (1H, d, *J*= 8.0Hz)	7.81 (1H, dd, *J*= 8.2 ; 1.5Hz,)
7	6.76 (1H, dd, *J*=8.0 ; 7.2Hz)	6.90 (1H, m)
8	7.37 (1H, dd, *J*=8.0 ; 7.2Hz)	7.16 (1H, d, *J*= 8,2Hz)
9	7.65 (1H, d, *J*= 8.0Hz)	7.28 (1H, m)
11	8.45 (1H, s)	8.46 (1H, s)
N-CH3	4.43 (3H, s)	4.32 (3H, s)

These information compared to those obtained in literature data (**Ablordeppey et *al*., 1990**) led to its characterization as cryptolepine.This compound have been reported to demonstrate promising antiplasmodial activity against chloroquine-resistant *P. falciparum* (**Parvatkar et *al*., 2011**)

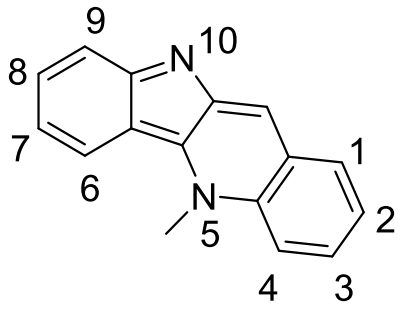

103

II.2.2.6 Steroids

II.2.2.6.1 Identification of SR1

The compound SR1 was isolated from the roots of *sida rhombifolia* as a white powder in a mixture Hex: AcOEt (9.5:0.5) and is soluble in chloroform. It responded positively to the Liebermann-Burchard test for steroids. Its (+)-ESI-MS spectrum showed proton adduct ions

at ([M + H]$^+$ 413.3 and 437.3 [M + Na]$^+$, respectively) (Figure 43) determined to have the molecular formula $C_{29}H_{48}O$ and $C_{29}H_{50}O$ with 6 and 5 degree of unsaturations respectively.

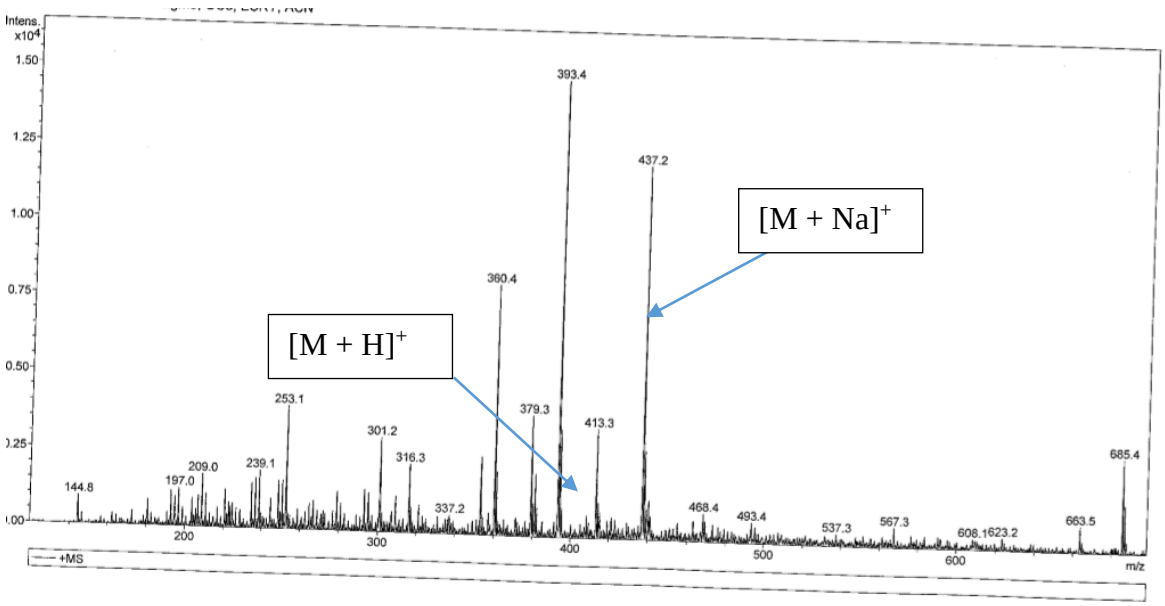

Figure 42: **(+)-ESI-MS spectrum of SR1**

Its ^{1}H NMR spectrum (Figure 44) indicates that compound SR1 is a phytosterol. As a matter of fact, on this spectrum we observe:

- A doublet at δ_H 5.40 (1H, d, *J*= 4.5Hz) assignable to the olefinic proton carried by carbon C-6 of the sterols;
- An AB system of proton each at δ_H 5.15 (1H, dd, *J*=15.2; 7.6) and 5.07 (1H, dd, *J*=15.3; 7.8Hz) ascribed to the olefinic protons H-22 and H- 23 in trans position;
- A multiplet at δ_H 3.42 (1H, m) corresponding to the proton of the oxymethine at C-3 following the biosynthetic pathway of sterols.
- Six methyls, with three appearing as doublets at δ_H 0.81 (1H, d, *J* = 6.3 Hz, H-26), 0.94 (1H, d, *J* = 6.3 Hz, H-27) and δ_H 1.05 (1H, d, J = 5.0 Hz, H-21); one appearing as a triplet at δ_H 0.85 (1H, t, *J* = 6.3 Hz, H-29) and two appearing as singlet is at
- δ_H 0.74 (3H, s) and δ_H 1.08 (3H, s).

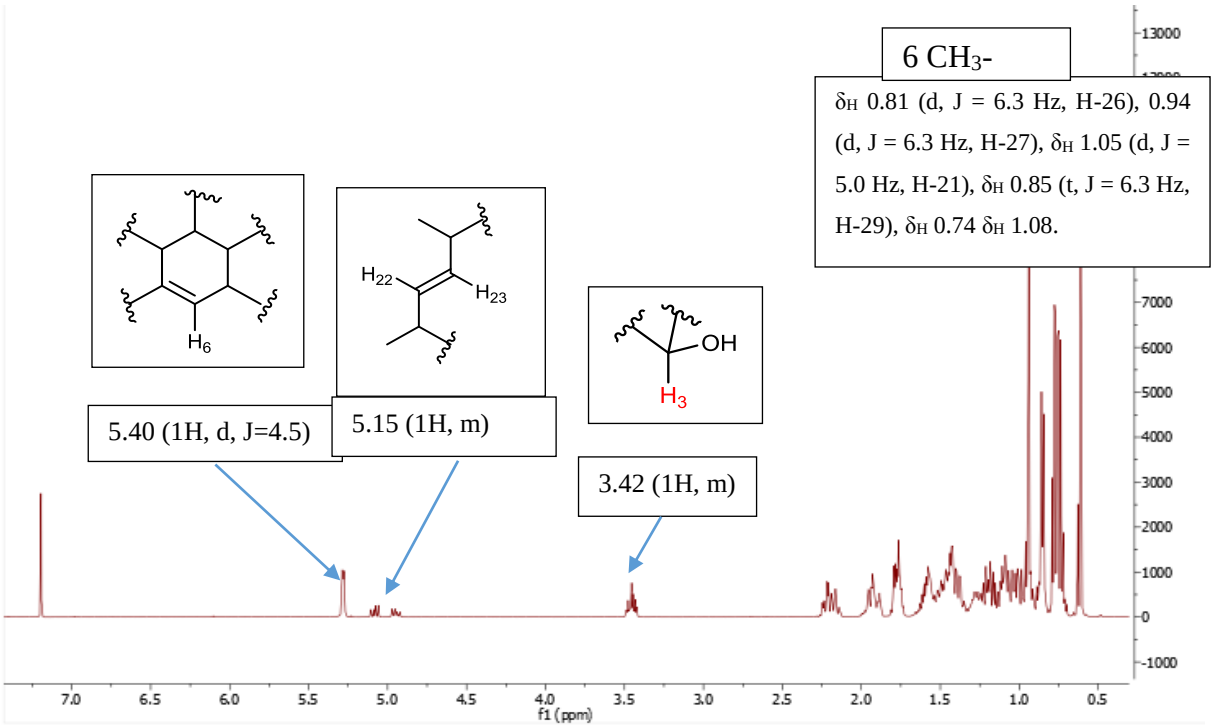

Figure 43: **^{1}H NMR spectrum (500 MHz, $CDCl_3$) of SR1**

The comparison TLC of compound SR1with mixture of *β*-sitosterol and stigmasterol in the laboratory and its comparison for the literature (**Chaturvedula and Prakash, 2012**) enable us to attribute compound SR1 to a mixture of stigmasterol and *β*- sitosterol previously isolated from *Astragalus altaicus* (**Ivorra et *al*., 1988**).

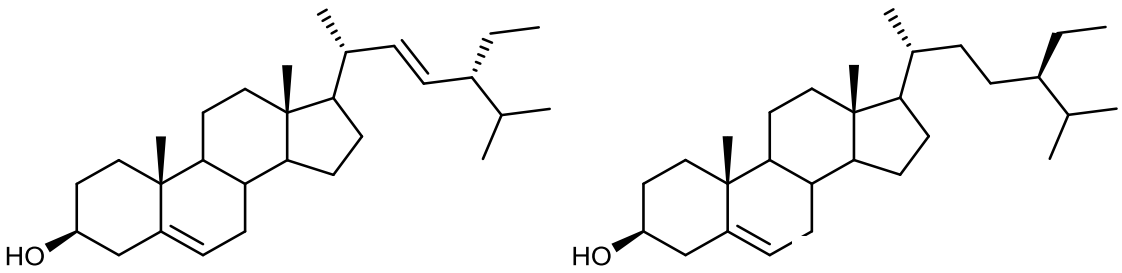

104 a stigmasterol **104 b *β*- sitosterol**

II.2.2.6.2 Identification of SR2

Compounds SR2 was isolated from the roots of *Sida rhombifolia*l, as a cream white powder in a mixture Hex: AcOEt 2:8. Its ESI-MS spectrum showed a molecular ion peak at m/z 574.4233 which was assigned to the molecular formula $C_{35}H_{58}O_6$ with 7 degrees of unsaturations.

Its ^{1}HNMR spectrum (Figure 44) is similar to that of SR1 because it also exhibited signals at δ_H 5.36; 5.15 and 5.06 assignable to the protons H-6, H-22, H-23 of stigmasterol. The signals between δ_H 3.25 and δ_H 4.39 were attributed to the proton of a sugar unit, with one of them at δ_H 4.36 (d, 7.8 Hz) value determined to be the signal of an anomeric proton. The coupling constant of the anomeric proton confirms the linkage of the sugar moiety was in a β orientation.

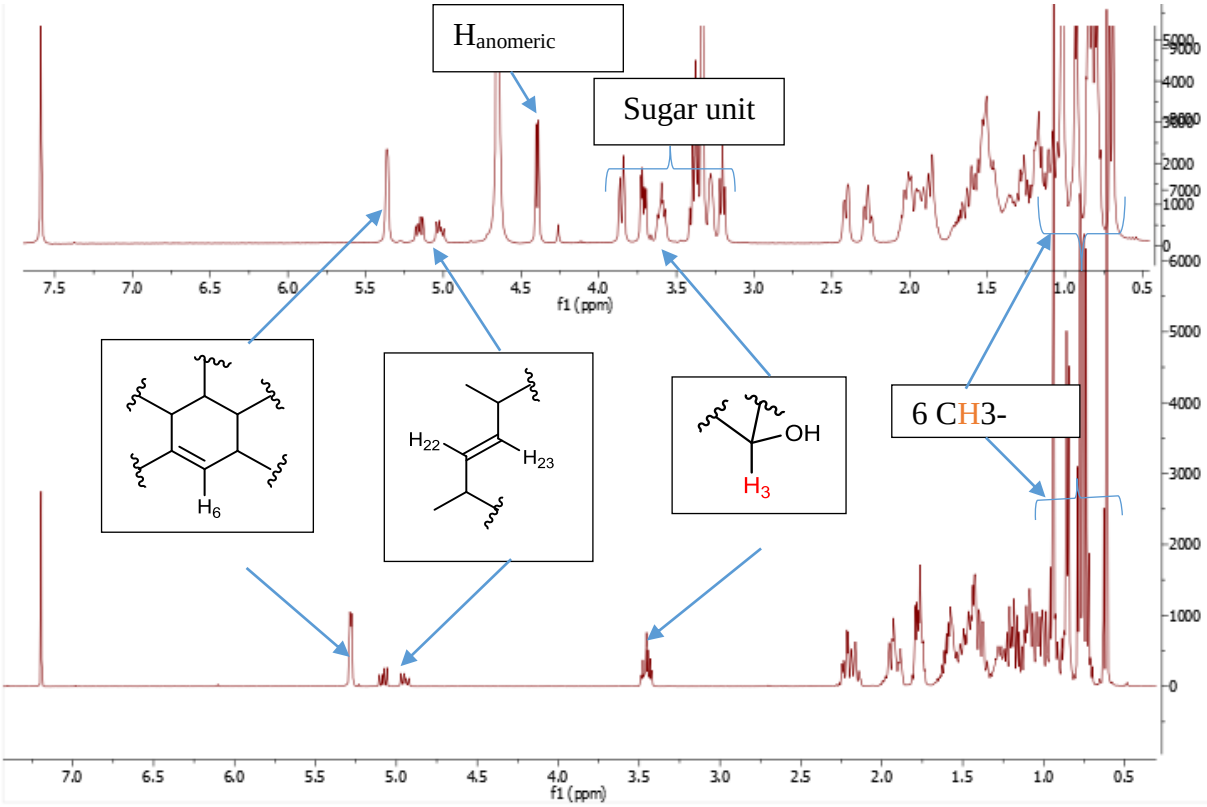

Figure 44: **Comparison of ^{1}H NMR spectrum ($CDCl_3/CD_3OD$, 500MHz) of SR2 and SR1**

Based on these data and by comparison with a sample available in the laboratory, SR2 was identified as stigmasterol 3-*O*-*β*-D-glucopyranoside, previously isolated from *Astragalus altaicus* and showed prominent cytotoxic activity against MOLT 4 (**Ivorra *et al*., 1988**).

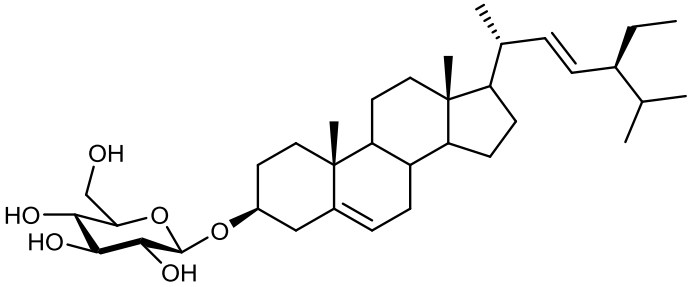

105

II.2.2.6.3 Identification of SB1 or 20-Hydroxyecdysone

SB1 was obtained as a white powder from *Sida rhombifolia* in mixure Hex-EA (60-4O). Its FAB in a positive mode mass spectrum showed a pseudo-molecular ion $[M + H]^+$ at *m/z* 481.1, thus a molecular mass of 480.3087 corresponding to the molecular formula $C_{27}H_{44}O_7$ with six degree of unsaturations.

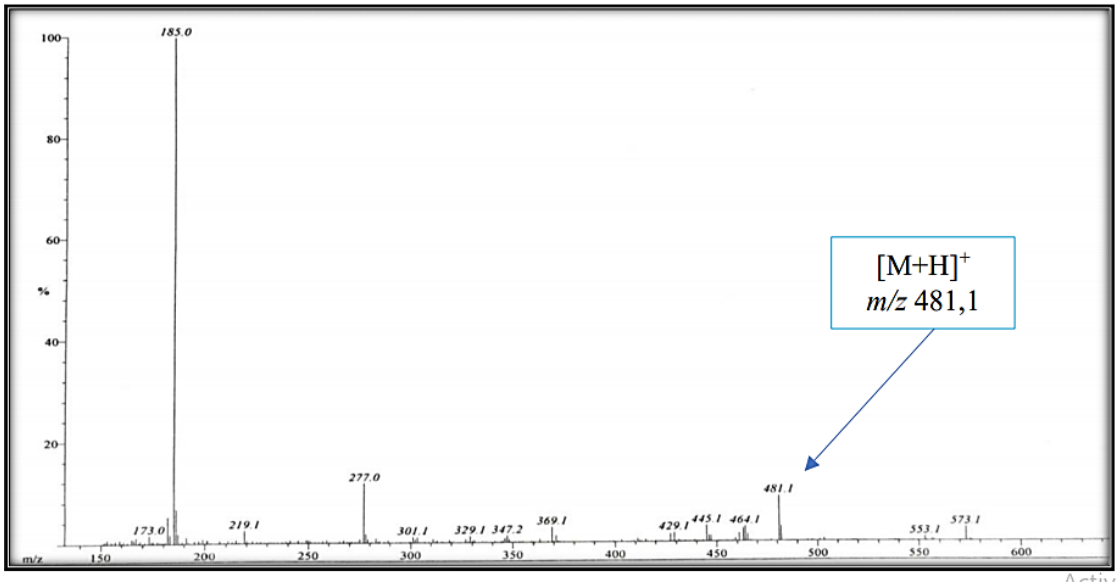

Figure 45: **FAB mass spectrum of SB1**

The compound exhibited signals of 27 carbons (Figure 46), among which a downfield signal for a carbonyl was observed at 206.5 ppm. In addition, signals appearing between δ_C 168.0 and 122.1 were assigned to olefinic bonds. The signals at δ_C 85.2, 78.4, 77.9, 71.3, 68.7 and 68.5 ppm attributable to six hydroxyl groups.

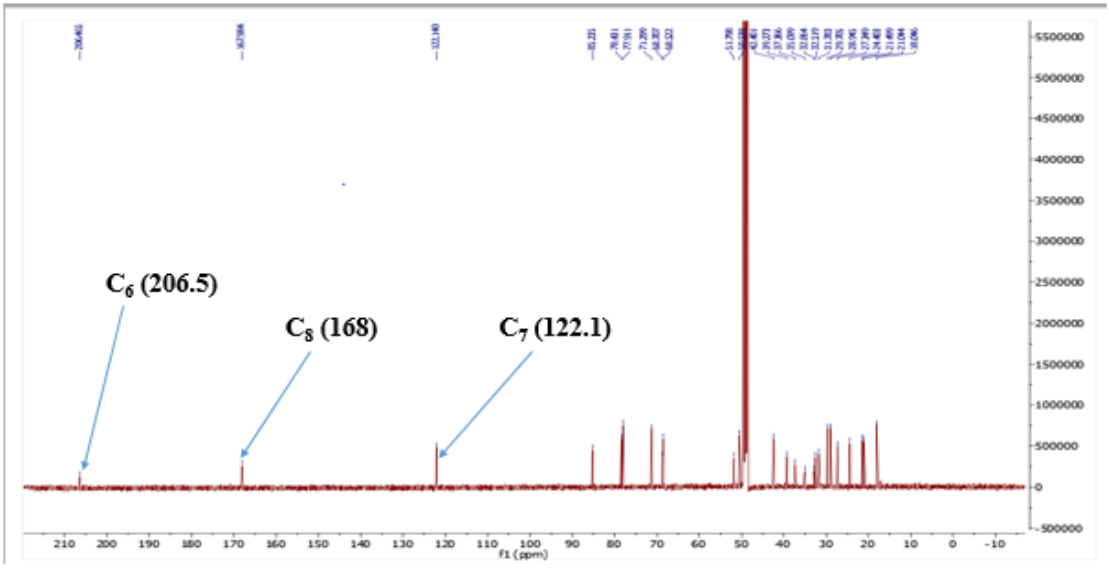

Figure 46:^{13}**C NMR broadband decoupled spectrum (125 MHz, CD_3OD) of SB1**

The ^{1}H NMR spectrum (Figure 47) showed resonances of five methyl singlets at 0.90; 0.98; 1.20; 1.21 and 1.22 ppm. The olefinic proton (H-7) signal at 5.82 ppm appeared as doublet due to allylic coupling (J = 2.6 Hz) with H-9 at 3.17 ppm.

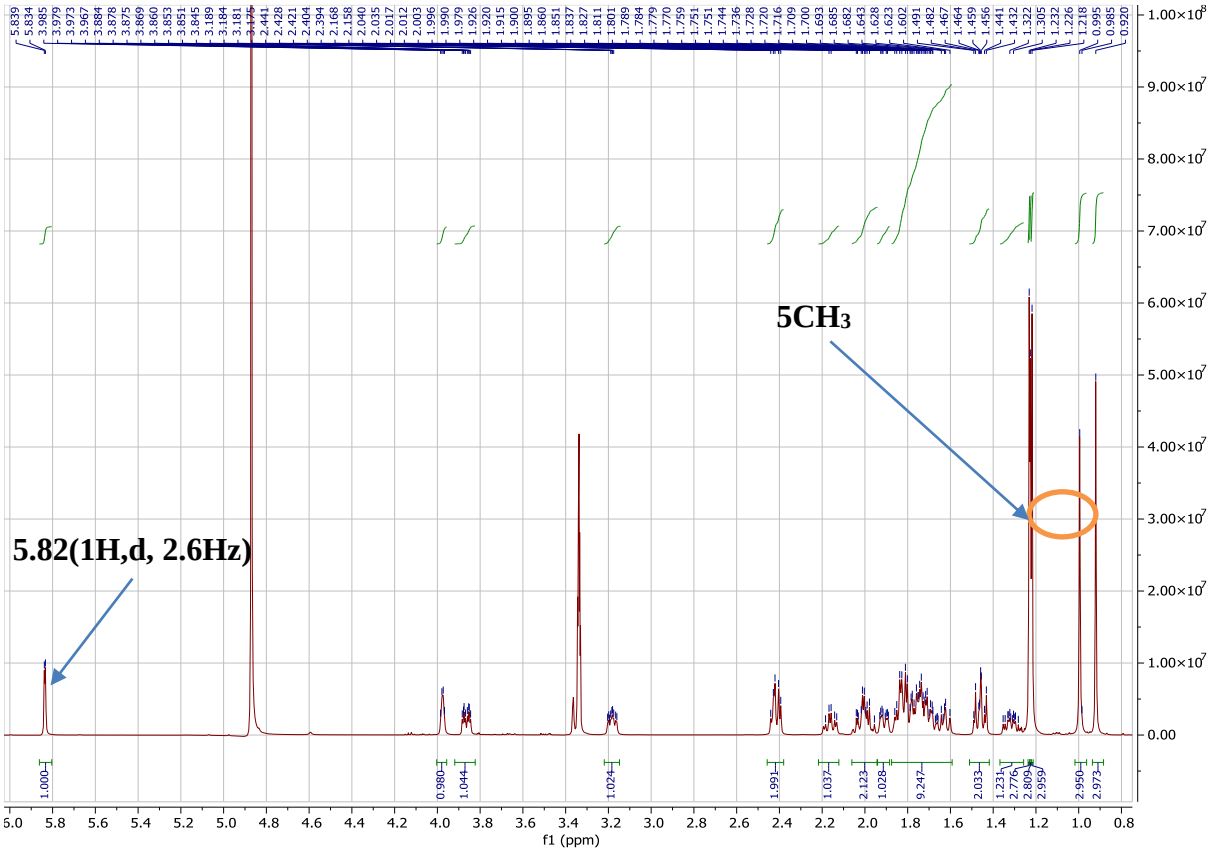

Figure 47: **^{1}H NMR spectrum (500 MHz, CD_3OD) of SB1**

The ^{13}C NMR (^{13}C:125 MHz, CD_3OD) data of SB1 in comparison with 20-Hydroxyecdysone of the literature are represented in the table 31:

Table 31: ^{13}C NMR (^{13}C:125 MHz, CD_3OD) data of SB1 in comparison with 20-Hydroxyecdysone of the literature (Maliński et *al.*, 2021).

Position	^{13}C NMR (125 MHz, CD_3OD) SB1	^{13}C NMR (125 MHz, CD_3OD) 20-Hydroxyecdysone
1	37.3	37.4
2	68.7	68.7
3	68.5	68.5
4	32.8	32.9
5	51.8	51.8
6	206.5	206.5
7	122.1	122.2
8	168.0	168.0
9	35.1	35.1
10	39.2	39.3
11	21.5	21.6

12	32.5	32.6
13	48.6	48.7
14	85.2	85.3
15	31.8	31.8
16	21.5	21.5
17	50.5	50.6
18	18.05.	18.1
19	24.4	24.5
20	77.9	77.9
21	21.1	21.5
22	78.4	78.5
23	27.3	27.4
24	42.4	42.4
25	71.3	71.3
26	28.9	29.0
27	29.7	29.8

These informations compared to 20-Hydroxyecdysone of the literature data led to its identification as 20-Hydroxyecdysone and improved sexual function in men (**Maliński *et al.* 2021**).

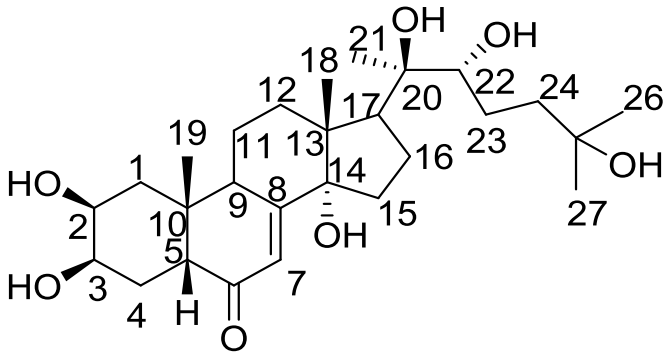

106

II.2.2.7 Triterpenes

II. 2.2.7.1. Identification of triterpene

Compound SR3 isolated as white powder from a mixture of Hex:EtOAc (95:5), was positive to Liebermann-Burchard test for triterpenes. Its ESI-MS spectrum showed an adduct ($[M + Na]^+$) at 449.3 with molecular formula $C_{30}H_{50}O$ having 6 degrees of unsaturation.

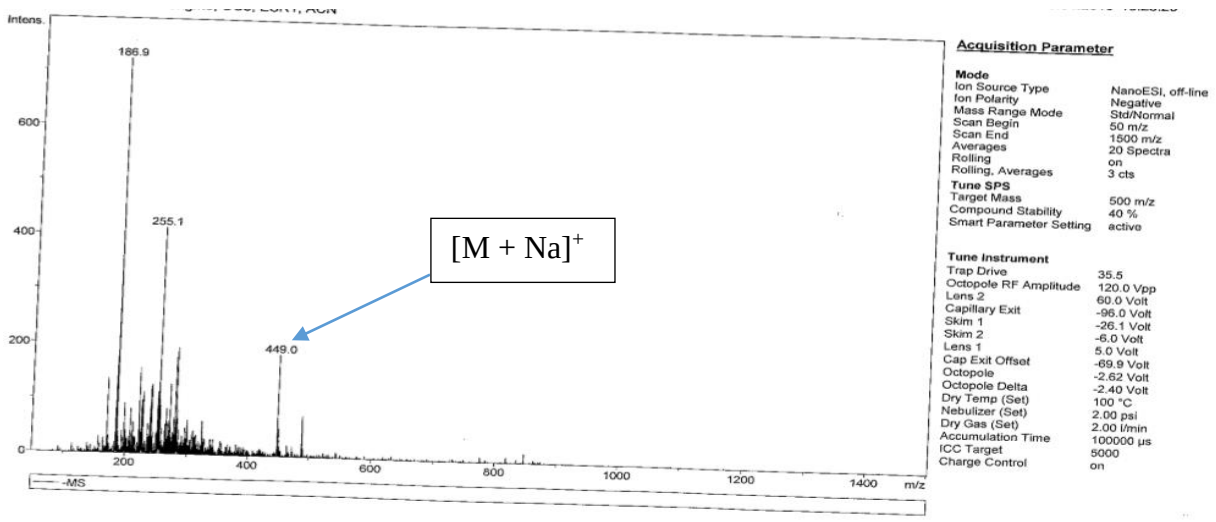

Figure 48: **(+)-ESI-MS spectrum of SR3**

Its ^{1}H NMR spectrum (Figure 49) showed six singlets for angular methyls between δ_H 0.75-0.97 (3H, s) each. It also showed a deshielded signal for sp2-bearing methyl at δ_H 1.62 (3H, s) and two broad singlets of olefinic protons at δ_H 4.61 (1H, s) and 4.50 (1H, s), typical characteristic of the propenyl group of a lupane-type pentacyclic triterpene (**Mahato and Kundu, 1994**). A doublet of doublet at δ_H 3.12 (1H, dd, J = 11.5; 4.8) was assigned to the proton of hydroxymethine.

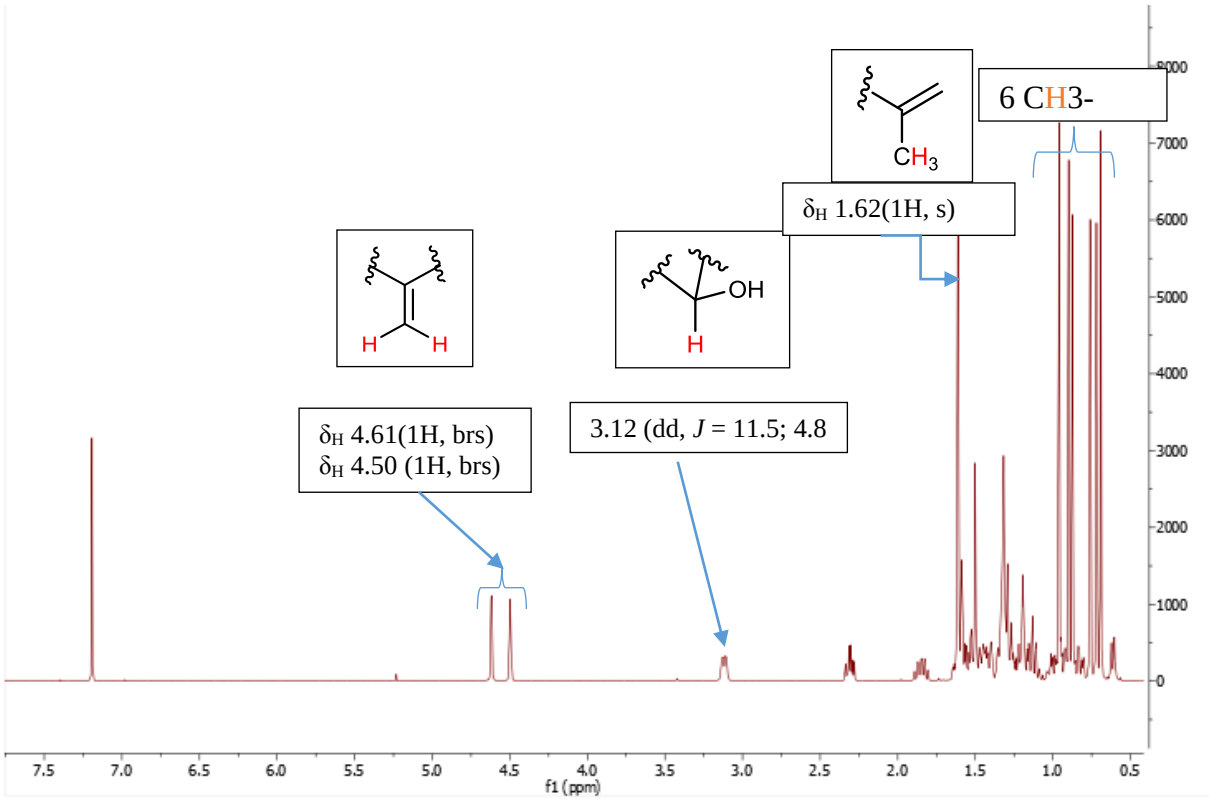

Figure 49: **^{1}H NMR spectrum (CDCl3, 500MHz) of SR3**

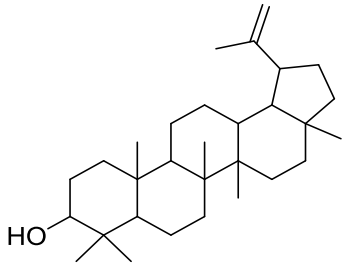

107

The ^{13}C NMR spectrum of SR4 (Figure 50) showed thirty signals corresponding to 30 carbon atoms. Among these signals:

- Two signals at δ_C 151.0 and 109.3 characteristic of carbons C-20 and C-29 of triterpenes of the lupane series **(Mbaze et *al*., 2007)**.
- A signal at δ_C 79.0 characteristic of the carbon of the hydroxymethine C-3 of pentacyclic triterpene **(Mbaze et *al*., 2007)**.

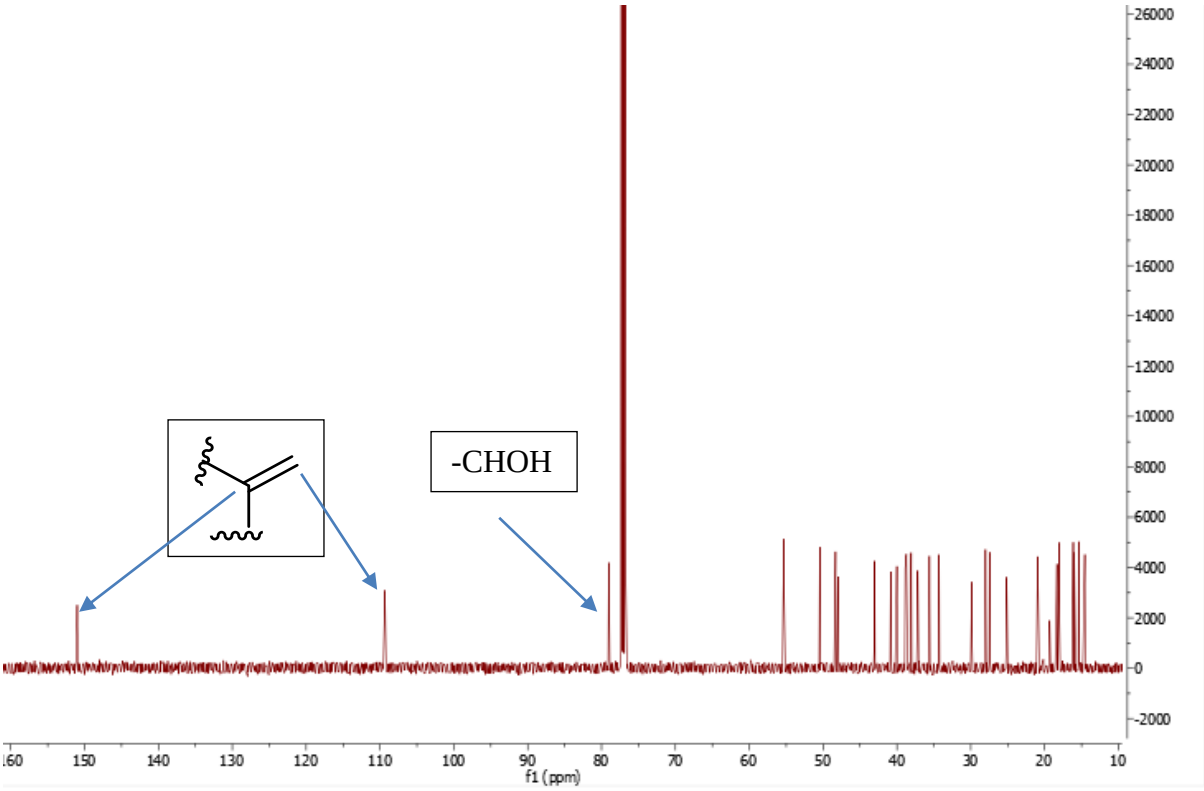

Figure 50: **^{13}CNMR broadband decoupled spectrum ($CDCl_3$, 125MHz,) of SR3**

The ^{13}C NMR (125 MHz) data of SR3 in $CDCl_3$ compared with lupéol of the literature value are represented in in the table 32.

Table 32: ^{13}C NMR (125 MHz) data for SR3 in $CDCl_3$ compared with lupeol of the literature (Thanakijcharoenpath et Theanphong, 2007).

SR3 (125 MHz,$CDCl_3$)		Lupeol (75 MHz,$CDCl_3$)
Position	δ_C	δ_C
1	38.8	38.7
2	27.3	27.4
3	79.0	78.9
4	38.8	38.8
5	55.4	55.3
6	18.4	18.3
7	34.3	34.2
8	40.9	40.8
9	50.5	50.4
10	37.1	37.1
11	21.0	20.9
12	25.2	25.1
13	38.1	38.0
14	42.8	42.8
15	27.4	27.4
16	35.5	35.5
17	43.1	43.0
18	48.2	48.2
19	47.9	47.9
20	151.0	150.9
21	29.9	29.8
22	40.1	40.0
23	28.1	28.0
24	15.5	15.4
25	16.2	16.1
26	16.0	15.9
27	14.6	14.5
28	18.1	18.0
29	109.3	109.3
30	19.3	19.3

All these data in comparison with those found in the literature enable us to assign Compound SR3 **108** lupeol previously isolated from *Diospyros glandulosa* (**Thanakijcharoenpath and Theanphong, 2007**).

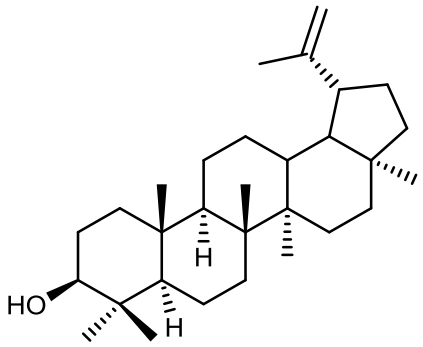

108

II.2.2.7.2 Identidfication of SR5

Compound SR5 was obtained as a cream white powder in the mixture of Hex:AcOEt (8.5:1.5). Its (+)-ESI-MS spectrum gave a sodium adduct ions at 457.1 ([M + Na]$^+$) (Figure 51) consistent with the molecular formular $C_{30}H_{48}O_3Na$ with 7 unsaturations.

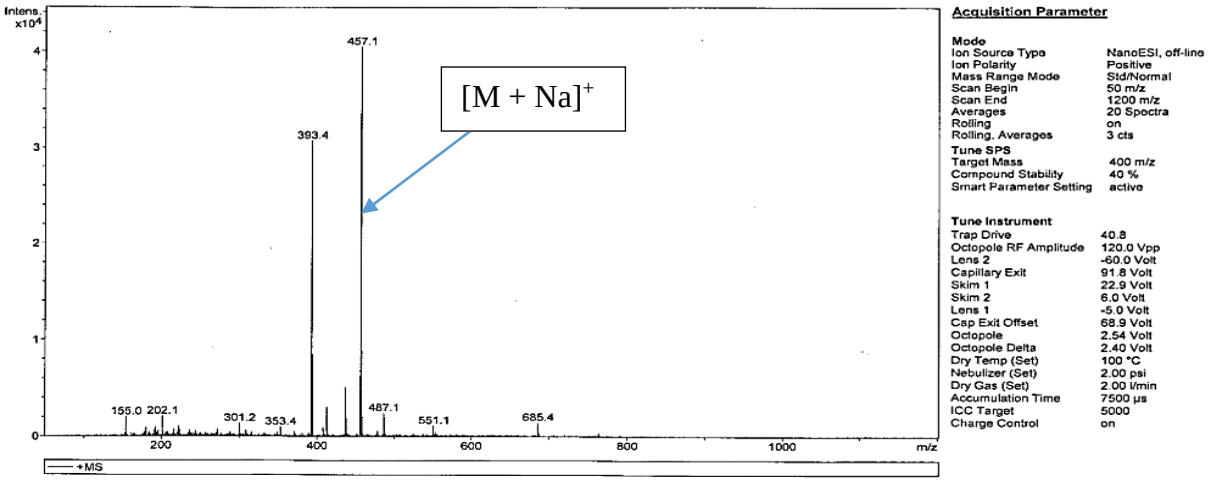

Figure 51: **(+)-ESI-MS spectrum of SR5**

Its ^{1}H NMR spectrum (Figure 52) is similar to that of SR4 since it showed a deshielded signal for Sp^2 bearing methyl at δ_H 1.62 (3H, s) and two broad singlets of an olefinic proton at δ_H 4.61 (1H, s) and 4.50 (1H, s) characteristic of the propenyl group of the lupane-type pentacyclic triterpene (**Mahato and Kundu, 1994**). It also showed signal for hydroxymethine proton at δ_H 3.12 (1H, dd, J = 11.5; 4.8). The main difference is the number of singlets for angular methyl groups between δ_H 0.75-0.97, one of which was oxidized.

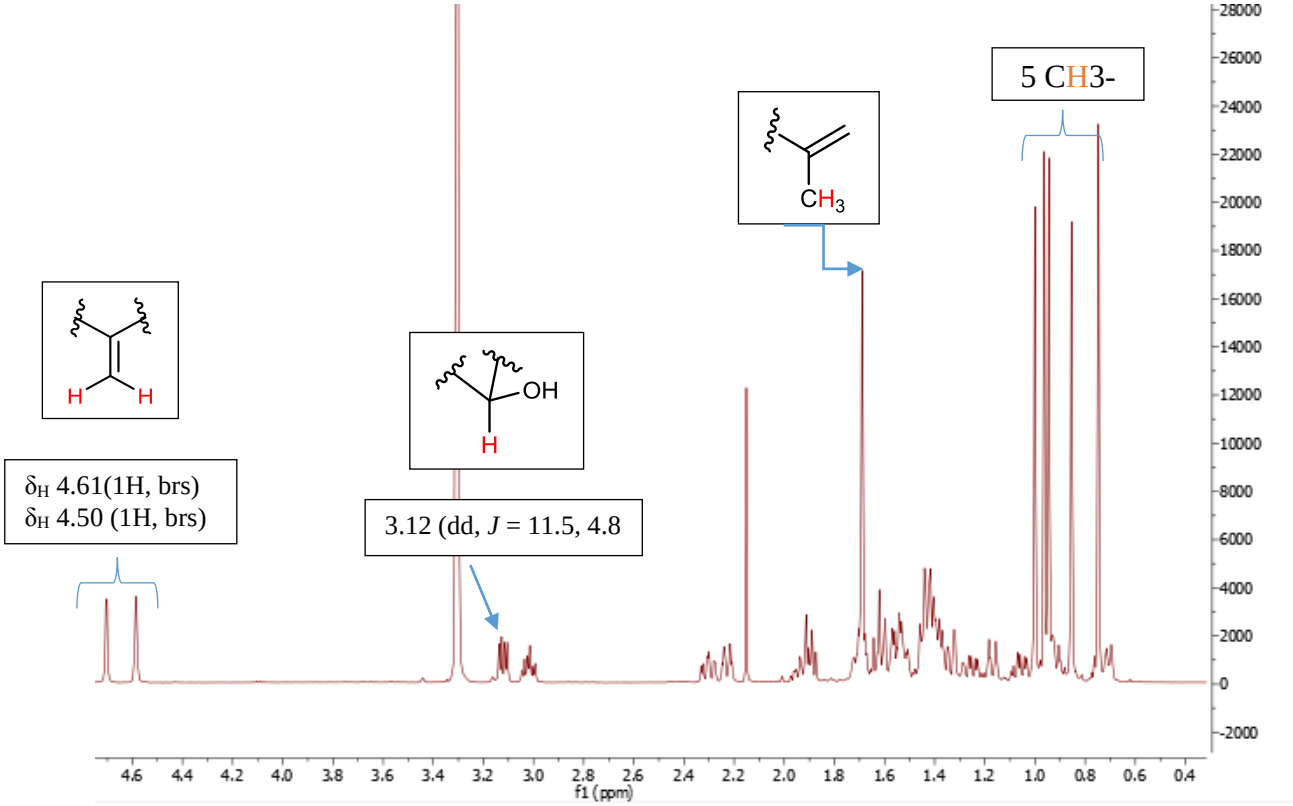

Figure 52: **^{1}H NMR spectrum (CD_3OD, 500MHz) of SR5**

The ^{13}C NMR spectrum of SR5 (Figure 53) showed thirty carbons among which were the characteristic signals of C-20 and C-29 of lupane series **(Mbaze et *al*., 2007)**. The main difference between the ^{13}C NMR of SR5 and that of SR3 is the carbonyl of an acid at δ_C 177.6, which confirmed the oxidation of one of the methyl.

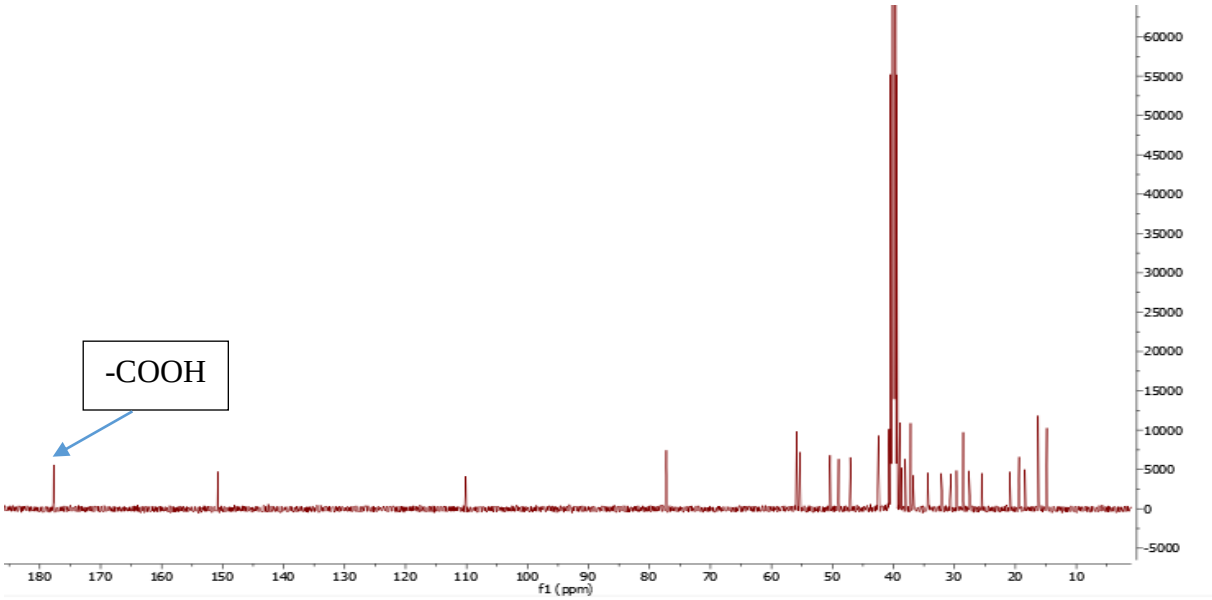

Figure 53: **^{13}C NMR broadband decoupled spectrum (CD_3OD, 125MHz) of SR5**

The ^{13}C NMR (125 MHz) data for SR3 in $CDCl_3$ compared with betulinic acid of the literature are represented in the table 33.

Table 33 : ^{13}C NMR (125 MHz) data for SR3 in $CDCl_3$ compared with betulinic acid the literature (Tangmouo *et al*., 2005).

Position	SR5 (125 MHz, $CDCl_3$)	Betulinic acid (100 MHz, $CDCl_3$)
N°	δ_C	δ_C
1	38.3	38.7
2	27.3	27.4
3	78.2	78.9
4	38.7	38.8
5	55.2	55.3
6	18.2	18.3
7	34.2	34.3
8	40.5	40.7
9	50.3	50.5
10	37.1	37.2
11	20.7	20.8
12	25.2	25.5
13	38.2	38.4
14	42.3	42.4
15	30.6	30.5
16	32.0	32.1
17	56.2	56.3
18	46.7	46.8
19	49.1	49.2
20	150.0	150.3
21	29.5	29.7
22	36.9	37.0
23	27.7	27.9
24	15.1	15.3
25	15.9	16.0
26	16.0	16.1
27	14.6	14.7
28	177.6	180.5
29	109.4	109.6
30	19.2	19.4

The deshielded nature of H-18 at δ_H 3.02 suggested that the acid group is located at the position C-28. This information compared to those obtained from the literature enabled us to assigned compound SR5 as betulinic acid **109**, previously isolated from *Diospyros canaliculata* (**Tangmouo *et al*., 2005**).

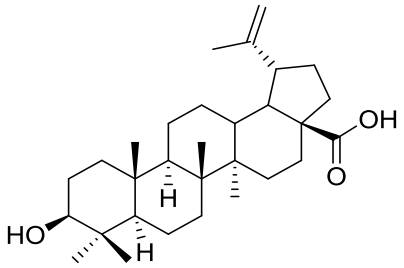

109

II.2.2.7.3 Identification of SRA1

Compound SRA1 isolated as white powder from a mixture of Hex:EtOAc (16.5:1.5), was positive to Liebermann-Burchard test for triterpenes. Its ESI-MS spectrum showed an adduct ([M + Na]$^+$) at 449.3 with molecular formula $C_{30}H_{50}ONa$ having 6 degrees of unsaturation.

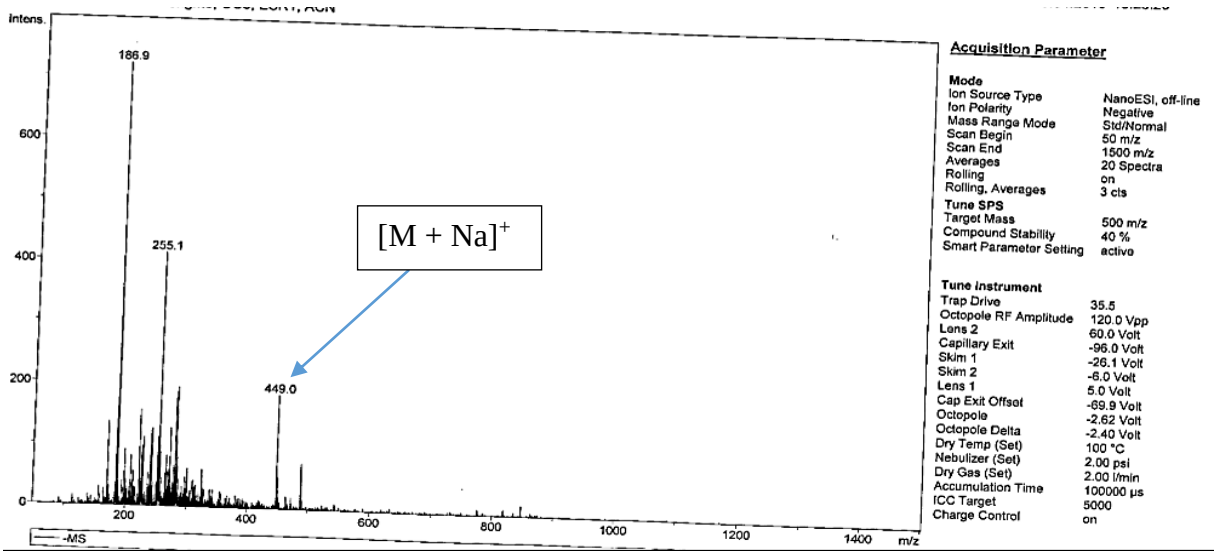

Figure 54: **(+)-ESI-MS spectrum of SRA1**

Its ^{1}H NMR spectrum (Figure 55) showed a set of eight singlets of three protons each at δ_H 0.73 (3H, s), δ_H 0.75 (3H, s), δ_H 0.83 (3H, s), δ_H 0.84 (3H, s), δ_H 0.85 (3H, s), δ_H 0.88 (3H, s), δ_H 0.91 (3H, s), δ_H 1.02 (3H, s) corresponding to eight angular methyl groups typical characteristic of pentacyclic triterpenes. In addition, it showed at signal δ_H 5.46 (1H, dd, *J*= 8.2, 3.2), characteristic of proton H-15 of pentacyclic triterpenes belonging to Taraxerene series **(Hernandez-Chavez et *al*., 2012)**. A multiplet of one proton at δ_H 3.12 (1H, dd, *J*= 11.3; 3.5) assign to hydroxymethine H-3, according to the biosynthesis of triterpene.

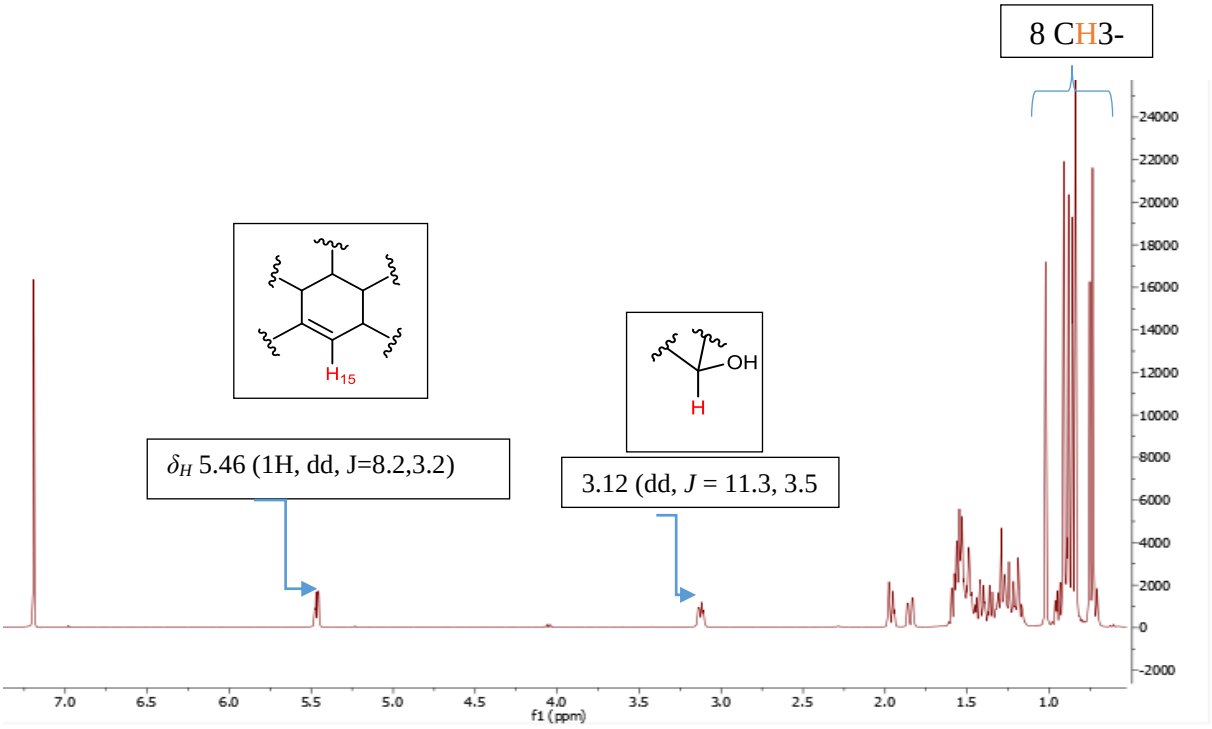

Figure 55: **^{1}H NMR spectrum ($CDCl_3$, 500MHz) of SAR1**

The ^{13}C NMR of SAR1 (Figure 56), showed thirty signals including that of carbon C-14 and C-15 of taraxerene series at δ_H 158.0 and 116.8, respectively **(Hernandez-Chavez et *al*., 2012)**. In addition, the signal of an oxyméthine (C-3) was observed at δ_C 79.0.

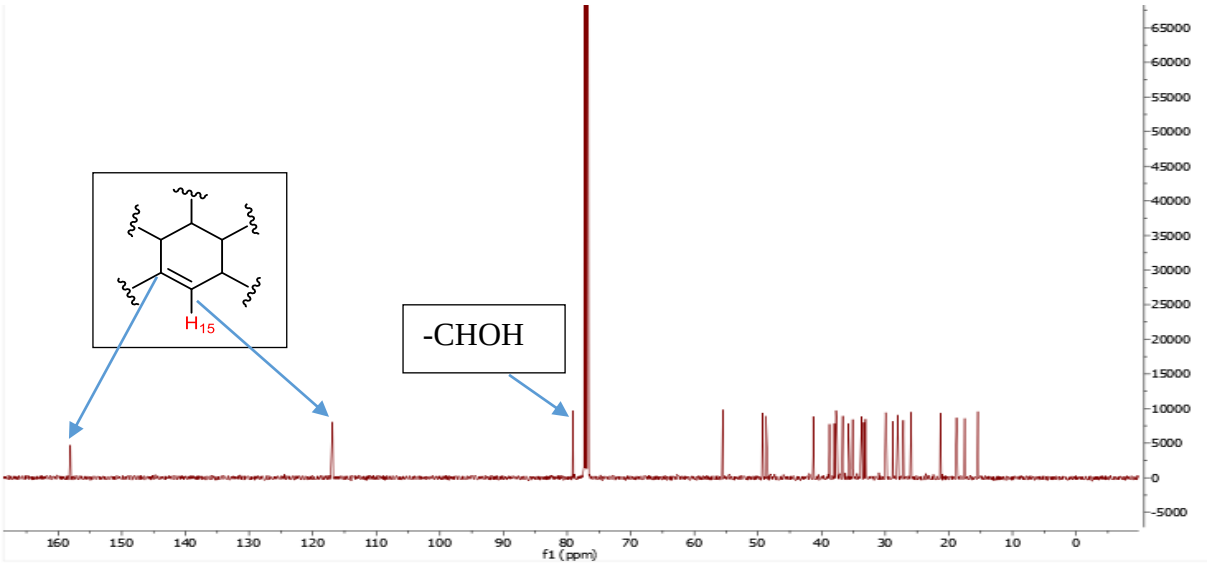

Figure 56: **^{13}C NMR broadband decoupling spectrum ($CDCl_3$, 125MHz) of SRA1**

The ^{13}C NMR (125 MHz) data for SRA1 in $CDCl_3$ compared with taraxerol of the literature are represented in the table 34 below:

Table 34: 13C NMR (125 MHz) data for SRA1 in CDCl3 compared with taraxerol of the literature (Oladoye et al., 2015).

SRA1 (125 MHz, $CDCl_3$)		Taraxerol (125 MHz, $CDCl_3$)
N°	δ_C	δ_C
1	38.0	38.0
2	27.0	27.1
3	79.0	79.1
4	39.0	39.0
5	55.4	55.5
6	18.7	18.8
7	35.0	35.1
8	38.6	38.7
9	48.6	48.7
10	37.4	37.5
11	17.4	17.5
12	35.7	35.8
13	37.5	37.6
14	158.0	158.1
15	116.8	116.9
16	36.5	36.6
17	37.6	37.7
18	49.1	49.2
19	41.2	41.3
20	28.7	28.8
21	33.6	33.7
22	33.0	33.1
23	28.0	28.0
25	15.3	15.4
26	29.7	29.8
27	25.8	25.9
28	29.8	29.9
29	33.2	33.3
30	21.3	21.4

Based on all these evidences and after comparing the above data with those recorded in the literature, SRA1 was characterized as taraxerol (**Oladoye *et al*., 2015**).

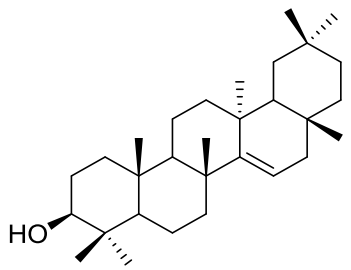

110

II.2.2.7.4 Identification of SRA2

Compound SRA2 isolated as white powder from a mixture of Hex:EtOAc (9.5:0.5), was positive to Liebermann-Burchard test for triterpenes. Its ESI-MS spectrum showed a proton adduct ion ($[M + H]^+$) at 469.2 with molecular formula $C_{32}H_{52}ONa$ having 7 degrees of unsaturation.

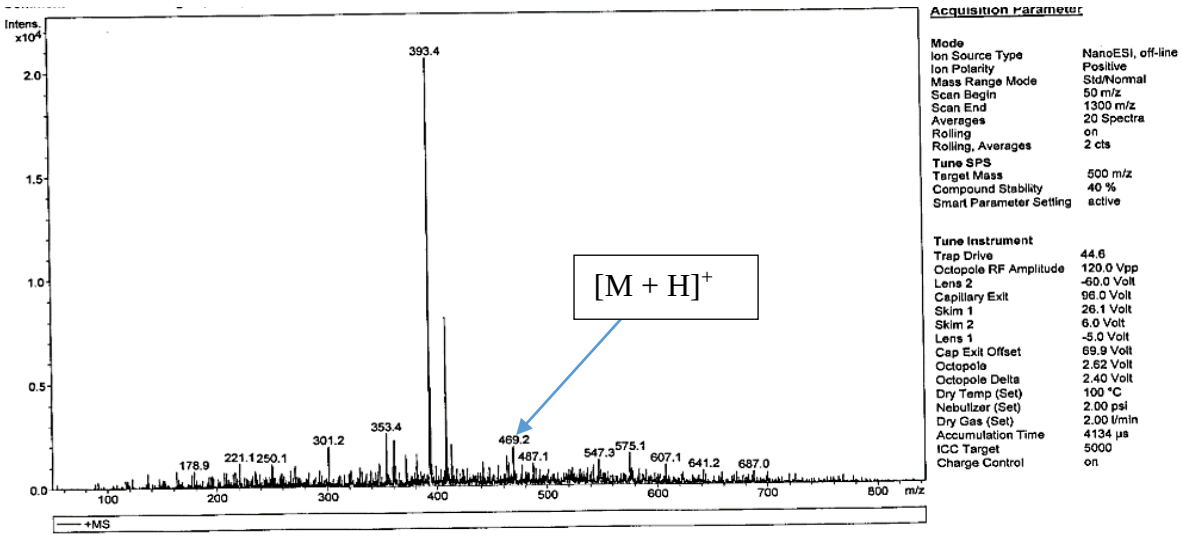

Figure 57: **(+)-ESI-MS spectrum of SRA2**

Its ^{1}H NMR spectrum (Figure 58) is similar to that of SAR1, since it also exhibited a set of eight singlets accounting for three protons each at δ_H 0.73 (3H, s), δ_H 0.75 (3H, s), δ_H 0.83 (3H, s), δ_H 0.84 (3H, s), δ_H 0.85 (3H, s), δ_H 0.88 (3H, s), δ_H 0.91 (3H, s), δ_H 1.02 (3H, s) which correspond to eight angular methyl groups. The signal at δ_H 5.46 (1H, dd, J= 8.2; 3.2 Hz) was assigned to proton H-15 of pentacyclic triterpenes belonging to taraxerene series. The two main differences between the ^{1}H NMR of SAR2 and SAR1 are:

- The shielded value of the hydroxymethine proton H-3, which appears at δ_H 4.39 (1H, dd, J= 8.2, 3.2), showing that the hydroxyl at C-3 has been acetylated.
- The presence of one more methyl signal at δ_H 1.97 (3H, s), which correspond to a methyl group attached to a carbonyl.

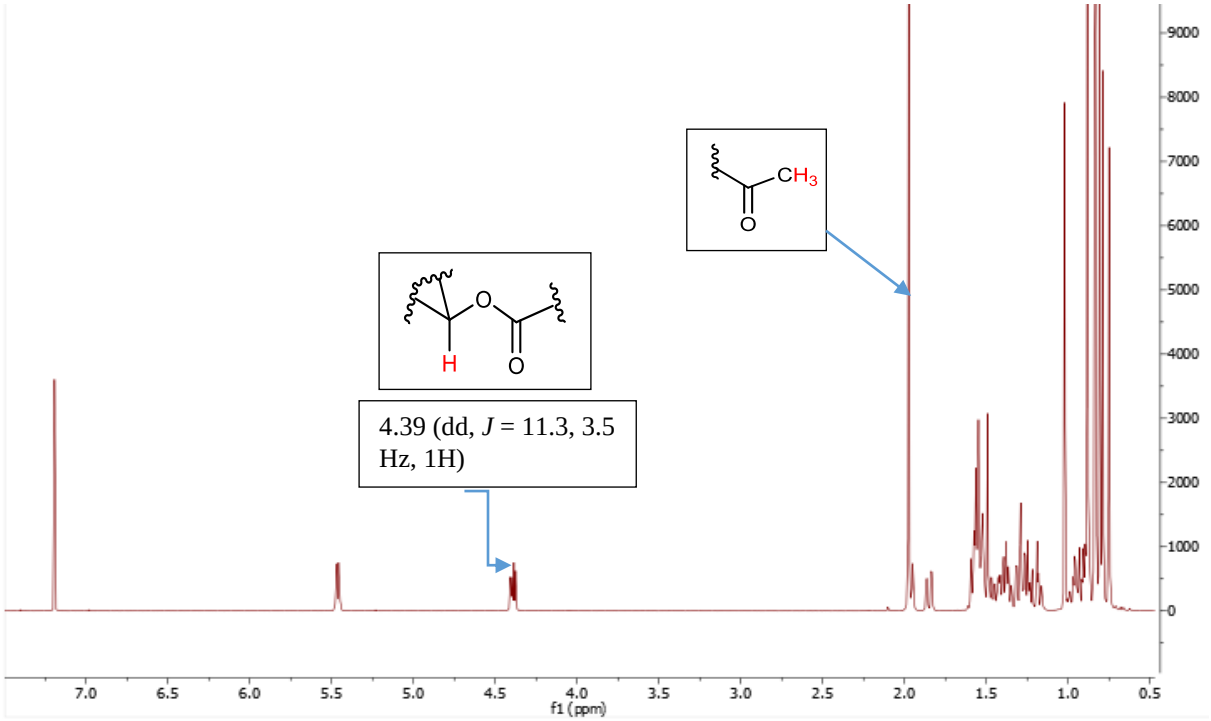

Figure 58: **^{1}H NMR spectrum ($CDCl_3$, 125MHz) of SRA2**

The ^{13}C NMR (Figure 59) confirmed the presence of two additional carbons since it showed thirty-two signals of carbons instead of thirty, among which the signal of a carbonyl of an ester at δ_C 171.0.

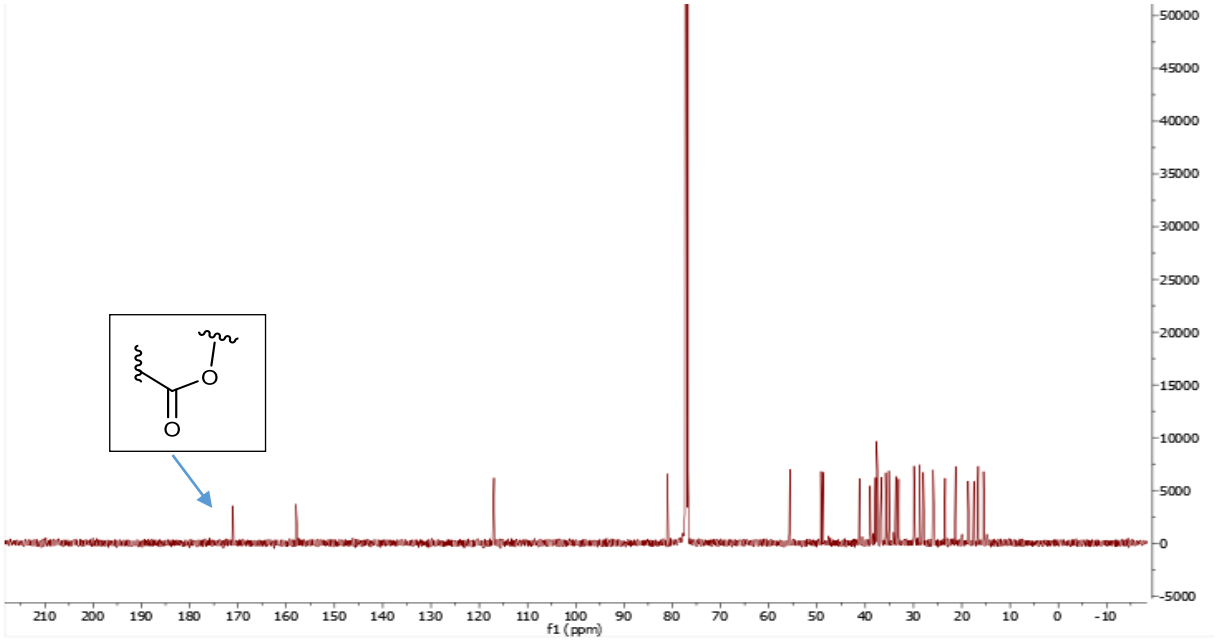

Figure 59: **^{13}C NMR broadband decoupled spectrum ($CDCl_3$, 125MHz) of SAR2**

The ^{13}C NMR (125 MHz) data for SAR2 in $CDCl_3$ in comparison with taraxeryl acetate of the literature are represented in the table 35 below:

Table 35: ^{13}C NMR (125 MHz) data for SAR2 in $CDCl_3$ in comparison with taraxeryl acetate of the literaure (Oladoye *et al.*, 2015).

	SAR2 (125 MHz, $CDCl_3$)	Taraxeryl acetate (125 MHz ,$CDCl_3$)
POSITION	δ_C	δ_C
1	38.0	38.0
2	27.1	27.1
3	80.1	80.0
4	39.3	39.2
5	55.6	55.5
6	18.9	18.7
7	35.2	35.0
8	38.9	38.8
9	48.9	48.8
10	37.7	37.6
11	17.7	17.6
12	36.0	35.9
13	37.8	37.7
14	158.2	158.1
15	116.9	116.8
16	36.6	36.6
17	37.9	37.8
18	49.3	49.2
19	41.4	41.3
20	28.9	28.8
21	33.9	33.8
22	33.2	33.2
23	28.0	28.0
25	15.4	15.4
26	29.9	29.8
27	25.9	25.9
28	30.0	29.9
29	33.7	33.6
30	21.4	21.4
$CH_3\underline{C}O$-	171.0	171.2
$\underline{C}H_3CO$-	21.6	21.8

On the basis of the above mentioned spectra data and by comparison with literature, compound SAR2 was assigned to **104** also known as taraxeryl acetate previously isolated from *Jatropha tanjorensis* (**Oladoye et *al.*, 2015**).

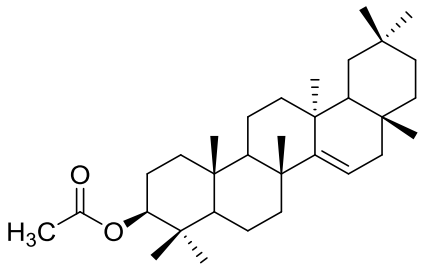

111

II.2.2.7.5 Identification of SR4.

SR4 was obtained as a white powder from a mixure Hex : EtoAc (17:3).

The ^{13}C NMR spectrum (Figure 60) showed 30 signals for 30 carbon resonances amongst which are the Urs-12-ene diagnostic signals at δ_C 138.1(C-13) and 126.1 (C-12) **(Mahato and Kundu, 1994)** as well as oxymethine and carboxylic acid carbon signals at δ_C 79.8 and δ_C 181.5, respectively.

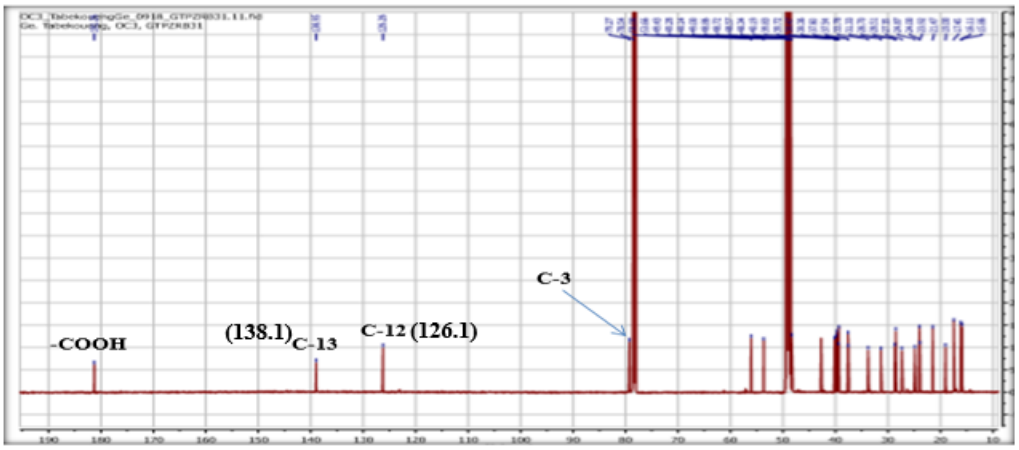

Figure 60: **^{13}C NMR broadband decoupled spectrum of compound SR4 (125MHz, CD_3OD)**

Its ^{1}H NMR spectrum (Figure 61) displayed signals for a vinyl proton as a triplet (J = 5.0 Hz) at δ_H 5.25 (H-12), two methyl groups as doublets at δ_H 0.88 (3H, d, J = 6.7 Hz) and 0.95 (3H, d, J = 6.3 Hz) attributable to methyls 29 and 30 of Urs-12-ene skeleton. Five intense angular methyl signals were also observed at δ_H 0.77, 0.79, 0.93, 0.98 and 1.08; an oxygenated methine multiplet at δ_H 3.23 assignable to H-3 of triterpene and a broad doublet at δ_H 2.30 (1H, brd, J = 10.5 Hz) ascribed to H-18 of C-28 oxidised ursane triterpene (**Furuya et *al*., 1987**).

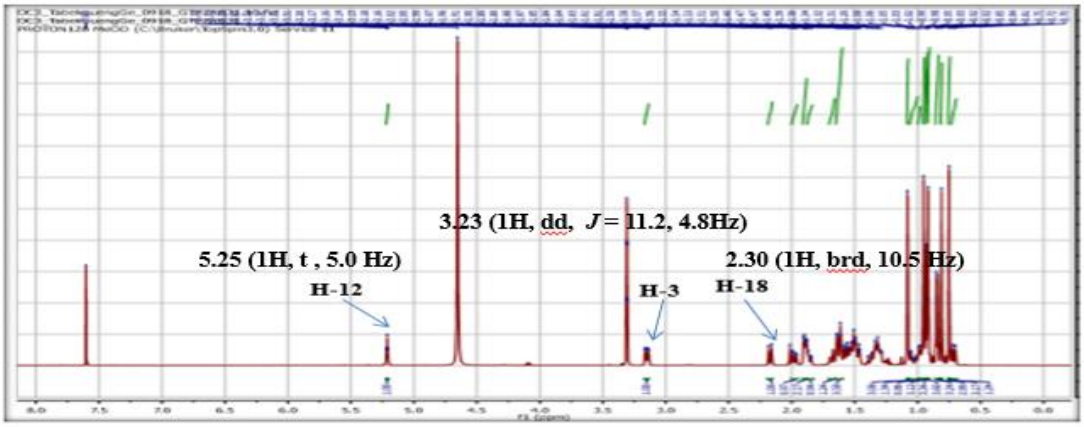

Figure 61: **^{1}H NMR spectrum of compound SR4 (500MHz, CD_3OD)**

The ^{13}C NMR (125MHz, CD_3OD) data of SR4 and ^{13}C NMR data of Ursolic acid (125MHz, C_5D_5N) are represented in the table 36 below.

Table 36: ^{13}C NMR (125MHz, CD_3OD) data of SR4 and ^{13}C NMR data of Ursolic acid (125MHz, C_5D_5N) (Kyeong et *al*. 2014).

POSITION	SR4, δ_C	Ursolic acid (Kyeong et *al*., 2014)
1	39.0	40.3
2	28.2	29.4
3	79.8	79.4
4	39.2	40.6
5	55.4	57.1
6	18.5	19.9
7	33.1	34.8
8	39.7	41.2
9	48.1	49.3
10	37.2	37.5
11	23.8	24.9
12	126.1	126.9
13	138.1	140.0
14	42.2	43.7
15	28.2	28.9
16	24.	26.2
17	48.1	49.3
18	52.9	54.8
19	39.2	40.7
20	39.0	40.6
21	30.8	32.3
22	38.8	38.7
23	28.3	30.1
24	15.8	17.5
25	15.6	16.4
26	17.2	18.5
27	24.3	25.2
28	181.5	181.2
29	17.3	18.6
30	21.3	22.3

Other signals were assigned to various carbons and protons by comparison of spectroscopic data with those reported by Kyeong et *al*. 2014. In addition to this, the TLC analysis of SR4 with an authentic sample in the laboratory enabled us to identify compound **112** as ursolic acid.

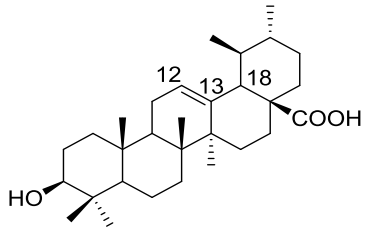

112

II.2.2.7.6 Identification of Oleanolic acid or SR7.

Compound SR7 isolated as white powder from a mixture of Hex:EtOAc (9:1), was positive to Liebermann-Burchard test for triterpenes. The EI-MS spectrum showed the molecular ion peak at *m/z* 456.3 which corresponding to molecular formula of $C_{30}H_{48}O_3$ with seven unsaturations.

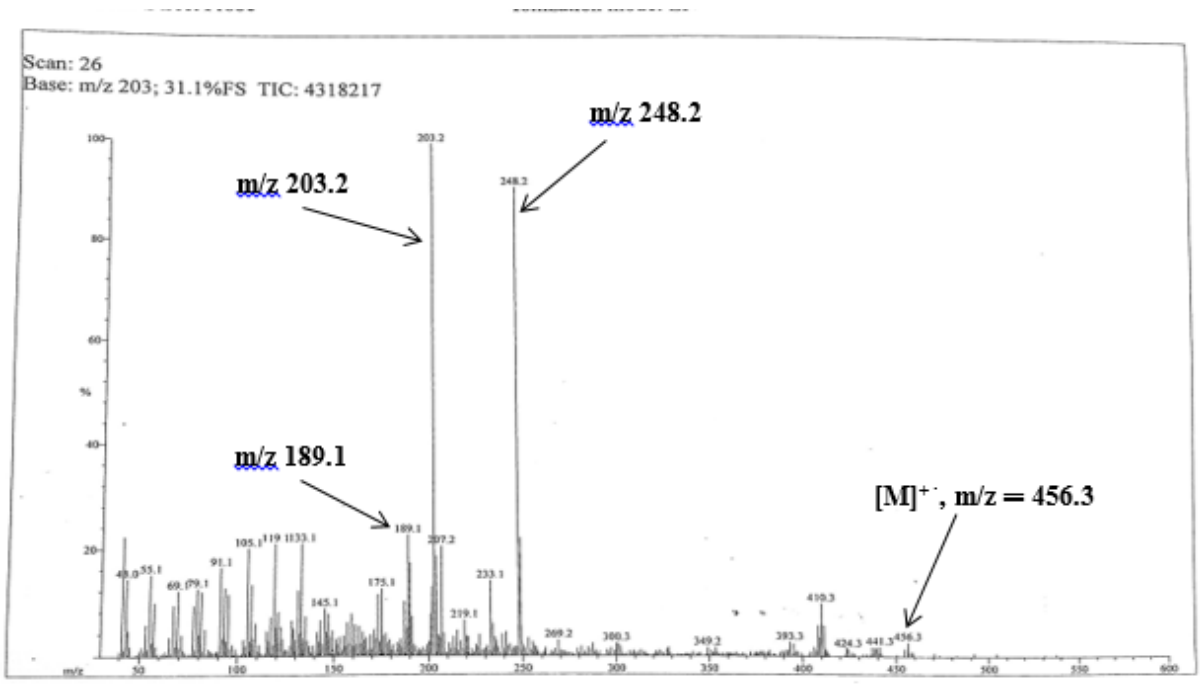

Figure 62: **EI-MS of SR7**

Its ^{1}H NMR spectrum (Figure 63**)** displayed a doublet of doublets (1H, *J* = 11.2, 4.8Hz) at δ_H 3.15 assignable to H-3 of triterpenes, suggesting the presence of a hydroxyl. It further displayed the following:

-Seven intense singlets of methyl groups appearing at δ_H 0.76, 0.81, 0.90, 0.95,0.97, 1.10, and 1.15 ppm, an olefinic proton appearing as a triplet (*J* = 3.6 Hz) at δ_H 5.24 typical characteristic of olean-12-ene triterpene (**Feumo et *al*. 2018**).

-A doublet of doublets (1H, *J* = 14, 4Hz) at δ_H 2.86 assignable to H-18 of oleanane oxidised at position C-28 **(Furuya et *al*. 1987)**.

-A cluster of signals between δ_H 1.01 - 2.08 revealing the presence of methylene and methine protons of the pentacyclic triterpene.

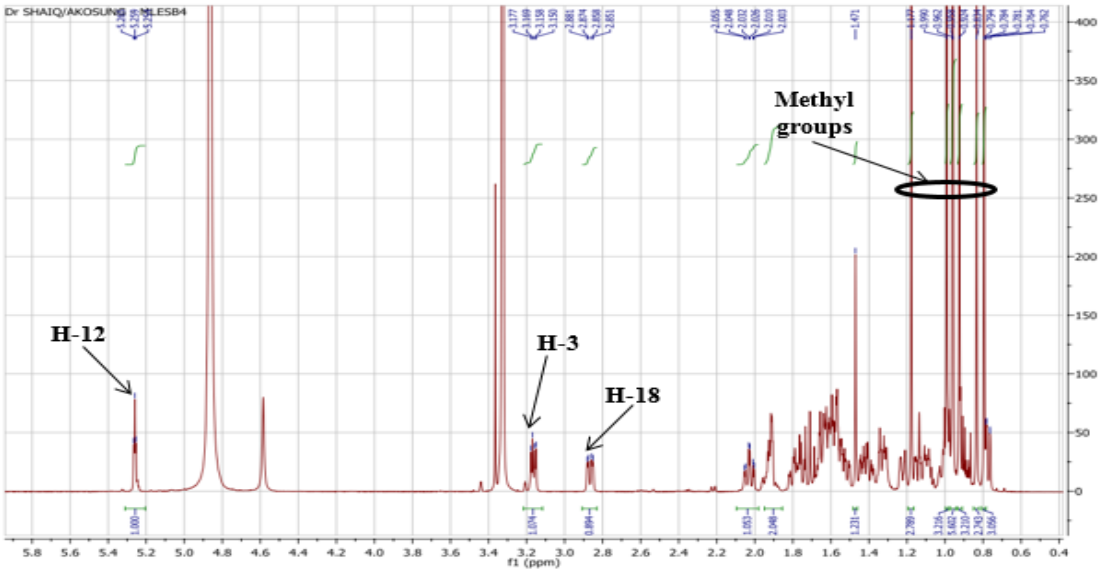

Figure 63: **^{1}H NMR spectrum of compound SR7 (600MHz, CD_3OD)**

The ^{13}C NMR spectrum (Figure 64) showed signals at δ_C 122.8 and at δ_C 143.7 assigned to C-12 and C-13 of the olean-12-ene respectively (**Mahato and Kundu, 1994**).

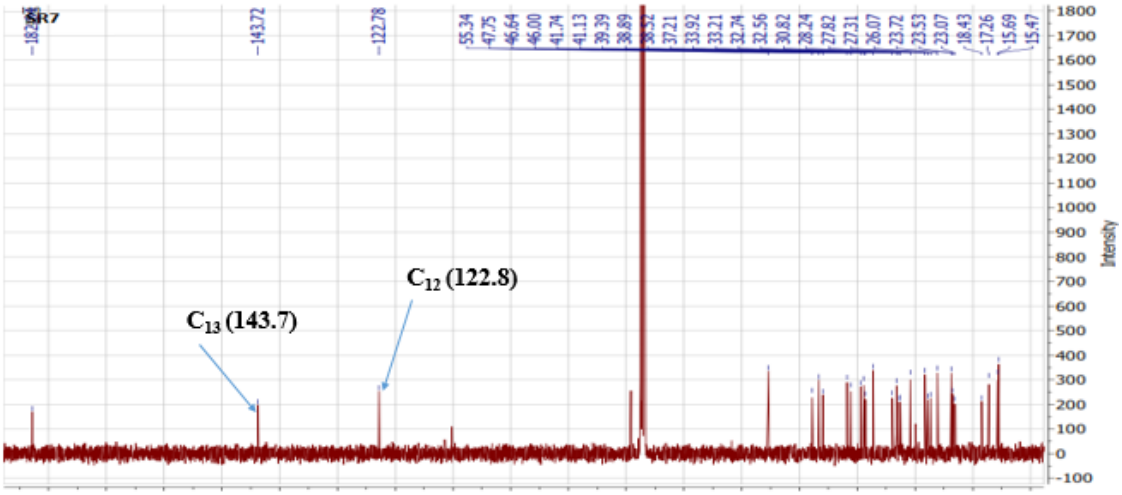

Figure 64 : ^{13}C NMR broadband decoupled spectrum of compound SR7 (75MHz, $CDCl_3$)

The ^{13}C NMR (75 MHz, $CDCl_3$) SR7 spectral data compared with those of oleanolic acid (100 MHz, $CDCl_3$) are represented in the table 37 below.

Table 37: ^{13}C NMR (75 MHz, $CDCl_3$) SR7 spectral data compared with oleanolic acid of the literature (100 MHz, $CDCl_3$) (Han S et *al*., 2014).

POSITION	SR7, δ_C	Oleanolic acid (Han S et *al*., 2014)
1	38.9	38.9
2	28.2	28.3
3	78.6	78.1
4	39.4	39.4
5	55.3	55.3
6	18.4	18.8
7	33.9	33.3
8	39.4	39.8
9	47.8	48.1
10	37.2	37.4
11	23.8	23.8
12	122.8	122.6
13	147.3	144.8
14	42.2	43.7
15	28.2	28.9
16	24.	26.2
17	48.1	49.3
18	52.9	54.8
19	39.2	40.7
20	39.0	40.6
21	30.8	32.3
22	38.8	38.7
23	28.3	30.1
24	15.8	17.5
25	15.6	16.4
26	17.2	18.5
27	24.3	25.2
28	181.5	181.2
29	33.2	33.3
30	21.3	22.3

Other signals were assigned to various carbons and protons by comparison of spectroscopic data with those reported by Kyeong et *al.* 2014. In addition to this, the TLC analysis of SR7 with an authentic sample in the laboratory enabled us to characterise compound **113** as oleanolic acid.

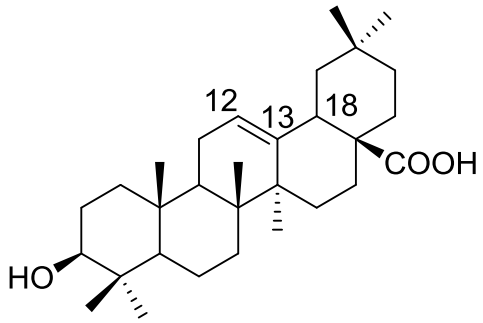

113

II.2.2.7.7 Identification of SRYK6 or Leontoside A

Compound SRYK6, named Leontoside A was obtained as a white powder in a mixture Hexane:Ethylacetate (1:1). It responded positively to Liebermann Burchardt test for triterpenoids and tests of glycosides. Its ESI-MS showed the sodium adduct peak $[M+Na]^+$ at *m/z* =627.3888, thus a molecular mass of 604.3975, which in conjunction with NMR data suggest a molecular formula $C_{35}H_{56}O_8Na$ corresponding to eight degrees of insaturation.

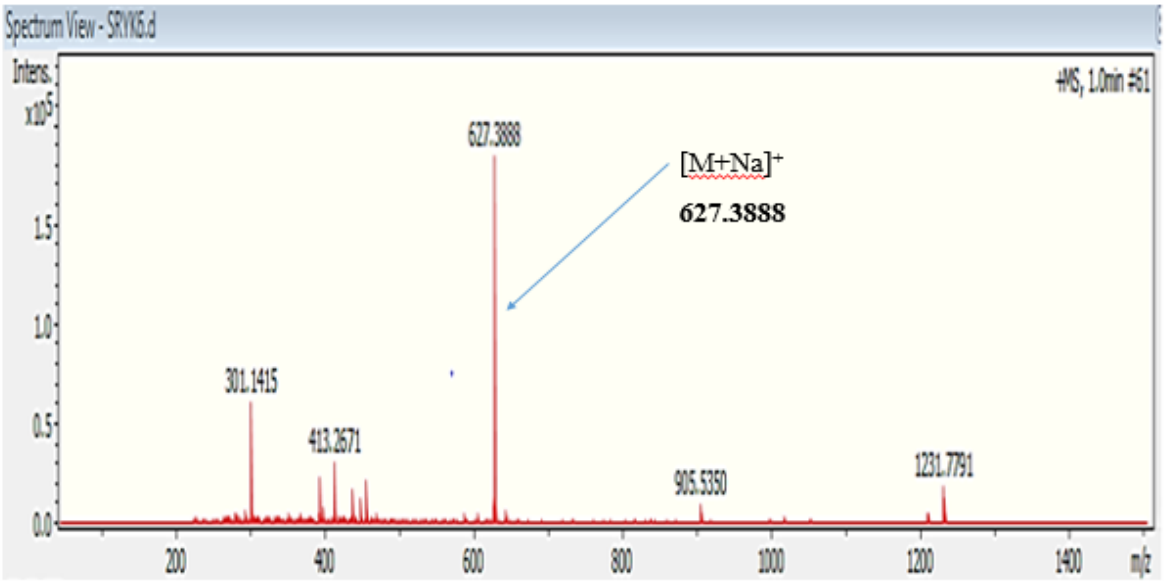

Figure 65: ESI-MS of SRYK6

The ^{1}H NMR spectrum (Figure 66) of SRYK6 is similar to oleanolic acid in the sense that it presents several peaks in common, including the signal of H-12 at δ_H 5.23.

The appearance of several other oxymethine and oxymethylene signals between 3.00 and 4.50 indicated the presence of a sugar moiety. Furthermore, the major changes of these spectra are the disappeareance of one of the oleanolic acid methyl signals in favour of the appearance of an oxymethylene on the SRYK6 spectrum indicating that one of the oleanolic acid methyls has been oxidised in the SRYK6 compound.

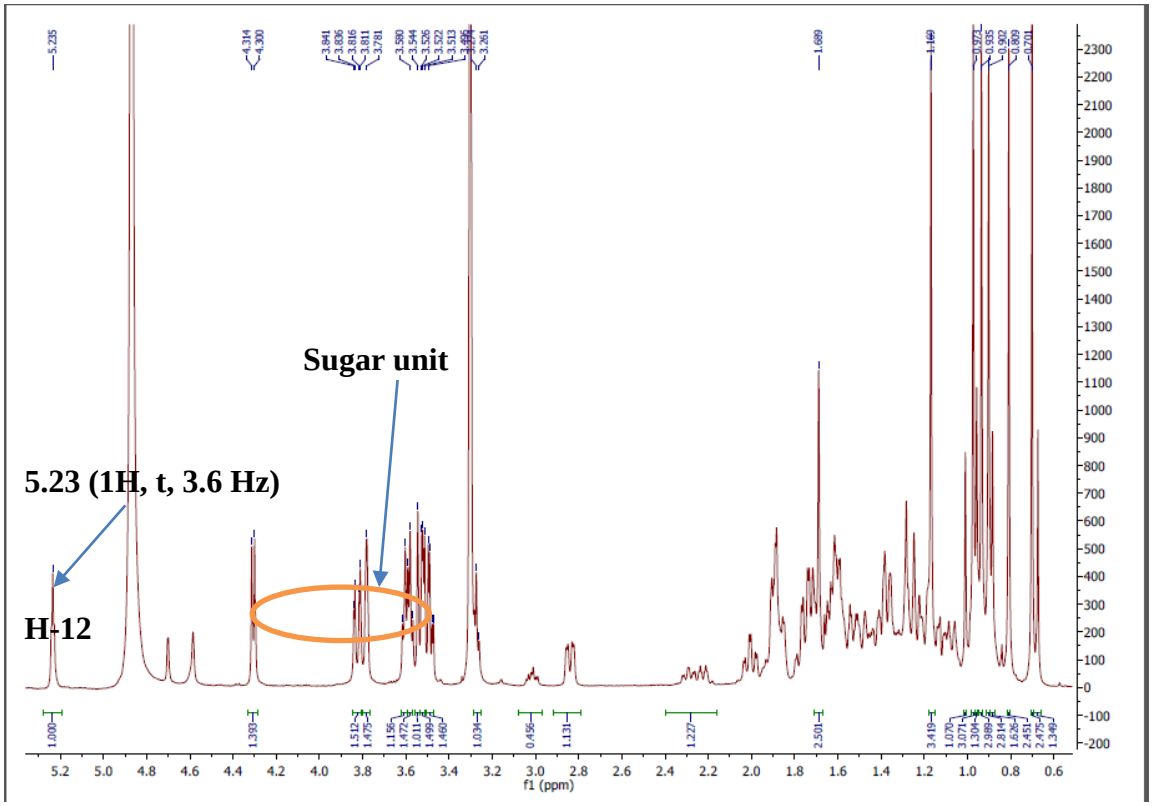

Figure 66: **^{1}H NMR spectrum of compound SRYK6 (500MHz, CD_3OD)**

The ^{13}C NMR spectrum (Figure 67) of SRYK6 is similar to that oleanolic acid since it presented the characteristic of oleanane peaks at δ_c 123.6 (C-12) and 144.2 (C-13). The major difference is the appearance of a set of signals between δc (66-75ppm) indicating the presence of a sugar moety with an anomeric carbon at δc 106.3.

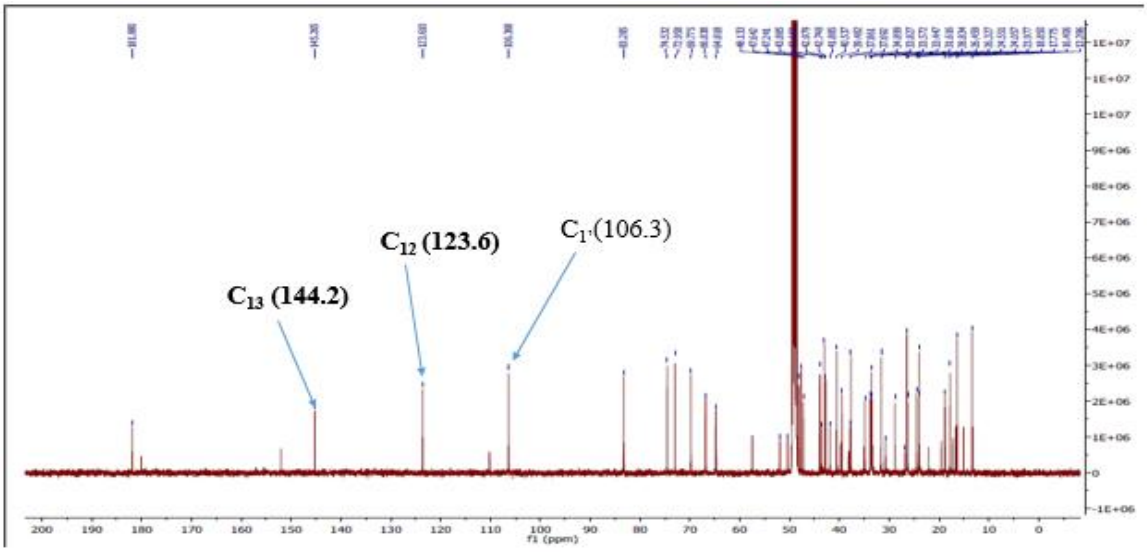

Figure 67: **^{13}C NMR broadband decoupled spectrum of compound SRYK6 (125MHz, CD_3OD)**

The ^{13}C NMR (125 MHz, CD_3OD) SRYK6 spectral data compared with leontoside A of the literature are represented in the table 38 below.

Table 38: ^{13}C NMR (125 MHz, CD_3OD) SRYK6 spectral data compared with Leontoside A of the literature (125 MHz, pyridine-d_5) (Park and Hahn, 1991).

Position	^{13}C NMR (75 MHz, CD_3OD) SRYK6	^{13}CNMR (125 MHz) pyridine-d_5 Leontoside A
1	37.8	38.7
2	26.3	26.0
3	83.2	81.0
4	43.6	43.4
5	47.6	47.5
6	18.8	18.1
7	33.4	32.8
8	39.4	39.7
9	48.1	48.1
10	37.6	36.9
11	23.9	23.8
12	123.6	122.4
13	144.2	144.8
14	41.8	42.1
15	28.8	28.2
16	23.9	23.6
17	47.2	46.4
18	41.8	41.9
19	47.6	46.7
20	30.8	31.6
21	34.8	34.1
22	33.4	33.1
23	64.8	64.7
24	13.3	13.5
25	16.4	16.0
26	17.7	17.4
27	26.3	26.0
28	181.8	180.2
29	33.4	33.1
30	23.9	23.7
1’	106.3	106.6
2’	72.9	73.0
3’	74.5	74.6
4’	69.7	69.5
5’	66.8	66.9

These informations compared to those obtained from the literature data (**Park and Hahn,1991**) led to the characterization of SRYK6 as **Leontoside A.**

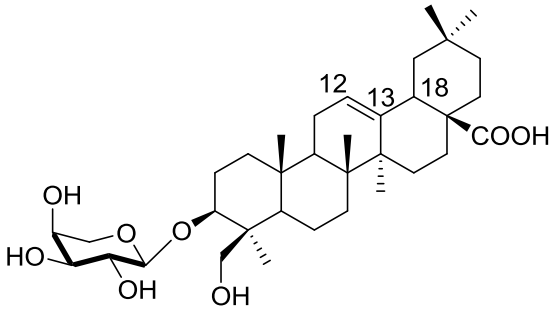

114

II.2.3 Summary of characterised compounds

- ***Sida rhombifolia***

The Ethyl acetate fraction (11.1 g) was submitted to silica gel column chromatography (20 g) and eluted with hexane followed by a gradient of ethyl acetate in hexane, methanol in ethyl acetate to yield taraxerol (SRA1,5.03mg), leontoside A (SRYK6, 4.01mg) , Kaempferol-3-0-β-D-(6-E-P-coumaroyl) glucopyranoside (SRA3, 5.06 mg), rhombifoliamide (SRP1, 5.21 mg), acetyl of taraxeryl (SRA2, 5.21 mg) and Oleanolic acid (SR7, 6.10 mg).

The hexane fraction (13.2 g) was submitted to silica gel column chromatography (25 g) and eluted with hexane followed by a gradient of ethyl acetate in hexane then methanol in ethyl acetate to yield Ursolic acid (SR4, 6.00mg), mixure of β-sitosterol and stigmasterol (SR1, 5.06 mg), 3-O-*β*-D-glucopyranosyl-β-sitosterol (SR2, 4.23 mg) and Lupeol (SR3, 5.12 mg).

The n-butanol fraction (10.3 g) was submitted to silica gel column chromatography (20 g) and eluted with hexane followed by a gradient of ethyl acetate in hexane then methanol in ethyl acetate to yield Kaempferol-3-O-*β*-D-glucopyranoside (SB4,6.32mg) and 20-hydroxyecdysone (SB1, 4.02mg) .

- ***Sida acuta***

The ethyl acetate fraction (10.1g) was submitted to silica gel column chromatography (20 g) and eluted with hexane followed by a gradient of ethyl acetate in hexane and methanol in ethyl acetate to yield xanthyletin (SAA1, 3.45 mg) , (E)-suberenol (SAA2 5.12 mg) , thamnosmonin (SAA3, 4.20 mg) and 5,5'-oxybis(pentane-1,2,3,4-tetraol) (SAR6, 6.32 mg).

The hexane fraction (12.2g) was submitted to silica gel column chromatography (20 g) and eluted with hexane followed by a gradient of ethyl acetate in hexane then methanol in ethyl acetate to yield 1-6 Dihydroxy-xanthone (SRYK3, 5.30 mg) and betulinic acid (SR5 6.50 mg)

The n-butanol fraction (11.3 g) was submitted to silica gel column chromatography (20 g) and eluted with CH_2Cl_2 followed by a gradient of MeOH in CH_2Cl_2 to yield cryptolepine (SAB3, 4.01 mg) and 4-methoxy-1-methylquinolin-2(1H)-one (SAB1**,** 5.12 mg).

- ***Garcinia ovalifolia***

The hexane-ethyl acetate (1:1) (50g), was submitted to silica gel column chromatography (70 g) and eluted with CH_2CL_2 followed by a gradient of MeOH in CH_2CL_2 to yield 2,6-dimethoxy-p-benzoquinone (GO9, 5.1 mg), isogarcignol (GOA**,** 408.5 mg), taxifolin 6-c-glucoside **(**GO-**S**1**,** 40.2 mg**),** rheediaxanthone A (GO4**,** 15.4 mg) and 7-épiisogarcinol (GOX**,** 20.4 mg).

The above mentioned separation and purification processes led to the isolation of a total of twenty four (**24**) compounds, their structures were elucidated .The structures of these compounds were determined by routine 1D and 2D spectroscopic techniques, MS, X-Ray, using their physical data and by comparison with data in literature. The compounds where found to belong to the class of pentacyclic triterpenes (**07**), Steroids (**03**), Xanthones (**02**), flavonoids (**03**), Alkaloid (**02**), Coumarines (**03**), Benzophenone (**03**), Ceramide (**01**), as indicated on Table below.

Table 39: **Summary of compounds elucidated from the different extracts.**

Plants	**compounds**	**name**
Sida rhombifolia (whole plant)	SR1	Mixure of β-sitosterol and stigmasterol
	SR2	Stigmasterol 3-O-*β*-D-glucopyranoside
	SR3	Lupeol
	SR4	Ursolic acid
	SRA1	Taraxerol
	SRA2	Taraxeryl acetyl
	SRYK6	Leontosise A
	SR7	Oleanolic acid
	SRA3	Kaempferol-3-0-β-D-(6-E-P-coumaroyl) glucopyranoside
	SRP1	Rhombifoliamide
	SB4	Kaempferol-3-O-*β*-D-glucopyranoside
	SB1	20-hydroxyecdysone
Sida acuta (whole plant)	SAA1	Xanthyletin

To be continued

Plants	**compounds**	**name**
	SAA2	(E)-suberenol
	SAA3	Thamnosmonin
	SAR6	5,5'-oxybis(pentane-1,2,3,4-tetraol
	SRYK3	1-6 Dihydroxy –xanthone
	SR5	Betulinic acid
	SAB1	4-methoxy-1-methylquinolin-2(1H)-one
	SAB3	Cryptolepine
G ovalifolia (stem bark)	GO9	2,6-dimethoxy-p-benzoquinone
	GP1	Isogarcignol
	GO-**S**1	Taxifolin 6-c-glucoside
	GO4	Rheediaxanthone A
	GOX	7-épiisogarcinol

To increase of the range of compounds to be tested for a structure-relation-activity study led us to make hemisynthesis.

II.3 Williamson reaction

In the last we introduced the Williamson ether synthesis, one of the most straightforward ways we know of to make an ether. The SN2 reaction between an alkoxide (RO-) and an alkyl halide (R-X) as shown below.

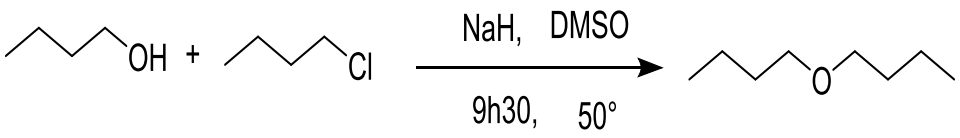

- **General mechanism**

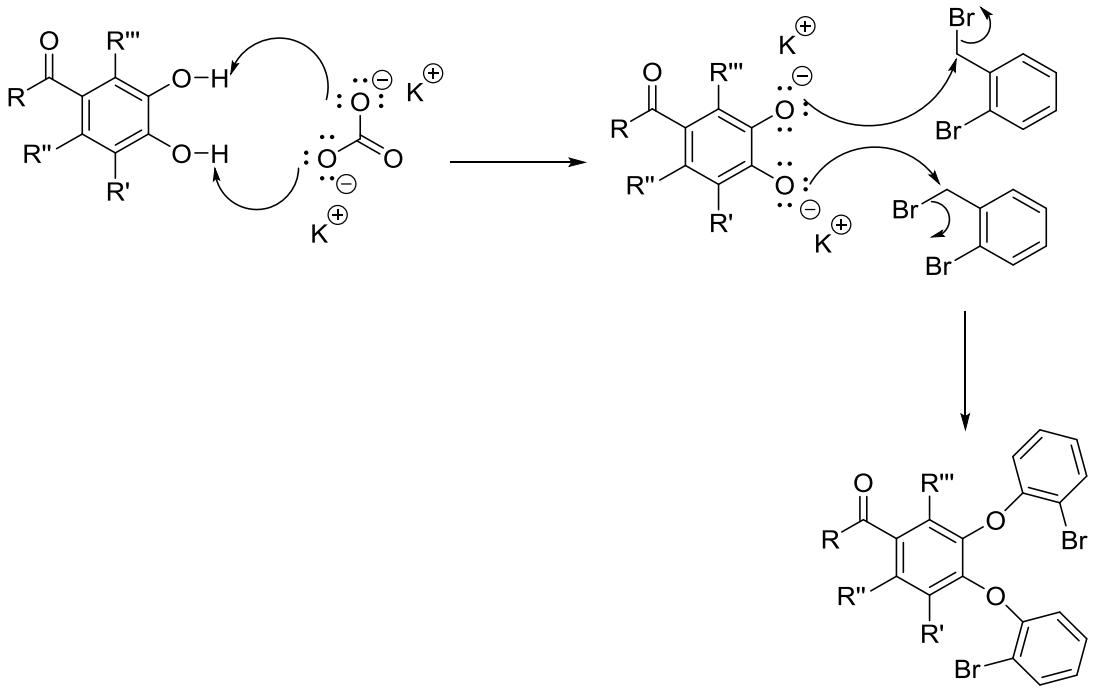

II.3.1 Hemisynthesis of (-) isogarcinol derivative by alkylation reaction of Williamson

In order to ameliorate the biological activities of some of the isolated compounds, five chemical transformations were carried out.

II.3 1.1 Alkylation by propargylbromide

In the mixture of **(-)** isogarcinol (103.3 mg; 0.17 mmol) and dry acetone (8 mL), K_2CO_3 (40 mg) was added followed by propargylbromide (16µL, d = 1.38, 0. 1.8 mmol). The reaction mixture was heated at 40 °C under reflux for 23 h. At the end of the reaction, the solvent was evaporated under reduced pressure and the residue was diluted in water (40 mL × 3). The aqueous mixture was extracted with ethyl acetate (3 × 60 mL) and the extract was dried by anhydrous Na_2SO_4. After evaporation of the solvent and purification by column chromatography on silica gel by elution with hexane- EtOAc of increasing polarity, compound named **13, 14-di-O-propargylisogarcignol** (81.9 mg, 0.12 mmol, 76.6 %, R_f 0.24, silica gel, hexane-EtOAc, 8:2 v/v) was obtained.

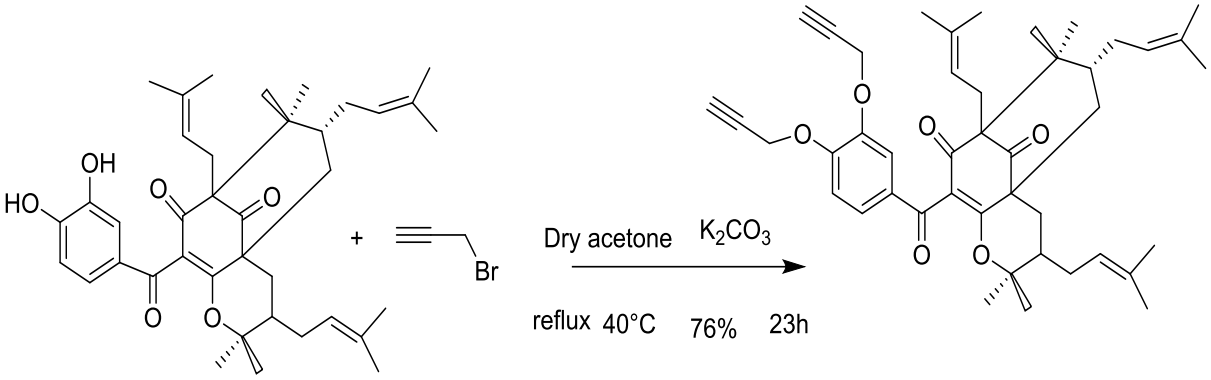

(-) Isogarcinol **13,14-di-O-propargylisogarcignol (115)**

This structure was confirmed by TOF-MS-ESI in which was observed a sodium adduct peak $[M+Na]^+$ at 701.

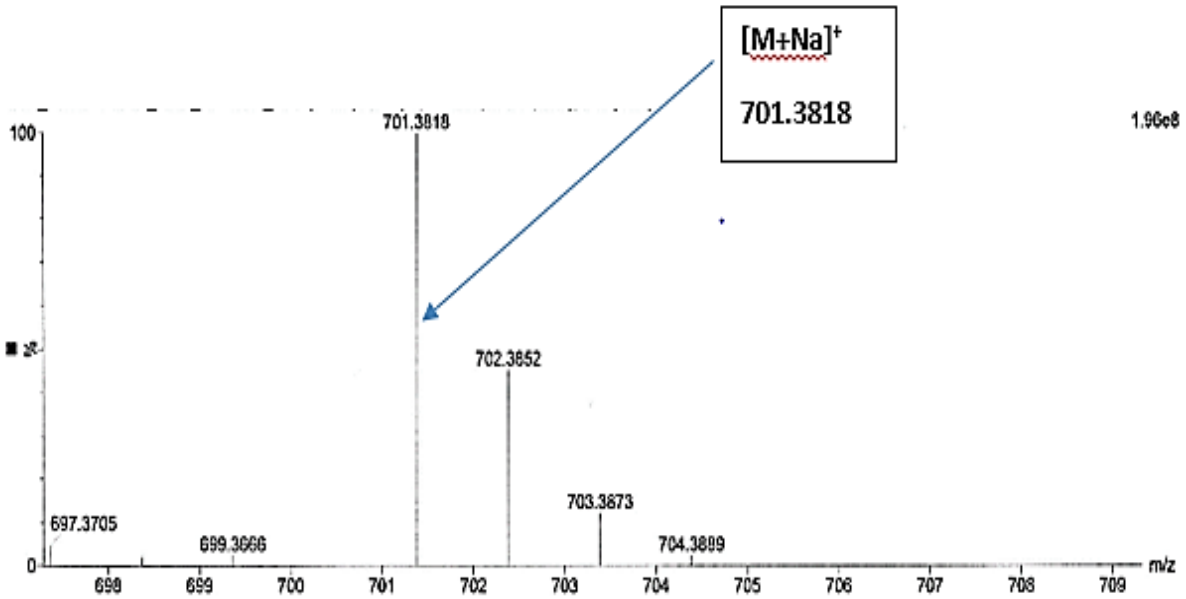

Figure 29: **TOF-MS-ESI spectrum of PB1**

On the ^{13}C NMR spectrum of 13, 14-di-O-propargylisogarcignol, we observed the signal of oxymethylene and alkyl group, which were absent on the ^{13}C NMR of isogarcinol.

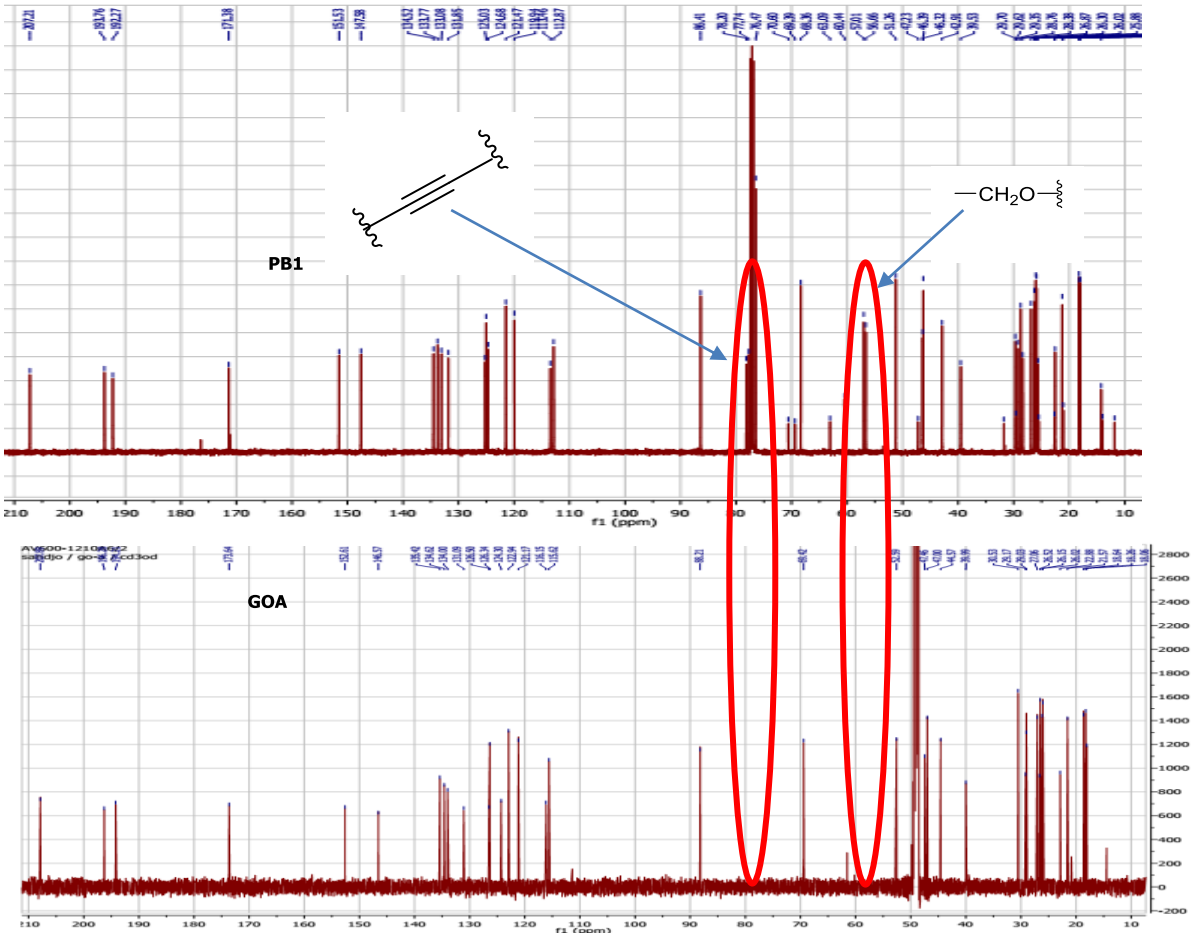

Figure 30: ^{13}**C NMR broadband decoupling spectrum of compound GOA and PB1**

II.3 1.2 Benzylation by benzylbromide

In a mixture of (**-**) isogarcinol (94.7 mg; 0.15 mmol) and dry acetone (10 mL), K_2CO_3 (30.0 mg) was added followed by benzylbromide (20.2 µL, d = 1.44, 0.17 mmol). The reaction mixture was heated at 40 °C under reflux for 20 h. At the end of the reaction, the solvent was evaporated under reduced pressure and the residue was diluted in water (40 mL × 3). The aqueous mixture was extracted with ethyl acetate (3 × 60 mL) and the extract was dried by anhydrous Na_2SO_4. After evaporation of the solvent and purification by column chromatography on silica gel using gradient elution with hexane- EtOAc of increasing polarity, compound named **13, 14-di-O-benzylisogarcinol** (43.0 mg, 0.06 mmol, 35 %, R_f 0.45, silica gel, hexane-EtOAc, 8:2 v/v) was obtained.

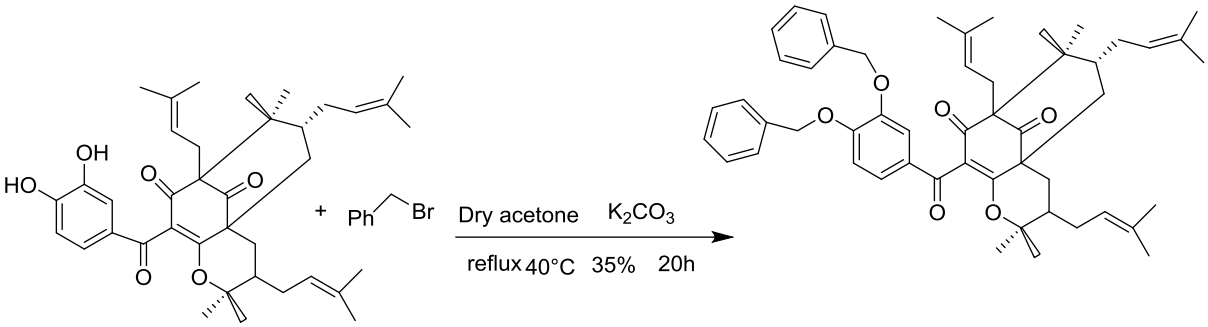

(-) Isogarcinol **13, 14-di-O-benzylisogarcinol (116)**

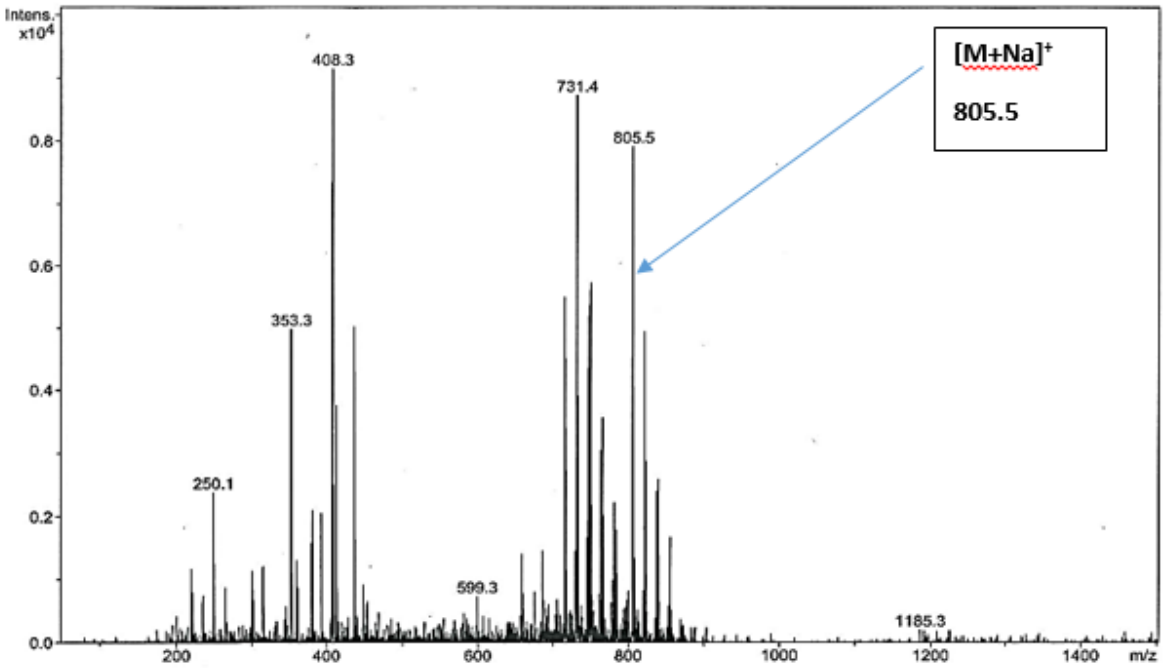

Figure 31: **MS-ESI spectrum of BB1**

This structure was confirmed by TOF-MS-ESI in which was observed a sodium adduct peak $[M+Na]^+$ at 805.5.

On the ^{1}H NMR spectrum of compound 13,14-di-O-benzylisogarcinol we observed the signal of oxymethyne, and two benzyl group which were absent on the ^{1}H NMR of isogarcinol.

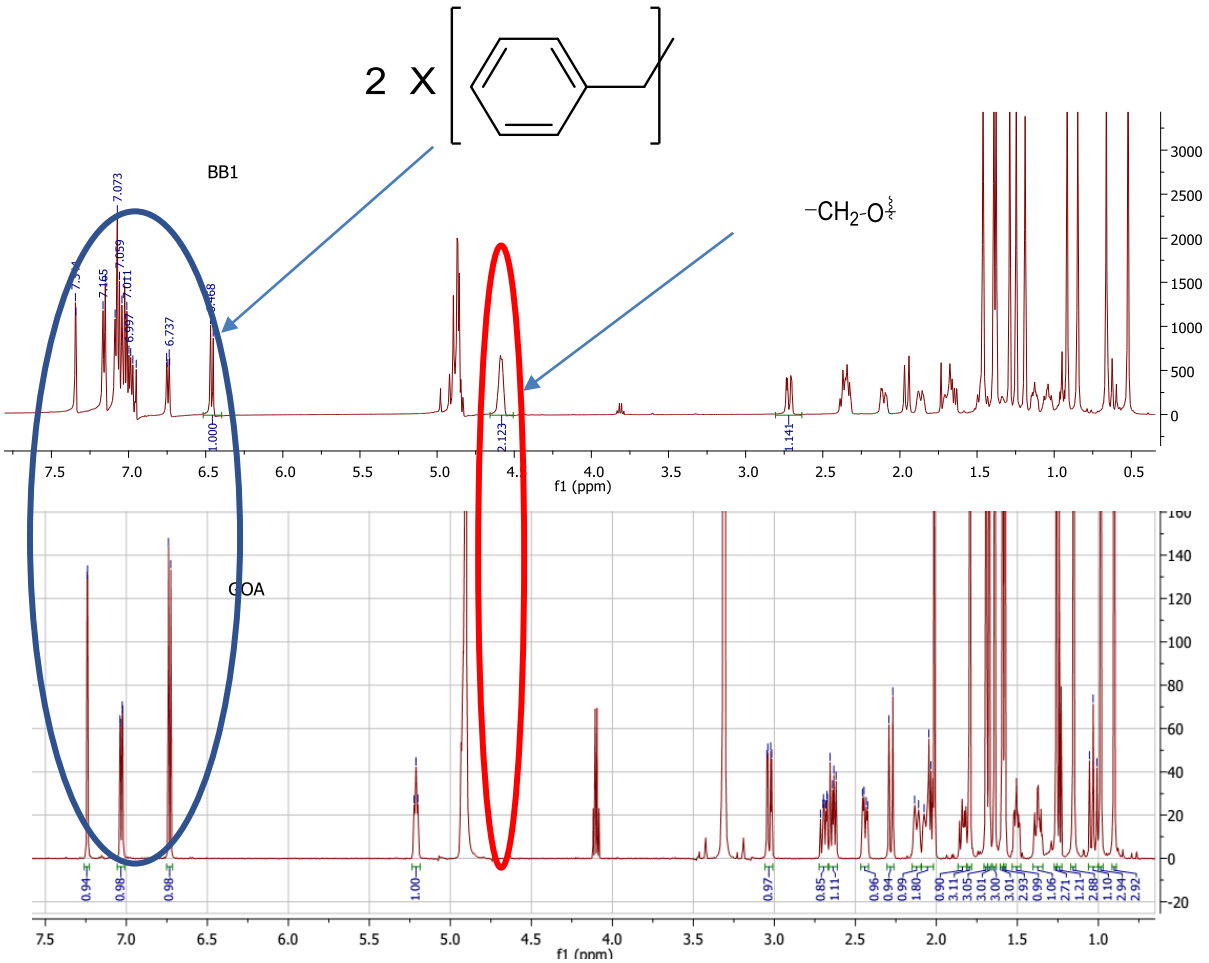

Figure 32:^{1}H NMR spectrum of compound GOA and BB1

II.2 1.3 Benzylation by 2-bromo benzylbromide

In a mixture of (-) isogarcinol (92.2 mg; 0.15 mmol) and dry acetone (10 mL), K_2CO_3 (1000.0 mg) was added followed by 2-bromo benzylbromide (40 mg, d = 1,44, 0.16 mmol). The reaction mixture was heated at 40 °C under reflux for 23 h. At the end of the reaction, the solvent was evaporated under reduced pressure and the residue was diluted in water (40 mL × 3). The aqueous mixture was extracted with ethyl acetate (3 × 60 mL) and the extract was dried by anhydrous Na_2SO_4. After evaporation of the solvent and purification by column chromatography on silica gel using gradient elution with hexane- EtOAc of increasing polarity, compound named **13,14-O-bis(3-bromobenzyl)isogarcinol** (112.0 mg, 0.11 mmol, 77.8 %, R_f 0.23, silica gel, hexane-EtOAc, 8:2 v/v) was obtained.

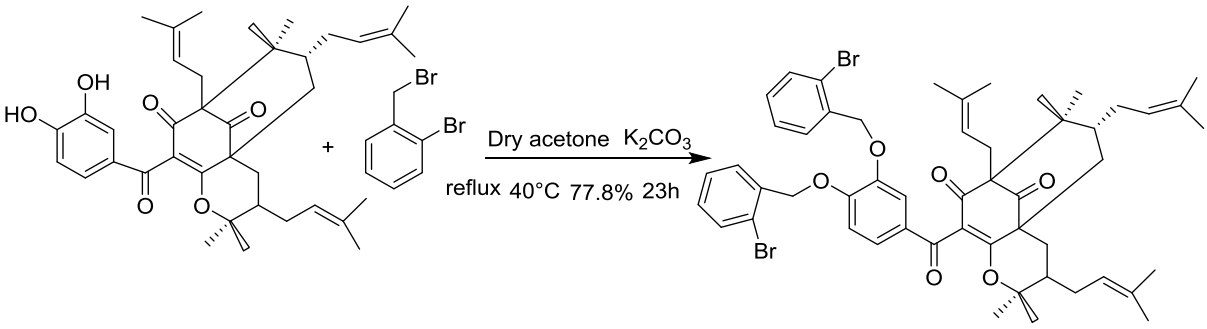

(-) Isogarcinol **13,14-O-bis(3-bromobenzyl)isogarcinol (117)**

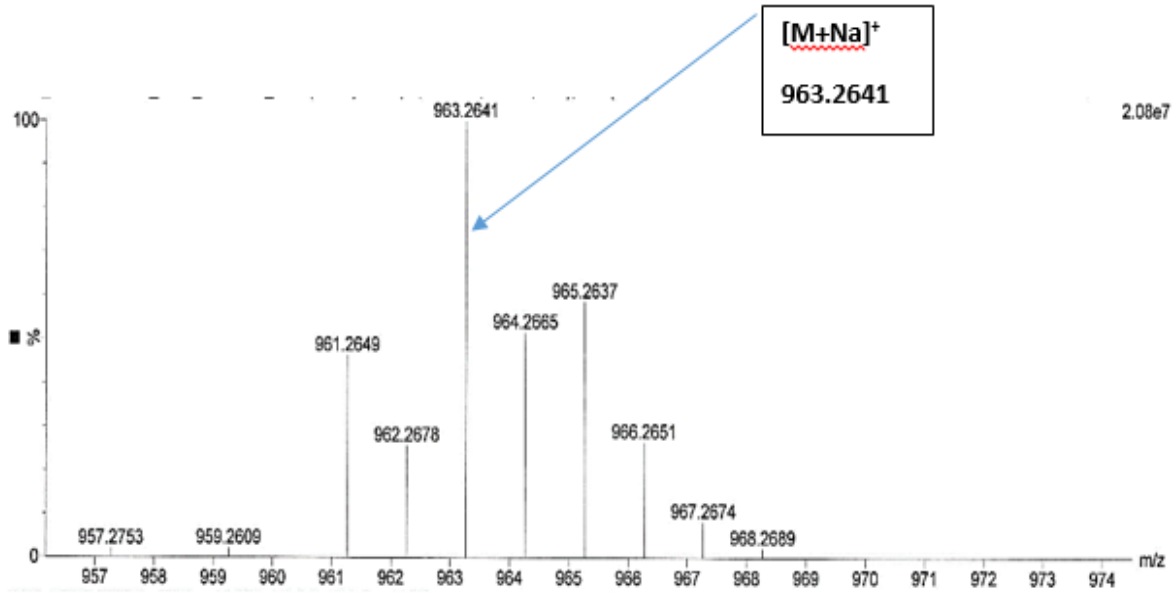

Figure 33 : **TOF-MS-ESI spectrum of BB3**

This structure was confirmed by TOF-MS-ESI in which was observed a sodium adduct peak $[M+Na]^+$ at 963.2641.

On the ^{1}H NMR spectrum of compound 13,14-O-bis(3-bromobenzyl)isogarcinol

We observed the signal of oxymethyne and signal of two ortho disubstituted aromatic ring which were absent on the ^{1}H NMR of isogarcinol.

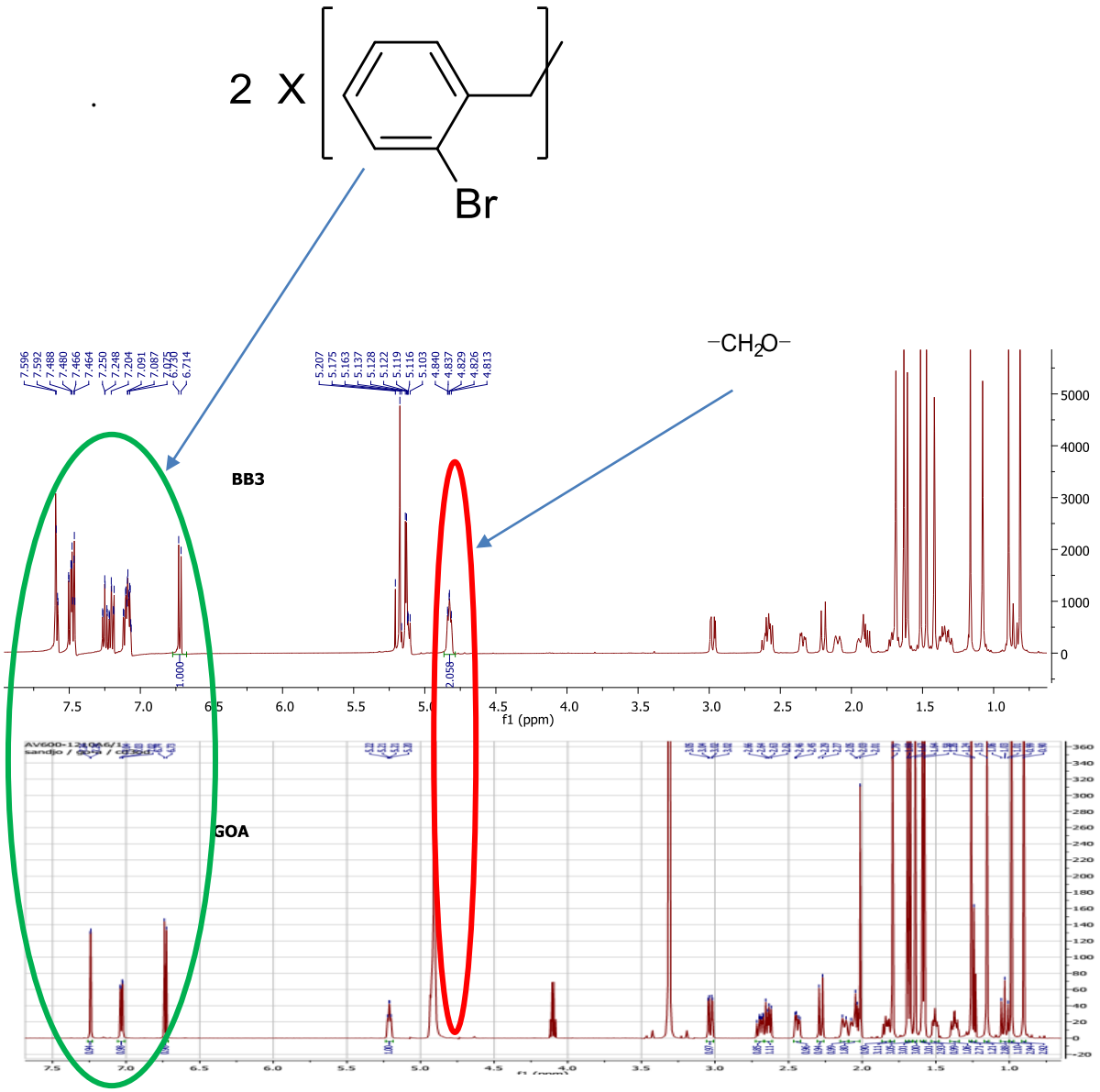

Figure 34:^{1}H NMR spectrum of compound GOA and BB3

II.2 1.4 Benzylation by 4-bromo benzylbromide

In a mixture of (-) isogarcinol (50.6 mg ; 0.15 mmol) and dry acetone (10 mL), K_2CO_3 (1000.0 mg), was added followed by 4-bromo benzylbromide (160 mg, d = 1,44, 1.43 mmol). The reaction mixture was heated at 40 °C under reflux for 22 h. At the end of the reaction, the solvent was evaporated under reduced pressure and the residue was diluted in water (40 mL × 3). The aqueous mixture was extracted with ethyl acetate (3 × 60 mL) and the extract was dried by anhydrous Na_2SO_4. After evaporation of the solvent and purification by column chromatography on silica gel using gradient elution with hexane- EtOAc of increasing polarity. Compound named **13,14-O-bis(5-bromobenzyl)isogarcinol** (67.2 mg, 0.07 mmol, 85 %, R_f 0.15, silica gel, hexane-EtOAc, 8:2 v/v) was obtained.

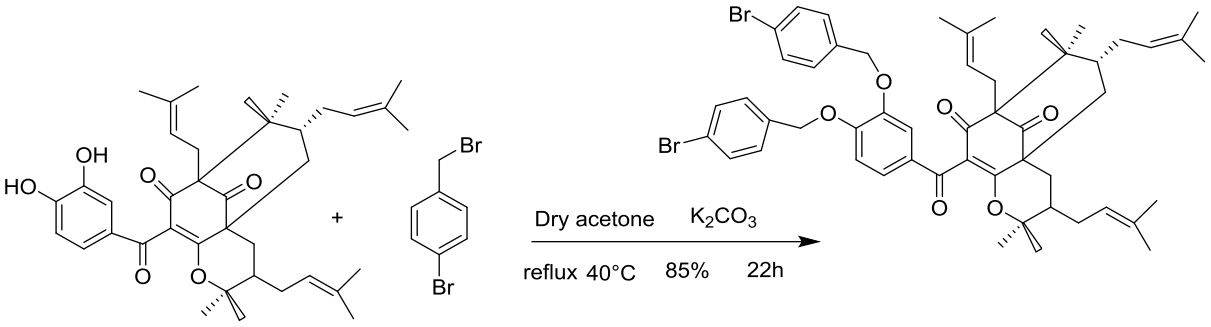

(-) Isogarcinol **13,14-O-bis(5-bromobenzyl)isogarcinol (118)**

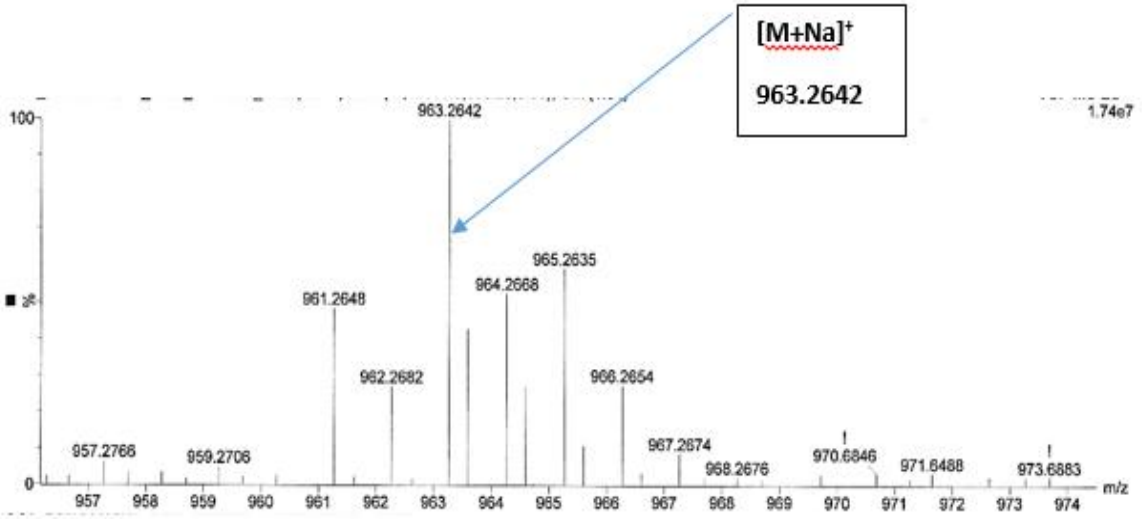

Figure 35 : **TOF-MS-ESI spectrum of BB4**

This structure was confirmed by TOF-MS-ESI in which was observed a sodium adduct Peak $[M+Na]^+$ at 963.2642.

On the ^1H NMR spectrum of compound 13,14-O-bis(5-bromobenzyl)isogarcinol we observed the signal of oxymethyne and signals of two protons in AA'BB' system which were absent on the ^1H NMR of isogarcinol.

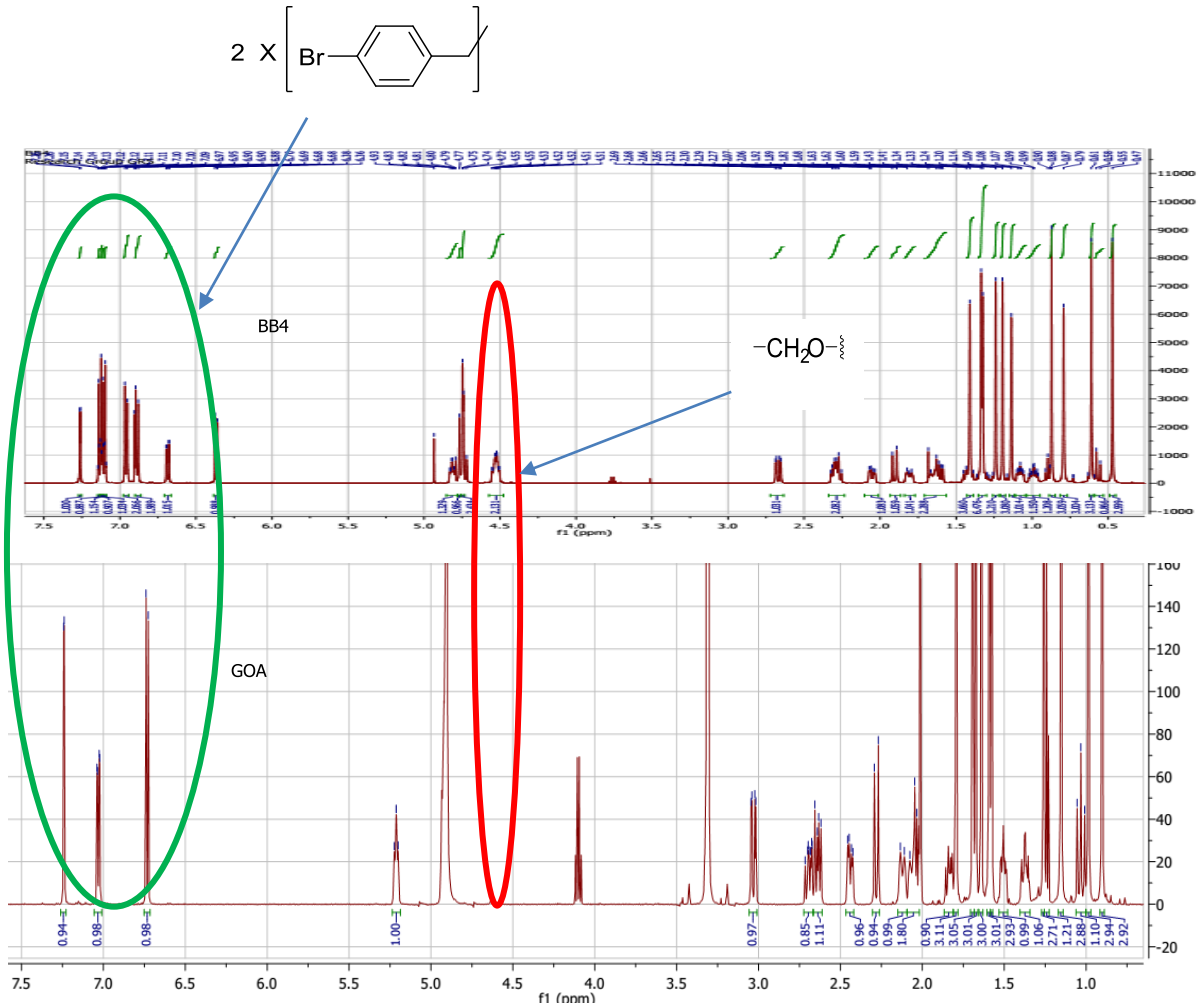

Figure 36:^{1}H NMR spectrum of compound GOA and BB4

II.2 1.5 Benzylation by 1.2-dibromoethane

In a mixture of (-) isogarcinol (73.8 mg; 0.123 mmol) and dry acetone (8 mL), K_2CO_3 (1000.0 mg) was added followed by 1.2-dibromoethane (0.5 mL, d = 2.18, 5.80 mmol). The reaction mixture was heated at 40 °C under reflux for 23 h. At the end of the reaction, the solvent was evaporated under reduced pressure and the residue was diluted in water (40 mL × 3). The aqueous mixture was extracted with ethyl acetate (3 × 60 mL) and the extract was dried by anhydrous Na_2SO_4. After evaporation of the solvent and purification by column chromatography on silica gel using gradient elution with hexane- EtOAc system of increasing polarity. Compound named 13, 14-dioxaethylisogarcinol (51.2 mg, 0.08 mmol, 77 %, R_f 0.25, silica gel, hexane-EtOAc, 8:2 v/v) was obtained.

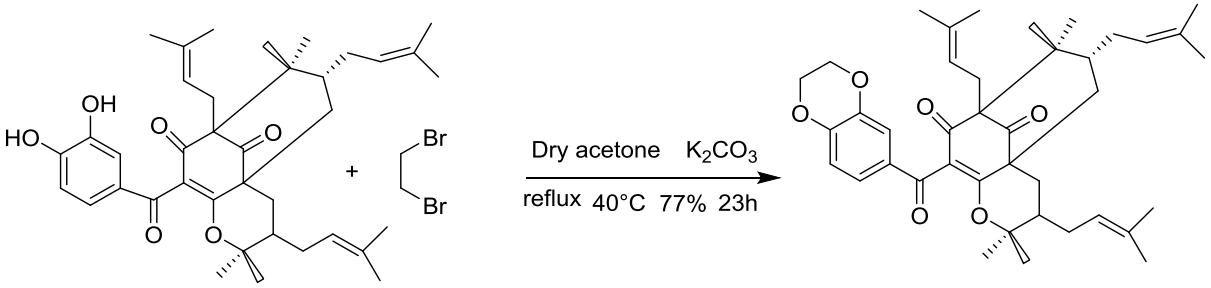

(-) Isogarcinol **13, 14-dioxaethylisogarcinol (119)**

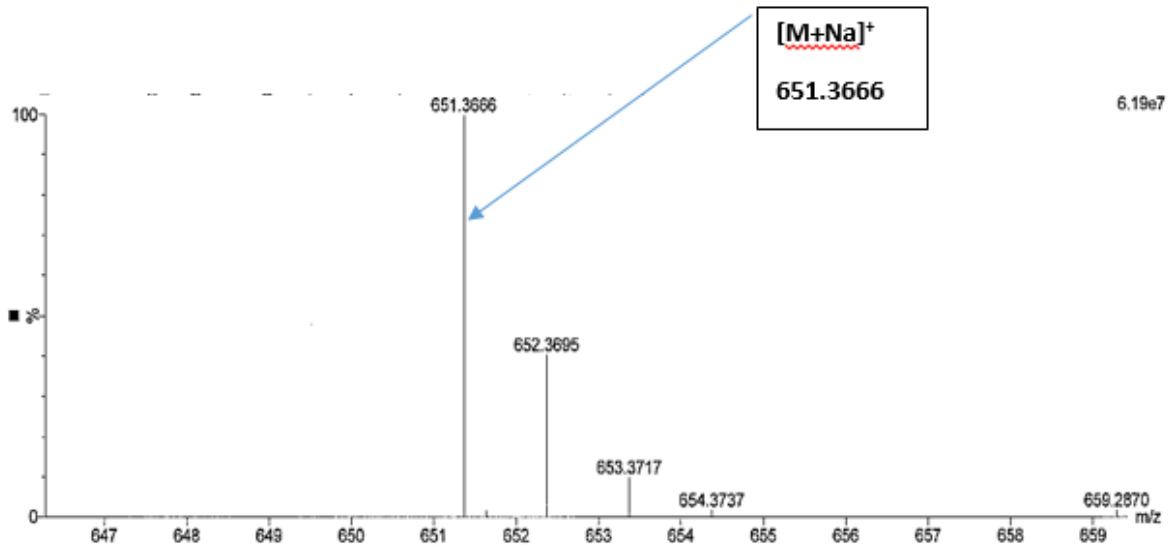

Figure 37 : **TOF-MS-ESI spectrum of BB6**

This structure was confirmed by TOF-MS-ESI in which was observed a sodium adduct

Peak $[M+Na]^+$ at 651.3666.

On the ^{1}H NMR spectrum of compound 13,14-dioxaethylisogarcinol, was observed two deshielded methylene protons at δ_H 4.14 (2H, d, J = 5.5Hz) and 4.20 (2H,d , J = 8.0Hz) which were absent on the ^{1}H NMR of isogarcinol.

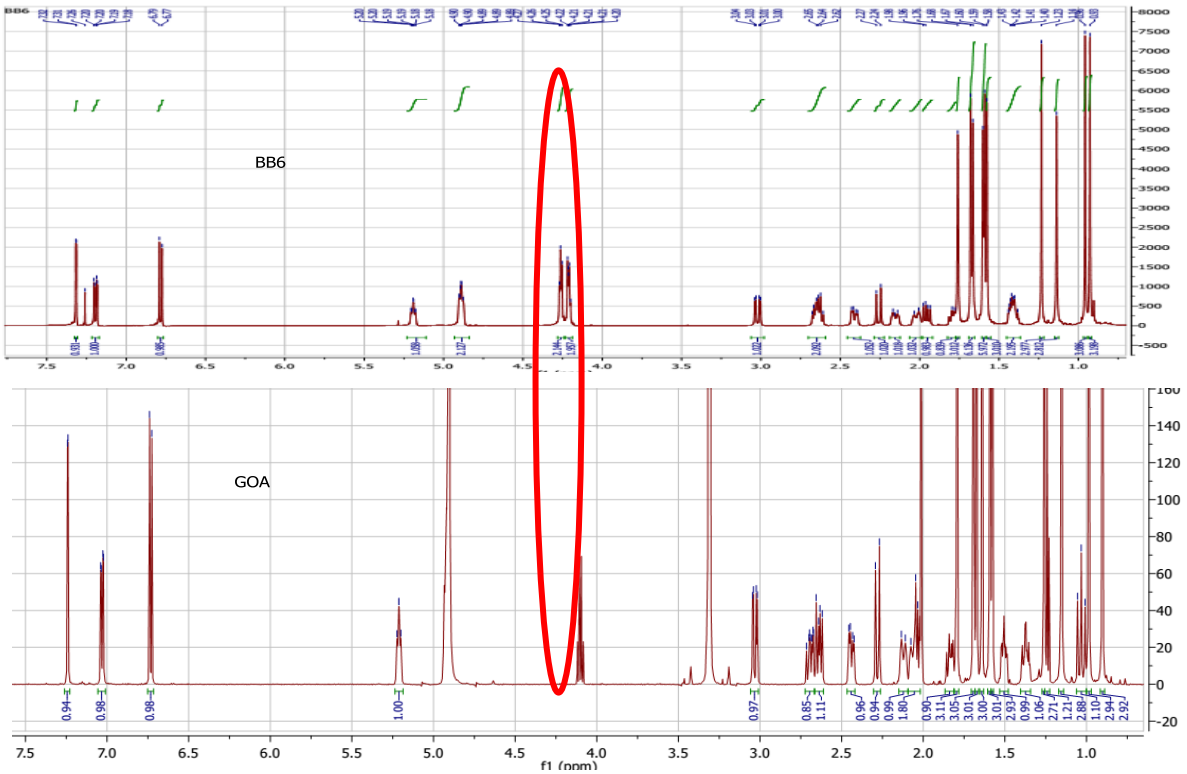

Figure 38 :^{1}H NMR spectrum of compound GOA and BB6

II.2 1.6 Discussion

The Williamson reaction led us to the product BB1 and we obtained a yield of 35% with a difference of 65% over 100%. This low yield can be explained by the fact that there were secondary products that were formed.

It can also be explained by the fact that during the treatment there were losses at the level of extraction, purification.

The extracts, fractions, compounds and one hemisynthetic derivative were subjected to antiplasmodial tests.

II.4 ANTIPLASMODIAL TEST OF EXTRACT FRACTIONS AND ISOLATED COMPOUNDS OR DERIVATIVES AGAINST 3D7 AND Dd2 STRAINS

Crude extracts, fractions and isolated compounds were screened for their antiplasmodial and cytotoxicity activities using SyBr Green-Based assay and resazurin-based assay

respectively. Results showed that, extracts and fractions exhibited moderate to strong antiplasmodial activities against 3D7 (IC_{50} values: 0.18-20.11 µg/mL) and Dd2 (IC_{50} values: 0.74-63.09 µg/mL) *Plasmodium falciparum* strains. Interestingly, two compounds, oleanolic acid and cryptolepine isolated from the EtOAc-soluble fraction of *S.*

rhombifolia and *S. acuta* displayed strong antiplasmodial activity with IC_{50} of (3.56 µg/mL ± 0.62 and 2.02 µg/mL ± 0.27); (0.18 µg/mL ± 0.01and 0.74 µg/mL ± 0.09) respectively against 3D7 and Dd2 *P. falciparum* strains (Table S1).

Table 40: Antiplasmodial activity of extract, fractions and isolated compounds and selectivity index of *Sida acuta* and *Sida rhombifolia*

	SBYR Green based assay			***Resazurin based* assay**		
	IC_{50} ± SD µg/mL		**Resistance Index (RI)**	**CC_{50}**	**Selectivity Index (SI)**	
	Pf3D7	**PfDd2**			Pf3D7	PfDd2
Extract						
SA	> 100	63.09 ± 0.11	-	> 500	-	> 7.92
SR	20.11 ± 0.39	37.51 ± 0.15	1.86	> 500	> 24.86	> 13.32
Fractions						
FSAB	15.85 ± 2.87	22.38 ± 0.17	1.41	> 500	> 31.54	> 22.34
FSAH	5.24 ± 0.50	11.93 ± 0.11	2.27	> 500	> 95.41	> 41.91
FSRB	> 100	> 100	-	> 500	-	-
FSRH	5.77 ± 0.11	14.59 ± 0.08	2.52	> 500	> 86.65	> 34.27
FSRA	4.18 ± 0.17	5.38 ± 0.04	1.28	> 500	> 119.61	> 92.93
Compounds						
1,6-dihydroxyxanthone	> 25	> 25	-	> 100	-	-
Cryptolepine	0.18 ± 0.01	0.74 ± 0.09	4.11	ND	-	-
20-Hydroxyecdysone	> 25	> 25	-	> 100	-	-
Mixture of stigmasterol and *β* -sitosterol	> 25	> 25	-	> 100	-	-
Rhombifoliamide	> 25	> 25	-	ND	-	-
Betulinic acid	> 25	> 25	-	> 100	-	-
Lupeol	> 25	> 25	-	> 100	-	-
Tiliroside	> 25	10.56 ± 0.28	-	> 100	-	> 9.46
Leontoside A	> 25	7.9 ± 0.18	-	ND	-	-
Oleanolic acid	3.56 ± 0.62	2.02 ± 0.27	0.56	ND	-	-
***β*-sitosterol glucoside**	> 25	> 25	-	> 100	-	-
Artemisinin (µg/mL)	0.41 ± 0.11	5.33 ± 0.13	0.12	-	-	-
Choroquine (µg/mL)	1.39 ± 0.53	42.54 ± 0.16	30.5	-	-	-

ND: Not Determinated; IC_{50}: Inhibitrice Concentration 50; CC_{50}: Cytotoxic Concentration 50; SD : Sensitive Deviation ; SA: *Sida acuta* hydroethanolic extract; SR: *Sida rhombifolia* hydroethanolic extract ; FSAB n-

butanol fraction of SA ; FSAH hexane fraction of SA ; FSRB n-butanol fraction of SR ; FSRH hexane fraction of SR ; FSRA Ethyl acetate fraction of SR.

Table 41: Antiplasmodial activity of compounds from *Garcinia*

	IC_{50} ± SD (µg/mL)			CC_{50} ± SD (µg/mL)	Selectivity Indices	
Extracts and compounds	**Pf3D7**	**PDd2**	**Resistance Indices (RI)**	**Raw Cells**	**SI (Pf3D7)**	**SI (PfDd2)**
GO	21.235	18.65	ND	ND	ND	ND
FAG	79.73	47.225	ND	ND	ND	ND
FHAG	11.21	3.88	ND	ND	ND	ND
13,14-dioxaethylisogarcinol	1.13 ± 0.22	0.64 ± 0.16	0.56	> 100	> 88.49	> 156.25
13,14-di-O-(4-bromobenzyl)isogarcignol	13.42 ± 0.17	11.47 ± 0.11	0.85	> 100	> 7.45	> 8.71
13,14-di-O-benzylisogarcignol	3.61 ± 0.23	2.08 ± 0.19	0.57	> 100	> 27.7	> 48.07
13,14-di-O-(2-bromobenzyl)isogarcignol	8.83 ± 0.12	8.84 ± 0.16	1	> 100	> 11.32	> 11.31
13,14-di-O-propargylisogarcignol	1.42 ± 0.28	1.01 ± 0.16	0.71	> 100	> 70.42	> 99.00
isogarcinol	9.35 ± 0.14	5.50 ± 0.08	0.58	> 100	> 10.69	> 18.18
c-aryl glucoside	> 50	7.39 ± 0.06	-	> 100	-	> 13.53
7-epiisogarcinol	> 50	33.75 ± 0.12	-	> 100	-	> 2.96
Rheediaxanthone A	24.80 ± 0.09	10.53 ± 0.15	0.42	> 100	> 4.03	> 9.49
Artemisinin (µg/mL)	0.41 ± 0.11	5.33 ± 0.13	0.12	-	-	-
Choroquine (µg/mL)	1.39 ± 0.53	42.54 ± 0.16	30.5	-	-	-

Go : *Garcinia ovalifolia* FAG: Ethyl acetate fraction of Go FHAG : hexane / Ethyl acetate (1:1)

Crude extracts, fractions and isolated compounds were screened for their antiplasmodial and compounds for cytotoxicity activities using SyBr Green-Based assay and resazurin-based assay respectively. Results showed that, extracts and fractions exhibited moderate to strong antiplasmodial activities against 3D7 (IC_{50} values: 11.21-79.73 µg/mL) and Dd2 (IC_{50} values: 3.88-18.65 µg/mL) *Plasmodium falciparum* strains. The Hexane/Acetate (1:1) -soluble

fraction of *G.ovalifolia* displayed strong antiplasmodial activity with IC_{50} of (11.21 µg/mL ± 0.16 and 3.88 µg/mL ± 1.31); respectively against 3D7 and Dd2 *P. falciparum strains*.

A set of plant-derived compounds were tested *in vitro* for their ability to inhibit the growth of sensitive (3D7) and multi-resistant (Dd2) intra-erythrocytic asexual of *P. falciparum* in culture using an SYBR green fluorescence assay. Chloroquine (CQ) and artemisinin (Art) were used as reference drugs to validate the assay. After that, antiplasmodial activities were classified using the classification criteria established by **Muganza et *al*. 2016**: $IC_{50} \leq 5$ µg/mL: pronounced activity; $5 < IC_{50} \leq 10$ µg/mL: good activity; $10 < IC_{50} \leq 20$ µg/mL: moderate activity; $20 < IC_{50} \leq 40$ µg/mL: low activity; $IC_{50} > 40$ µg/mL: inactive. Based on the above criteria, all tested compounds exhibited pronounced to low activity on both strains of *P. falciparum*. Compounds 13,14-dioxaethylisogarcinol; 13,14-di-O-benzylisogarcignol; 13,14-di-0-propargylisogarcignol displayed pronounced activity and 13,14-di-0-(2-bromobenzyl)isogarcignol and isogarcinol exhibited good activity on both sensitive and resistant strains of *P. falciparum* . Besides, Rheediaxanthone A showed low activity on sensitive strain and moderate activity on multi-resistant strain of *P. falciparum*. Interestingly, isogarcinol and 7-epiisogarcinol showed activity on multi-resistant strain of *P. falciparum* which could be attributed to their novel mode of action. Following the antiplasmodial activity, all compounds were subjected to *in vitro* cytotoxicity assay in order to verify their safety against mammalian cells lines. All active compounds against asexual *P. falciparum* parasites exhibited no cytotoxicity against Raw cells (selectivity index (SI) > 10) and $SI=CC_{50} / IC_{50}$. According to the work of Valdes *in* 2006, SI ≥10 selectif and SI < 10 not selectif.

II.4.1 General discussion

Crude extract of *Sida rhombilfolia*, *Sida acuta* and *Garcinia ovalifolia* with IC_{50} of 37.51, 63.09 and 18.65 on Dd2 strains respectively exhibited moderate to inactive activities. Whereas the fractions of ethyl acetate (SR) 5.38 and hexane/acetate 50% (Go) 3.88 showed pronounced to good activities. The variation of activity could be due to antagonist effet and these fractions have a good activity than reference drug. Interestingly, two compounds, oleanolic acid and cryptolepine isolated from the EtOAc-soluble fraction of *S.rhombifolia* and *S. acuta* displayed strong antiplasmodial activity with IC_{50} of (3.56 µg/mL ± 0.62 and 2.02 µg/mL ± 0.27); (0.18 µg/mL ± 0.01and 0.74 µg/mL ± 0.09) respectively against 3D7 and Dd2 *P. falciparum* strains (Table S1). leontoside A and tiliroside showed moderate activity only against the multidrug resistant (Dd2) and no activity against sensitive strain of *P. falciparum*. Except for cryptolepine, all

extracts, fractions and compounds with activity against asexual *P. falciparum* parasites exhibited no cytotoxicity against Raw cells (selectivity indices (SI) > 10. To the best of our knowledge, this study provides the first report of antiplasmodial activity of isolated oleanolic acid against chloroquine-sensitive (3D7) and chloroquine-resistant (Dd2) *P. falciparum* strains. However, previous studies showed that the strong antiplasmodial activity of dichloromethane twig extract of *keetia leucantha* is attributed to the presence of eight triterpenic esters and the major antiplasmodial triterpenic acids, ursolic and oleanolic acids identified by HPLC-UV methods (**Beaufay *et al*., 2017**). In addition, cryptolepine previously showed varied interaction with the 4- aminoquinolines, amodiaquine, and chloroquine.

The combination of cryptolepine with amodiaquine showed a synergistic effect in *vitro* (mean RFIC ¼ 0.235 ± 0.15), whereas an additive effect (mean RFIC ¼ 1.342 ± 0.34) have been seen with chloroquine (Forkuo *et al*. 2016). In addition, cryptolepine has already been reported to show high inhibitory activity against the late-stage gametocytes (IC50 ¼ 1965 nM) (Forkuo et al. 2016) of *P. falciparum* (NF54). Summing-up, these studies reports the potential of cryptolepine as a promising antimalarial hit for both malaria treatment and transmission-blocking therapy (**Forkuo *et al*., 2016**). Based on the pronounced antiplasmodial activity of this compound, further chemical studies such as structural-activity relationship is needed to obtain a lead compound that responds to pharmacokinetics and pharmacodynamics properties for antimalarial drugs. All experiments were performed in triplicate and the main results obtained are recorded in Table S2.

GENERAL CONCLUSION AND PROSPECTS

General conclusion

The aim of this work was to search for new safe and efficient antiplasmodial therapeutic agents from three Cameroonian medicinal plants namely *Sida rhombifolia* Linné.C, *Sida acuta* Burm. F. (Malvaceae) and *Garcinia ovalifolia* Oliv. (Clusiaceae).

The methanolic and hydroethanolic extracts were treated by liquid-liquid partitioning to obtain fractions. The fraction from different parts of plants were subjected to liquid column chromatography techniques. This led to the isolation of twenty-four compounds characterized. They belong to six classes of natural substances and were classified as follows:

- Seven Triterpenes: lupéol (**108**) oleanolic acid **(113)** taraxeryl acetate **(111)** leontoside A (**114**) taraxerol (**110**) ursolic acid **(112) ,** betulinic acid **(109);**
- Three steroids: 3-O-*β*-D-glucopyranosyl-β-sitosterol (**105**) mixure of β-sitosterol and stigmasterol **(104)** 20-hydroxyecdysone (**106**);
- Two alkaloids: 4-methoxy-1-methylquinolin-2(1H)-one **(102)** cryptolepine **(103)**
- Eleven phenolic derivatives: kaempferol-3-O-D-glucopyranoside **(96)** kaempferol-3-O-β-D-(6-*E*-*P*-coumaroyl) **(97)** 1-6 dihydroxy-xanthone **(94)** isogarcinol (**99)** taxifolin 6-C-glucoside **(98)** 7-epiisogarcinol **(100)** rheediaxanthone **(95)**: thamnosmonin **(93),** xanthyletin **(92),** suberenol **(91)** 2,6-dimethoxy-p-benzoquinone **(101);**
- One ceramide: rhombifoliamide **(90).**

Williamson synthesis reaction was performed on isogarcinol leading to five compounds among which three are reported for the first time **(**13,14-dioxaethylisogarcinol **(119),** 13,14-di-O-(4-bromobenzyl)isogarcignol**(118)** **,** 13,14-di-O-(2-bromobenzyl)isogarcignol **(117))**.

Ethyl acetate fraction of *S. rhombifolia* showed the most potent activity with IC_{50} values of 4.18 and 5.38 µg/mL respectively, against strains of *Plasmodium* 3D7 and Dd2 with selectivity index of 119.61 and 92.93.

Hexane fraction of *S. acuta* showed good antiplasmodial activity against the strains 3D7 with IC_{50} values of 5.24 µg/mL with selectivity index of 95.41.

Hexane/ethylacetate 50 % fraction of *Garcinia ovalifolia* were also tested against the strains 3D7 and Dd2 and we observed IC_{50} values of 11.21 and 3.88 µg/mL respectively.

Among twenty-four isolated compounds which were screened for their antiplasmodial activity against those strains cryptolepine and oleanolic acid have a very good activity.

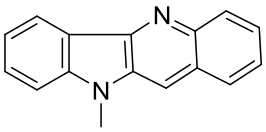

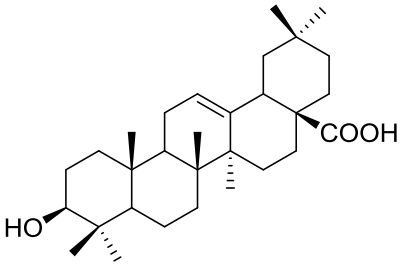

Cryptolepine

IC_{50} = **0.18 Pf3D7**

IC_{50} = **0.74 PfDd2**

Oleanolic acid

IC_{50} = 3.56 Pf3D7 IC_{50} = 2.02 PfDd2

The semi-synthetic compounds were screened against the strains 3D7 and Dd2 of *Plasmodium* and 13,14-dioxaethylisogarcinol showed pronounced activity against strains 3D7 and Dd2 with IC_{50} values of **1.13** and **0.64** µg/mL respectively**.**

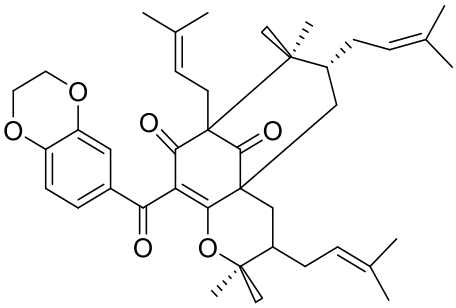

Cryptolepine and oleanolic acid are potential antimalarials and can be explored in the design of drugs against *Plasmodium falciparum* that justifying the traditional use of *Sida rhombifolia* and *Sida acuta* as antimalarial agents.

We plan to:

- Study the Structure Activity Relationship of cryptolepine
- Evaluate the anti-plasmodial activity of the fractions *in-vivo*
- Evaluate the sub-acute toxicity of the plant extracts
- Evaluate the *in-silico* predictions of the compounds obtained on the target proteins of plasmodium
- Study the mechanism of action of active compounds (isogarcinol, oleanolic acid and cryptolepine) against resistant strains

- Test the cytotoxicity of the active compounds to have a selectivity index of the most promising compound
- Screen the new ceramide Rhombifoliamide against a larger panel of pathogens

CHAPTER III

EXPERIMENTAL PART

III.1. INSTRUMENTS AND GENERAL METHODS

Melting points were measured on a Buchii melting point apparatus. Optical rotations were recorded on a Perkin-Elmer-241 MC Polarimeter. IR spectra were recorded on a Bruker Fourier transform/infrared (ATR) spectrophotometer. Mass spectra (ESI–MS) were obtained with a Thermo-Finnigan LCQ DECA mass spectrometer and HRESIMS spectra were measured with a FTHRMS-Orbitrap (Thermo-Finnigan) mass spectrometer.

1D- and 2D- NMR spectra were recorded in deuterated solvents on either Bruker ARX 500 or AVANCE DMX 600 NMR spectrometers (proton at 500 MHz and carbon ^{13}C at 125 MHz). All chemical shifts (δ) were measured in parts per million (ppm) using a residual solvent signal as secondary reference relatively to tetramethyl silane (TMS) as internal standard, while coupling constants (*J*) are given in *Hz*. Solvents were distilled prior to their use. Analytical grade solvents were used for LCMS.

Column chromatography (CC) were performed using Merck MN silica gel 60 M (0.04–0.063 nm) and thin layer chromatography (TLC) on aluminum silica gel 60 F_{254} (Merck) precoated plates (0.2 mm layer thickness). Spots were visualized on TLC either by UV lamp (254 and 366 nm) or by heating after spraying with 20% H_2SO_4 (v/v) solution. Different mixtures of *n*-hexane, EtOAc, CH_2Cl_2 and MeOH were used as eluting solvents.

III.2. EXPERIMENTAL

COLLECTION, EXTRACTION AND ISOLATION COMPOUNDS

The whole plant of *Sida rhombifolia* L.was collected in October 2017 from Bagangte in the Western region of Cameroon. The plant was identified by the staff of Cameroon National Herbarium in Yaoundé, where voucher specimens were conserved under the specimen N°: 20113/HNC.

The whole plant of *Sida rhombifolia* L, was dried and ground to give 2.5 kg of powder. This powder was extracted by maceration at room temperature with EtOH/H_2O (7:3) for 72 hours. After evaporation of the solvent under reduced pressure, we obtained 105.3 g of crude extract. The hydro ethanolic extract obtained of plant was dissolved in 300 mL of water and submitted to the liquid-liquid partition successively with *n*-hexane (500 mL), EtOAc (500 mL) and *n*-butanol (500 mL) fraction.

The whole plant of *Sida acuta* Burm. F.was collected in February 2017 from Ebolowa in the South region of Cameroon. The plants were identified by the staff of Cameroon

National Herbarium in Yaoundé, where voucher specimens were conserved under the specimen N°: 46188/HNC.

The whole plant of *Sida acuta* Burm was dried and ground to give 2.5 kg of powder. This powder was extracted by maceration at room temperature with EtOH/H2O (7:3) for 48 and 24 hours. After evaporation of the solvent under reduced pressure, we obtained 130.3 g of crude extract. The hydro ethanolic extract obtained of plant was dissolved in 300 mL of water and submitted to the liquid-liquid partition successively with *n*-hexane (400 mL), EtOAc (400 mL) and *n*-butanol (400 mL) fraction.

The Stem bark of *Garcinia ovalifolia*, was collected in Mont kala, in 2018, crushed, sun dried and grinded. The plant was identified by Mr. *Nana Victor*, botanist at the National Herbarium, Yaoundé, Cameroon, where a voucher specimen N° 55523/HNC was deposited.

The air-dried and powdered stem bark of *G. ovalifolia* (3 kg) was macerated in either a mixture of CH_2Cl_2/MeOH (1:1) for 48h and MeOH for 24h respectively, at room temperature. The removal of solvent under reduced pressure yielded 230 g of brown extract. A mass of 225 g of this organic extract was submitted to flash liquid chromatography on silica gel and eluted with hexane- ethyl acetate (EtOAc) solutions:, (1:1), (1:3), and finally with pure EtOAc to give 40 fractions of 250 ml each.

III.2.1. *In vitro* Antiplasmodial assays

P. falciparum growth inhibition assay

Dilution of samples for antiplasmodial activity

Stock solutions of plant isolated compounds and positive control (Chloroquine and Artemisinin) were prepared in DMSO 100% at 10mg/mL for isolated compounds and 1mM for Chloroquine and Artemisinin. After which, the required concentrations of each sample were achieved by adding a volume of sample from stocks into a 96-well plate containing incomplete RPMI 1640 medium followed by a five-fold serial dilution. For each compound, the intermediate concentrations were ranged from 0.04 to 25 µg/mL.

In vitro cultivation of *Plasmodium falciparum*

The Chloroquine-sensitive (Pf3D7-(MRA-102)) and Chloroquine-resistant (PfDd2) of *Plasmodium falciparum* strains was cultured in fresh O^+ human red blood cells at 4% haematocrit in complete RPMI 1640 medium [500 mL RPMI 1640 (Gibco, UK) supplemented with 25 mM HEPES (Gibco, UK), 0.50% Albumax I (Gibco, USA), 1X hypoxanthine (Gibco, USA) and 50mg/mL gentamicin (Gibco, China)] and incubated at 37°C

in a humidified atmosphere with 5% CO_2. The medium was replaced with fresh complete medium daily to propagate the culture. Giemsa-stained thin blood smears were examined microscopically under immersion oil to monitor cell-cycle transition and parasitaemia evolution

Synchronization of parasite culture

Before each experiment, synchronized ring stage parasite was obtained by 5% sorbitol (w/v) treatment in respect to **Lambros and Vanderberg, 1979**. It is important to note that, the use of synchronized cultures over mixed stage cultures can enable the test molecules to interact with all the three stages (ring, trophozoite and schizont) of the 48 hrs long life cycle of *P. falciparum* in culture. Moreover, starting the experiment with synchronized ring stage culture provides the distinct advantage of observing growth inhibitory effects without a rise in parasitemia during the ring-trophozoite-schizont transitions.

SYBR green I based fluorescence assay

Drug sensitivity assay was carried out in 96-well microtitration plates using SYBR green I fluorescence based assay **(Smilkstein *et* al., 2004).** This assay specifically based on the ability of SYBR green to give strong fluorescence in the presence of parasite DNA during cell proliferation. The absence of nucleus in human red blood cells where the malarial parasite proliferates allows the use of SYBR green for the specific monitoring of the growth of malarial parasite.

Sorbitol-synchronized ring stage parasites (haematocrit: 1%, parasitaemia: 2%, 90 µl) under normal culture conditions were incubated in the presence of pre-diluted compounds and reference drug (10µL) followed by the incubation at 37°C for 72h. After what, 100 µL of SYBR Green I buffer [6 µL of 10,000 × SYBR Green I (Invitrogen) + 600µL of Red Blood Cells lysis buffer {Tris (25 mM; pH 7.5)} + 360µL of EDTA (7.5 mM) + 19,2µL of parasites lysis solution {saponin (0.012%; wt/vol) } and 28,8µL of Triton X-100 (0.08%; vol/vol)}] were added to each well, mixed twice gently with multi-channel pipette and incubated in the dark at 37°C for 1h. Fluorescence was measured using a TECAN M200 Microplate reader with excitation and emission at 485 and 538 nm, respectively. The fluorescence counts were plotted against the logarithm of sample concentration and the 50% inhibitory concentration (IC_{50}) was determined by analysis of dose–response curves using GraphPad Prism 5. Experiments were done in duplicate.

III.2.2 *In vitro* cytotoxicity assay.

The cytotoxicity profile of compounds were assessed using the resazurin based assay **(Bowling et *al*., 2012)** against RAW 264.7 cells duly cultivated in complete Dulbecco's Modified Eagle's Medium (DMEM) containing 13.5 g/L of DMEM (Sigma Aldrich), 10% Fetal Bovine Serum (Sigma Aldrich), 0.2% sodium bicarbonate (w/v) (Sigma Aldrich) and 50 μg/mL of gentamicin (Sigma Aldrich). Globally, macrophages were seeded into 96-wells cell-culture flat-bottomed plates at a density of 10^4 cells in 100 μL of complete medium/well and incubated for 24 hours at 37°C, 5% CO_2 to allow cell adhesion. Following cell adhesion, ten microliter of each serially diluted test samples solution were added in assay plates and were then incubated for 48 h in the same experimental conditions. Growth control (0.1%DMSO-100% growth) and positive control wells (Podophyllotoxin at 20 μM) were included in the experiment plates. Cell proliferation was checked by adding 10 μL of a stock solution of resazurin (0.15 mg/mL in sterile PBS) to each well followed by an incubation of 4 h in the same culture condition. Fluorescence was then read on an Infinite M200 fluorescence multi-well plate reader (Tecan) at an excitation/emission of 530/590 nm. Results were expressed as 50% cytotoxic concentrations (CC_{50}) and selectivity indices (CC_{50} Mammalian cell/IC50 *Pf*3D7) were calculated for each tested compound.

Table 42: Chromatogram for acetate fraction of the whole plant of *Sida rhombifolia*

Eluent	Sub fractions	Observations after TLC analysis
Hex – EA (100-0)	1 – 10	Yellow oil
Hex – EA (95-5)	11 – 19	**SRA2**+ mixture of 3 compound
Hex – EA (90-10)	20 – 30	**SR7** +Mixture of 4 compound
Hex – EA (85-15)	31 – 50	**SRA1**+ Mixture of 2 compound
Hex – EA (80-20)	51 – 77	Mixture of 2 compound
Hex – EA (75-25)	78 – 95	+ trails
Hex – EA (70-30)	96 – 116	**SRA3**+Mixture of 2 compounds + trails
Hex – EA (65-35)	117 – 124	Mixture of 2 compound + trails
Hex – EA (60-40)	133 – 140	**SRP1**+Mixture of 2 compound
Hex – EA (50-50)	141 – 151	**SRYK6**+Mixture of 4 compound
Hex – EA (25-75)	152 – 169	+ Mixture of 4 compound
Hex – EA (0-100)	170 – 176	Mixture of 4 compound
EA – MeOH (95-5)	177 – 185	trails
EA – MeOH (90-10)	186 – 195	trails

The hexane fraction (13.2 g), adsorbed on 25 g of silica gel was mounted on silica gel column (100 g) and eluted with hexane, Hex-EA, EA-MeOH in gradient conditions to yield Ursolic acid (**SR4**,6.00mg), mixure of β-sitosterol and stigmasterol (**SR1**, 5.06 mg). 3-O-*β*-D-glucopyranosyl-β-sitosterol (**SR2**, 4.23 mg) Lupeol (**SR3**, 5.12 mg).

Table 43: Chromatogram for hexane fraction of the whole plant of *Sida rhombifolia*

Eluent	Sub fractions	Observations after TLC analysis
Hex – EA (100-0)	1 – 8	Yellow oily mixture
Hex – EA (95-5)	9 – 17	**SR3**+ mixture of 3 compound
Hex – EA (90-10)	18 – 47	**SR1**+ 2 compound
Hex – EA (85-15)	48 – 64	**SR4**+Mixture of 2 compounds + trails
Hex – EA (80-20)	65 – 78	Mixture of 2 compound + trails
Hex – EA (75-25)	79 – 90	Mixture of 2 compound + trails
Hex – EA (70-30)	91 – 104	Mixture of 2 compound + trails
Hex – EA (65-35)	105 – 117	trails
Hex – EA (60-40)	118 – 139	**SR2**
Hex – EA (50-50)	140 – 177	Mixture of 2 compound
Hex – EA (40-60)	180 – 196	Mixture of 3 compound
Hex – EA (25-75)	197 – 207	trials
Hex – EA (0-100)	208 – 221	trials
EA – MeOH (95-5)	222 – 230	Mixture of 2 compound + trails
EA – MeOH (90-10)	231 – 240	Mixture of 2 compound + trails
EA – MeOH (80-20)	241– 250	trails

The n-butanol fraction (10.3 g), adsorbed on 20 g of silica gel was mounted on silica gel column (90 g) and eluted with hexane, Hex-EA, EA-MeOH in gradient conditions to yield Kaempferol-3-O-*β*-D-glucopyranoside (**SB4**,6.32mg) and 20-hydroxyecdysone (**SB1**,4.02mg)

Table 44: Chromatogram for the n-butanol fraction of the whole plant of *Sida rhombifolia*

Eluent	Sub fractions	Observations after TLC analysis
Hex – EA (50-50)	1 – 15	Yellow oily mixture
Hex – EA (40-60)	16 – 35	**SB1**+Mixture of 3 compound
Hex – EA (25-75)	36 – 50	**SB4**+ Mixture of 3 compound
EA – MeOH (95-5)	51 – 65	trails

Scheme 8: Extraction and isolation procedure from the whole plant of *Sida acuta*

The ethyl acetate fraction (10.1 g), adsorbed on 20 g of silica gel was mounted on silica gel column (90 g) and eluted with hexane, Hex-EA, EA-MeOH in gradient conditions to yield xanthyletin (**SAA1**, 3.45 mg) (E)-suberenol (**SAA2** 5.12 mg) , Thamnosmonin (**SAA3**, 4.20 mg). 5,5'-oxybis(pentane-1,2,3,4-tetraol) (**SAR6**, 6.32 mg).

Table 45: Chromatogram for acetate fraction of the whole plant of *Sida acuta*

Eluent	Sub fractions	Observations after TLC analysis
Hex – EA (100-0)	1 – 10	Yellow oil
Hex – EA (95-5)	11 – 19	mixture of 3 compound
Hex – EA (90-10)	20 – 30	**SAA1**+Mixture of 4 compound
Hex – EA (85-15)	31 – 50	Mixture of 2 compound
Hex – EA (80-20)	51 – 77	**SAA2**+ Mixture of 2 compound
Hex – EA (75-25)	78 – 95	+ trails
Hex – EA (70-30)	96 – 116	Mixture of 2 compounds + trails
Hex – EA (65-35)	117 – 124	Mixture of 2 compound + trails
Hex – EA (60-40)	133 – 140	**SAA3**+Mixture of 2 compound
Hex – EA (50-50)	141 – 151	Mixture of 4 compound
Hex – EA (25-75)	152 – 169	Mixture of 4 compound
Hex – EA (0-100)	170 – 176	Mixture of 4 compound
EA – MeOH (95-5)	177 – 185	Mixture of 3 compound
EA – MeOH (90-10)	186 – 195	Mixture of 2 compound
EA – MeOH (80-20)	196-210	Mixture of 2 compound
EA – MeOH (60-40)	211-220	**SAR6**+Mixture of 2 compound

The hexane fraction (12.2 g), adsorbed on 20 g of silica gel was mounted on silica gel column (90 g) and eluted with hexane, Hex-EA, EA-MeOH in gradient conditions to yield 1-6 Dihydroxy –xanthone (**SRYK3**, 5.30 mg) and betulinic acid (**SR5** 6.50 mg)

Table 46: Chromatogram for hexane fraction of the whole plant of *Sida acuta*

Eluent	Sub fractions	Observations after TLC analysis
Hex – EA (100-0)	1 – 10	Yellow oil
Hex – EA (95-5)	11 – 19	Yellow oil
Hex – EA (90-10)	20 – 30	**SRYK3**+Mixture of 4 compound
Hex – EA (85-15)	31 – 50	**SR5**+Mixture of 2 compound
Hex – EA (80-20)	51 – 77	Mixture of 2 compound
Hex – EA (75-25)	78 – 95	+ trails

The n-butanol fraction (11.3 g), adsorbed on 20 g of silica gel was mounted on silica gel column (90 g) and eluted with, CH_2CL_2-MeOH in gradient conditions to yield Cryptolepine (**SAB3**, 4.01 mg) and 4-methoxy-1-methylquinolin-2(1H)-one (**SAB1,** 5.12 mg).

Table 47: Chromatogram for n-butanol fraction of the whole plant of *Sida acuta*

Eluent	Sub fractions	Observations after TLC analysis
CH_2CL_2 – MeOH (100-0)	1 – 10	mixture of 2 compound
CH_2CL_2 – MeOH (95-5)	11 – 19	mixture of 3 compound
CH_2CL_2 – MeOH (90-10)	20 – 30	Mixture of 4 compound
CH_2CL_2 – MeOH (85-15)	31 – 50	**SAB3+SAB1**+Mixture of 2 compounds
CH_2CL_2 – MeOH (80-20)	51 – 77	Mixture of 2 compound
CH_2CL_2 – MeOH (75-25)	78 – 95	trails

.

Table 48: Chromatogram for hexane/acetate 50% fraction of the stem bark of G. *ovalifolia*

Eluent	Sub fractions	Observations after TLC analysis
CH_2CL_2 – MeOH (100-0)	1 – 10	mixture of 3 compound
CH_2CL_2 – MeOH (95-5)	11 – 19	**GO4** + mixture of 3 compound
CH_2CL_2 – MeOH (90-10)	20 – 30	**GP1** +Mixture of 4 compound
CH_2CL_2 – MeOH (85-15)	31 – 50	**GOX**+ Mixture of 2 compound
CH_2CL_2 – MeOH (80-20)	51 – 77	Mixture of 2 compound
CH_2CL_2 – MeOH (75-25)	78 – 95	**GO-S1**+ trails
CH_2CL_2 – MeOH (70-30)	96 – 116	Mixture of 2 compound + trails
CH_2CL_2 – MeOH (65-35)	117 – 124	trails

III.3. HEMISYNTHESIS

III.3.1 Williamson alkylation reaction

To 80.4 mg (0.13 mmol) of (-) isogarcinol in dry acetone (8 mL), was added K_2CO_3 (0.3 g) followed by 1.2-dibromoethane (0.12 mL, d = 2.18, 0.17 g, 1.43 mmol). The reaction mixture was heated at 40 °C under reflux for 23 h. we use benzylbromide, 2-bromo benzylbromide, 4-bromo benzylbromide and 1.2-dibromoethane.

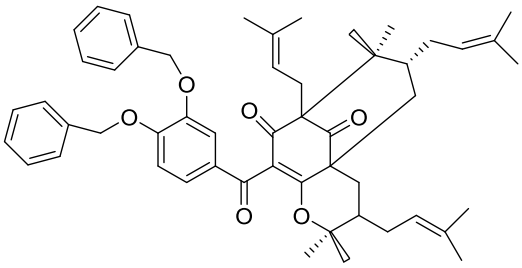

13, 14-di-*O*-benzylisogarcinol

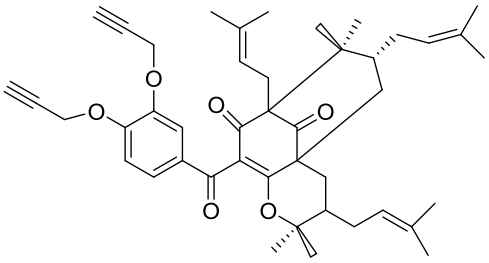

13, 14-di-*O*-propargylisogarcignol

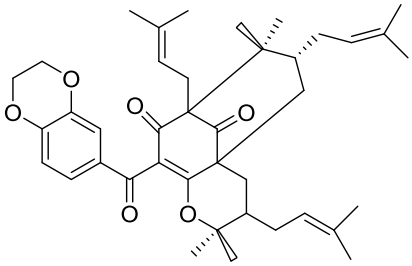

13,14-dioxaethylisogarcinol

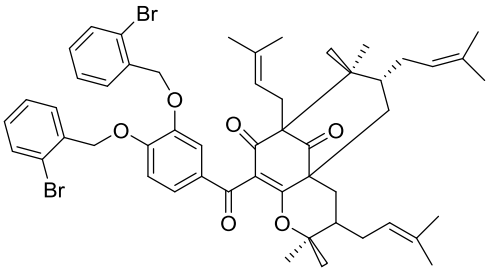

13,14-*O*-bis (3-bromobenzyl)isogarcinol

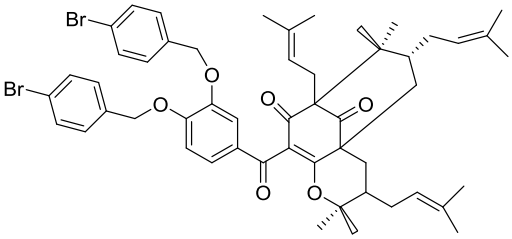

13,14-*O*-bis (5-bromobenzyl)isogarcinol

III.4 PHYSICO-CHEMICAL CHARACTERISTICS OF COMPOUNDS AND DERIVATIVES

Rhombifoliamide (90) or SRP1

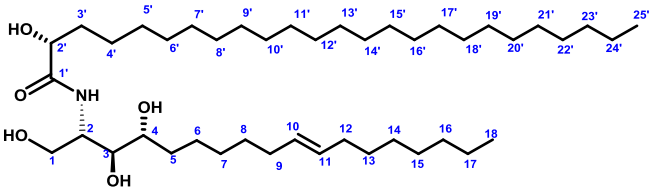

Physical state: white powder

Molecular formula $C_{43}H_{85}NO_5$

^{1}H NMR (600 MHz, $CDCl_3/CD_3OD$)

^{13}C NMR (150 MHz, $CDCl_3/CD_3OD$)

IR (KBr): 3329 cm^{-1}, 3215 cm1 and 1620 cm^{-1} ;

HRESI-MS: m/z 696.6506 ($C_{43}H_{86}NO_5$þ; calcd. 696.6501

SAA2 or (E) - Suberenol (91)

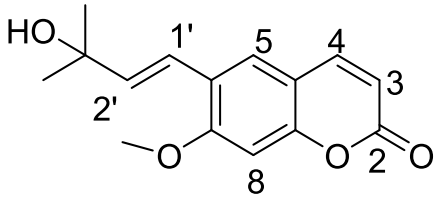

Physical state: white powder

Molecular formula $C_{15}H_{16}O_4$

^{1}H NMR (500 MHz, acetone)

^{13}C NMR (126 MHz, acetone)

SAA1 or xanthyletin (92)

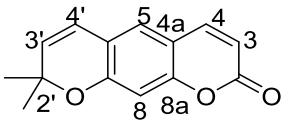

Physical state: white powder

Molecular formula $C_{14}H_{12}O_3$

^{1}H NMR (500 MHz, acetone)

^{13}C NMR (126 MHz, acetone)

Thamnosmonin or SAA3 (93)

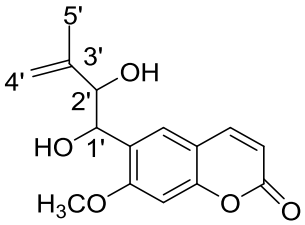

Physical state: white powder

Molecular formula $C_{15}H_{16}O_5$

^{1}H NMR (500 MHz, acetone)

^{13}C NMR (126 MHz, acetone)

1.6-dihydroxyxanthone or SRYK3 (94)

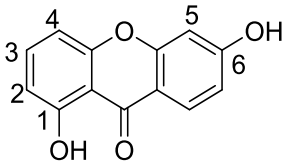

Physical state: yellow powder

Molecular formula $C_{13}H_8O_4$

^{1}H NMR (500 MHz, Methanol-d4)

4-Methoxy-1-methyl-2-quinolone or SAB1 (102)

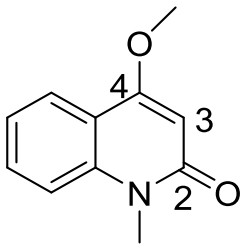

Physical state: crystalline solid needles

Molecular formula $C_{11}H_{11}NO_2$

^{1}H NMR (500 MHz, $CDCl_3$)

^{13}C NMR (125 MHz, $CDCl_3$)

Melting point**:** 199-200 °C

Astragaline or SAB4 (96)

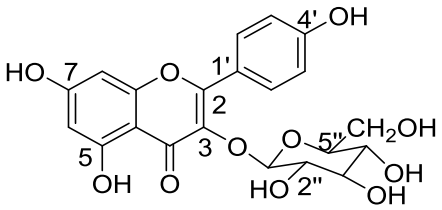

Physical state: white powder

Molecular formula $C_{15}H_{16}O_5$

^{1}H NMR (500 MHz, Methanol-d4)

^{13}C NMR (125 MHz, $CDCl_3$)

Tiliroside or SRA3 (97)

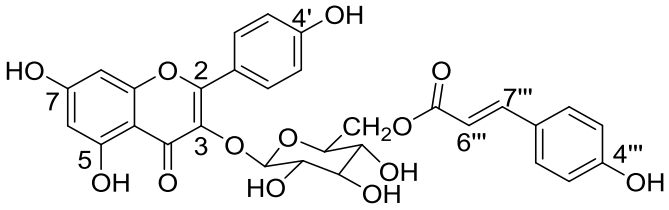

Physical state: yellow powder

Molecular formula $C_{30}H_{26}O_{13}$

ESI-MS m/z= 595.1414,

^{1}H NMR (500 MHz, CD_3OD)

Cryptolepine or SAB3 (103)

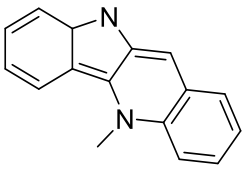

Physical state: yellow powder

Molecular formula $C_{16}H_{13}N_2$

^{1}H NMR (500 MHz, CD_3OD)

APCI: 233.27

SR1 or mixture of stigmasterol and *β*- sitosterol (104)

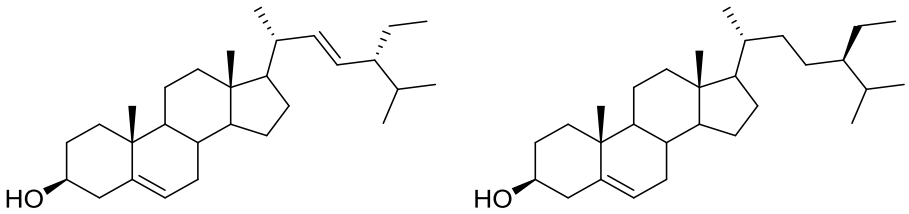

Physical state: white powder

Molecular formula $C_{29}H_{48}O$ and $C_{29}H_{50}O$,

^{1}H NMR (500 MHz, $CDCl_3$)

SR2 or Stigmasterol 3-O-*β*-D-glucopyranoside (105)

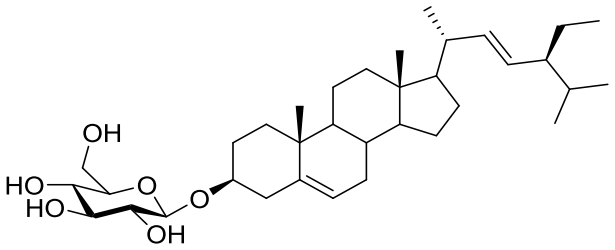

Physical state: Beige powder

Molecular formula $C_{35}H_{62}O_6$

^{1}H NMR ($CDCl_3$/ CD_3OD, 500MHz,)

ESI-MS: m/z 615.2

SR3 or Lupeol (108)

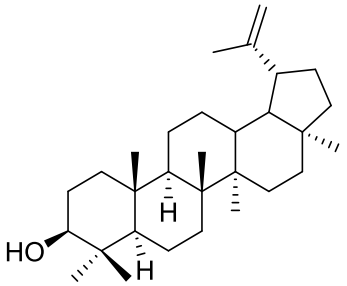

Physical state: white powder

Molecular formula $C_{30}H_{50}O$

^{1}H NMR ($CDCl_3$, 500MHz)

^{13}C NMR ($CDCl_3$, 125MHz,)

(+)-ESI-MS: m/z 449.3

SR5 or Betulinic acid (109)

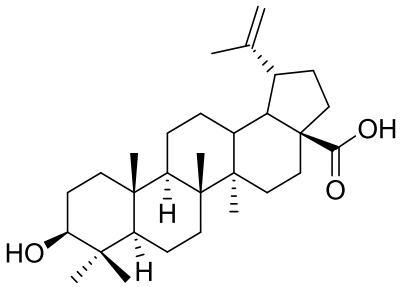

Physical state: beige powder

Molecular formula $C_{30}H_{48}O_3Na$

^{1}H (MeOD, 500MHz,)

^{13}C NMR (CD_3OD, 125MHz,)

(+)-ESI-MS: m/z 457.1

SRA1 or Taraxerol (110)

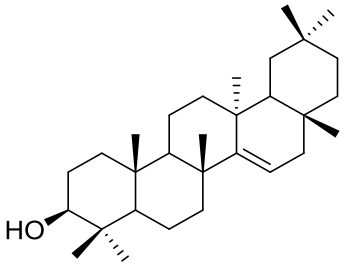

Physical state: white powder

Molecular formula $C_{30}H_{50}ONa$

^1H NMR ($CDCl_3$, 500MHz)

^{13}C NMR ($CDCl_3$, 125MHz)

SRA2 or Taraxeryl acetyl (111)

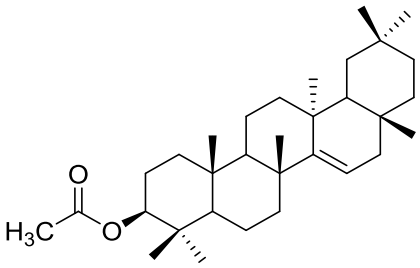

Physical state: white powder

Molecular formula $C_{32}H_{52}O_2Na$

^1H NMR ($CDCl_3$, 500MHz)

^{13}C NMR ($CDCl_3$, 125MHz)

SR4 or Ursolic acid (112)

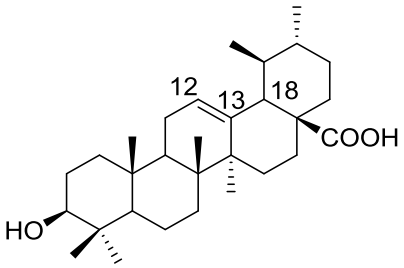

Melting point 256.7-258.6 ^0C

Physical state: white powder

Molecular formula $C_{32}H_{52}O_2Na$

^{1}H NMR (500MHz, CD_3OD)

^{13}C NMR (125MHz, CD_3OD*)*

SR7 or oleanolic acid (113)

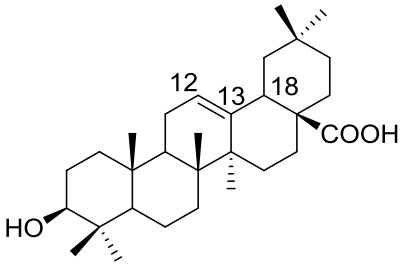

Physical state: white powder

Molecular formula $C_{30}H_{48}O_3$

^{1}H NMR (600MHz, $CDCl_3$)

^{13}C NMR (150 MHz, $CDCl_3$)

EIMS m/z 456.3

SRYK6 or Leontoside A (114)
Physical state: white powder

Molecular formula $C_{35}H_{56}O_8$

^{1}H NMR (500MHz, CD_3OD)

^{13}C NMR (125 MHz, CD_3OD)

EIMS m/z 604.3975

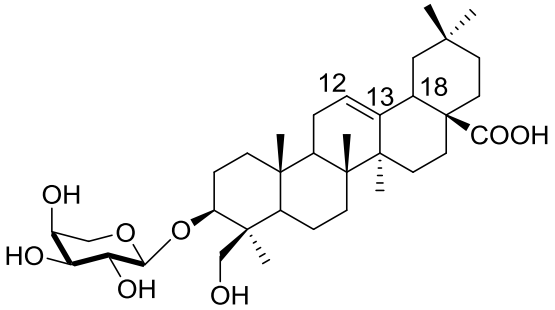

SB1 or 20-Hydroxyecdysone (106)

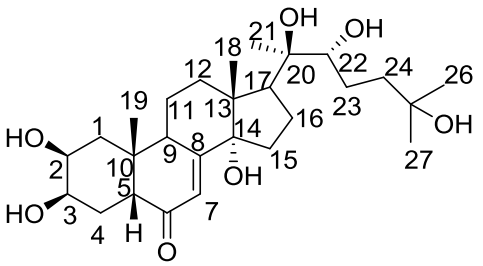

Physical state: white powder

Molecular formula $C_{27}H_{44}O_7$

^{1}H NMR (500 MHz, CD_3OD)

^{13}C NMR (125 MHz, CD_3OD)

FAB mass: 480.3087

GO4 or Rheediaxanthone A (101)

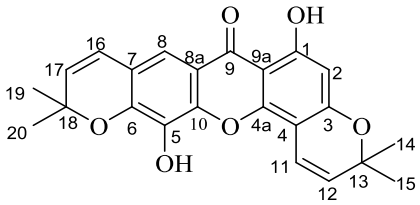

Physical state: yellow powder

Molecular formula $C_{23}H_{20}O_6$

^{1}H NMR (300 MHz, $CDCl_3$)

^{13}C NMR (75 MHz, $CDCl_3$)

7-épiisogarcinol or GOX (100)

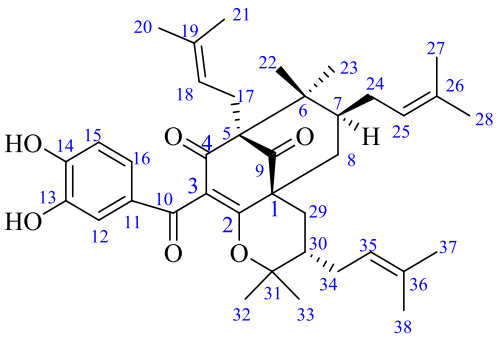

$[\alpha]_D^- = -158$ (C=1, 0; $CHCl_3$)

Physical state: yellow powder

Molecular formula $C_{38}H_{50}O_6$

^{1}H NMR (300 MHz, $CDCl_3$)

^{13}C NMR (75 MHz, $CDCl_3$)

Taxifolin 6-c-glucoside or GO-S1 (98)

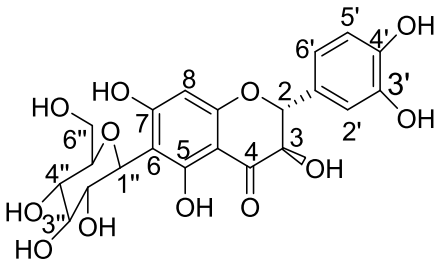

Physical state: white powder

Molecular formula $C_{21}H_{22}O_{12}$

^{1}H NMR (300 MHz, CD_30D)

^{13}C NMR (75 MHz, CD_30D)

(-)Isogarcignol or GO-A (99)

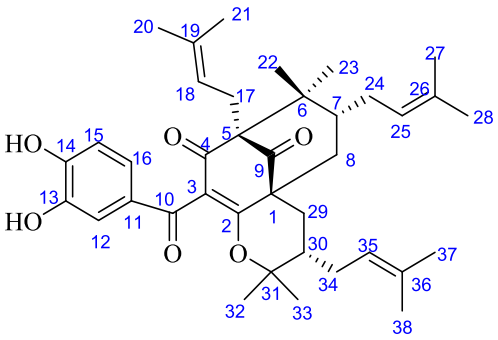

Physical state: brown crystals

Molecular formula $C_{38}H_{50}0_6$

^{1}H NMR (300 MHz, $CDCl_3$)

^{13}C NMR (75 MHz, $CDCl_3$)

2,6-dimethoxy-p-benzoquinone or GO9 (101)

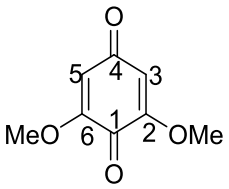

Physical state: white powder

Molecular formula $C_8H_8O_2$

^{1}H NMR (300 MHz, $CDCl_3$)

^{13}C NMR (75 MHz, $CDCl_3$)

13, 14-di-*O*-propargylisogarcignol

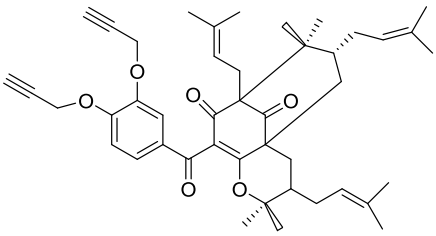

Physical state: white powder

Molecular formula $C_{44}H_{54}O_6$

^1H NMR (300 MHz, $CDCl_3$)

13, 14-di-*O*-benzylisogarcinol

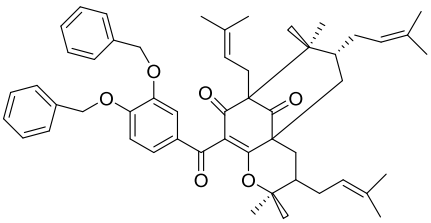

Physical state: white powder

Molecular formula $C_{52}H_{62}O_6$
^1H NMR (300 MHz, $CDCl_3$)

13,14-dioxaethylisogarcinol

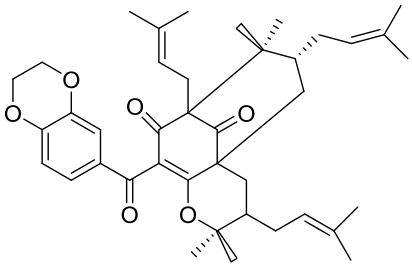

Physical state: white powder

Molecular formula $C_{40}H_{52}O_6$
^1H NMR (300 MHz, $CDCl_3$)

13,14-*O*-bis (3-bromobenzyl)isogarcinol

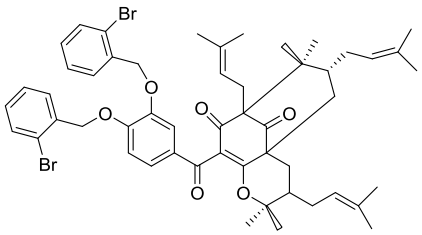

Physical state: white powder

Molecular formula $C_{52}H_{60}Br_2O_6$
^{1}H NMR (300 MHz, $CDCl_3$)

13,14-*O*-bis (5-bromobenzyl)isogarcinol

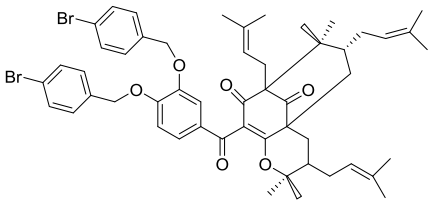

Physical state: white powder

Molecular formula $C_{52}H_{60}Br_2O_6$
^{1}H NMR (300 MHz, $CDCl_3$)

III.5. CHARACTERISTIC ANALYTICAL TESTS

III.5.1. Molisch's Test

Objective: Identification of sugars.

Reagents: EtOH, α-naphthol, concentrated H_2SO_4

The sample to be analyzed, is introduced into a test tube and dissolved in a solution of 1% ethanol in α-naphthol. A few drops of concentrated H_2SO_4 are added, letting it flow down the side of the tube. The appearance of a purple-red ring at the interface, between the liquids indicates the presence of a sugar or sugars**. (Hamid et *al*., 2018).**

III.5.2. Liebermann-Burchard test: identification of terpenes and sterols.

Objective: Identification of triterpenes and sterols.

Reagents: $CHCl_3$, Ac_2O, concentrated H_2SO_4 (50 mL/20 mL/1 mL).

To a $CHCl_3$ solution of the sample to be analyzed, we have added a few drops of acetic anhydride, followed by concentrated H_2SO_4. The presence of triterpenes and their saponins is indicated by a change of color from brick red, through purple, then blue and finally to green. Sterols give a blue color that rapidly changes to green **(Hamid et *al*., 2018).**

III.5.3. Ferric Chloride Test

Objective: Identification of phenols.

Reagents: $FeCl_3$, MeOH

To an alcoholic solution of the sample, add a few drops of $FeCl_3$. A color change from yellow to purple indicates the presence of phenols **(Hamid et *al*., 2018).**

III.5.4. Shinoda's Test

Objective: Identification of flavonoids.

Reagents: Mg, MeOH, concentrated HCl

To an alcoholic solution of the sample, add a few drops of concentrated HCl and a pinch of Mg fillings. The presence of flavonoids is indicated by effervescence and a deep pink (purplish) color **(Hamid et *al*., 2018).**

REFERENCES

Abat JK, Kumar S, Mohanty A. **2017**. Ethnomedicinal, phytochemical and ethnopharmacological aspects of four medicinal plants of Malvaceae used in Indian traditional medicines: A review. *Medicines*. 4:75.

Ablordeppey SY, Hufford CD, Borne RF, Dwuma-Badu D. **1990**. ^{1}H-NMR and ^{13}C-NMR Assignments of Cryptolepine, A 3: 4-Benz-δ-carboline Derivative Isolated from *Cryptolepis sanguinolenta*. *Planta medica*. 56: 416-417.

Achan J, Mwesigwa J, Edwin CP, D'alessandro U. **2018**. Malaria medicines to address drug resistance and support malaria elimination efforts. *Expert Review* of *Clinical Pharmacology*. 11: 61-70.

Adetutu A, Morgan WA, Corcoran O. **2011**. Ethnopharmacological survey and in vitro evaluation of wound-healing plants used in South-western Nigeria. *Journal of Ethnopharmacology*. 137: 50-56.

Adhikari BS, Babu MM, Saklani P, Rawat G. **2010**. Medicinal plants diversity and their conservation status in Wildlife Institute of India (WII) campus, Dehradun. *Ethnobotanical leaflets*. 2010: 6.

Ageta H, Arai Y. **1983**. Fern constituents: pentacyclic triterpenoids isolated from *Polypodium niponicum* and *P. formosanum*. *Phytochemistry*. 22: 1801-1808.

Ali S, Goundar R, Sotheeswaran S, Baulieu C, Spino C. **2000**. Benzophenone of *Garcinia pseudoguttifera*. *Phytochemistry.* 53 : 281-284.

Allard S, Ourisson G. **1957**. Remarques sur la nomenclature des triterpènes. *Tetrahedron*.1: 277-283.

Amaratunga C, Sreng S, Suon S, Phelps S, Stepniewska K, Lim P, Zhou C, Mao S, Anderson M, Lindegardh N. **2012**. Artemisinin-resistant *Plasmodium falciparum* in Pursat province, western Cambodia: a parasite clearance rate study. *The Lancet Infectious Diseases* 12: 851-858

Aminah NS, Laili ER, Rafi M, Rochman A., Insanu M, Tun W. **2021**. Secondary metabolite compounds from *Sida* genus and their bioactivity. *Heliyon*. 7: 6682.

Anyango R, Julius M, Heydenreich M, Masanja H, Waweru J, Owor R, Kerubo L, Ogweno Midiwo J. **2019**. Antiplasmodial Biflavanones from the Stem Bark of *Garcinia buchananii.*

Arwa P, Zeraik M, Ximenes V, da Fonseca L, Bolzani V, Siqueira D. **2015**. Redox-active bioflavonoids from *Garcinia brasiliensis* as inhibitors of neutrophil oxidative burst and human erythrocyte membrane damage. *Journal of Ethnopharmacol*. 174: 410-418.

Asha A, Farsana S, Baiju E. **2018**. Phytochemical profiling and antibacterial activity of selected Sida species against common human pathogenic bacteria: An in vitro study. *Journal of Pharmacognosy*. 7: 1201-1205.

Ashley A, Dhorda M, Fairhurst M, Amaratunga C, Lim P, Suon S, Sreng S, Anderson M, Mao S, Sam B. **2014**. Spread of artemisinin resistance in *Plasmodium falciparum* malaria. *The New England Journal of Medicine*. 371: 411-423.

Asif M, Saleem M, Yousaf S, Saadullah M, Zafar M, Khan R, Yuchi A. **2019**. Antidiabetic activity of aqueous extract of *Sigesbeckia orientalis* (St. Paul's Wort) in alloxan-induced diabetes model. *Brazilian Journal of Pharmaceutical Sciences*. 55.

Aubreville, A. **1959**. Forest Flora of the Ivory Coast. Tropical Forestry Technical Centre, 2nd Revised ed. 325-329.

Augustin J, Kuzina V, Andersen S, Bak S. **2011.** Molecular activities, biosynthesis and evolution of triterpenoid saponins. *Phytochemistry*. 72: 435-457.

Bamps P. **1970**. Flora of the Congo, Rwanda and Burundi: Spermatophytes, Guttiferae. National Botanic Garden of Belgium, Bruxelles. 1-61.

Bandeira S, Gaspar F, Pagula F. **2001**. African ethnobotany and healthcare: emphasis on Mozambique. *Pharmaceutical Biology*. 39 : 70-73.

Banzouzi J-T, Prado R, Menan H, Valentin A, Roumestan C, Mallié M, Pelissier Y, Blache Y. **2004**. Studies on medicinal plants of Ivory Coast: Investigation of *Sida acuta* for *in vitro* antiplasmodial activities and identification of an active constituent. *Phytomedicine*. 11: 338-341.

Barreto-Bergter E, Pinto M, Rodrigues L. **2004**. Structure and biological functions of fungal cerebrosides. *Anais da Academia Brasileira Ciências*. 76 : 67-84.

Bati K, Kwape TE, Chaturvedi P. **2018**. The Inhibitory Effect of An Ethanol Extract of *Sida rhombifolia* Leaves on Key Carbohydrate Hydrolyzing Enzymes. *Journal of Complementary Medicine Research*. 9: 1-10.

Beaufay C, Herent MF, Quetin-Leclercq J, Bero J. **2017**. In *vivo* anti-malarial activity and toxicity studies of triterpenic esters isolated form *Keetia leucantha* and crude extracts. *Malaria Journal*. 16: 8.

Benkiki N, Benkhaled M, Kabouche Z, & Bruneau, C. **2002**. Heraclenol and isopimpinellin: two rare furocoumarins from *Ruta montana*. In *Biodiversity*. 303-307.

Biloa M, Cressend D, Perron K, Nkengfack A, Hostettmann K, Cuendet M. **2014**. Isolation and biological activity of compounds from *Garcinia preusii*. *Pharmaceutical Biology*. 1–6.

Bissim SM , Kenmogne SB, Lobe JS, Atangana AF, Bissoue AN, Langat M, Isyaka S, Lateef M, Nguefa H, Ali M, Waffo KA, Wansi JD. **2020**. The chemistry and biological activities of *Citrus clementina* Hort. Ex Tanaka (Rutaceae), a vegetatively propagated species. *Natural Product Research*. 35(22):1-4.

Blasco B, Leroy D, Fidock DA. **2017**. Antimalarial drug resistance: linking Plasmodium falciparum parasite biology to the clinic. *Natural Mededecine*. 23: 917-28.

Bouquet A. **1969**. Fetishes and Traditional Medicines of the Congo. Memory of l'ORSTOM. 35: 123.

Bowling T, Mercer L, Don R, Jacobs R, Nare B. **2012**. Application of a resazurin-based high-throughput screening assay for the identification and progression of new treatments for human African trypanosomiasis. *International Journal for Parasitology*. 2: 262-270.

Bruneton J, **1993**. Pharmacognosy, Phytochemistry and Medicinal Plants. 2nd edition, Paris. 230–585.

Burkill, I. **1966**. A. Dictionary of the Economic Products of the Malay Peninsular, 2ème Ed. Kuala Lumpur.

Busson, F. **1965**. Food plants of West Africa: Botanical, biological and chemical study Edition le conte, Marseille. 211–215.

Campos P, Horinouchi C, Prudente A, Cechinel-Filho V, Cabrini D, Otuki. **2013**. Effect of *Garcinia garderiana* (Planchon and Triana) Zappi hydroalcoholic extract on melanogenesis in B16F10 melanoma cells. *Journal of Ethnopharmacol*. 148: 199-204.

Casalino, E**. 2004.** Paludisme. EMC – Médecine. 1: 580–591.

Castillo M, Osorio L, and Palma G. **2002**. Assessment of therapeutic response of *Plasmodium vivax* and *Plasmodium falciparum* to chloroquine in a Malaria transmission free area in Colombia. *Memórias do* Instituto Oswaldo Cruz. 97: 559-562.

Chang, P, Cordell G, Aynilian G, Fong H, Farnsworth N. **1976**. Alkaloids and coumarins of *Thamnosma montana. Journal of Natural Products*. 39: 134-140.

Chaturvedula V, Prakash I. **2012**. Isolation of Stigmasterol and *β*-Sitosterol from the dichloromethane extract of *Rubus suavissimus*. *International Current Pharmaceutical Journal*. 1: 239-242.

Chaves J, De Souza M, Da Silva L, Lachos-Perez D, Torres-Mayanga P, da Fonseca Machado A, Forster-Carneiro T, Vázquez-Espinosa M, González-de-Peredo A, Barbero G. **2020**. Extraction of flavonoids from natural sources using modern techniques. *Frontiers in Chemistry*. 8.

Chaves O, Gomes R, Tomaz A, Fernandes M, Das Graças Mendes Junior L, de Fátima Agra M, Braga V, De Fátima Vanderlei de Souza M. **2013**. Secondary metabolites from *Sida rhombifolia* L. (Malvaceae) and the vasorelaxant activity of cryptolepinone. *Molecules*. 18 : 2769-2777.

Chen H, Chen T, Huang W, Tsai J, Kuo, C. **2012**. 4-Ketopinoresinol, a novel naturally occurring are activator, induces the Nrf2/HO-1 axis and protects against oxidative stress-induced cell injury via activation of PI3K/AKT signaling. *Free Radical Biology and Medicine*. 52: 1054-1066.

Chen S, Wan M, Loh B. **1996**. Active constituents against HIV-1 protease from *Garcinia mangostana*. *Planta Medica*. 62: 381–382.

Chen, C. R., Chao, L. H., Liao, Y. W., Chang, C. I.,Pan, M. H. **2007**. Tocopherols and triterpenoids from *Sida acuta*. *Journal of the Chinese Chemical Society*, 54*:* 41-45.

Chin W, Kinghorn D. **2008**. Structural characterization, biological effects, and synthetic studies on xanthones from mangosteen (*Garcinia mangostana*), a popular botanical dietary supplement. *Mini-reviews in Organic Chemistry*. 5: 355-364.

Chukwuemeka N-AP, Adejoh I, Osafanme I, Duniya S, Boniface M. **2019**. Laxative effects of aqueous extract of *Sida acuta* leaves in loperamide-induced constipation in wistar rats. *Asian Journal of Research in Medical*. 1-7.

Ciochina R, Grossman R. **2006.** Polycyclic polyprenylated acyphloroglucinols. *Chemical Reviews*. 106**:** 3963–3986.

Colodel E, Gardner D, Zlotowski P, Driemeier D. 2002. Identification of swainsonine as a glycoside inhibitor responsible for *Sida carpinifolia* poisoning. *Brazilian Journal of Veterinary Research* . 44 : 177-178.

Cottrell G, Musset L, Hubert V, Bras J, Clain J. **2014.** Emergence of Resistance to Atovaquone-Proguanil in Malaria Parasites: Insights from Computational Modeling and Clinical Case Reports. Antimicrob. Agents Chemother. *American Society for Microbiology Journals*. 58 :4504-14.

Cuca-Suarez L, Barrera, E & Caballero J. **2011**. Quinoline alkaloids and friedelane-type triterpenes isolated from leaves and wood of *Esenbeckia alata* kunt (Rutaceae). *Química Nova*. 34 : 984-986.

Da Costa D, Silva D, Cavalcanti A, de Medeiros M, de Lima J, Cavalcante J, de Fatima Vde Souza M. **2007**. Chemical constituents from *Bakeridesia pickelii* Monteiro (Malvaceae) and the relaxant activity of kaempferol-3-O-beta-D-(6"-Ep-coumaroyl) glucopyranoside on guinea-pig ileum. *Química Nova*. 30: 901.

Da Silva C, Benchimol JL. **2014** Malaria and Quinine Resistance: A Medical and Scientific Issue between Brazil and Germany. *Medical History*. 58 : 1-26

Darwish F, Reinecke MG. **2003**. Ecdysteroids and other constituents from *Sida spinosa* L. *Phytochemistry*. 62: 1179-1184.

Das N, Mishra S, Bishayee A, Ali S, Bishayee A. **2021**. The phytochemical, biological, and medicinal attributes of phytoecdysteroids: An updated review. *Acta Pharmaceutica Sinica B*. 11: 1740-1766.

Das N, Saha T, Bhattacharjee S. **2014**. A new biologically active ecdysteroid from the aerial parts of *Sida glutinosa*. *Journal of Pharmacognosy*. 3 : 73-78.

De Lima, L. F., de Oliveira, J. O., Carneiro, J. N. P., Lima, C. N. F., Coutinho, H. D. M., & Morais-Braga, M. F. B. **2021**. Ethnobotanical and antimicrobial activities of the Gossypium (Cotton) genus: A review. *Journal of Ethnopharmacology*. 279 : 114-363

Debalke D, Birhan M, Kinubeh A, Yayeh M. **2018**. Assessments of antibacterial effects of aqueous-ethanolic extracts of *Sida rhombifolia's* aerial part. *The Scientific World Journal*. Doi: 10.1155/2018/8429809.

Deepralard K, Kawanishi K, Moriyasu M, Pengsuparp T, Suttisri R. **2009**. Flavonoid glycosides from the leaves of *Uvaria rufa* with advanced glycation end-products inhibitory activity. *Thai Journal of Pharmaceutical Sciences*. 33 : 84-90.

Desalegn A, Andualem B. **2014**. Synergistic antibacterial effect of *Sida rhombifolia* leaf extracts and *Apis mellifera* honey against standard and drug resistant clinical isolated pathogenic bacteria. *World Applied Sciences Journal*. 32 : 1600-1610.

Dey T, Dutta P, Manna P, Kalita J, Boruah D, Buragohain , Unni B. **2018**. Anti-proliferative activities of vasicinone on lung carcinoma cells mediated via activation of both mitochondria-dependent and independent pathways. *Biomolecules & Therapeutics*. 26: 409.

Dinda B, Das N, Dinda S, Dinda M, SilSarma I. **2015**. The genus *Sida* L.–A traditional medicine: Its ethnopharmacological, phytochemical and pharmacological data for commercial exploitation in herbal drugs industry. *Journal of ethnopharmacology*.176 : 135-176.

Dorling R, Colegate M, Huxtable R. **1983**. The biological activity of swainsonine: An indolizidine alkaloid isolated from *Swainsona canescens*. Toxicon. 21: 93-96.

Draper J, Sack K, King R, Nielsen M, Rayner C, Higgins K. **2018**. Malaria Vaccines: Recent Advances and New Horizons. *Cell Host Microbe*. 24 :43-56.

Duarte R, Polycarpo C, Wait R, Hartmann R, Bergter E. **1998**. Structural characterization of neutral glycosphingolipids from Fusarium species. *Biochimica et Biophysica Acta*. 1390 : 186-196.

Elfita E, Muharni M, Maddyawati L, Darwati D, Ari W, Supriyatna, S, Husein H, Dachriyanus D, Paul C, Louis M. **2009**. Antiplasmodial and other constituents from four Indonesian *Garcinia* spp. *Phytochemistry*. 70 : 907-912.

Elufioye T, Agbedahunsi J. **2004**. Antimalarial activities of *Tithonia diversifolia* (Asteraceae) and *Crossopteryx febrifuga* (Rubiaceae) on mice *in vivo*. *Journal of Ethnopharmacol*. 93: 167-171.

Fogh S, Jepsen S, Effersoe P. **1979**. Chloroquine-resistant *Plasmodium falciparum* malaria in Kenya. *Transactions of the Royal Society of Tropical Medicine and Hygiene*. 73: 228-229.

Forkuo A, Charles A, Kwesi M, Johnson N, Elvis O, Ben A, Andrea T, Michael F. **2016**. Synergistic antimalarial action of cryptolepine and artemisinins. *Malaria Journal*. 15:12.

Forno I, Kassulke R, Harley K. **1992**. Host specificity and aspects of the biology of *Calligrapha pantherina* (Col.: Chrysomelidae), a biological control agent of *Sida acuta* [Malvaceae] and *S. rhombifolia* in Australia. *Entomophaga*. 37: 409-417.

Fotso, G.W., Ntumy, A.N., Ngachussi, E., Dube, M., Maptise, R., Kapche, G.D.F., Andrae-Marobela, K., Bonaventure Ngadjui, B. T. and Abegaz, B. M., **2014.** Epunctanone, a new benzophenone, and further secondary metabolites from *Garcinia epunctata* Stapf (Guttiferae). *Helvetica Chimica Acta.* 97: 957–964.

Furuya T., **1987**. Saponins (ginseng saponins). In Vasil, I.K. (Ed.), "Cell Cultures and Somatic Cell Genetics of Plants". 5, Academic Press, San Diego, CA: 213-234.

Gaillard T, Madamet M, Tsombeng FF, Dormoi J, Pradines B. **2016**. Antibiotics in malaria therapy: which antibiotics except tetracyclines and macrolides may be used against malaria. *Malaria Journal*. 15 : 556

Giang M, Otsuka H. **2018**. New compounds and potential candidates for drug discovery from medicinal plants of Vietnam. *Chemical and Pharmaceutical Bulletin*. 66 : 493-505.

Girach R, Aminuddin, Siddiqui P, Khan SA. **1994**. Traditional plant remedies among the Kondh of District Dhenkanal (Orissa). *International Journal of Pharmacognosy*. 32 : 274-283.

Gontijo D, Leite J, Nascimento M, Brandão G, Oliveira A. **2019.** Bioprospection for antiplasmodial activity, and identification of bioactive metabolites of native plants species from the *Mata Atlântica biome*, Brazil. *Natural Product Research*. 1-6.

Gontijo V, Judice W, Codonho B, Pereira I, Assis D, Januário J, Caroselli E, Juliano M, de Carvalho-Dosatti A, Marques M. **2012**. Leishmanicidal, antiproteolytic and antioxidant evaluation of natural bioflavonoids isolated from *Garcinia brasiliensis*

and their semi synthetic derivatives. Eur. *Journal* of *Medicinal Chemistry*. 58 : 613-623.

Gonzalez M., Rosazza J., **2004**. Microbial transformation of chalcones: hydroxylation, *O*-dimethylation and cyclisation to flavanones. *Journal of Natural Products.* 67: 553-558.

Goodwin T, Mercer E. **1983**. Introduction to plant biochemistry. Second Edition: Pergamon Press, Oxford, England..

Guedje N, Fankap R, Nkongmeneck B. **2000**. The genus *Garcinia* (Guttiferae) in Cameroon, diversity and traditional uses. In xvth Congress of AETFAT. *Scripta Botanica Belgica*. 20: 37-38.

Gupta S, Gunter J, Novak R, Regens J. **2009**. Patterns of Plasmodium vivax and *Plasmodium falciparum* malaria underscore importance of data collection from private health care facilities in India. *Malaria Journal*. 8: 1-8.

Gurjar V, Pal D. **2021**. Natural compounds extracted from medicinal plants and their immunomodulatory activities. *Bioactive Natural Products for Pharmaceutical Applications*. 197-261.

Haifang D, Hanxiang L , WU P. **2021.** α-Glucosidase inhibitory pentacyclic triterpenoids from the leaves of *Cleistocalyx conspersipunctatus*. *Phytochemistry Letters*. 41: 109-113.

Hamid, E. H., Moncef, B., Assia, B., Hind, T., & Rachid, B. **2018**. Phytochemical screening of a medicinal plant: *Mentha Spicata* L. *American Journal* of *Applied* Scientific *Research.* 12: 2429-5396.

Han S, Kim Y, Kang H, Huh J , Kim J , Baek N . **2014**. Oleanolic acid from Fragaria ananassa calyx leads to inhibition of α-MSH-induced melanogenesis in B16-F10 melanoma cells. *Journal of the Korean Society for Applied Biological Chemistry*. 57: 735-742

Hemshekhar M, Sunitha K, Santhosh MS, Devaraja S, Kemparaju K, Vishwanath BS, Niranjana SR, Girish KS. **2011**. An overview on genus *Garcinia*: phytochemical and therapeutical aspects. *Phytochemistry Reviews*. 10: 325-351

Herath H, Müller K, Diyabalanage H. **2004**. Synthesis of acrimarins from 1, 3, 5-trioxygenated-9-acridone derivatives. *Journal of Heterocyclic Chemistry*. 41 : 23-28.

Hernandez-Chavez I, Torres-Tapia L, Sima-Polanca P, Cedillo-Rivera R, Moo-Puc R, Peraza-Sanchez S**. 2012**. Antigiardial Activity of *Cupania dentate* Bark and its Constituents. *Journal of Mexican Chemical Society*. 56: 105-108.

Holdsworth D, Lacanienta E. **1981**. Traditional medicinal plants of the Central Province of Papua New Guinea. Part II. *Quarterly Journal of Crude Drug Research*. 19 : 155-167.

Huang H.-C, Chen L.-C, Chang, T.-H, Zhu T.-F, Chen C.-L, Cheng M.-J, Chen J.-J. **2019**. A new Lignanamide derivative and bioactive constituents of *Lycium chinense*. *Chemistry of Natural Compounds*. 55: 1002-1006.

Hung W, Liu C.-M, Lai C, Ho C, Pan M. **2015**. Inhibitory effect of garcinol against 12-O-tetradecanoylphorbol 13- acetate-induced skin inflammation and tumorigenesis in mice. *Journal of Functional Foods*. 18 : 432-444.

Hutchinson. **1972**. The families of Flowering Plants. Oxford University Press, London. 33

Ishii T, Okino T, Mino Y. **2006**. A ceramide and cerebroside from the starfih asterias a murensis lütken and their plant-growth promotion activities. *Journal of Natural Products*. 6: 1080-1082.

Ito C, Matsui T, Kobayashi T, Tokuda H, Shanmugam S, Itoigawa M. **2018**. Cancer chemopreventive activity of xanthones from *Calophyllum elatum*. *Natural Product Communications*. 13: 232-240.

Ivorra M, D'ocon M, Paya M, & Villar A. **1988**. Antihyperglycemic and insulin-releasing effects of beta-sitosterol 3-beta-D-glucoside and its aglycone, beta-sitosterol. *Archives internationales de pharmacodynamie et de thérapie*. 296 : 224-231.

Jain A, Choubey S, Singour K, Rajak H, Pawar S. **2011**. Sida cordifolia (Linn)–an overview. *Journal of Applied Pharmaceutical Science*. 1: 23-31.

Jang D, Park E, Kang Y-H, Su B-N, Hawthorne M, Vigo J, Graham J, Cabieses F, Fong H, Mehta R. **2003**. Compounds obtained from *Sida acuta* with the potential to induce quinone reductase and to inhibit 7, 12-dimethylbenz-[a] anthracene-induced

preneoplastic lesions in a mouse mammary organ culture model. *Archives of Pharmacal Research*. 26 : 585-590.

Jayaprakasha G, Jena B, Sakariah K. **2003**. Improved liquid chromatographic method for determination of organic acids in leaves, pulp, fruits, and rinds of *Garcinia*. *Journal of* AOAC International. 86: 1063-1068.

Johnson A, Obot I, Ukpong U. **2014**. Green synthesis of silver nanoparticles using *Artemisia annua* and *Sida acuta* leaves extract and their antimicrobial, antioxidant and corrosion inhibition potentials. *Journal of Materials and Environmental Science*. 5 : 899-906.

Kanthal L, Bhar K, Ravali P. **2017**. Evaluation of *in vitro* cytotoxic activity of chloroform extract of *Sida acuta* burm.f. *Evaluation*. 10.

Karaket N, Supaibulwatana K, Ounsuk S, Bultel-poncé V, Pham V, Bobo B. **2012**. Chemical and bioactivity evaluation of the bark of *Neonouclea purpurea*. *Natural Product Commun.* 7 : 160-169.

Karthivashan G, Kweon H, Park Y, Kim S, Kim H, Ganesan P, Choi K. **2019**. Cognitive-enhancing and ameliorative effects of acanthoside B in a scopolamine-induced amnesic mouse model through regulation of oxidative/inflammatory/cholinergic systems and activation of the TrkB/CREB/BDNF pathway. *Food and Chemical Toxicology*. 129: 444-457.

Kasahara K, Sanai Y. **2000**. Functional roles of glycosphingolipids in signal transduction via lipids rafts. *Glycoconjugate Journal*. 17: 153-162.

Kim J, Park S. **2020**. Recent insights into the biological functions of apigenin. *Experimental and Clinical Sciences.* 19: 984-991.

Kim R, Park G, & Jung Y. **2014.** Acacetin (5, 7-dihydroxy-4'-methoxyflavone) exhibits *in vitro* and *in vivo* anticancer activity through the suppression of NF-κB/Akt signaling in prostate cancer cells. *International Journal of Molecular Medicine*. 33: 317-324.

Komgeum J, Meli AL, Manfouo RN, Lontsi D, Ngounou FN, Kuete V, Kamdem W, Tane P, Ngadjui T, Sondenganm L, Connolly D. **2005**. Xanthone from *Garcinia smeathmannii* (Oliver) and their antimicrobial activity. *Phytochemistry.* 66 : 1713-1717.

Kumar M, Bussmann R, Mukesh J, Kumar P. **2011**. Ethnomedicinal uses of plants close to rural habitation in Garhwal Himalaya, India. *Journal of Medicinal Plants Research*. 5 : 2252-2260.

Kyeong W, Ji Y, Sang U, Ki H, Kang R. **2014.** Triterpenes from *Perilla frutescens* var. acuta and their cytotoxic activity. *Natural Products Sciences.* 20 : 71-75

Lambros C, Vanderberg J. **1979**. Synchronization of *Plasmodium falciparum* Erythrocytic Stages in Culture. *The Journal of Parasitology.* 65: 418.

Levery S, Toledo M, Doong R, Straus A, Takahashi H. **2005**. Comparative analysis of ceramide structural modification found in fungal cerebrosides by electrospray tandem mass spectrometry with low energy collision induced dissociation of Li^+ adductions. *Rapid Communications in Mass Spectrometry*. 14 : 551-563.

Li F, Awale S, Zhang H, Tezuka Y, Esumi H, Kadota S. **2009**. Chemical constituents of propolis from Myanmar and their preferential cytotoxicity against a human pancreatic cancer cell line. *Journal of Natural Products*. 72: 1283-1287.

Li Guan, M. R. Wenk., **2006**. Mass spectrometry-based profiling of phospholipids and sphingolipids in extracts from Saccharomyces cerevisiae. *Yeast.* 23: 465-477.

Lien-Hoa D, Hau T, Hung D, Connolly J, Harrison L. **2003**. Xanthones from the bark of *Garcinia merguensis*. *Phytochemistry*. 63: 467–470.

Lin Y, Anderson H, Flavin M, Pai Y. **1997**. In vitro anti-HIV of biflavonoïds isolated from *Rhus succedanea* and *Garcinia multiflora*. *Journal of Natural Product.* 60 : 884-888

Mahato, S.B., Kundu, A.P. **1994**. ^{13}C NMR spectra of pentacyclic triterpenoids. A compilation and some salient features. *Phytochemistry*. 37: 1517-1575.

Maliński M, Budzianowski J, Kikowska M, Derda M, Jaworska M, Mlynarczyk D, & Thiem B. **2021**. Two Ecdysteroids Isolated from Micropropagated Lychnis flos-cuculi and the Biological Activity of Plant Material. *Molecules*. 26 : 904.

Marques G, Monteiro R, Leão W, Lyra M, Peixoto M, Rolim-Neto P, Xavier H, Soares LAdL. **2012**. Avaliação de procedimentos para quantificação espectrofotométrica de flavonoides totais em folhas de *Bauhinia forficata* Link. *Química Nova*. 35 : 517-522.

Marti G, Eparvier V, Moretti C, Prado S, Grellier P, Hue N, Thoison O, Delpech B, Guéritte F, Litaudon M. **2010**. Antiplasmodial benzophenone derivatives from the root barks of *Symphonia globulifera* (Clusiaceae). *Phytochemistry.* 71 : 964-974.

Marti G, Eparvier V, Moretti C, Susplugas S, Prado S, Grellier P, Retailleau P, Guéritte F, Litaudon M. **2009**. Antiplasmodial benzophenones from the trunk latex of *Mocronobea coccina* (Clusiaceae). *Phytochemistry*. 70: 75-85.

Martins C, Campos M, Irioda A, Stremel D, Trindade A, Pontarolo R. **2017**. Anti-inflammatory effect of *Malva sylvestris*, *Sida cordifolia*, and *Pelargonium graveolens* is related to inhibition of prostanoid production. *Molecules*. 22 : 1883.

Mathew G, Lincy J, Aravind A. **2017**. A review on antibacterial activity of alkaloids from *Sida acuta. Journal of Pharmaceutical Innovation*. 6 :1029.

Mbafor J, Fomum Z, Promsattha R, Sanson D, Tempesta M. **1989**. Isolation and characterization of taxifolin 6-C-glucoside from *Garcinia epunctata*. *Journal of Natural Products*. 52 : 417-419.

Mbaze L, Poumale H, Wansi J, Lado J, Khan S, Iqbal M, Ngadjui B, Laatsch H. **2007**. α-Glucosidase inhibitory pentacyclic triterpenes from the stem bark of *Fagara tessmannii* (Rutaceae). *Phytochemistry.* 68: 591-595.

Meli A, Komguem J, Ngounou N, Tangmouo J, Lontsi D, Ajas A, Choudhary M, Ranjit R, Devkota K, Sondengam L. **2005**. Bangangxanthone A and B, two xanthones from the stem bark of *Garcinia polyantha* Oliv. *Phytochemistry.* 66 : 2351-2355.

Meshnick SR, Dobson MJ. **2001** The History of Antimalarial Drugs. In: Rosenthal PJ, éditeur. Antimalar. Chemother. *Humana Press* . 15-25.

Mgbemena C, Okwuosa C, Mene A, Nwofe J, Akhaumere E. **2015**. Hepatoprotective activity of n-hexane and ethyl acetate fractions of *Sida acuta* on thioacetamide induced liver injury in rats. *International Journal of Herbs Pharmacological Research*. 4 : 65-74.

Michael W. **2013**. The medical biochemistry page.org.

Michio K. **2011**. Biologically Active Molecules from Soybeans, Soybean and Health. El-Shemy H, editor. *InTech, hlm*. 213-214.

Minodier P, Noël G, Laporte R. **2011**. Chimioprophylaxie du paludisme. *Journal of Paediatrics and Childcare*. 24: 244-252.

Mishra M, Mishra VK, Kashaw V, Iyer AK, Kashaw SK. **2017.** Comprehensive review on various strategies for antimalarial drug discovery. *Journal of Medicinal Chemistry*. 125: 1300-1320.

Morris H, Panico M, Barber M, Bordoli R, Sedgwick R, Tyler A. **1981**. Fast atom bombardment: a new mass spectrometric method for peptide sequence analysis. *Biochemical and Biophysical Research Communication*. 101 : 623-631.

Muffler K, Leipold D, Scheller M-C, Haas C, Steingroewer J, Bley T, Neuhaus H, Mirata M, Schrader J, Ulber R. **2011**. Biotransformation of triterpenes. *Process Biochemistry*. 46 : 1-15.

Muganza D, Fruth B , Lami N, Tuenter E, Foubert K, Maes L. **2016**. *In Vitro* Antiprotozoal Activity and Cytotoxicity of Extracts and Isolated Constituents from *Greenwayodendron Suaveolens*. *Journal of Ethnopharmacology*. 193: 510-516.

Murali M, Mahendra C, Hema P, Rajashekar N, Nataraju A, Sudarshana M, Amruthesh Ky. **2017**. Molecular profiling and bioactive potential of an endophytic fungus *Aspergillus sulphureus* isolated from *Sida acuta*: a medicinal plant. *Pharmaceutical Biology*. 55 : 1623-1630.

Murphy R, Mathews W, Rokach J, Fenselau C. **1982**. Comparison of biological-derived and synthetic leukotriene C4 by fast atom bombardment mass spectrometry. *Prostaglandins*. 23 : 201–206.

Nájera JA, González-Silva M, Alonso PL. **2015**. Some Lessons for the Future from the Global Malaria Eradication Programme (1955–1969). *PLoS Medecine*. 8 : 145-234

Neto S, Prada A. Achod R., Torquato V, Lima C, Paredes-Gamero E, Amado R. **2021**. α-amyrin-loaded nanocapsules produce selective cytotoxic activity in leukemic cells. *Biomedicine & Pharmacotherapy*: 139: 111656.

Nguyen H, Trinh B, Tran Q, Pham H, Hansen P, Connolly J, Nguyen L-H. **2012**. Friedolanostane, fredocycloartane and benzophenone of the bark and leaves of *Garcinia benthami*. *Phytochemistry* . 72: 290-295.

Nisha C, Bhawana P, Fulekar M. **2017**. Antimicrobial potential of green synthesized silver nanoparticles using *Sida acuta* leaf extract. *Journal for Nanoscience and Nanotechnology*. 11: 111-119.

Noedl H, Se Y, Schaecher K, Smith L, Socheat D, Fukuda M. **2008**. Artemisinin Resistance in Cambodia 1 (ARC1) Study Consortium . Evidence of artemisinin-resistant malaria in western Cambodia. *The New England Journal of Medicine* 359: 2619-2620

Normand, D. **1955**. Atlas of Ivory Coast Woods .Tropical Forestry Technical Centre, Tome II, Nogent-Sur-Marne (Seine). 123–132.

Noudou, B. S., Djama, C. M., Mamdem, N. M., Komguem, J., Kkengfack, A. E., mbafor, j., & Wandji, J. **2015**. Banfoxanthone, a new prenylated xanthone from the stem bark of *Garcinia ovalifolia* (Guttiferaceae). *Journal of Applied Pharmaceutical Science*, 5 :136-139.

Noumi E, Yomi A. **2001**. Medicinal plants used for intestinal diseases in Mbalmayo Region, Central Province, Cameroon. *Fitoterapia*.72:246-254.

Nsangou M, Happi E, Fannang S, Atangana A, Waffo A, Wansi J. **2021**. Chemical composition and synergistic antimicrobial effects of a vegetatively propagated Cameroonian lemon, *citrus x limon* (l.) osbeck. *Journal* of *Agricultural and Food Chemistry*. 1 : 354-361.

Nyemba A, Mpondo T, Connolly J, Rycroft D. **1990**. Cycloartane derivatives from *Garcinia lucida*.*Phytochemistry*. 29: 994-997

Ogunkoya L. **1981**. Application of mass spectrometry in structural problems in triterpenes. *Phytochemistry.* 19 : 121-126.

Okombo J, Ohuma E, Picot S, Nzila A. **2011.** Update on genetic markers of quinine resistance in *Plasmodium falciparum. Molecular and Biochemical Parasitology*. 177: 77-82.

Oladoye S, Ayodele E, Abdul-hammed M**. 2015**. Characterisation and Identification of Taraxerol and Taraxer-14-en-3-one from *Jatropha tanjorensis* . 58 : 46-50.

Osafo N, Mensah K., Yeboah K. **2017**. Phytochemical and pharmacological review of *Cryptolepis sanguinolenta* (Lindl.) Schlechter. *Advances in Pharmacological Sciences*. 20: 125.

Padye S, Ahmed A, Oswal N, Sarkar F. **2009**. Emerging role of Garcinol, the antioxidant chalcone from *Garcinia indica* Choisy and its synthetic analogs. *Journal of* Hematology *and Oncology*. 2 : 38-40.

Papitha N, Jayshree N, Sreenivasan S, Kumar V. **2013**. Anti-tubercular activity on leaves and roots of *Sida rhombifolia* L. *International Journal of Pharmaceutical Sciences Review and Research.* 20 : 135-137.

Park J. **2011**. Effects of typheramide and alfrutamide found in Allium species on cyclooxygenases and lipoxygenases. *Journal of Medicinal Food*. 14: 226-231.

Park M, Hahn D . **1991**. Saponins from the stem bark of *Kalopanax pictum* var. magnificum (I). *Archives of Pharmacal Research*. 14 : 7-11.

Parveen N, Khan N. **1987**. Luteolin 7, 4′-dimethyl ether 3′-glucoside from *Gelonium multiflorum*. *Phytochemistry*. 26 : 2130-2131.

Payne, D. **1987**. Spread of chloroquine resistance in *Plasmodium falciparum*. *Parasitology*. 3: 241-246.

Piccinelli L, Cuesta-Rubio O, Chica B, Mahmood N, Pagano B, Pavone M, Baronee V, Rastrelli L. **2005**. Structural revision of clusianone and 7-*epi*-clusianone and anti-HIV activity of polyisoprenylated benzophenones. *Tetrahedron*. 61: 8206-8211.

Pieme C, Ambassa P, Yankep E, Saxena AK. **2015**. Epigarcinol and isogarcinol isolated from the root of *Garcinia ovalifolia* induce apoptosis of human promyelocytic leukemia (HL-60 cells). *Journal of Biological Engineering* . 8 :1-10.

Prakash A, Varma R, Ghosal SJPm. **1981**. Alkaloid constituents of *Sida acuta, S. humilis, S. rhombifolia* and *S. spinosa. Thai Journal* of *Pharmaceutical Sciences*.43: 384-388.

Qi J, Ojika M, Sakagami Y. **2000**. Termitomycesphins A-D, novel neuritogenic cerebrosides from the edible Chinese mushroom *Termitomyces albuminosus*. *Tetrahedron*. 56: 5835-5841.

Ramalhete C, Lopes D, Mulhovo S, Rosário V, Ferreira M. **2008**. Antimalarial activity of some plants traditionally used in Mozambique. In Workshop Plantas Medicinais e Fitoterapêuticas nos Trópicos. 29: 30

Ramalho L, Dias G, Guedes E, da Silva M, Lira AB, de Oliveira K, Chaves O, do Amaral R, da Paz A, Padilha J. **2019**. Acute toxicity evaluation of ethanolic extract of the air parts of *Sida rhombifolia* L., in wistar rats. *African Journal of Pharmacy*.13:181-187.

Reddy C, Diwakar P, Murthy YK. **2017**. Sustainable biodiversity management in India: remote sensing perspective. *Proceedings of the National Academy of Sciences*.87: 617-627.

Rieckmann H, Davis R, Hutton C. **1989**. *Plasmodium vivax* resistance to chloroquine. *Lancet 2*: 1183-1184.

Roberts R, Tren R, Hess K. **2013.** Perspectives on Barriers to Control of Anopheles Mosquitoes and Malaria. In: Manguin S, éditeur. Anopheles Mosquitoes. *Malaria journal*.

Rosli N, Melati K, Zuhair J. **2020.** Phytochemical and Biological Activity Studies of The Leaves of *Garcinia hombroniana* Pierre. *Malaysian Institute of Chemistry*. 81-102.

Sanon S, Azas N, Gasquet M, Ollivier E, Mahiou N, Barro N, Cuzin-ouattara N,Traore S, Esposito F, Balansard G, Timon-David P. **2003**. Antiplasmodial activity of alkaloid extracts from *Pavetta crassipes* (K. Schum) and *Acanthospermum hispidium* (DC), two plants used in traditional medicine in Burkina Faso. *Parasitology Research*. 90 : 314-317.

Sarma R, Kumari S, Elancheran R, Deori M, Devi R. **2016**. Polyphenol rich extract of *Garcinia pedunculata* fruit attenuates the hyperlipidemia induced by high fat diet. *Frontiers* in *Pharmacology*. 7: 294.

Sassaki G, Souza L, Serrato R, Cipriani T, Gorin P, Iacomini M. **2008**. Application of acetate derivatives for gas chromatography-mass spectrometry: novel approaches on carbohydrates, lipids and amino acids analysis. *Journal of Chromatography*. 1208 : 215-222.

Sbai H, Zribi I, DellaGreca M, & Haouala R. **2017**. Bioguided fractionation and isolation of phytotoxic compounds from *Apium graveolens* L. aerial parts (Apiaceae). *South African Journal of Botany*. 108: 423-430.

Scandroglio F, Loberto N, Valsecchi M, Chigorno V, Prinetti A, Sonnino S. **2009**.Thin layer chromatography of gangliosides. *Glycoconjugate Journal*. 26: 961-973.

Schobert R, & Biersack B. **2019**. Chemical and biological aspects of garcinol and isogarcinol: Recent developments. *Chemistry & biodiversity*. 16 :1900-366.

Senthilkumar R, Bhuvaneshwari V, Malayaman V, Chitra G, Ranjithkumar R, Dinesh K, Chandarshekar B. **2019**. Biogenic method of cerium oxide nanoparticles synthesis

using wireweed (*Sida acuta* Burm. f.) and its antibacterial activity against *Escherichia coli*. *Materials Research Express*. 6 : 105-126.

Shao J, Qing C, Wang F, Zhang L, Luo Q, Liu K. **2005**. A new cytotoxic lanostane triterpenoid from the basidiomycete *Hebeloma versipelle*. *The Journal of Antibiotics*. 58: 828-831.

Shi-Yie C, Zhi-Hong, W Shu-Fen, C Chung-Wei, T Shang-Kewi W, Chi-Hsin H, Chang-Feng D, Songue L, Koum Dongo E, Mpondo N, White L. **2012**. Constituents from Stem bark and Roots of *Clausena anisata*. *Molecules*. 17: 13673-13686.

Sibley H, Hyde J, Sims G, Plowe V, Kublin G, Mberu K. **2001**. Pyrimethamine-sulfadoxine resistance in *Plasmodium falciparum*. *Trends Parasitol*. 17: 570-1.

Silja V, Varma KS, Mohanan K. **2008**. Ethnomedicinal plant knowledge of the Mullu kuruma tribe of Wayanad district, Kerala.

Silva T, Almeida A, Moura T, Silva A, Freitas S, Jesus FG. **2016**. Effect of the flavonoid rutin on the biology of *Spodoptera frugiperda* (Lepidoptera: Noctuidae).*Acta Scientiarum Agronomy*. 38 :165-170.

Simo C, Kouam S, Poumale H, Simo I, Ngadjui B, Green I, Krohn K. **2008**. Benjaminamide: a new ceramide and other compounds from the twigs of *Ficus benjamina* (Moraceae). *Biochemical Systematics and Ecology*. 36 : 238-24.

Singh S, Gray AI, Waterman P. **1993.** Mesuabixanthone-A and mesuabixanthone-B: novel bisxanthones from the stem bark of *Mesua ferrea* (Guttiferae). *Natural Product Research*. 3: 53-58.

Sirajunnisa A, Mohamed M, Subramania A. **2014**. Influence of aqueous extract of *Sida acuta* leaves on corrosion inhibition of aluminium in alkaline solution. *Der Chemica Sinica*. 5 : 148-156.

Smilkstein M, Sriwilaijaroen N, Kelly J, Wilairat P, Riscoe M. **2004**. Simple and Inexpensive Fluorescence-Based Technique for High-Throughput Antimalarial Drug Screening. *Antimicrobial Agents and Chemotherapy.* 48: 1803-1806.

Sobreira A. **2019**. Phytochemical profiling by LC/MS and first isolated metabolites from *Sida planicaulis* Cav . (Malvaceae) and antimicrobial activity. 62-80

Sreedevi P, Owais S, Khan H, Ahmed S. **2009**. Morphometric analysis of a watershed of South India using SRTM data and GIS. *Journal of the geological society of india*.73:543-552.

Steck, Warren, Mazurek. **1972.** Identification of natural coumarins by NMR spectroscopy. *Lloydia* 35 : 418-439.

Subeki M, Yamasaki M, Yamato O, Maede Y, Katakura K, Suzuki M, Trimurningsih C, Yoshihara T. **2004**. Effects of central kalimantan plant extracts on intraerythrocytic Babesia gibsoni in culture. *Journal of Veterinary Medical Science* . 66: 871-874.

T Parvatkar P, S Parameswaran G Tilve S. **2011**. Isolation, biological activities and synthesis of indoloquinoline alkaloids: cryptolepine, isocryptolepine and neocryptolepine. *Current Organic Chemistry*. 15 : 1036-1057.

Talebi M, Talebi M, Farkhondeh T, Simal-Gandara J, Kopustinskiene M, Bernatoniene J, Samarghandian S. **2021**. Emerging cellular and molecular mechanisms underlying anticancer indications of chrysin. *Cancer Cell International*. 21: 1-20.

Tangmouo J, Lontsi D, Ngounou F, Kuete V, Meli A, Manfouo R, Kamdem H, Tane P, Beng V, Sondengam B. **2005**. Diospyrone, a new coumarinylbinaphthoquinone from *Diospyros canaliculata* (Ebenaceae): structure and antimicrobial activity. *Bulletin of the Chemical Society of Ethiopia*. 19 : 81-88.

Tanumihadja M, Mattulada K, Natsir N, Subehan S, Mandey F, Muslimin L. **2019**. Structural Assessment of Chemical Constituent of Sidaguri (*Sida rhombifolia* Linn) and Its Ability to Inhibit Cyclooxygenase. *Pesquisa Brasileira em Odontopediatria e Clínica Integrada*. 19.

Tanumihardja M, Natsir N, Mattulada I, Lukman M. **2016**. Pharmacological evaluation of ethanol extract of *Sida rhombifolia* L. roots (Malvaceae). *Journal* of *Chemical* and *Pharmaceutical Research.* 8 : 770-774.

Thanakijcharoenpath W, Theanphong O. **2007**. Triterpenoids from the stem of *Diospyros glandulosa*. *Thai Journal of Pharmaceutical Sciences*. 31 :1-8.

Thondawada M, Mulukutla S, Raju KRS, Dhanabal S, Wadhwani A. **2016**. *In vitro* and *In vivo* Evaluation of *Sida Acuta* burm. f.(Malvaceae) for its Anti-oxidant and Anti-Cancer Activity. Der *Pharma Chemica Journal for Medicinal Chemistry*. 8: 396-402.

Tian-Shung W, Chang-Sheng K, Furukawa, H. **1983**. Acridone alkaloids and a coumarin from *Citrus grandis*. *Phytochemistry*. 22 : 1493-1497.

Tona L, Cimanga RK, Mesia K, Musuamba CT, De Bruyne T, Apers S, Hernans N, Van Miert S, Pieters L, Totté J, Vlietinck AJ. **2004**. *In vitro* antiplasmodial activity of extracts and fractions from seven medicinal plants used in the Democratic Republic of Congo. *Journal of Ethnopharmacology*. 93: 27-32.

Ukpanukpong R, Uyabeme R, Adebiyi F, Basiru D, Akinfesola B, Aigbadumah P. **2019**. Heamatological Studies on *Sida rhombifolia* Ethanolic Leaf Extract of Micronor Induced Infertility in Female Rats. *International Journal* of *Current Microbiology* and *Applied* Sciences. 8: 1751-1759.

Vadivel V. **2016**. Distribution of flavonoids among Malvaceae family members–A review. *International Journal of Green Pharmacy*. 10.

Vatcharin R. Somksa S, Pueksa K, Souwalak P. **2005**. Friedolanostane and Lanostanes from the leaves of *Garcinia hombroniana*. *Journal of Natural Products.* 68: 1222-1225.

Viera L, Kijoa A, Silva A, Mondranondra I-O, Kengthong S, Gales L, Damas A, Herz W. **2004**. Lanostanes and friedolanostanes from the bark of *Garcinia speciosa*. *Phytochemistry*. 65: 393-398.

Wang R, Liu R, Zhang T, Wu T. **2010**. A new natural ceramide from *Trollius chinensis* Bunge. *Phytochemistry* .15: 7467-7471.

Weihong W, Chanhyeok J, Yongjin L, Chanyoon P, Eunseok O, Kyu-Hyung P, Youbin C, Eunmo K, JunI L, Yeon-Jin C, Jung P, Young-Ji, Ki Won L, and Heonjoong K. **2022.** Flavonoid Glycosides from Ulmus macrocarpa Inhibit Osteoclast Differentiation via the Downregulation of NFATc1. *American Chemical Society.* 7 : 4840-4849.

Weng J.-R, Tsao L.-T, Wang J.-P, Wu R.-R, Lin C.-N. **2004**. Anti-inflammatory phloroglucinols and terpenoids from *Garcinia subelliptica*. *Journal of Natural Products* 67: 1796-1799.

William W. **2014**. Ceramides, structure, biosynthesis and analysis. *American Oil Chemists Society*. 1-9.

Wong L, Klemmer P. **2008**. Severe lactie acidosis associated with juice of the mangosteen fruit, *Garcinia mangostana*. *American Journal of kidney Diseases.* 51: 829-833.

Wootton C, Feng X , Ferdig T, Cooper A, Mu J, Baruch I, Magill J, Su Z. **2002**. Genetic diversity and chloroquine selective sweeps in *Plasmodium falciparum*. *Nature*. 418:320-323.

World Health Organization. **2015**. Global Technical Strategy for Malaria Control 2016-2030.

World Health Organization. **2014**. Summarizes information received from malaria-endemic countries and other sources, and updates the analyses presented in the 2013 report.

World Health Organization**. 2017.** Tracks investments in malaria programmes and research as well as progress across all intervention areas: prevention, diagnosis, treatment and surveillance.

World Health Organization. **2018**. Procedures for testing insecticide resistance in malaria mosquito vectors.

World Health Organization. **2019.** Comprehensive update on global and regional malaria data and trends.

World Health Organization. **2020.** Historical look at key milestones that helped shape the global response to the disease over the last 2 decades.

Wouamba N, Happi G, Lenta B, Sewald N, Kouam S. **2020**. Vernoguinamide: A new ceramide and other compounds from the root of *Vernonia guineensis* Benth. and their chemophenetic significance. *Biochemical Systematics and Ecology*. 88 : 103988.

Yao X., Ding Z, Xia Y, Wei Z, Luo Y, Feleder C, Dai Y. **2012**. Inhibition of monosodium urate crystal-induced inflammation by scopoletin and underlying mechanisms. *International Immunopharmacology*. 14: 454-462.

Yemele M, Telefo P, Lienou L, Tagne S, Fodouop C, Goka C, Lemfack M, Moundipa F. **2015**. Ethnobotanical survey of medicinal plants used for pregnant women′ s health conditions in Menoua division-West Cameroon. *Journal of Ethnopharmacology*. 160 :14-31.

Yue J, Fan C, Xu J, Sun H . **2001**. Novel ceramides from the fungus *Lactarium volemus*. *Journal of Natural Product*. 64: 1246-1248.

Yu-Qing, T.; Qian, Y.; He, H.; Wei-Yi, Z. **2020.** An Overview of Available Antimalarials: Discovery, Mode of Action and Drug Resistance. *Current Molecular Medicine.* 20: 583-592.

Zakaria N, Mahdzir A, Yusoff M, Mohd Arshad N, Awang K, Nagoor H. **2018**. Cytotoxic effects of pinnatane A extracted from *Walsura pinnata* (Meliaceae) on human liver cancer cells. *Molecules*. *23*: 2733.

Zanetta J, Timmerman P, Leroy Y. **1999**. Determination of constituents of sulphated proteoglycans using a methanolysis procedure and gas chromatography/mass spectrometry of heptafluorobutyrate derivatives. *Glycoconjugate Journal*. 16: 617-627.

Zeb M, Khan S, Rahman T, Sajid M, Seloni S. **2017**. Isolation and Biological Activity of *β*-Sitosterol and Stigmasterol from the Roots of *Indigofera heterantha*. *Pharmacy & Pharmacology International.* 5: 139.

Zhang J. **2005**. A detailed chronological record of Project 523 and the discovery and development of qinghaosu (artemisinin) . *Yangcheng Evening News.* 193

LIST OF PUBLICATION

Blaise Cedric Kamdoum, Ingrid Simo, Steven Collins Njonte Wouamba, Brice Mariscal Tchatat Tali, Bathelemy Ngameni, Ghislain Wabo Fotso, Pantaléon Ambassa, Fekam Boyom Fabrice, Bruno Ndjakou Lenta, Norbert Sewald & Bonaventure Tchaleu Ngadjui (2021): Chemical constituents of two Cameroonian medicinal plants: *Sida rhombifolia* L. and *Sida acuta* Burm. f. (Malvaceae) and their antiplasmodial activity, Natural Product Research, DOI:10.1080/14786419.2021.1937156.

APENDICE

Natural Product Research

Formerly Natural Product Letters

ISSN: (Print) (Online) Journal homepage: https://www.tandfonline.com/loi/gnpl20

Chemical constituents of two Cameroonian medicinal plants: *Sida rhombifolia* L. and *Sida acuta* Burm. f. (Malvaceae) and their antiplasmodial activity

Blaise Cedric Kamdoum, Ingrid Simo, Steven Collins Njonte Wouamba, Brice Mariscal Tchatat Tali, Bathelemy Ngameni, Ghislain Wabo Fotso, Pantaléon Ambassa, Fekam Boyom Fabrice, Bruno Ndjakou Lenta, Norbert Sewald & Bonaventure Tchaleu Ngadjui

To cite this article: Blaise Cedric Kamdoum, Ingrid Simo, Steven Collins Njonte Wouamba, Brice Mariscal Tchatat Tali, Bathelemy Ngameni, Ghislain Wabo Fotso, Pantaléon Ambassa, Fekam Boyom Fabrice, Bruno Ndjakou Lenta, Norbert Sewald & Bonaventure Tchaleu Ngadjui (2021): Chemical constituents of two Cameroonian medicinal plants: *Sida rhombifolia* L. and *Sida acuta* Burm. f. (Malvaceae) and their antiplasmodial activity, Natural Product Research, DOI: 10.1080/14786419.2021.1937156

To link to this article: https://doi.org/10.1080/14786419.2021.1937156

NATURAL PRODUCT RESEARCH
https://doi.org/10.1080/14786419.2021.1937156

Taylor & Francis
Taylor & Francis Group

Chemical constituents of two Cameroonian medicinal plants: *Sida rhombifolia* L. and *Sida acuta* Burm. f. (Malvaceae) and their antiplasmodial activity

Blaise Cedric Kamdoum[a], Ingrid Simo[b], Steven Collins Njonte Wouamba[a,c], Brice Mariscal Tchatat Tali[d], Bathelemy Ngameni[e], Ghislain Wabo Fotso[a], Pantaléon Ambassa[a], Fekam Boyom Fabrice[c], Bruno Ndjakou Lenta[d], Norbert Sewald[f] and Bonaventure Tchaleu Ngadjui[a]

[a]Department of Organic Chemistry, Faculty of Science, University of Yaounde I, Yaounde, Cameroon; [b]Department of Chemistry, Faculty of Science, University of Dschang, Dschang, Cameroon; [c]Department of Chemistry, Higher Teacher Training College, University of Yaounde I, Yaounde, Cameroon; [d]Department of Biochemistry, Faculty of Science, University of Yaounde I, Yaounde, Cameroon; [e]Department of pharmacy, Faculty of Medicine and Biomedical Sciences, University of Yaounde I, Yaounde, Cameroon; [f]Organic and Bioorganic Chemistry, Faculty of Chemistry, Bielefeld University, Bielefeld, Germany

ABSTRACT

An extensive phytochemical investigation of the EtOH/H_2O (7:3) extracts of *Sida rhombifolia* L. and *Sida acuta* Burm. f., yielded a previously undescribed ceramide named rhombifoliamide (**1**) and a xylitol dimer (**2**), naturally isolated here for the first time, as well as the thirteen known compounds *viz*, oleanolic acid (**3**), β-amyrin glucoside (**4**), ursolic acid (**5**), β-sitosterol glucoside (**6**), tiliroside (**7**), 1,6-dihydroxyxanthone (**8**), a mixture of stigmasterol (**9**) and β-sitosterol (**10**), cryptolepine (**11**), 20-Hydroxyecdysone (**12**), (*E*)-suberenol (**13**), thamnosmonin (1**4**) and xanthyletin (1**5**). Their structures were elucidated by the analyses of their spectroscopic and spectrometric data (1 D and 2 D NMR, and HRESI-MS) and by comparison with the previously reported data. The crude extracts, fractions, and some isolated compounds were tested against chloroquine-sensitive (3D7) and chloroquine-resistant (Dd2) *Plasmodium falciparum* strains. All the tested samples demonstrated moderate and/or significant activities against 3D7 (IC_{50} values: 0.18-20.11 µg/mL) and Dd2 (IC_{50} values: 0.74-63.09 µg/mL).

ARTICLE HISTORY
Received 12 April 2021
Accepted 25 May 2021

KEYWORDS
Sida rhombifolia L; *Sida acuta* Burm. f; Malvaceae; rhombifoliamide; xylitol dimer; antiplasmodial activities

CONTACT Bonaventure Tchaleu Ngadjui ngadjuibt@yahoo.fr; Ghislain Wabo Fotso ghis152001@gmail.com

Supplemental data for this article can be accessed at https://doi.org/10.1080/14786419.2021.1937156.

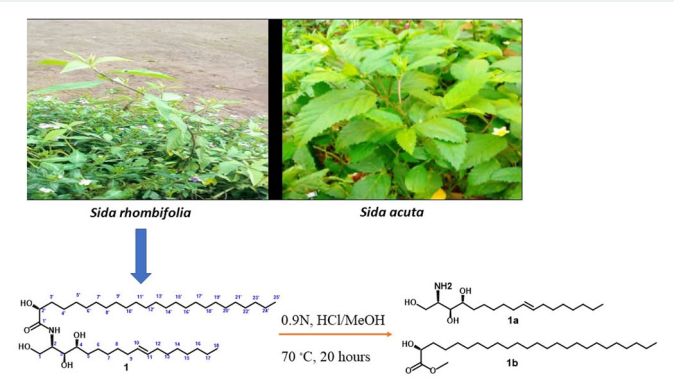

1. Introduction

Malaria is a parasitic disease caused by a protozoan of the genus *Plasmodium* asexually replicating inside the human body and transmitted from mosquitos to humans during a blood meal. Despite the continuous evolution of drug search, malaria is the deadliest and most dangerous parasitic infection in Sub-Saharan Africa, making the search for new antimalarial drugs an imperative of the overall health goal and probably one of the greatest public health challenges facing humanity (Gontijo et al. 2019). Despite extensive control efforts, the incidence of the disease is not decreasing and constitutes a major public health issue, principally in developing countries. According to the latest *World malaria report*, released on 30 November 2020, around 229 million malaria cases were reported compared to 228 million cases in 2018 where children under 5 years of age are the most vulnerable group affected by malaria; in 2019 and accounting for 67% (274 000) of all malaria deaths worldwide (WHO. 2020). Responsible for 99.7% of malaria cases in 2017, *Plasmodium falciparum* is the most prevalent malaria parasite in Sub-Saharan Africa. Until the development of an effective vaccine, chemotherapy remains a major frontline strategy for the control and future elimination of malaria. The current chemotherapy against malaria relies on Artemisinin Combination Therapy (WHO 2020). Plants of the genus *Sida* (Malvaceae) are widely used in indigenous communities for their nutritive values and for treating various ailments such as gonorrhoea, piles, rheumatism, gastrointestinal infections, varicella, variola, and malaria (Gupta et al. 2009). *Sida* genus is one of the most diverse in the Malvaceae family, with about 200 species distributed worldwide (Brandao et al. 2017). Phytochemical and pharmacological studies performed on some species have led to the identification of antibacterial lipid compounds from *S. cordata* Burm. f. and *S. acuta* Burm. f. (Adindu and Oguzie 2017), alkaloids with anti-inflammatory and antiparasitic potential from *S. rhombifolia* L. and *S. cordifolia* L. (Chaves et al. 2017; da Rosa et al. 2018). Polyphenols, triterpenes, and steroids have also been identified (da Rosa et al. 2015; Mah et al. 2017; Kumar et al. 2019). Currently, there are various empiric formulations based on *Sida* species (e.g., *S. acuta* Burm. f., *S. cordifolia* L. and *S.*

rhombifolia L.) for the treatment of neurological and rheumatic problems, and which also act as antimalarial drugs (Rodrigues and Oliveira 2020) but little is known about their chemical composition. In our continuous search for bioactive compounds from Cameroonian medicinal plants (Fotso et al. 2017, Mbougnia et al. 2020), we have carried out the chemical and biological study of two Cameroonian medicinal plants: *S. rhombifolia* L. and *S. acuta* Burm. f. The choice of these plants was motivated by the fact that they are traditionally used to treat malaria, but no antiplasmodial constituent has been described from them to date. We herein report the isolation and structure elucidation of a new ceramide named rhombifoliamide (**1**) and a xylitol dimer (**2**), naturally isolated for the first time, together with thirteen known compounds as well as their antiplasmodial activity.

2. Results and discussion

2.1. Isolation and structure elucidation

S. rhombifolia whole plant was extracted using the mixture of EtOH/H_2O (7:3, v/v). It is worth noting that this solvent system was chosen firstly because the hydroethanolic extract displayed the best antiplasmodial activity after micro-extraction compared to the DCM-MeOH extract and secondly because of the use of white wine in traditional medicine for plant maceration. The resulting crude extract was subjected to repeated silica gel and Sephadex LH-20 column chromatography (CC) to afford a previously undescribed ceramide named rhombifoliamide **(1**, 10.4 mg**)**, together with eight known compounds *viz*, oleanolic acid **(3**, 6.2 mg**)** (Wouamba et al. 2020), β-amyrin glucoside (**4**, 7.8 mg**)** (Alam et al. 2012), ursolic acid (**5**, 4.3 mg**)** (Wouamba et al. 2020), *β*-sitosterol glucoside (**6**, 9.7 mg**)** (Wouamba et al. 2020), tiliroside (**7**, 8.1 mg**)** (Danielly et al. 2007), 1,6-dihydroxyxanthone (**8**, 6.4 mg**)** (Lien Do et al. 2020), mixture of stigmasterol (**9**) and *β*-sitosterol (**10)** (Wouamba et al. 2020) and 20-hydroxyecdysone (**12**, 2.2 mg**)** (da Rosa et al. 2018). Similarly, *S. acuta* whole plant was extracted using the same solvent mixture. The crude extract obtained was subsequently purified using the above-mentioned chromatographic techniques to yield a xylitol dimer (**2**, 9.3 mg), naturally isolated for the first time, together with five known secondary metabolites namely: cryptolepine (**11**, 3.9 mg**)** (Banzouzi et al. 2004), 20-hydroxyecdysone (**12**, 5.3 mg**)** (da Rosa et al. 2018), (E)-suberenol (**13**, 5.1 mg**)** (Bissim et al. 2019), thamnosmonin (1**4**, 4.2 mg**)** (Tian-Shung et al. 1994) and xanthyletin (1**5**, 5.4 mg**)** (Ngo et al. 2020) (Figure 1). The structures of the known compounds were identified by comparison of their spectroscopic and spectrometric data with those reported in the literature.

Compound **1** was obtained as a white powder. Its molecular formula $C_{43}H_{85}NO_5$ was established from its HRESI-MS spectrum (Figure S1), showing the pseudo-molecular ion peak $[M+H]^+$ at *m/z* 696.6506 ($C_{43}H_{86}NO_5{}^+$; calcd. 696.6501), indicating two degrees of unsaturation. Its IR spectrum (Figure S2) showed characteristic absorption bands for free OH groups (3329-3215 cm^{-1}) and an amide group (1620 cm^{-1}) (Yue et al. 2001; Wonkam et al. 2020). The structure of **1** was fully assigned after careful analyses of its ^1H, ^{13}C, ^1H-^1H COSY, HMQC, HMBC, tandem MS spectra and methanolysis reaction (Figure S3–S12, Table 1). Indeed, the ^1H NMR spectrum of **1** (Figure S4) in

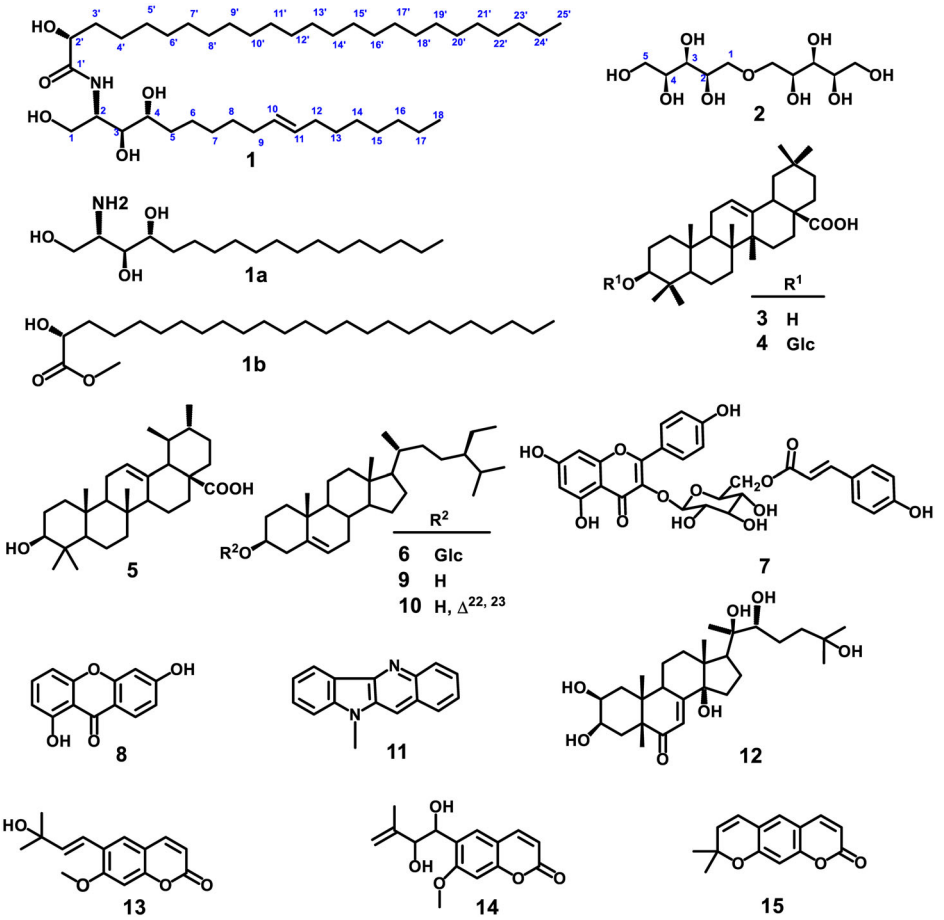

Figure 1. Structures of the isolated compounds **(1–15).**

conjunction with ^{13}C-NMR DEPT 135 spectra and HSQC (Figure S5–S7) displayed a set of signals characteristic of a ceramide as described by Simo et al. 2008. This was confirmed by the signals of the carbonyl of an amide at δ_C 175.4 and the signal of a nitrogen-attached sp^3 carbon at δ_C 51.5. Specifically, the NC-H proton appeared at $\delta_{H/C}$ 4.03(1H, m)/51.5 while the broad signal centered at δ_H 1.18 was attributed to the methylene protons of the aliphatic long chain; a distorted triplet at δ_H 0.79 (6H, t, 6.9) characterized the two terminal methyl groups. In addition, the spectrum displayed two diastereotopic protons of an oxymethylene at $\delta_{H/C}$ 3.72 (1H, dd, 4.6, 11.5, H-1a)/60.9 and 3.66 (1H, dd, 4.6, 11.4, H-1b)/60.9 as well as three oxymethine protons at δ_H/δ_C 3.46/75.3 (C-3), 3.45/72.1 (C-4) and 3.95/71.8 (C-2′) respectively. Correlations between these protons were observed on the ^{1}H–^{1}H COSY spectrum (Figure S8). In addition, the presence of a signal at δ_H 5.32(2H, m) showing cross peaks on the HSQC with two olefinic carbons at 129.8 and 130.5 ppm suggested the presence of a double bond in the structure of **1** (Wouamba et al. 2020). The length of this fatty acid moiety was deduced by the analysis of the ESI-MS/MS spectra of **1** (Figure S11) showing the fragment ion peak $[(CH_3(CH_2)_{22}CH(OH)CO + 2H]^+$ at *m/z* 383.4 and further confirmed

by the methanolysis using 0.9 N, HCl/MeOH, at 70 °C for 20 H to yield the fatty acid methyl ester (**1a**) and the sphingosine (**1 b**) (Simo et al. 2008 (Figure S3). Specifically, the peak at *m/z* 216.2 $[M+H]^+$ corresponding to molecular formula $C_{18}H_{38}NO_3^+$ was attributable to the long chain base (**1 b**) and implying one degree of unsaturation. Furthermore, this molecular formula of sphingosine suggested that the olefinic moiety is located in the long chain base (LCB). In the HMBC spectrum of compound **1** (Figure S9), ^2J correlations were observed between the olefinic proton at δ_H 5.32 and carbon C-12 (δ_C 32.5); H-15 at δ_H 1.21 with C-16 carbon (δ_C 31.8). Finally, H-17 at δ_H 1.20 correlates in ^3J with C-18 carbon corresponding to the terminal methyl. All of these correlations (Figure S11) made it possible to locate the double bond at Δ^{10} on the long basic chain. This information was confirmed by the ESI-MS/MS spectrum (Figure S12a and S12b) on which the ions peaks $[M+H\text{-}C_9H_{17}]^+$ at *m/z* 571.5 and $[M+H\text{-}C_7H_{15}]^+$ at *m/z* 619.5 corresponding to the allylic cleavages of the double bond, respectively for C_9-C_{10} and C_{11}-C_{12} were observed (Figure S10). The *trans* configuration of the C = C bond was evident from the chemical shifts of the allylic C-atoms at δ_C 32.5 and 32.0, which should have been less than 29.0 ppm if the configuration was cis (Simo et al. 2008, Wouamba et al. 2020). In addition, the absolute configurations at C(2), C(3), C(4), and C(2′) were determined as (*S*), (*S*), (*R*), and (*R*) according to biogenetic consideration and previously reported data (Ishii et al. 2006, Wonkam et al. 2020). Therefore, the structure of **1** was unambiguously determined as (2*S*,2′*R*,3*S*,4*R*,10*E*)-*N*-[2′-hydroxypentacosanoyl]-2-amino-octadec-10-ene-1,3,4-triol, to which the trivial name rhombifoliamide was given.

2.2. Antiplasmodial and cytotoxicity activities

Crude extracts, fractions and isolated compounds were screened for their antiplasmodial and cytotoxicity activities using SyBr Green-Based assay and resazurin-based assay respectively. Results showed that, extracts and fractions exhibited moderate to strong antiplasmodial activities against 3D7 (IC_{50} values: 0.18-20.11 µg/mL) and Dd2 (IC_{50} values: 0.74-63.09 µg/mL) *Plasmodium falciparum* strains. Interestingly, two compounds, oleanolic acid (**3**) and cryptolepine (**11**) isolated from the EtOAc-soluble fraction of *S. rhombifolia* and *S. acuta* displayed strong antiplasmodial activity with IC_{50} of (3.56 ± 0.62 and 2.02 ± 0.27) for **3; (**0.18 ± 0.01and 0.74 ± 0.09) for **11** respectively against 3D7 and Dd2 *P. falciparum* strains (Table S1). β-amyrin glucoside (**4**) and tiliroside (**7**) showed moderate activity only against the multidrug resistant (Dd2) and no activity against sensitive strain of *P. falciparum*. Except for cryptolepine (**11**), all extracts, fractions and compounds with activity against asexual *P. falciparum* parasites exhibited no cytotoxicity against Raw cells (selectivity indices (SI) > 10. To the best of our knowledge, this study provides the first report of antiplasmodial activity of isolated oleanolic acid against chloroquine-sensitive (3D7) and chloroquine-resistant (Dd2) *P. falciparum* strains. However, previous studies showed that the strong antiplasmodial activity of dichloromethane twig extract of *keetia leucantha* is attributed to the presence of eight triterpenic esters and the major antiplasmodial triterpenic acids, ursolic and oleanolic acids identified by HPLC-UV methods (Beaufay et al. 2017). In addition, cryptolepine previously showed varied interaction with the 4-

aminoquinolines, amodiaquine, and chloroquine. The combination of cryptolepine with amodiaquine showed a synergistic effect *in vitro* (mean $\Sigma FIC = 0.235 \pm 0.15$), whereas an additive effect (mean $\Sigma FIC = 1.342 \pm 0.34$) have been seen with chloroquine (Forkuo et al. 2016). Additionally, cryptolepine has already been reported to show high inhibitory activity against the late-stage gametocytes ($IC_{50} = 1965$ nM) (Forkuo et al. 2016) of *P. falciparum* (NF54). Summing-up, these studies report the good potential of cryptolepine as a promising antimalarial hit for both malaria treatment and transmission-blocking therapy (Forkuo et al. 2016). Based on the pronounced antiplasmodial activity of this compound, further chemical studies such as structural-activity relationship and/or medicinal chemistry are needed to obtain a lead compound that responds to pharmacokinetics and pharmacodynamics properties for antimalarial drugs. All experiments were performed in triplicate and the main results obtained are recorded in **Table S2**.

3. Experimental (supplementary data)

3.3.1. Rhombifoliamide *(1)*

White powder; IR (KBr): 3329 cm^{-1}, 3215 cm^{-1} and 1620 cm^{-1}; HRESI-MS: $[M+H]^+$ at *m/z* 696.6506 ($C_{43}H_{86}NO_5^+$; calcd. 696.6501); ^{1}H-NMR (600 MHz, $CDCl_3/CD_3OD$) & ^{13}C-NMR (150 MHz, $CDCl_3/CD_3OD$) see Table S1.

4. Conclusion

The phytochemical investigation on the EtOH/H_2O (7:3) extracts of *S. rhombifolia* and *S. acuta* yielded a previously undescribed ceramide named rhombifoliamide (**1**) and a xylitol dimer (**2**), naturally isolated here for the first time, as well as the thirteen known compounds viz, oleanolic acid (**3**), β-amyrin glucoside (**4**), ursolic acid (**5**), β-sitosterol glucoside (**6**), tiliroside (**7**), 1,6-dihydroxyxanthone (**8**), a mixture of stigmasterol (**9**) and β-sitosterol (**10**), cryptolepine (**11**), 20-Hydroxyecdysone (**12**), (*E*)-suberenol (**13**), thamnosmonin (1**4**) and xanthyletin (1**5**). Crude extracts, fractions, and compounds **1**-**12** were evaluated for their *antiplasmodial activity* against chloroquine-sensitive (3D7) and chloroquine-resistant (Dd2) *P. falciparum* strains. Two tops 'hits' antiplasmodial compounds **3** and **11**, with $IC_{50} < 3$ µg/mL isolated from EtOAc-soluble fraction of *S. rhombifolia* and *S. acuta* respectively, were identified in this study as potential lead compounds for antimalarial drug discovery. The hydroethanolic extract of *S. rhombifolia* and EtOAc-soluble fractions from *S. rhombifolia* and *S. acuta* had a good *antiplasmodial* activity with low preparation cost may be useful for further investigation in view to develop improved traditional medicines (ITM) to combat malaria disease.

Supplementary material

Experimental section, NMR, and MS data of compounds **1** are available alongside Figures S1–S12.

Acknowledgements

The authors are thankful to the German Academic Exchange Service (DAAD) for the financial support to the Yaounde-Bielefeld Graduate School of Natural Products with Antiparasite and Antibacterial activities (YaBiNaPA), project N° 57316173. Also, the NMR and MS departments at Bielefeld University, Germany, and Dr Jouda Jean-Bosco are grateful for their excellent work during the analysis of different samples.

Disclosure statement

No conflict of interest was reported by the authors.

Funding

This work was supported by the DAAD with funds from the Federal Ministry for Economic Cooperation and Development (BMZ) through the YaBiNaPA project (YaBiNaPA, www.yabinapa.de).

References

Adindu CB, Oguzie E. 2017. Investigating the extract constituents and corrosion inhibiting ability of *Sida acuta* leaves. World News Nat Sciences. 13:63–-81.

Alam P, Ali P, Aeri V. 2012. Isolation of keto alcohols and triterpenes from tubers of *Cyperus rotundus* Linn. J Nat Prod Plant Resour. 2:272–280.

Banzouzi JT, Prado R, Menan H, Valentin A, Roumestan C, Mallie M, Pelissier Y, Blache Y. 2004. Studies on medicinal plants of Ivory Coast: Investigation of *Sida acuta* for *in vitro* antiplasmodial activities and identification of an active constituent. Phytomedicine. 11:338–341.

Beaufay C, Hérent MF, Quetin-Leclercq J, Bero J. 2017. In vivo anti-malarial activity and toxicity studies of triterpenic esters isolated form *Keetia leucantha* and crude extracts. Malar J. 16(1):8.

Bissim SM, Kenmogne SB, Tcho AT, Lateef M, Ahmed A, Happi EN, Wansi JD, Ali MC, Waffo AF. 2019. Bioactive acridone alkaloids and their derivatives from *Citrus aurantium* (Rutaceae). Phytochem Lett. 29:148–153.

Bowling T, Mercer L, Don R, Jacobs R, Nare B. 2012. Application of a resazurin-based high-throughput screening assay for the identification and progression of new treatments for human African trypanosomiasis. Int J Parasitol Drugs Drug Resist. 2:262–270.

Brandao JL, Baracho GS, Sales MF, Viegas MP. 2017. Synopsis of *Sida* (Malvaceae, Malvoideae, Malveae) in the state of Pernambuco. Phytotaxa. 307:205–227.

Chaves OS, Teles YC, Monteiro MM, Junior LG, Agra MF, Braga VA, Silva TM, Souza MF. 2017. Alkaloids and phenolic compounds from *Sida rhombifolia* L. (Malvaceae) and vasorelaxant activity of two indoquinoline alkaloids. Molecules. 22(1):94.

da Rosa HS, Camargo VB, Camargo G, Garcia CV, Fuentefria AM, Mendez AS. 2015. Ecdysteroids in *Sida tuberculata* RE Fries (Malvaceae): Chemical composition by LC–ESI-MS and selective anti-*Candida krusei* activity. Food Chem. 182:193–199.

da Rosa HS, Koetz M, Santos MC, Jandrey EH, Folmer V, Henriques AT, Mendez AS. 2018. Extraction optimization and UHPLC method development for determination of the 20-hydroxyecdysone in *Sida tuberculata* leaves. Steroids. 132:33–39.

Danielly A, Davi A, Aline C, Marcos A, Julianeli T, José M, Bagnólia A, Maria FA, Maria FV. 2007. Chemical constituents from *Bakeridesia pickelii* Monteiro (Malvaceae) and the relaxant activity of kaempferol-3-O-β-D-(6″-Ep-coumaroyl) glucopyranoside on guinea-pig ileum. Quim Nova. 30:901–903.

Forkuo AD, Charles A, Kwesi MB, Johnson NB, Elvis OA, Ben AG, Andrea TA, Michael FO. 2016. Synergistic antimalarial action of cryptolepine and artemisinins. Malar J. 15(1):12.

Fotso GW, Kamga J, Ngameni B, Uesugi S, Ohno M, Kimura KI, Ngadjui BT. 2017. Secondary metabolites with antiproliferative effects from *Albizia glaberrima* var glabrescens Oliv. (Mimosoideae). Nat Prod Res. 31:1981–1987.

Gontijo DC, Leite JP, Nascimento MF, Brandão GC, Oliveira AB. 2019. Bioprospection for antiplasmodial activity, and identification of bioactive metabolites of native plants species from the Mata Atlântica biome, Brazil. Nat Prod Res. 10 :1732–1737.

Gupta S, Gunter JT, Novak RJ, Regens JL. 2009. Patterns of *Plasmodium vivax* and *Plasmodium falciparum* malaria underscore importance of data collection from private health care facilities in India. Malar J. 8:1–8.

Ishii T, Okino T, Mino Y. 2006. A ceramide and cerebroside from the starfish asterias a murensis lütken and their plant-growth promotion activities. J Nat Prod. 69:1080–1082.

Kumar S, Lakshmi PK, Sahi C, Pawar RS. 2019. *Sida cordifolia* accelerates wound healing process delayed by dexamethasone in rats: Effect on ROS and probable mechanism of action. J Ethnopharmacol. 235:279–292.

Lien Do TM, Duong TH, Nguyen VK, Phuwapraisirisan P, Doungwichitrkul T, Niamnont N, Jarupinthusophon S, Sichaem J. 2020. Schomburgkixanthone, a novel bixanthone from the twigs of *Garcinia schomburgkiana*. Nat Prod Res. :1–6.

Mah SH, Teh SS, Ee GC. 2017. Anti-inflammatory, anti-cholinergic and cytotoxic effects of *Sida rhombifolia*. Pharm Biol. 55(1):920–928.

Mbougnia JF, Bitchagno GT, Wouamba SC, Jouda JB, Awouafack MD, Tene M, Lenta NB, Kouam SF, Tane P, Sewald N. 2020. Two new triterpenoid fatty acid esters from *Schefflera barteri* Harms (Araliaceae). Nat Prod Res. :1–12.

Ngo TC, Mai TV, Pham TT, Jeremic S, Markovic Z, Huynh LK, Dao DQ. 2020. Natural acridones and coumarins as free radical scavengers: Mechanistic and kinetic studies. Chem Phys Lett. 746:137–312.

Rodrigues FC, Oliveira AF. 2020. The genus *Sida* L. (Malvaceae): An update of its ethnomedicinal use, pharmacology and phytochemistry. S Afr J Bot. 132:432–462.

Simo CC, Kouam SF, Poumale HM, Simo IK, Ngadjui BT, Green IR, Krohn K. 2008. Benjaminamide: A new ceramide and other compounds from the twigs of *Ficus benjamina* (Moraceae). Biochem Syst Ecol. 36(3):238–243.

Smilkstein M, Sriwilaijaroen N, Kelly JX, Wilairat P, Riscoe M. 2004. Simple and inexpensive fluorescence-based technique for high-throughput antimalarial drug screening. Antimicrob Agents Chemother. 48:1803–1806.

Tian-Shung W, Shiow-Chyn H, Jeng-Shiow L. 1994. Stem bark coumarins of *Citrus grandis*. Phytochemistry. 36(1):217–219.

Wonkam AK, Ngansop CA, Wouamba SC, Jouda JB, Happi GM, Boyom FF, Sewald N, Lenta BN. 2020. Rothmanniamide and other constituents from the leaves of *Rothmannia hispida* (K. Schum.) Fagerl. (Rubiaceae) and their chemophenetic significance. Biochem Syst Ecol. 93: 104–137.

Wouamba SC, Happi GM, Lenta BN, Sewald N, Kouam SF. 2020. Vernoguinamide: A new ceramide and other compounds from the root of *Vernonia guineensis* Benth. and their chemophenetic significance. Biochem Syst Ecol. 88:103–988.

Yue JM, Fan CQ, Xu J, Sun HD. 2001. Novel ceramides from the fungus *Lactarium volemus*. J Nat Prod. 64:1246–1248.